THE DEVELOPMENT AND COMMISSIONING OF AN 8-CHANNEL ASTRONOMICAL PHOTOMETER

Christopher A. Pollard

A Thesis Submitted for the Degree of PhD
at the
University of St Andrews

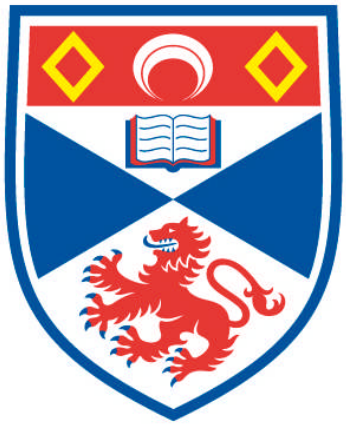

1988

The Development and Commissioning of an 8-Channel Astronomical Photometer.

by

C. A. Pollard

A dissertation submitted for the degree of Doctor of Philosophy at the University of St. Andrews.

St. Andrews April 1988

CERTIFICATE

I certify that Christopher Pollard has spent nine terms in research work at the University Observatory, St. Andrews, that he has fulfilled the conditions of Ordinance General No. 12 and Senate Regulations under resolution of the University Court, 1967, No. 1, and that he qualified to submit the accompanying dissertation in application for the degree of Ph.D.

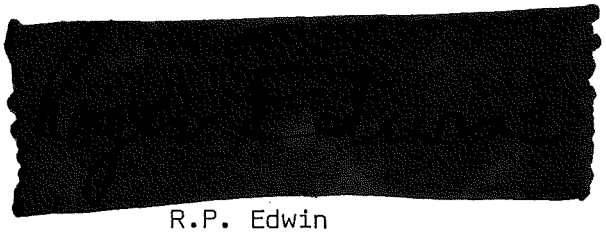

R.P. Edwin

DECLARATION

Except where reference is made to the work of others the research described in this thesis and the composition of the thesis are my own work. No part of this thesis has previously been submitted in application for a higher degree. I was admitted to the Faculty of Science of the University of St. Andrews as a research student under Ordinance General No. 12 on the 1st October, 1984. I was accepted as a candidate for the degree of Ph.D. on the 1st October, 1985, under Resolution of the University Court, 1967, No. 1.

Christopher Pollard

In submitting this thesis to the University of St. Andrews I understand that I am giving permission for it to be made available for use in accordance with the regulations of the University Library for the time being in force, subject to any copyright vested in the work not being affected thereby. I also understand that the title and abstract will be published, and that a copy of the work may be made and supplied to any bona fide library or research worker.

AKNOWLEDGEMENTS

I am indebted to my supervisor Dr.R.P. Edwin for his sustained interest and guidance throughout this project. I should like to thank Dr.R.W. Hilditch for his advice and assistance in preparing an astronomical programme.

It is a pleasure to acknowledge the help and encouragement of many members, past and present, of the Observatory. In particular the (then) workshop staff, Bill, George and Jimmie, for their willingness to help at all times. Also to Mr.Carr for his valuable discussions and practical help with the electronics. Not forgetting my fellow students Andy, Steve, Tam, Rab, Mark, Quentin, Ian, Keith, Eddie Jam Jar, Simon, Don, Helen, Paul and Kevin. Thanks especially to Graham, for getting me back on the right tracks on numerous occasions. For Clive, with whom I visited parts of the Old Course most golfers don't know exist ! To the Guinness family, who helped keep me sane, if not solvent, and to Louise for her help with tiping the daigrms.

I would like to extend my thanks to Professors D.W.N. Stibbs and W. Sibbet for making available the facilities at the University Observatory. I acknowledge the partial funding of this work by the Science and Engineering Council.

Looking back, into what now seems the very distant past, I would like to record here the debt I owe to the people who started me off down what has turned out to be a long and yet very rewarding path. Were it not for the encouragement and confidence given to me by Prof. Ian Robson and Drs Ian Butchart and Doug Whittet, none of this would have come about.

The debt I owe to my parents could not be adequately described here, nor could it ever be fully repaid. This work will always remind me of their sacrifices and love for me.

For Mum and Dad

ABSTRACT

The development and commissioning of an 8-channel astronomical photometer is described. The design is based on a low dispersion grating spectrograph in which the spectrum produced is focussed onto a mosaic of mirrors which redirect the radiation in the spectral bands into the appropriate detector channels. Filters are used to further define the spectral passbands. The detectors used are photomultipliers, whose response features have been matched to the individual channels. The instrument is under the control of a dedicated microprocessor with a further microprocessor used for data acquisition.

The photometer has been employed in an observing programme on the 0.9m James Gregory telescope at St.Andrews. Observations of standard uvby stars have allowed transformations equations to be derived for the Strömgren system. The eclipsing binary SV Cam has been observed and a revised ephemeris found.

Table of Contents

Chapter 1 : HISTORY OF PHOTOMETERS

1.1 Introduction
1.2 Early Observations
1.3 Introduction of the Photographic Plate
1.4 First use of Physical Detectors
1.5 Introduction of the Photomultiplier Tube
1.6 Development of Pulse Counting Techniques
1.7 Improvement of Photometric Detection Systems
1.8 Establishment of Photometric systems
1.9 Advantageous of Simultaneous Observations
1.10 Chopping Photometers
1.11 Dual Beam Photometers
1.12 Multi-Channel Photometers
1.13 The St.Andrews-DAO 8-Channel Photometer

Chapter 2 : OPTICAL AND MECHANICAL LAYOUT

2.1 Introduction
2.2 Optical Details
2.2.1 James Gregory Telescope
2.2.2 Optical Coupling
2.2.3 Acquisition Mirror
2.2.4 Acquisition Eyepiece
2.2.5 Aperture Slide
2.2.6 Neutral Density Filter
2.2.7 Post-Acquisition Eyepiece
2.2.8 Collimator
2.2.9 Grating
2.2.10 Camera Mirror
2.2.11 Mirror Mosaic
2.2.12 Photomultiplier Filters
2.2.13 Window Heaters
2.2.14 Fabry Lenses
2.2.15 Photomultiplier Tubes
2.3 Mechanical Details
2.3.1 Mechanical Overview
2.3.2 Calibration Source Unit
2.3.3 Acquisition Mirror
2.3.4 Offset Guider Counters
2.3.5 Aperture Slide
2.3.6 Aperchopper Assembly
2.3.7 Neutral Density Filter Wheel
2.3.8 Post-Aperture Viewer
2.3.9 Grating Rotator
2.3.10 Photomultiplier Filter Units

Chapter 3 : SYSTEM HARDWARE

3.1 Introduction
3.2 Control Electronics
3.2.1 Acquisition Mirror
3.2.2 Calibration Source
3.2.3 Filter Shutter
3.2.4 Grating Rotator
3.2.5 Photomultiplier Filters
3.3 Pulse Counting Electronics
3.3.1 The Aperchopper

3.3.2 Integration Timer
3.3.3 Pulse Counters
3.4 Associated Electronics
3.4.1 Power Supplies
3.4.2 Connectors
3.4.2.1 Backplane Modifications

Chapter 4 : SYSTEM SOFTWARE

4.1 Philosophy Behind the System
4.2 Processing Capabilities
4.3 Description of the Software Environment
4.4 Development Work with the System
4.5 Description of the Control Software
4.6 Description of the Data Acquisition Software
4.7 Communication Between the Two Systems
4.8 File Transfer Protocol

Chapter 5 : COMMISSIONING THE PHOTOMTETER

5.1 Introduction
5.2.1 Calibration Unit
5.2.2 Neutral Density Filter Wheel
5.2.3 Aperchopper
5.2.4 Grating Rotator
5.2.5 Photomultiplier Filter Units
5.2.6 Phtomultiplier Operating Voltage
5.2.7 Setting Grating Angle
5.3.1 Optical Assembly
5.3.2 Balancing the Telescope
5.3.3 "O" Rings
5.3.4 Flexure Testing
5.3.5 Testing the Counters
5.3.6 Focussing on the Apertures
5.3.7 Aperture Slide Selection
5.3.8 Fabry lenses
5.3.9 Dark Counts
5.3.10 Dead-Time Calculations
5.3.11 Neutrality of Neutral Density Filters
5.3.12 Sensitivity Variations Over the Aperture

Chapter 6 : ASTRONOMICAL PHOTOMETRY

6.1 Introduction
6.1.1 The Stromgren Four-Colour System
6.1.2 Photoelectric Reduction Procedure
6.1.3 Magnitude and Colour Transformations
6.1.4 Difficulties in Establishing Accurate Extinction Coefficients
6.1.5 The Observations
6.1.6 Reduction Procedure
6.1.7 The Derived Transformation Equations
6.2 Photometric Observations of SV Camelopardis
6.2.1 Introduction
6.2.2 The Observations
6.2.3 Time of Minima and Revised Orbital Period
6.2.4 Results of Observations

Chapter 7 : SUMMARY

Appendix A : CONTROL SOFTWARE

Appendix B : DATA ACQUISITION SOFTWARE

Appendix C : SIGNAL-TO-NOISE RATIO

Appendix R : REFERENCES

CHAPTER 1

A HISTORY OF PHOTOMETERS

1.1 INTRODUCTION

1.2 EARLY OBSERVATIONS

The history of photometry is as old as the history of astronomy itself. In the earliest of star catalogues, estimates of the brightness of the stars were established as an aid to identification.

A quantitative numerical scale was established by Hipparchus almost 2000 years ago. The first critical estimates of the apparent brightness of stars were made by Ptolemy in his Almagest. This was later revised and refined by al-Sufi.

In 1609, with the introduction of the telescope as an astronomical tool, Galileo extended Ptolemy's system of magnitudes.

Sir William Herschel devised a method of estimating stellar brightness by forming short sequences of stars and arranging them according to their apparent brightness. The degree of difference between successive members was indicated by symbols.

Argelander made use of this same method for estimating the light changes of variable stars but used "grades" instead of symbols. In 1843 he published his "Uranometrica Nova" which contained positions and apparent magnitudes for all objects visible to the unaided eye

from Bonn.

But throughout most of this time no standard scale of brightness existed. Whilst each observer generally based his work on that of the other observers, each defined his own scale or system of brightness. Furthermore, photometry was still seen as an aid to stellar identification rather then as being of merit in itself.

The first photometric instrument was introduced in 1725 when P.Bouger made measurements of the brightness of the Sun and Moon using a simple illumination photometer with a candle as a standard source. In 1740, A.Celsius and A.Tulenius, using an extinction photometer, made the first measurements of stellar magnitudes.

In 1836 Sir John Herschel invented his astrometer with which he determined the light ratios of a number of Southern stars. The brightness of a star was measured by comparing its brightness with a minified image of the moon. At the same time in Munich, C.A.Steinhill was using a more advanced method . His prism-photometer consisted of a small telescope with a divided objective. The two halves could be moved independently along the optical axis of the telescope. This motion allowed the intensities of two images, one from each half of the objective which were diffused into small discs by defocusing, to be varied. The relative brightness of the stars could be calculated from the relative positions of the two half-objectives when the images were seen to be of equal intensity.

By now, using the eye to check for equality or inequality, the typical error in estimating a stars magnitude was reduced from 0.2mag. to 0.06mag., (Weaver, 1946a).

That there was a functional relationship between the visually estimated magnitudes and the physical intensities of the stars was only established slowly. Newton had assumed that a 2nd magnitude star was twice as far away as a 1st magnitude star and a 3rd, 3 times as far away. This would imply that the apparent brightness was inversely proportional to the square of the magnitudes, which is a good approximation. This belief was still held a century later by Herschel and it was not until 1837 that C.A.Steinhill introduced the logarithmic relation which was to be adopted by nearly all later workers.

1.3 INTRODUCTION OF THE PHOTOGRAPHIC PLATE

The next major advance came in the use of the photographic plate. Just a few years after the photographic process had become available, Fizeau and Foucault were able to compare the brightness of the Sun to that of a carbon arc using the photographic principle.

In 1850 the first photographic stellar image (of Vega) was made by J.A.Whipple at the Harvard College Observatory, but such was the low sensitivity of the plates that no image of Polaris was possible, regardless of the length of exposure and the use of the medium stopped.

By 1857 the sensitivity of the plates had increased sufficiently to make possible photography of sixth and seventh magnitude stars using the 15-inch telescope at Harvard and so photographic photometry acquired new favour.

In 1881 using the new gelatin silver bromide emulsion, A.A.Common was the first to photograph stars too faint to be seen with the naked eye.

It should be noted though, that the photographic plate is not actually an improved detector over the eye. It still retains all the failures of the eye, ie. variable sensitivity, non-linearity, wavelength dependence along with a complicated time-dependence (reciprocity failure). The eye was still the final detector in much of the early photographic photometry. The main advantage of photography is the ability to integrate and store light. Longer exposures are able to average out the effects of scintillation and the observer can make his measurements in a more comfortable environment.

1.4 FIRST USE OF PHYSICAL DETECTORS

During the period 1911-1916, H.T.Stetson designed an instrument which eliminated the use of the eye and relied on purely physical methods for the determination of stellar magnitudes from photographic stellar images (Stetson, 1914; 1916). The energy absorbed from a beam of light by the silver grains in the stellar image on the plate was measured and interpreted in terms of stellar magnitude. J.Schilt at Groningen was to construct a very similar device to that of Stetson just a few years later (Schilt, 1922). This form of instrument is essentially similar to those which are still used today, ie. the microdensitometer.

The use of physical instruments in photometry could be said to precede the use of the photographic plate. In 1800 Sir William Herschel (1800) used a thermometer which he placed in a solar spectrum and demonstrated that heating could be observed beyond the

visible portion.

Shortly after the discovery of the thermoelectric effect in 1825 by Seeback, instruments employing thermoelements were made by d'Asonval (1886) and Boys (1889), though without much success. Huggins (1868) used a similar device some years later to successfully obtain measurements of Sirius, Pollux, Regulus and Arcturus. However the instruments required long exposure times and were impractical for routine use.

The first practical observations were made in 1913 by Pfund (1913) employing a vacuum thermocouple. Measurements were made of Jupiter and Vega with integration times of a few seconds, rather than minutes. This work was extended by Coblentz (1914) who, using the 36-inch Crossley at the Lick Observatory measured some 120 celestial objects, some down to 6.7th magnitude.

Concurrent with these developments was the introduction of the photocell. The principle of the photocell had been discovered in 1839 by E.Bequerel. One of the first successful uses of the photocell was in 1895 by G.M.Minchin (1895) who obtained measurable electrical effects when the cell was irradiated with light from Jupiter and Saturn.

More significant advances came with the use of selenium cells. The first observations made in the United States were by J.Stebbins and F.C. Brown (Stebbins, 1907). In spite of the selenium cell's low sensitivity, narrow wavelength response and poor availability, in 1910 Stebbins published a light curve of the eclipsing variable Algol (Stebbins, 1910). In his observations Stebbins used two stars of constant light, α Persei and δ Persei as comparison objects. These observations probably formed the most accurate set of observations in

existence at the time, with a probable error of only +/- 0.023mag. near the primary minimum.

The discovery of the photoelectric cell, by Elster and Geitel, in 1911 held the promise of more sensitive measurements. They were also more linear in their response than the selenium cells. In 1913, Schulz and Kunz used a photoelectric cell to record light from Arcturus and Capella (Schulz, 1913). Similar systems were being developed by Guthnick in Berlin (1913) and Rosenberg in Tubingen (1913).

Prior to 1932 the photocells were used in conjunction with comparatively inefficient electrometers. Then in 1932 Whitford perfected the thermionic amplifier which eliminated the necessity for electrometers (Whitford , 1932). The amplification was of the order of 2 million and the current generated could now be measured using a galvanometer. Although the combination of photocell amplifier and galvanometer was by far the most convenient way of measuring the magnitude of bright stars, there was a major drawback. Unlike the electrometer, where no amplifier is used, the amplification process introduces "noise" which, for faint stars, dominates the signal. There seemed little hope of decreasing the amplifier noise as it was already close to its theoretical limit.

1.5 INTRODUCTION OF THE PHOTOMULTIPLIER TUBE

The invention of the photomultiplier tube in the late 1930s offered the possibility to push the accuracy limit several magnitudes beyond that obtainable with either the electrometer or amplifier/galvanometer. (The internal amplification that takes place within the photomultiplier tube is, essentially, noise free).

Whitford and Kron in 1937 were the first to use a photomultiplier tube as auxiliary equipment (for guiding) on a telescope (Whitford, 1937). These initial experiments indicated that the devices were inferior to the photocell because of the low efficiency of the emitting surfaces, and little further interest was shown in them.

The photomultiplier tube came of age in the early 1940s with the use of antimony-caesium emission surfaces. RCA produced their first type 931 just before the Second World War and the 1P21 during the war. Kron (1946) was one of the first to use the new tubes and in conjunction with the 36-inch Lick refractor was able to measure down to 11th magnitude.

Up to this point the final measuring instrument, usually some form of galvanometer, had been used to measure the output current, after DC amplification, from the photomultiplier tube. The limits of accuracy with this technique were now beginning to be reached, especially for the fainter stars, where the currents produced could be of the order 10^{-15}, 10^{-18} ampere.

1.6 DEVELOPMENT OF PULSE COUNTING TECHNIQUES

From the earliest days of photoelectric photometry attempts had been made to count the individual electrons emitted from the photocathode. Although several early attempts had been successful (Elster and Geitel, 1916; Steinke, 1926; Rajewsky, 1931) the methods used were somewhat unreliable and were not adapted for photoelectric photometry. However, these experiments had been performed using photocells.

A HISTORY OF PHOTOMETERS

The introduction of the photomultiplier tube, with its internal amplification producing a sizeable output pulse at the anode, renewed attempts to count individual electrons. Kron had speculated on the use of pulse counting electronics (Kron , 1946) though at this time had not actually produced anything. In 1947, R.W.Engstrom was able to make simple measurements by visually counting the output pulses appearing on a cathode ray oscilloscope (Engstrom, 1947).

The first systems to be successfully used in astronomical applications were produced independently by Yates (1948) in Cambridge and Blitzstein (1951) at the Flower Observatory Pennsylvania .

The output pulse from the photomultiplier tube is amplified and fed into a discriminator. All pulses greater then a selected reference level cause the discriminator to generate a standard pulse. A gating circuit then either passes or blocks them, the action being controlled by a timer, which determines the length of the integration.

Since this period the use of pulse counting electronics has gradually become standard, particularly after the introduction of the transistor, which has made low noise amplifiers and fast reliable counters cheap and easily available. It has been shown by several authors that photon counting techniques produce better results in the detection of faint sources than other methods. This is due to the ability to reject output signals that do not originate from photons striking the cathode (eg. thermal electrons emitted from lower stages of the amplification chain), thereby improving the signal-to-noise ratio. (Morton, 1968; Nakamura and Schwarz, 1968; Tull, 1968). However, for high luminous fluxes, DC methods are to be preferred due to the non-linearity of the photomultiplier tubes at

high count rates which arises from the dead time associated with the devices, (Johnson , 1960).

1.7 IMPREOVEMENT OF PHOTOMETRIC DETECTION SYSTEMS

EHT supplies are now far more stable resulting in less drift in the gain of the tubes, though pulse counting techniques are less sensitive to these variations than DC techniques. Effective and stable cooling systems are now available helping to reduce the dark current of the tubes.

Improvements in the photomultiplier tubes themselves have centred mainly on the use of higher efficiency materials for the photocathode. The S20 type was the first to use bi-alkali metals, which extended the sensitivity range out to 700nm, sufficient to include the Hα line. The S1 photocathode pushed the cutoff response into the infra-red at 1100nm. At the other end of the wavelength range caesium-iodide and potassium-bromide photocathodes have extended the response to 105 to 200 nm, which is of particular use in spaceborne observatories.

Another area where improvements have been made is in the timing of integrations. Unfortunately, in photographic work, for integrations of longer than one second, the reciprocity law fails making time-scale photometry very difficult. With photoemissive detectors this problem is avoided. Studies by Latham (1968) have shown that effects found in photoemissive devices, producing a similar effect to the reciprocity failure, such as gain-drift or fatigue, can be reduced to 1 to 2%.

The overall trend then, has been towards the removal of various systematic effects, with an emphasis on those connected with averaging.

1.7.1 Establishment Of Photometric Systems

Along with this development of detectors came a parallel development of photometric systems. The development of photography had enabled spectroscopists to begin to study the physical nature of the stars. But, for the photometrist, the photographic plate does not readily yield precise mean numbers due to the diffuse mass of silver grains which form the scattered image. The introduction of the photomultiplier changed this.

At first progress was rather uncoordinated with various observatories and astronomers using different colour filters to define the bands and also using an assorted number of filters.

It was not until the introduction of the UBV system by Johnson and Morgan (1953) that some order was imposed. They systematically compared their measurements with the MK classifications which, with the discovery by Eggen that stars in associations and clusters have colours which fall along narrow sequences, made the system a powerful tool. To this day a great majority of photometric measurements are either taken using this system or else transformed to it.

Many other photometric systems have been developed, some of which employ very narrow filters to measure individual line strengths, or to investigate specific properties in selected groups of stars. For example, the Strömgren uvby system (1966) was created for the study of A F and G stars and the DDO system (McClure and Van den Bergh, 1968) for late type stars. For a more detailed discussion of

photometric systems and their applications see Golay, 1974.

1.9 ADVANTAGES OF SIMULTANEOUS OBSERVATIONS

So far we have just been considering conventional single beam photometers. Here magnitudes, either through different filters and/or between object sky and comparison, must be measured sequentially. Now it has been shown that, for ground based photoelectric photometry, the limiting factors are photodetection-noise and variable atmospheric transparency (Belvedere and Paterio, 1976). Therefore, this non-simultaneous measurement procedure requires either good atmospheric stability (ie. constant sky transparency and seeing) or else frequent alternations of object and sky, which results in a considerable loss of efficiency. Even with frequent alternations, errors arise from inconsistent centring of the stellar image in the photometer aperture and poor tracking.

It has been shown that simultaneous observations at several wavelengths can largely eliminate errors arising from transparency fluctuations and also, to an extent, errors due to inconsistent centring of the stellar image (see eg. Walraven and Walraven, 1960; Griffin and Redman, 1960; Oke, 1969.). But if the simultaneous colour observations are to be independent of sky-transparency fluctuations the fluctuations must be, to a first order, grey. Also the stars being measured must be sufficiently bright so that accompanying changes in sky brightness introduce an insignificant error (Walker, 1969). Using a quasi-simultaneous procedure Serkowski reports a change in colour of only 0.01 magnitude per magnitude of cloud absorption for the UBV photometric system (Serkowski, 1970). This means that otherwise non-photometric nights may be used profitably.

An additional advantage of simultaneous observations is the increase in observations over a given period. Simultaneous measurements also allow the monitoring of colour changes in stars which exhibit rapid phenomena eg. flickering of flares.

Numerous photometers have been developed which exploit the concept of simultaneous measurements. It would be impractical, and undesirable, to list here each multi channel/beam instrument which has been built. Instead, specific photometers will be considered which exemplify the various design approaches.

The approaches that have been taken can be split into three general groups which tend to increase in complexity. They are

(i) Chopping Photometers

(ii) Dual beam photometers and

(iii) Multi channel/beam photometers.

It is convenient to consider each group in turn.

1.10 CHOPPING PHOTOMETERS

None of the instruments in this section provide true simultaneous measurements as all use a single detector. The underlying theme is the reduction of time between successive measurements through different filters and/or different objects.

The simplest consist of a rotating filter wheel, generally under computer control, that allows rapid changing of filters between observations.

A typical example of this type of photometer is that described by Gianni et. al. (1975). An optical diagram of the photometer is shown in Figure 1.1. The various colours are measured by a single photomultiplier successively. The six filters used (UBV from Johnson (1955) plus-two bands at R (600nm) and I (800nm), differing from the standard R and I used by Stebbins (1956)), are held in a circular filter-stand disc. The disc is mounted on the shaft of a stepping motor, whose rotation is controlled by the data acquisition system. A single counting device is used.

Although fast electronics were used in the counting system, allowing photoemissions occurring within a time interval of the order of 20ns to be detected, the integration times used in each channel were generally of the order of 10 sec.

But Sorvari (1975) has pointed out that whilst atmospheric transparency variations occur at all frequencies, it is most apparent on a time scale of several tens of seconds. So, changing the filters on this time scale will not reduce the effect of these variations. It was with this in mind that Sorvari constructed a photometer incorporating a rapid change filter wheel.Four filters are mounted in a filter wheel. Associated with each of the four filters is one channel in a four-channel scaler, which is used to record the pulses generated by photons arriving through that particular filter.

A control unit is used to gate the scalers and also control the position of the filter wheel. It also "enables" the appropriate scaler. Approximately every 3 seconds counting is inhibited for about 0.25sec whilst a stepper motor advances the filter wheel. This results in a dead time of about 8%.

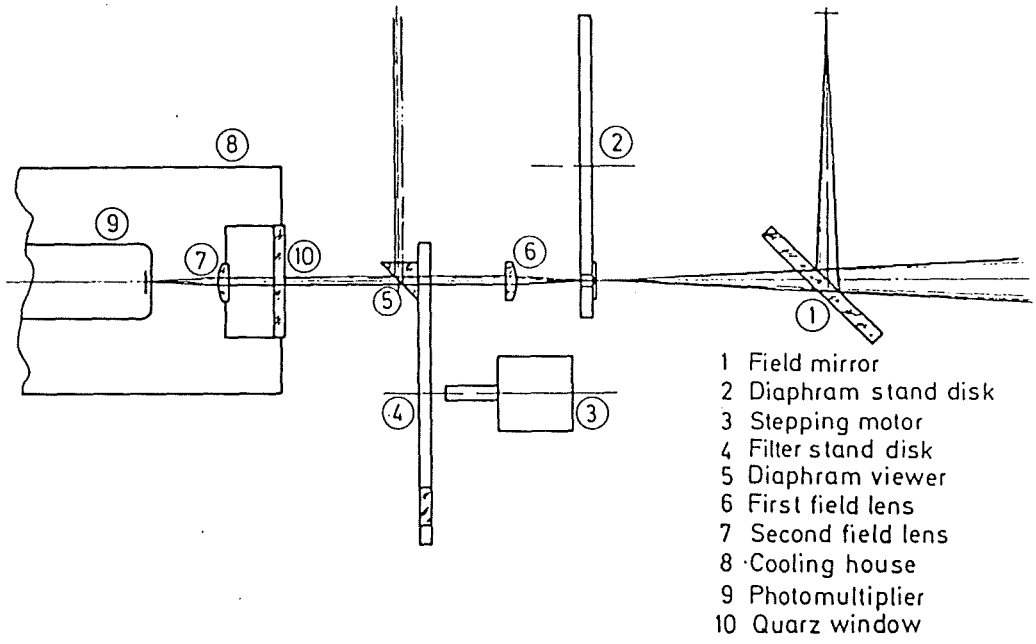

Fig.1.1 Optical diagram of the photometer designed by Gianni et al.

After each filter has been in place ten times, the scalers are read. For fainter stars a series of the standard length integrations is summed.

That this method is effective in removing the effects of variable sky transparency in the colour indices was demonstrated by Sorvari, by comparing both conventional and rapid-filter-change measurements of the same star on two different nights.

The first night was of good photometric quality. The standard deviation, for a set of 8 measurements was $\sigma = 0.004$ for conventional photometry and $\sigma = 0.003$ for the rapid-filter-change photometry. (This demonstrates that the rapid-filter-changing introduces no new source of noise).

The second night was chosen because of its obviously poor quality. This time the standard deviation for conventional photometry rose to $\sigma = 0.043$, whilst that for the rapid-filter-change increased to only $\sigma = 0.008$, a reduction in σ of approximately a factor of 6.

Other photometers which have been built to exploit this increased accuracy in colour determination include that of Caplan and Grec (1975). This was built specifically to measure the line and continuum intensities in emission nebulae. Again, the technique of repeating short integrations through many rotations of the filter wheel to average out the effects of variations in atmosphere transparency is used.

A design by Kinman and Mahaffey (1974) incorporates a paddle device which can be used to cover one of a pair of apertures. (Figure 1.2).The position of the paddle is computer controlled , as is the filter wheel. This design marks the transition between the

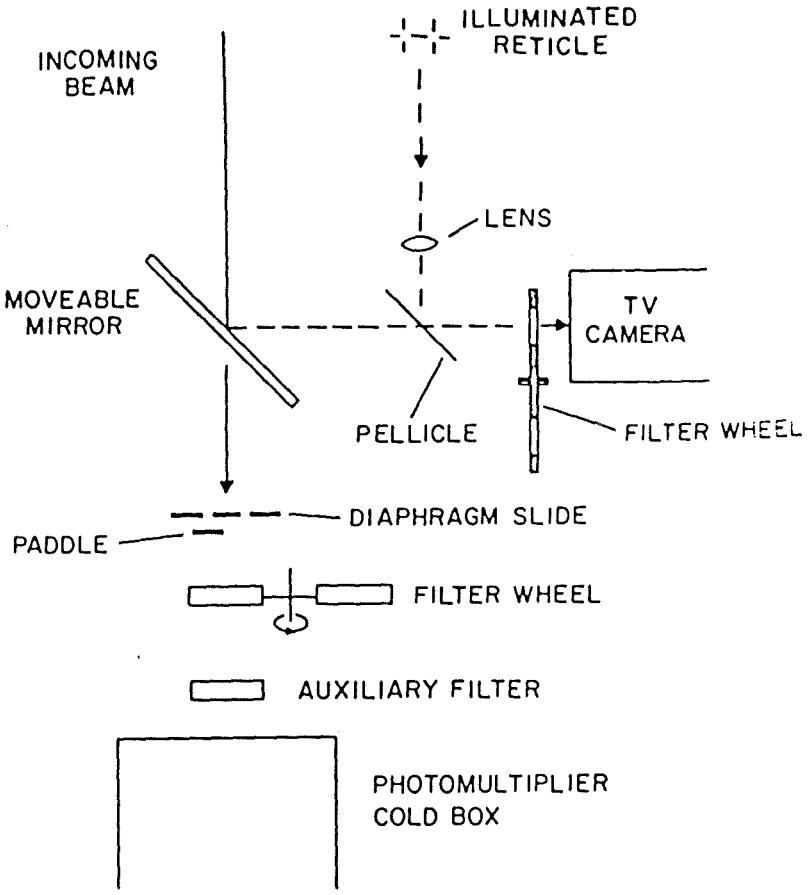

Fig.1.2 A schematical diagram showing the layout of the photometer designed by Kinman and Mahaffey.

simple repetitive filter-cycle photometer and the chopping photometer.

A chopping photometer is described by Davidson (1976). A schematic diagram is shown in Figure 1.3. A spring loaded solenoid moves a stainless steel mirror which is set at a 45^{o} angle with the optical axis, in a plane parallel to the focal plane. A 0.75mm hole (giving a circular diaphragm with an angular diameter of 30 arc seconds) is drilled into the mirror. The mirror is oscillated at either 1Hz or 5Hz. The light from the object passes alternately through the filters and onto the photomultiplier tube or else to the viewing mirror. The diaphragm is stationary in one of the two positions, sky or star, for approximately half of the time. By using the mirror the objects position in the diaphragm can be continuously monitored using the viewing telescope. The filters are located in two stacked filter wheels, each containing five filters.

Control electronics are used to gate the pulses to the appropriate counter, depending on the mirrors position and to inhibit counting whilst the mirror is moving from one position to the next.

Whilst the system allows quasi-simultaneous monitoring of the object and sky, the different colours are still separated in time with the possibility that there may be changes in the sky transparency between measurements made through different filters.

Several photometers have been built which, whilst still single beam instruments, have attempted to overcome this difficulty.

Burnet and Rufener (1979) have constructed a photometer which they claim can measure objects simultaneously, see Figure 1.4. Object A is situated on the optical axis of the telescope and object B can be in any direction up to 13' from A (with a minimum separation of 1').

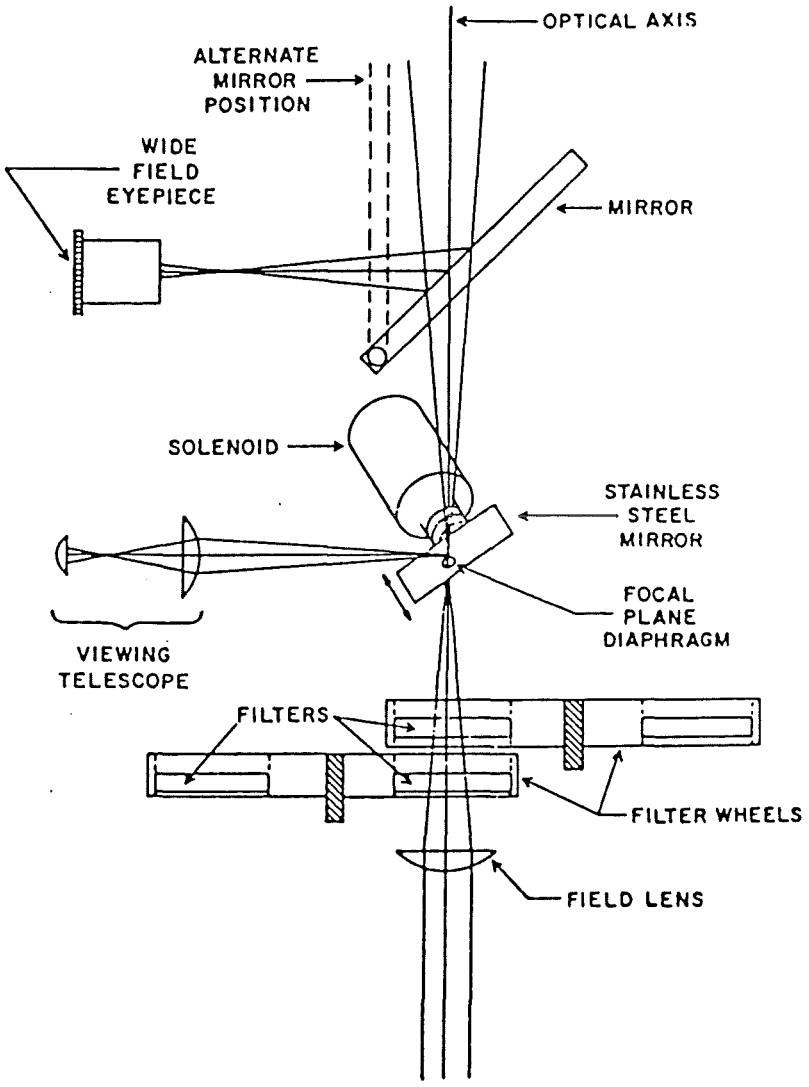

Fig.1.3 A schematical diagram of the sky-compensating photometer designed by Davidson et al.

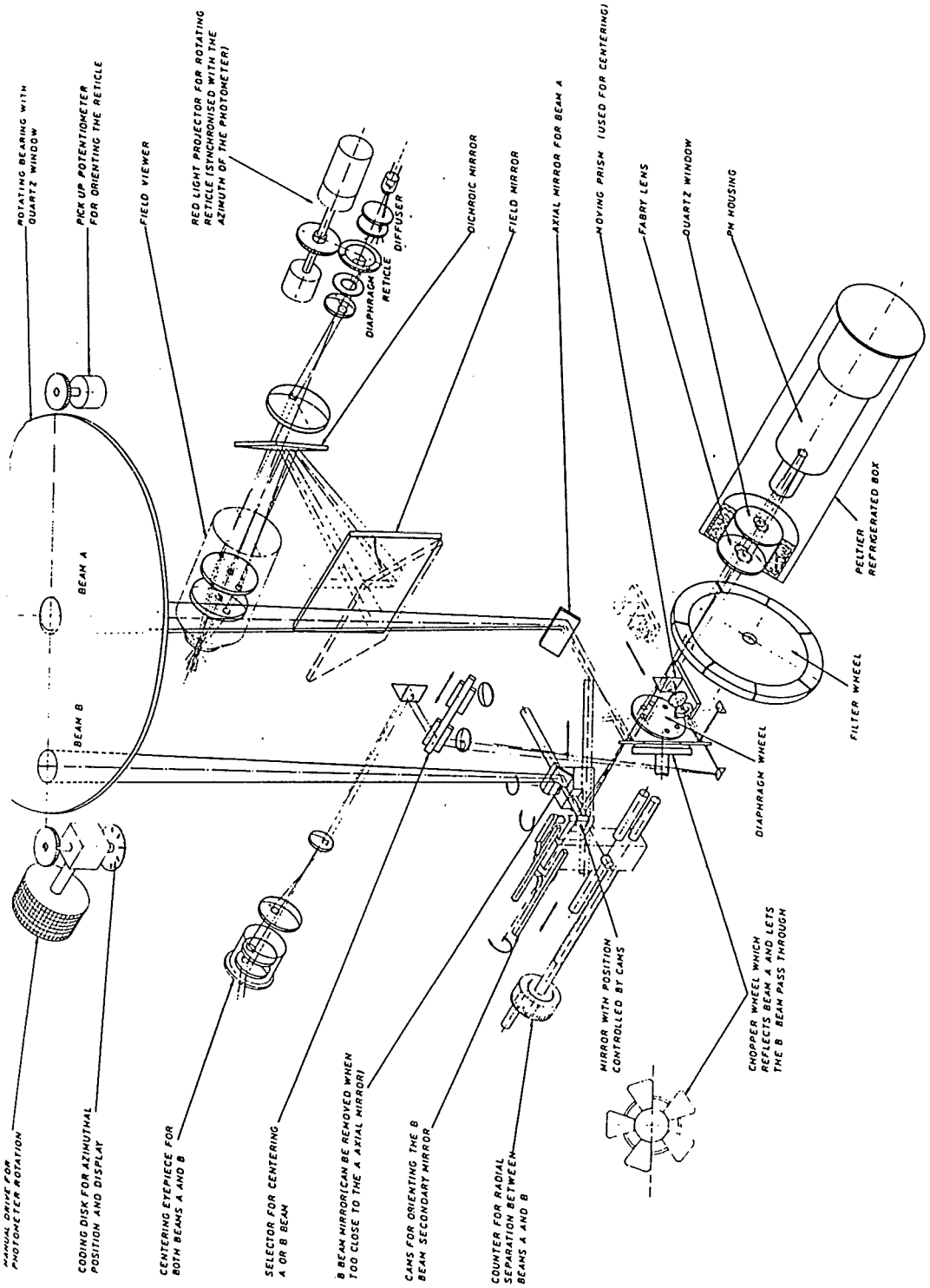

Fig.1.4 A schematical diagram of the differential photometer designed by Burnet and Rufener.

A 150mm diameter wheel holds seven filters. As each filter is brought into the optical beam an optical chopper wheel switches between the two data channels, allowing each to be incident in turn on the photomultiplier tube.

The period of rotation of the filter wheel, as well as that of the optical chopper, is variable, allowing different lengths of integration to be used.

The photometer can be used for differential photometry, comparing a variable star with a reference star, allowing short term variation to be followed, or it can be used in a star/sky mode.

Clearly, the two channels are not being sampled simultaneously, but this rapid changing between the two objects and through different filters will help reduce the effects due to changes in sky transparency.

Visvanathan (1972) has constructed a similar device, though this is restricted to the star/sky mode. Here two apertures, of equal size, separated by 8mm, have been mounted in an aperture wheel in the focal plane of the photometer. A small circular plate chopper with two semicircular slots is mounted eccentrically behind the apertures. As the chopper rotates, only light from one aperture can reach the photomultiplier at any time. A magnetic pickup, mounted near the edge of the chopper produces one positive and one negative pulse for each rotation of the wheel. The wheel is rotated at 60 cycles per second, therefore the star and sky are seen alternatively by the photomultiplier tube sixty times per second.

The photometer can be used either in conjunction with a continuous circular interference filter or with a filter wheel which holds six wideband filters.

The continuous variable filter wheel covers a wavelength range from the ultraviolet to 750nm, with a bandwidth of about 20nm. It is rotated about the optical axis using a stepping motor, with the whole of the wavelength range being covered in 20 steps. The movement of the filter is controlled by the positive pulse generated by the chopper. With the wideband filter wheel (used for UBVR and H photometry) the filter wheel is rotated in steps of 60°. So a measurement for both star and sky are taken before a new filter position is moved to.

Taylor (1980) has used the same general approach in his repetitive filter cycle photometer built for the Behlen Observatory.

Here the filter wheel is driven directly on the shaft of a stepper motor with the chopper disc mounted on the same shaft. In this way the filter changing motion also accomplishes the chopping (Figure 1.5).

The chopping scheme utilizes a double focal-plane diaphragm with the star in one and the sky in the other. As the chopper wheel and filter wheel turn, the chopper hole and associated filter line up in turn behind each of the two diaphragms.

Two light emitting diodes along with two photo-transistors provide positional information for each of the 16 possible star and sky positions.

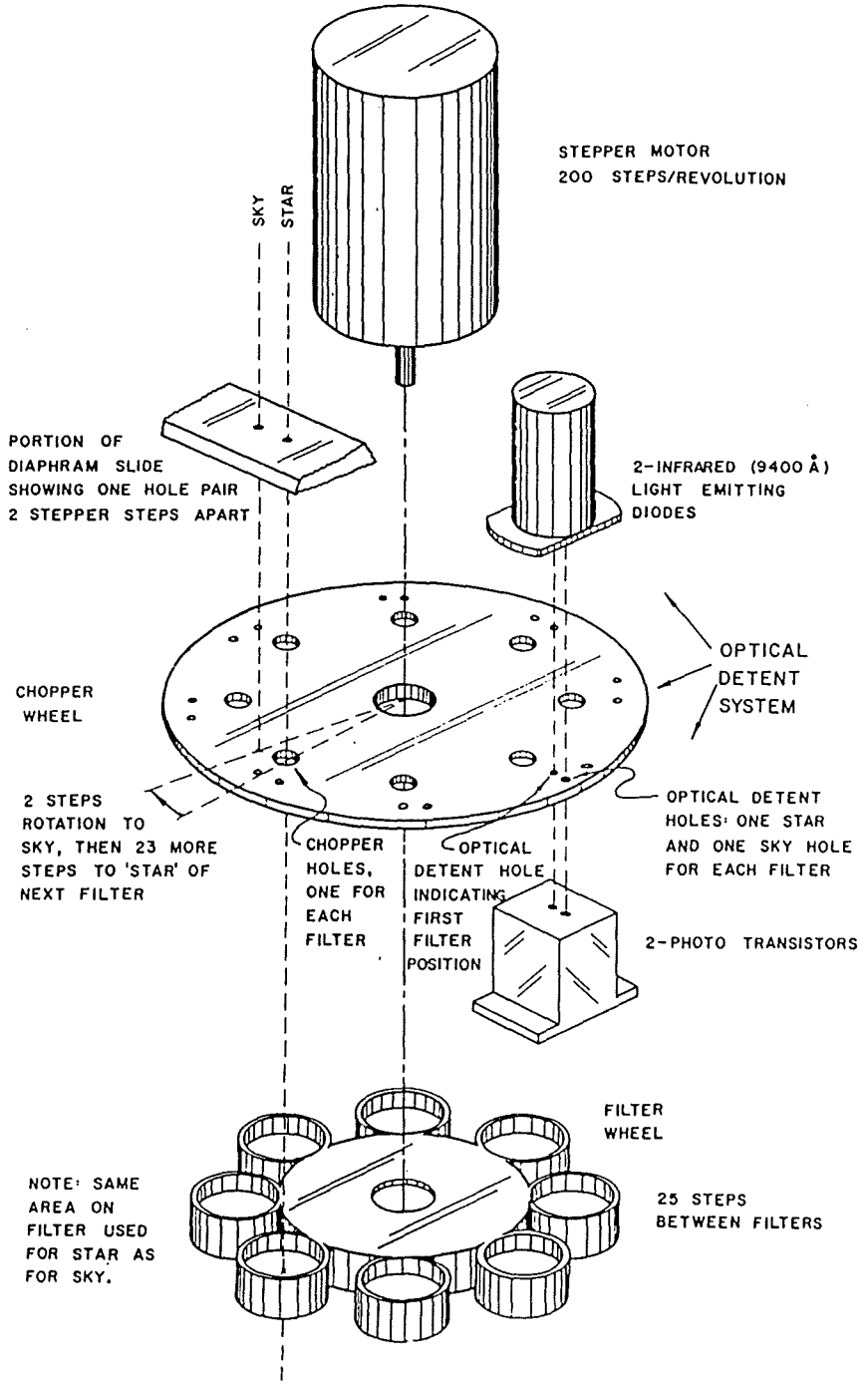

Fig.1.5 A schematical diagram of the dual-diaphragm photometer designed by Taylor.

These last three photometers represent just about as far as one would wish to go, in terms of complexity, to overcome the problem of variable sky transparency, using just a single photomultiplier tube. These systems all try to mimic double beam photometers and it is these that are considered next.

1.11 DUAL-BEAM PHOTOMETERS

Nather and Warner (1971) constructed a photometer with the aim of observing rapid blue variables. The rapid light variation in these objects necessitated that the time scale of the measurements be as low as 1ms. In order to define the character of the variations in as much detail as possible, the photometer was normally operated without filters so that a sufficiently large count rate would be achieved during the short integrations. This along with the fact that very few measurements of comparison stars were made, made the system very susceptible to changes in sky transparency. They suggested the construction of a photometer with a second channel dedicated to monitoring a comparison star, so that measurements of the variable star could be continued uninterrupted.

Warner went on to build a photometer using a second channel (Warner, 1971 and 1972). The main photometer was left unchanged, but a second miniature photometer was attached to the guiding eyepiece. The variable star is set in the main photometer's diaphragm and then the eyepiece of the offset guider is moved until a suitable comparison star is found. A flip mirror diverts the light into the miniature photometer, thus enabling the comparison star to be monitored simultaneously with the variable. Associated with each channel is a 4-position filter wheel, driven by stepping motors, which allow sequential photometry to be performed. Figure 1.6 shows how the

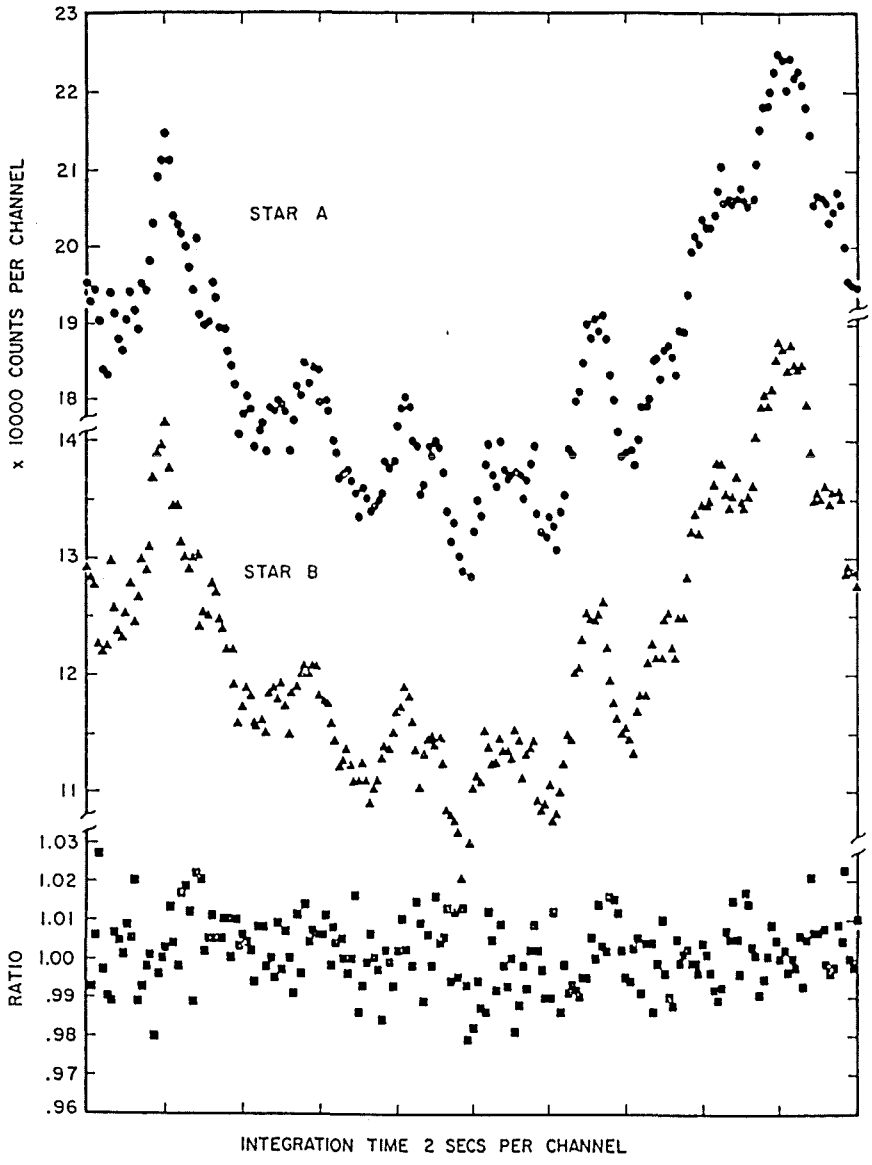

Fig.1.6 An example of the use of the two-channel photometer, designed by Warner, on non-variable stars under cloudy conditions.

instrument performs under poor observing conditions. Both star A and star B were non variable stars, observed on a night with drifting cirro-stratus. In each channel variation of up to 1 magnitude was recorded within very short time intervals. The normalized ratio of the output of the two channels is shown in the lower portion of the diagram. The average magnitude variation is now reduced to about 0.03 magnitudes. So the second channel serves not only as a check on good nights, but makes observing possible through relatively thin clouds.

A similar photometer based on this design was constructed and used by Grauer and Bond (1981). They, like Warner and Nather, made sky readings, on average, only every twenty minutes. It has already been stated that Serkowski has shown that absorption by cloud is essentially neutral. But Warner (1971) pointed out that this assumption breaks down on moonlit, cloudy nights, as clouds are very much better scatterers than absorbers. Therefore the first presence of moonlit clouds causes a large increase in the total brightness, (due to an increased sky brightness), followed by a diminution as the thicker clouds begin to absorb the starlight. If rapid measurements of the sky brightness levels are not taken then the signal ratio method will break down. It was suggested by Grauer and Bond (1981) that a design which rapidly chops between star and sky would eliminate this problem. A far better solution would be to monitor them simultaneously.

Many photometers capable of doing this have been built. Some rely on optical means, such as beam splitters, to direct the incident light into the two separate photomultipliers, whilst others use separate photometer heads mounted on moveable carriages.

In the first category, one of the earliest double beam photometers was designed by Johnson (1958). The optical layout is shown in Figure 1.7. The light from the star and sky passes through identical holes in the diaphragm disc. The beams are then split by an aluminised prism and are directed to the two 1P21 photomultiplier tubes. Johnson claimed that the simultaneous recording of both star and sky improves the accuracy by 20 to 100%, depending on the amount of variation in the sky transparency. On this instrument the 3 colours used had to be measured sequentially. Johnson had originally planned to develop the system into a "sextuple-beam" photometer ie. six photomultipliers, measuring star and sky simultaneously through each of the 3 colours (yellow, blue, and ultraviolet). At the time he felt that the increased sensitivity that would be gained could not justify the threefold increase in complexity and expense. (Such a system was subsequently built by Hiltner, in collaboration with Johnson, and is described elsewhere in this chapter).

Another photometer which typifies this design approach was constructed by Goudis and Meaburn (1973). This has 4 different modes of use derived from two configurations. From the layout shown in Figure 1.8 come three of the modes;

(i) A small central diaphragm is used with a dichroic beamsplitter with reflection and transmission of the same efficiency. This allows simultaneous 2-colour photometry on a single object.

(ii) The beamsplitter used is now a thin sheet of glass, reflecting 8% of the parallel beam onto photomultiplier 2 and the remaining 92% onto photomultiplier 1. The 8% is passed through a broadband filter and the 92% through a narrow filter, centred on a nebular emission line (eg. Hβ or [NII])

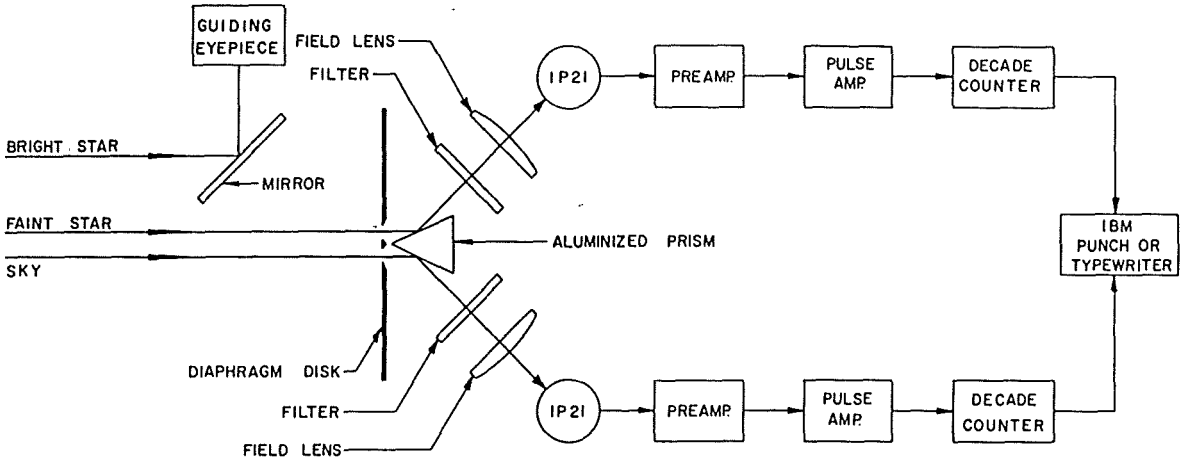

Fig.1.7 A schematical diagram of the two-channel photometer designed by Johnson.

(iii) The beamsplitter from (ii) is replaced by a partially aluminised one, so that two nebular lines could be detected simultaneously. The reflection and transmission of the beamsplitter would be chosen to match the expected brightness ratio of the top line.

Using the arrangement shown in Figure 1.9, a single star and the sky brightness immediately adjacent to it, can be monitored simultaneously, or, two stars within 5' of each other can be observed. To achieve this the beamsplitter is removed and photomultiplier 2 repositioned. A completely aluminised mirror, with a central hole is inserted into the focal plane. A diaphragm with both a central hole and an off-axis hole is placed in the focal plane. Light passing through the central hole is detected by photomultiplier 2. If colour photometry is desired then, once again, this must be performed sequentially.

The second category of double beam devices do not use beam splitters but measure the two sources simultaneously but completely independently. Usually one, if not both, of the photometer heads will be mounted on a movable carriage.

Bernacca (1978) describes the construction of a two channel photometer which typifies the design of this classification. The photometer head consists of a box containing two identical sets of focal plane diaphragms. Two photometers of identical design are mounted on a slide carriage attached to the diaphragm box. Each diaphragm and photometer pair can be moved independently of the other, allowing two separate sources to be centred in the diaphragms. (For sources separated by more than 206'' two aluminised rectangular, fuzed-quartz prisms are used to deflect the beam into the diaphragm).

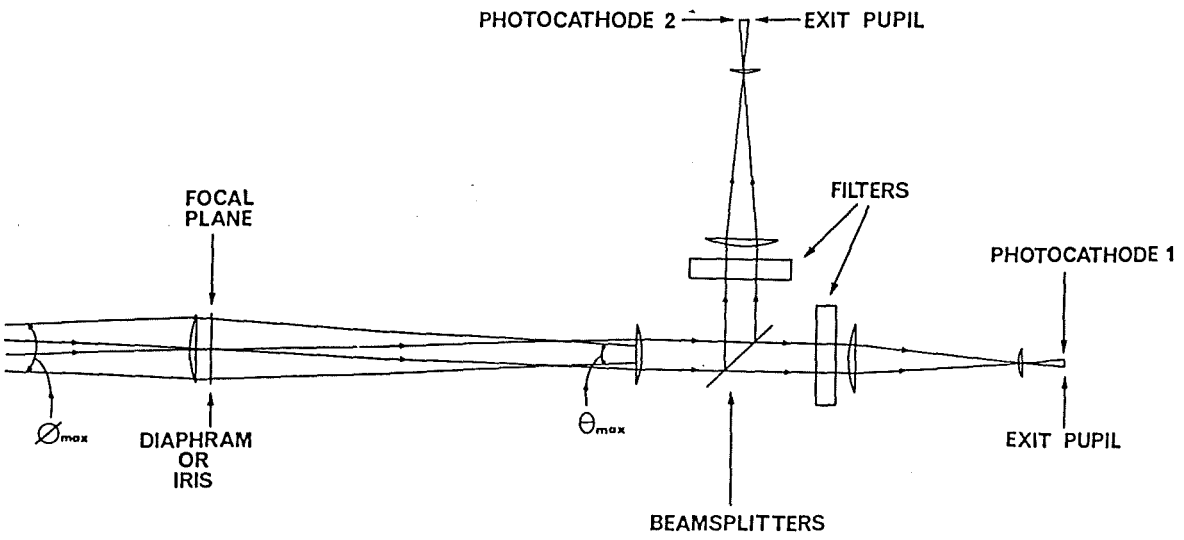

Fig.1.8 Optical layout for mode A of the photometer designed by Goudis and Meaburn.

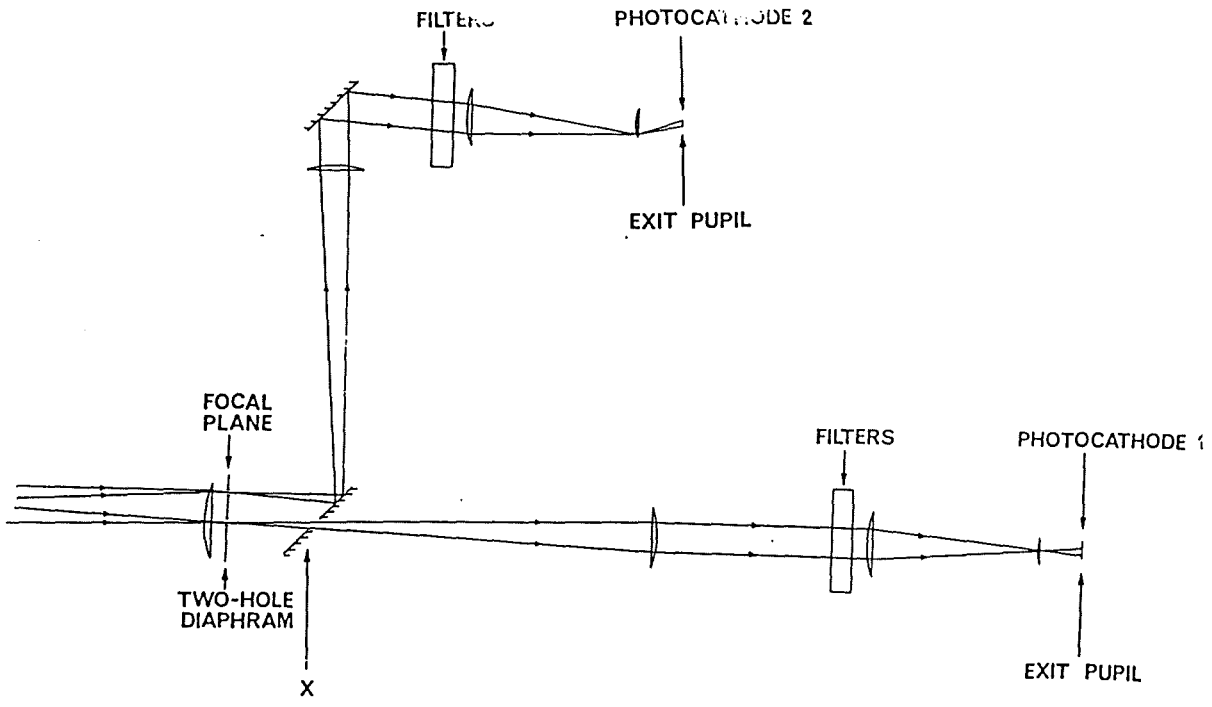

Fig.1.9 Optical layout for mode B of the photometer designed by Goudis and Meaburn.

Each channel has a separate filter wheel associated with it and each channel drives a separate counter.

A similar device has been built by Geyer and Hoffman (1974). The layout is schematically shown in Figure 1.10. Again the two photometers are mounted on moveable carriages, each capable of moving independently, in a direction perpendicular to the optical axis of the telescope. The whole framework is free to rotate around the optical axis. Each photomultiplier box contains its own interchangeable focal-plane diaphragm, Fabry lens and filter wheel, which holds up to 4 filters.

An almost identical design to this has been built by Piccioni (1979) at the Bologna Observatory. Here, the major difference is that pulse counting has been used rather than the DC-integrating method chosen by Geyer and Hoffman.

De Baise (1978) also reports the construction of a photometer similar to that of Geyer and Hoffman. A schematic diagram of the optical parts is shown in Figure 1.11, the other channel being identical to that shown. They claim an improved efficiency and precision over that of Geyer and Hoffman's, largely due the use of pulse counting techniques and the switching time of the "optical multiplexer" ie. filter wheel.

The photometers described in this section have a distinct advantage over those described previously. They all have the ability to measure either object and sky, or object and comparison simultaneously. But none are able to do so whilst measuring in more than one passband at the same time. The next section looks at some of the instruments which have been designed to measure through at least two channels and several wavelengths simultaneously.

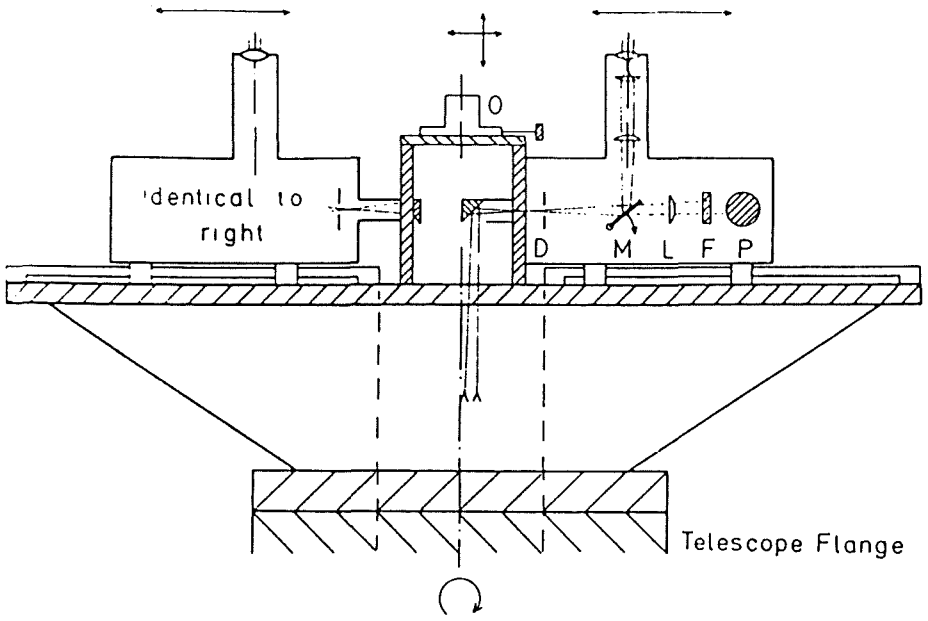

Fig.1.10 A schematical drawing of the photometer designed by Geyer and Hoffman.

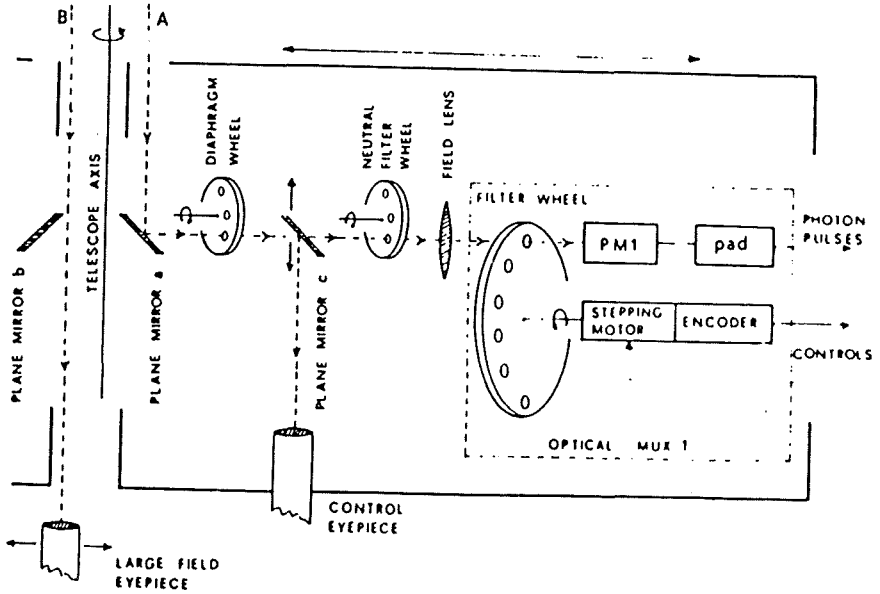

Fig.1.11 A schematical diagram of channel A of the photometer designed by De Baise et al. Channel B is identical to channel A.

1.12 MULTI CHANNEL/BEAM PHOTOMETERS

Following on from Johnson's photometer (Johnson, 1958), Hiltner constructed a six-channel photometer. This possibility had been suggested by Johnson but at the time he was of the opinion that the filters available were not sufficiently well defined. Nevertheless the photometer was constructed a year later. A schematic diagram of the photometer is shown in Figure 1.12.

The first stage is identical to Johnson's in that it splits the light from the two sources (star+sky and sky) using an aluminised prism. A further 4 dichroic filters, 2 to each channel, are used to separate the several filter bands. The filter system used is the UBV system as defined by Johnson and Morgan (1951). It should be noted that the dichroic filters do not have exactly the same spectral pass-band characteristics as the standard UBV filters and so a transformation to the UBV system is necessary. Johnson's earlier reservations about the ultraviolet filters seem to be borne out, since Baum (1959) noted difficulties with the system and did not attempt to use the U channel.

Giovannelli (1980) has used a similar beamsplitting technique to construct a 4 channel photometer. The instrument was designed specifically to observe the optical counterpart of X-ray sources, in particular, phenomena such as bursts or flickering. Since these occur on time-scales comparable with those of atmospheric phenomena (Paerno, 1979) it is advantageous that colour measurements can be made simultaneously, along with the monitoring of a comparison object. Otherwise the effects of sky transparency variation, scintillation and seeing would seriously reduce the reliability of the readings.

The instrument is able to measure the object star in UBV colours simultaneously and a comparison star in B. A schematic of the layout is shown in Figure 1.13.

The mirror M, tilted at 45^{o} with respect to the optical axis of the telescope, has a hole in it which allows the light to reach the Cassegrain focal plane. The prism, P, can be inserted to allow centring of the star in one of the diaphragms, DP. When the prism is removed, the incident beam is split by two partial transmission mirrors, MP, providing 3 beams which are incident upon the 3 photomultipliers, PM1, PM2 and PM3.

The mirror M also provides an auxiliary focal plane, FC, which allows viewing through a large field eyepiece, EC. A comparison star identified in this field can then be centred in a diaphragm, DC, by moving the whole of the auxiliary photometer head. The comparison star is then monitored by the fourth photomultiplier tube, PM4. All of the photomultipliers are used in the photon counting mode.

As a final example of an instrument which utilizes the beamsplitting technique let us consider Tinbergens 12 channel photometer.

The objective in designing the photometer was to produce an instrument that was efficient in its use of available light and also flexible enough to perform photometery of various spectral features. With the additional requirements of measurements of the equivalent widths of stellar absorption lines came the decision to split the channels into pairs to allow "Hβ" photometry with each pair.

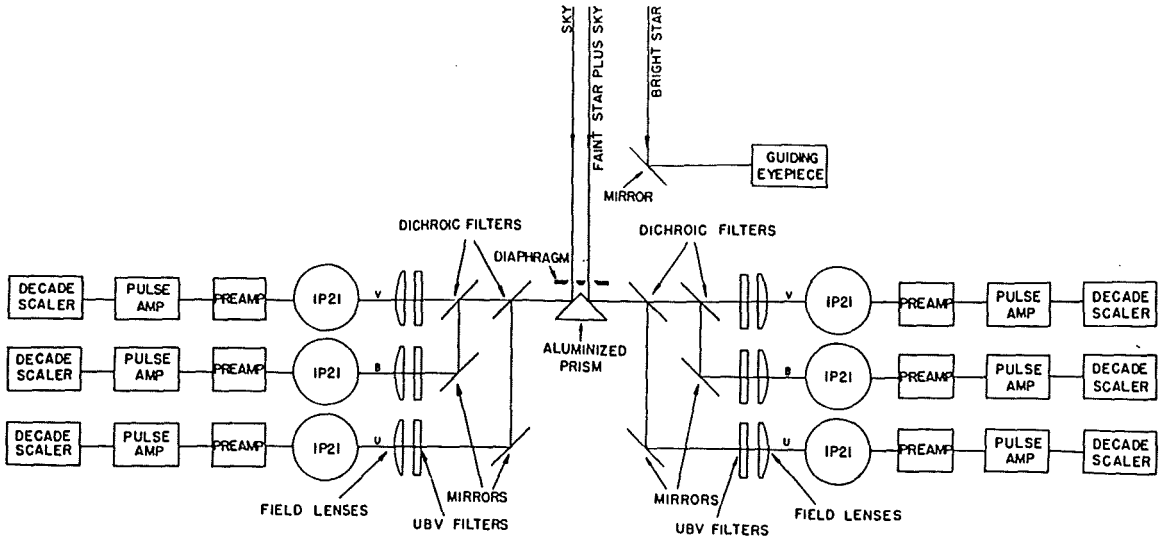

Fig.1.12 A schematical diagram of Hiltner's six-channel photometer.

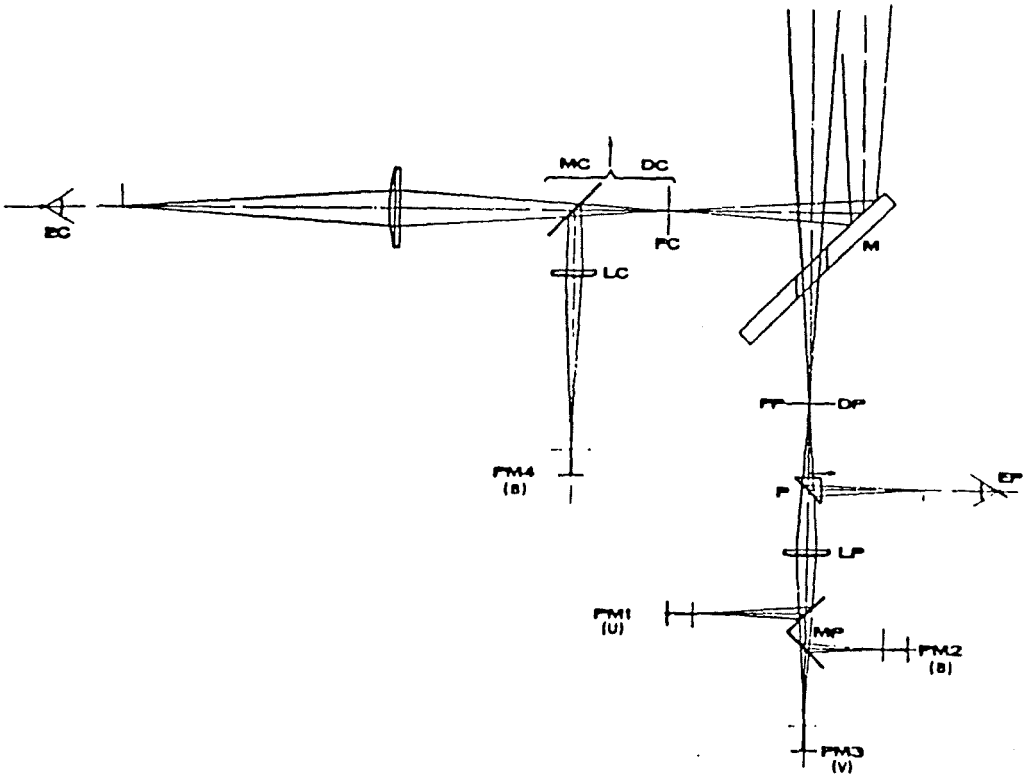

Fig.1.13 Optical diagram of the four-channel photometer designed by Giovannelli et al.

A schematic of the layout, reproduced from the users manual, is shown in Figure 1.14. Light passes through a calibrator (optional) and is focussed in a single diaphragm. (A double diaphragm will eventually be available for sky-chopping). The light then passes through an optional neutral density filter. The beam then proceeds to a collimator with an electro-mechanical shutter situated behind it. Five dichroic beamsplitters are used to produce up to 6 separate beams (3 between 300 and 600 nm and the other 3 between 450 and 900nm). Each of these 6 beams is then subsequently split by a "neutral" beam splitter to produce "Hβ" pairs of beams. These final beams then pass through 3-position filter slides and Fabry lenses before arriving at the photomultiplier tubes.

Since dichroic beamsplitters are wavelength-dependent polarisers the incoming light was depolarised to avoid photometric errors occurring with polarised objects. A time averaging polariser, consisting of a rotating achromatic halfwave plate was used. This led to the decision to include an optional polariser, so that linear polarimetry could be done using half of the light.

Whilst this instrument allows for (potentially) two objects to be monitored simultaneously in up to 12 channels there are, as is inevitable with such a complex design, certain difficulties.

For example, in deciding that the dynamic range should extend from very faint to very bright stars, a wide range of neutral density filters have been included. Unfortunately these filters are not neutral enough to allow UBV or similar broad-band photometry to be feasible. Also the high count of optical components leads to a loss of efficiency.

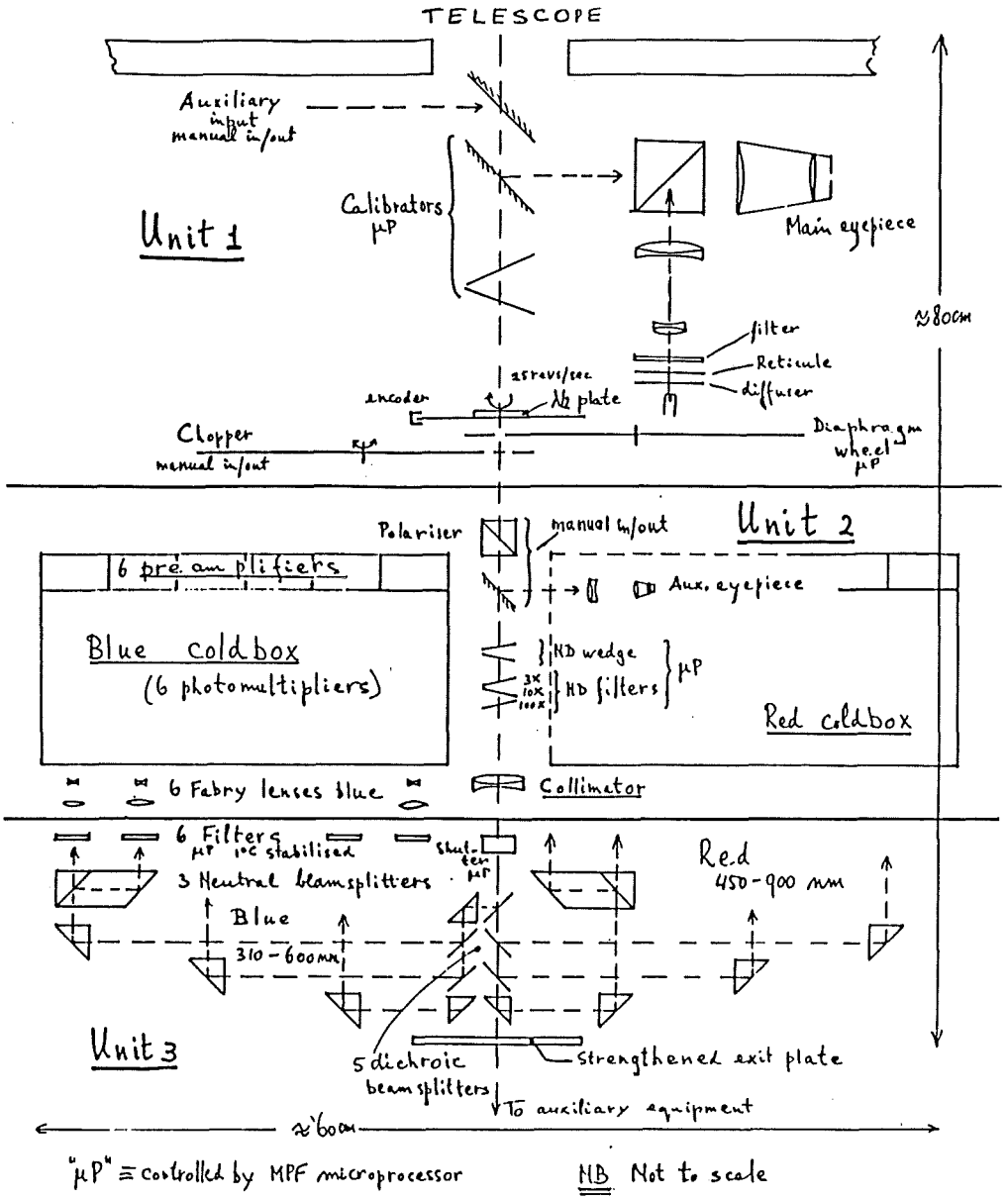

Fig.1.14 A schematical diagram of the multi-purpose photometer (MPF) designed by Tinbergen.

A more efficient approach than using a beam splitter is to have multiple photometer units mounted on an X-Y carriage. This is basically the same design as used by De Baise, Piccioni etc. described earlier.

E.N.Walker (1984) has constructed such a device using fibre optics.

Four X-Y arms are provided, one for each side of a square. At their innermost ends they are provided with an aperture to be centred upon each area of the sky plus star. Underneath each aperture is a Fabry lens/prism assembly. This deflects the light path through 90° so that the light is directed towards the outer end of each arm. A 1.7mm image of the primary mirror is produced on the end of a fibre optic bundle. The stars are centred in their apertures by moving each lens/prism/fibre bundle outwards and using a travelling microscope mounted on X-Y slides positioned above those which carry the arms.

The 4 incoming fibre bundles then enter a chopper unit. Each bundle has an active area of 2mm and the emergent light has an angle of approximately one radian. Each diverging cone of light is collected by a 3mm diameter fibre bundle which is one arm of a 4-into-1 fibre optic integrator, which has a common 6mm diameter output. There is a 1mm gap between the 2mm diameter input and the 3mm diameter collector and it is in this gap that the chopper is situated. The chopper is a rotating disc with an 85° cut out slot. The speed of rotation is 25 revolutions each second.

Light emerging from the 6mm diameter common end is scrambled using a Fabry lens before striking the photocathode of the single EMI 9863/350QB photomultiplier. A filter wheel with 6 filters is situated adjacent to the Fabry lens.

This system can not really claim simultaneity for any of its measurements, though it does offer an improvement over the earlier chopping devices mentioned by being able to sample either 4 stars, or 3 stars plus sky, in rapid succession.

However, Caton and Pollock (1986) have built a device, using stepper motor controlled X-Y stages, which allows for up to 4 objects to be monitored simultaneously.

The instrument is coupled to the telescope through a rotational stage, driven by a stepper motor, to allow for optimization of alignment within a given stellar field.

Directly beneath the rotating coupling is an upper plate which carries the full-field filter wheel. Each of the 4 stepper motor driven X-Y stages is mounted on another plate beneath the filter wheel. Each X-Y stage carries a detector which nominally serves one quadrant of the field of view, though any of the detectors is capable of reaching any point in the 30 arc-minute focal plane.

The light from the four beams is brought to the detectors using 1mm diameter, solid, fused silica optical fibres. The fibres are used as Fabry lenses relying on them to randomize the star/sky image before it reaches the detectors. The 1mm bundle provides a 24 arc-second aperture.

Viewing is provided by a set of 4 coherent fibre bundles attached at a specific offset from the fibres leading to the photomultipliers. A computer is used to reposition the fibres after acquisition.

An alternative approach that enables simultaneous colour measurements, is to use a dispersing element and then isolate various spectral regions. An instrument of this nature is described by Walraven and Walraven (1960).

In designing the instrument they realised that the greatest difficulty they would have to overcome would be that of the stability of the spectrum. Unlike a spectrograph, a slit can not be used to stabilize the position of the light source as the amount of light cut out of the moving stellar image would be large. Also, even at small zenith distances, the image of the star is no longer achromatic, due to atmospheric dispersion, which would result in serious errors in the observed colours. So a sufficiently wide diaphragm, as used in classical photoelectric photometry, must be used and consequently the spectrum produced will be moving erratically to and fro.

To overcome this problem, a very large dispersion would be required, in order to reduce the effects of the erratic motion. A sufficiently large dispersion could be provided by a flint-glass prism or a diffraction grating. A flint-glass prism, though, would make observations in the ultraviolet region of the spectrum impossible and it was felt that a grating would make simultaneous observations of widely separated spectral regions impractical, as the light would be concentrated in a relatively small space.

But producing the spectrum by means of 2 prisms and lenses of fused quartz, as done in a spectrograph, would not allow the spectral regions to be isolated using geometrical cutting of the spectrum, as the stellar image could not be kept stable enough in the aperture to ensure sufficient stability of the resulting spectrum.

The solution found is shown in Figure 1.15. The Iceland Spar divider separates the incoming beam into 2 separate beams. The roof shaped prism restores their parallelism and they then pass through 2 equally thick adjacent slabs of crystal quartz. The pieces of quartz rotate the planes of polarization for one beam in a clockwise direction and for the other anti-clockwise, the amount of rotation varying on the wavelength of the light and on the thickness of the quartz.

Since the amount of rotation for both beams is equal, but in opposite sense, then for a certain wavelength the plane of polarization will become equal to 0^{o}, that is, parallel to the plane of symmetry of the spectrum analyser. At another wavelength the beams will be polarised in a plane perpendicular to the plane of symmetry.

The light then passes through another double-refracting prism of Iceland Spar, which splits the beams into a part polarised parallel to the plane of symmetry and one perpendicular. One beam contains light only of certain wavelengths with the other wavelengths present in the other beam. Only the light polarised parallel to the plane of symmetry is directed towards the spectrum analyser. Thus a spectrum is formed which consists of bright and dark bands.

If the condenser lenses, which are used to concentrate the different bright regions onto the respective photocells, have their edges placed into the dark intervals, a large displacement of the spectrum can be tolerated before the total amount of light received by each lens is appreciably affected.

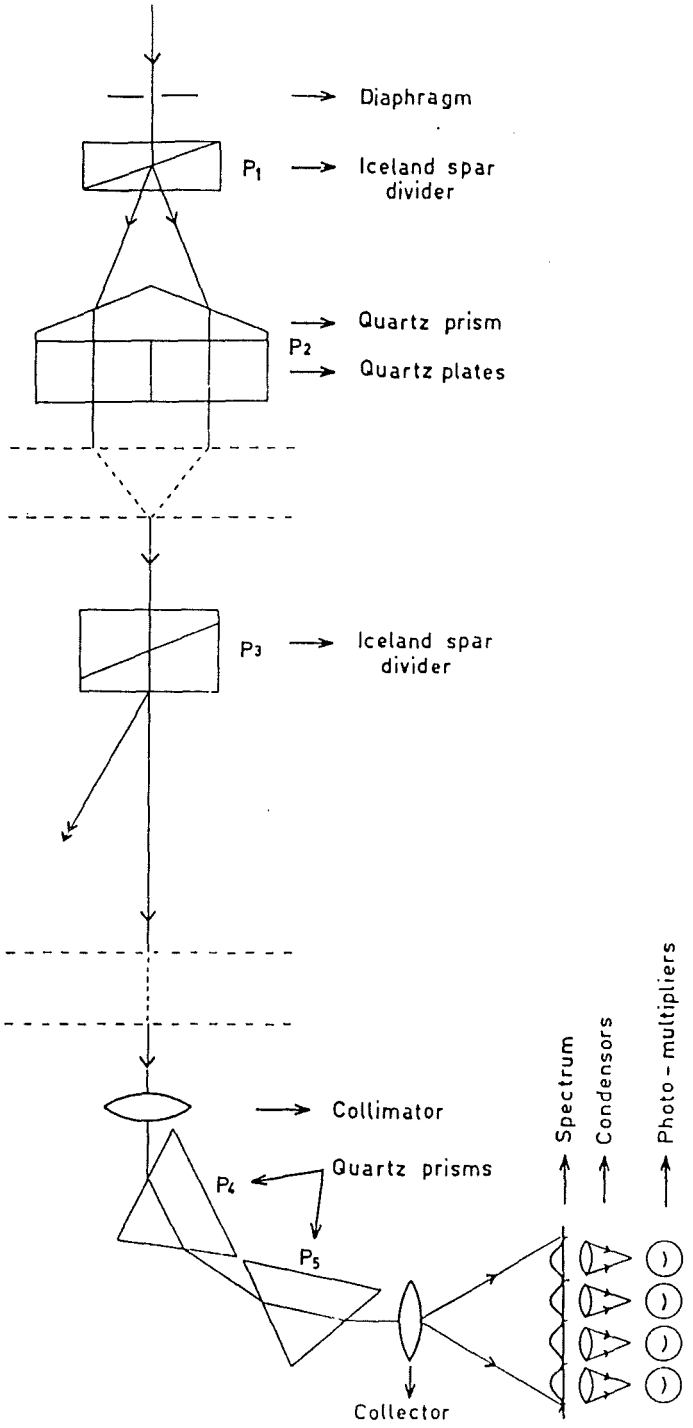

Fig.1.15 A schematic diagram of Walraven's five-colour photometer.

This method of stabilizing the wavelength region does however restrict the choice of the positioning of the regions. By varying the thickness of the quartz plates the bright regions in the spectrum can be shifted to other wavelengths, but they will still be regularly spaced. Walraven built the instrument specifically to carry out a programme of observations to attempt to classify O- and B-type stars according to luminosity and spectral type. Consequently spectral regions were chosen that would provide colour parameters best suited to this task. The transmission curves of the photometer are as shown in Figure 1.16 with the Johnson and Morgan UBV standards shown for reference.

G.A.Walker (1970) also reports the construction of a multichannel photometer designed to isolate specific spectral regions. This instrument differs from that of Walraven's in that it uses a diffraction grating as its dispersive element. Windows in the curved focal surface of the camera are used to isolate the chosen spectral regions. An additional two regions are isolated by using a mask which covers up half of each of the long wavelength windows for alternate observations.

As with Walraven's photometer, the normal spectrograph slit is replaced with an entrance diaphragm. To avoid shifting of the spectrum, due to movement of the image in the stellar aperture, a grating with a large number of line/mm (1200) is used, thus reducing any shift to a few percent, even for the smallest window (15nm). A total of 4 photomultipliers are used. Figure 1.17 shows the position of the spectral regions defined by the photometer in comparison with other photometric systems.

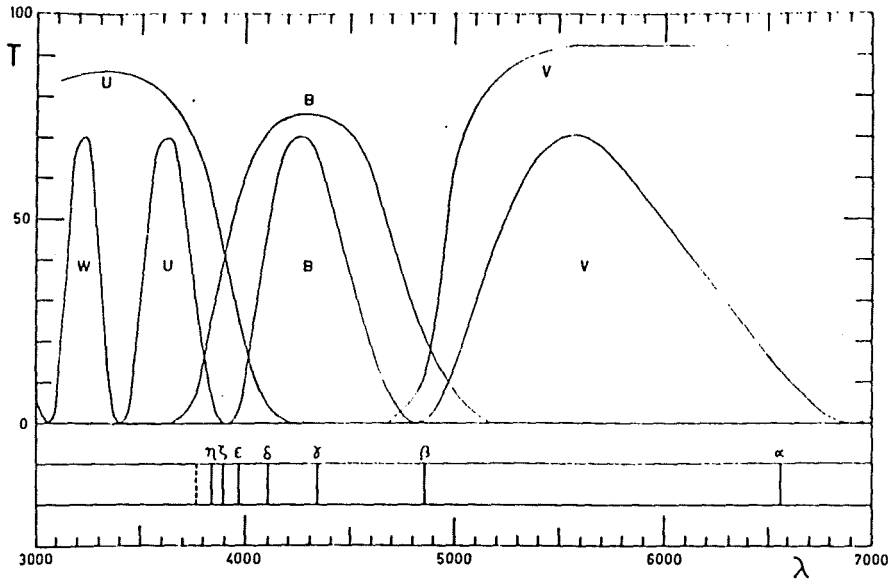

Fig.1.16 Transmission curves of Walraven's photometer. For comparison the transmission curves as used in the UBV system are also included.

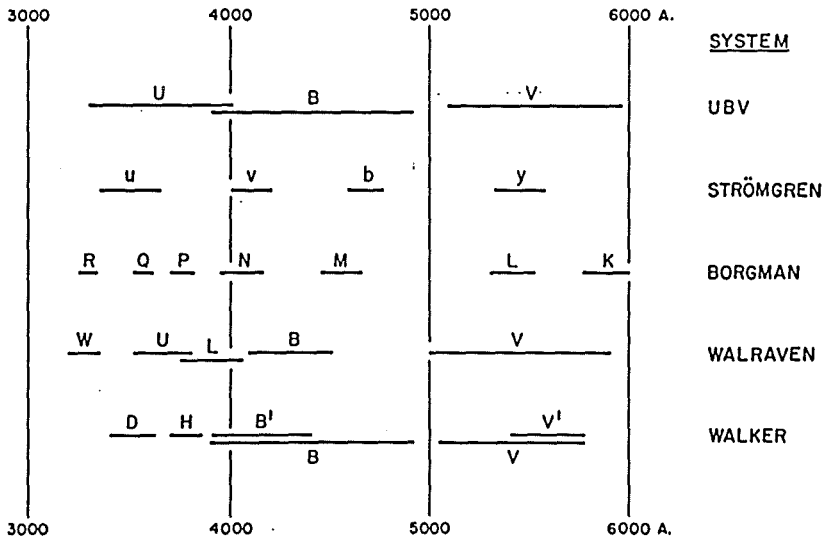

Fig.1.17 Comparison of the passbands defined by Walker's photometer, shown at the bottom, with other multi-colour systems.

Nielsen (1983), in conjunction with Strömgren, has developed a 4 channel photometer for use in the uvby system, as well as for Hβ photometry. It is based on existing 4 channel photometers which have been built in Denmark (see eg. Grønbech, 1976). Again, it uses a high dispersion grating (1200 lines/mm). The spectrum is formed on a curved surface on which exit slots are used to select the spectral bands. (Two sets of slots are available, one for use with optical filters and one which defines the spectral bands itself). A combination of spherical mirrors and Fabry lenses are then used to image the light spot from the grating onto the 4 photomultipliers. For Hβ photometry a beamsplitter is inserted, which gives a split of approximately 85/15%. The photometer can be operated in either uvby or Hβ mode.

All of these instruments allow simultaneous multicolour photometry to be carried out, but only on a single object.

Whilst this makes more efficient use of the telescope time, it would be advantageous if we could combine the above facility with that of the double/multibeam photometers, ie. observe more than one object in several colours simultaneously.

Barwig and Schoembs (1984, 1986 and 1987) have developed such a system. The instrument has been developed over a number of years and can now measure 3 separate objects in 5 different colours simultaneously. To do so it combines several of the techniques which have been described previously.

A schematic diagram is shown in Figure 1.18. Light from 3 sources in the focal plane of the telescope is guided through optical fibres to 3 separate, but identical, spectrographs. A bundle of quartz and plastic fibres split the resulting spectrum into 5 colours (the

passbands are based on the Kron-Cousins UVBRI system). The resulting 15 optical fibre outputs are linked to 15 photomultipliers. The relative transmission curves of the colour bands are shown in Figure 1.19.

The benefits that are gained from an instrument such as this are obvious, the most immediate being the greatly increased efficiency over classical photometers due to the simultaneous data acquisition. As with the double/multiple beam, and to a lesser extent the chopping photometers, useful data can be acquired even if the stability of the atmospheric transparency is marginal. This gives a considerable gain in usable photometric time. It is also possible to measure the colours of rapidly varying objects and with the simultaneous monitoring of a second (non-varying) object verify the validity of the data.

1.13 THE ST.ANDREWS - D.A.O. 8-CHANNEL PHOTOMETER

In the remainder of this thesis the construction and commissioning of an 8-channel photometer is described. The instrument was designed by Graham Hill and associates at the Dominion Astrophysical Observatory, Canada. A schematic layout of the photometer is show in Figure 1.20.

The photometer uses a dispersive element to produce a spectrum on a mosaic of mirrors. These mirrors then reflect segments of the spectrum onto 8 photomultipliers. Filters, in front of the photomultipliers, are used to define the pass bands. Two diaphragms are placed in the telescope's focal plane and a chopping device allows for rapid alternations between star+sky and sky.

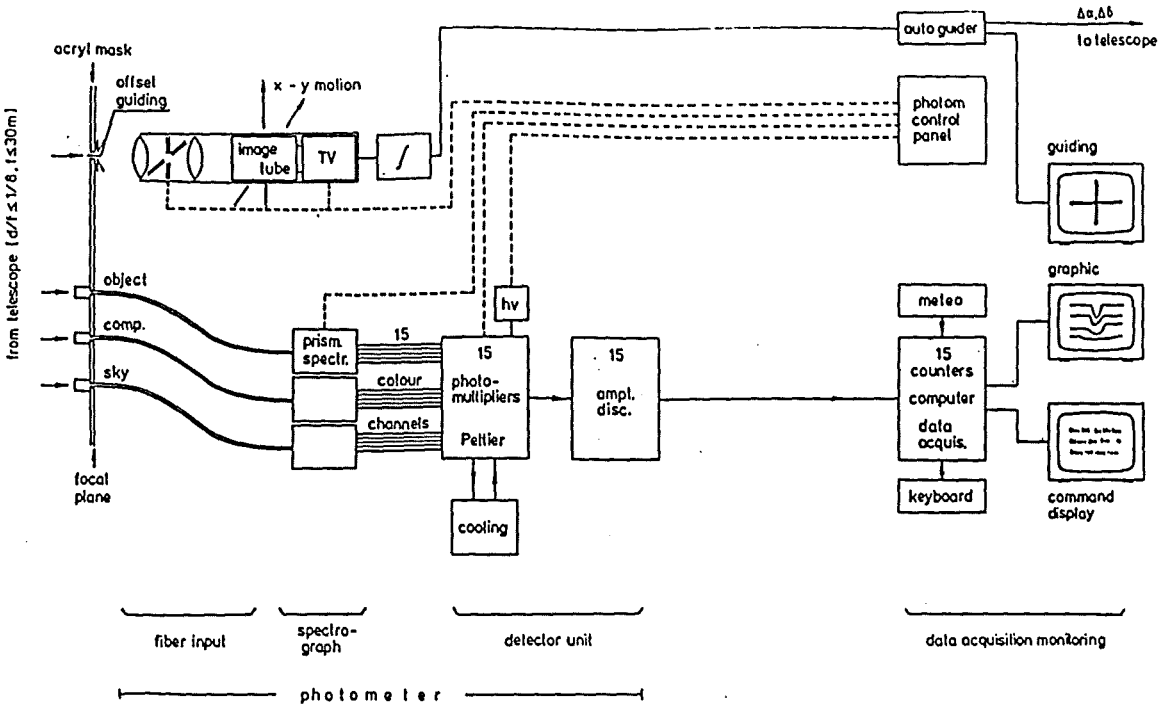

Fig.1.18 A block diagram of the three-channel, five-colour photometer designed by Barwig and Schoembs.

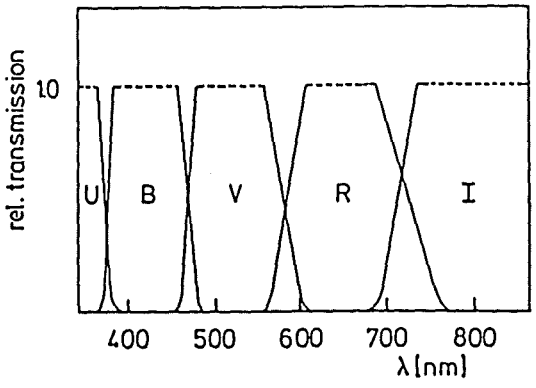

Fig.1.19 Relative transmission curves of the colour channels for Barwigs multi-colour photometer.

The primary advantages of the photometer are obvious. Simultaneous measurements can be made in all 8-channels, which is far more efficient than using, for example, a rotating filter wheel. The chopping action between star and sky, which results in only a 12% loss of observing time, gives the advantages of dual-beam photometers described earlier. Further, the use of a grating to "split" the light is far less wasteful than using beamsplitters.

Secondary advantages include more productive use of the available observing time and the ability to acquire useful data on nights of marginal photometric quality.

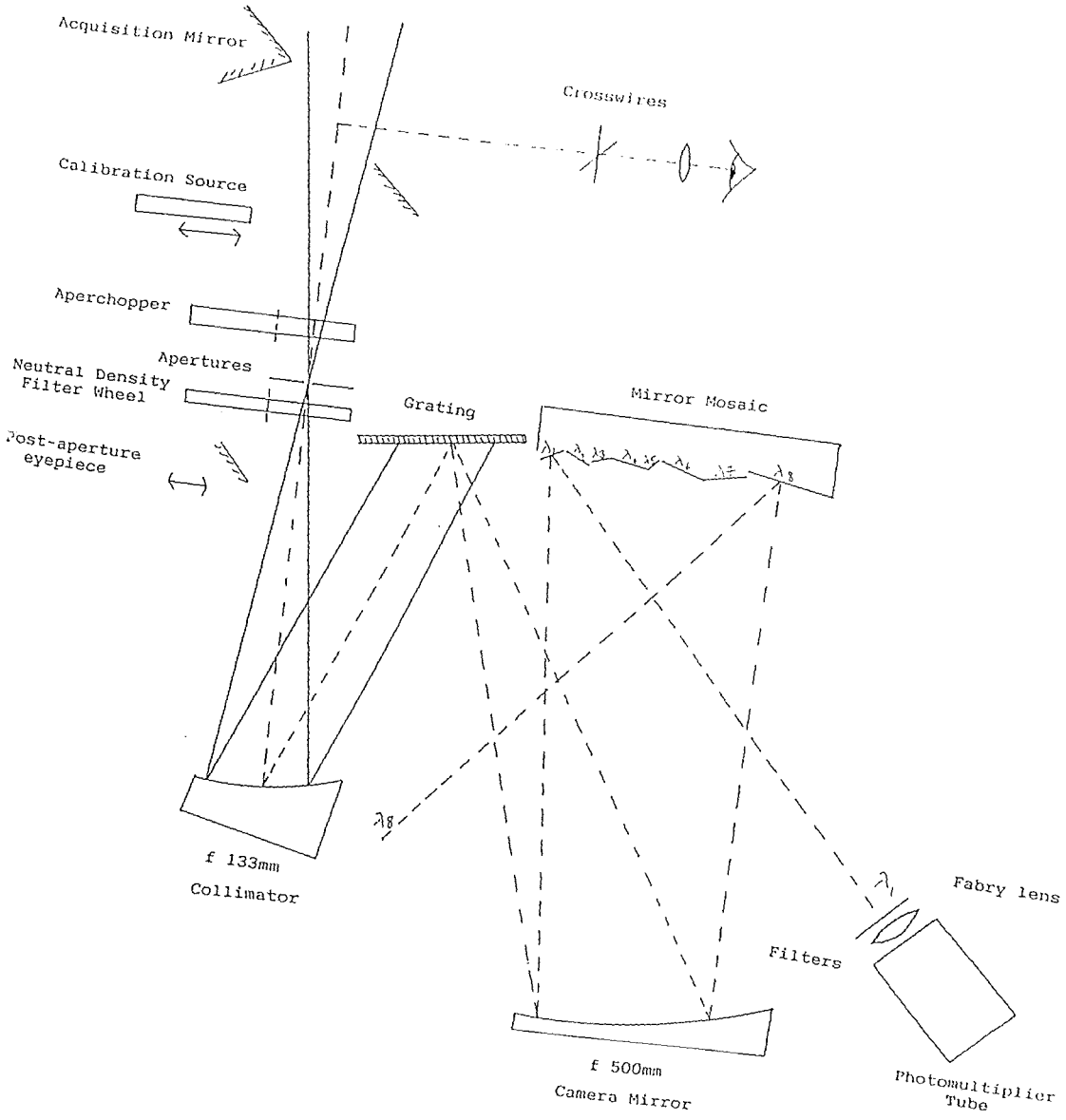

Fig.1.20 Schematic layout of the St.Andrews - D.A.O. 8-Channel photometer

CHAPTER 2

OPTICAL AND MECHANICAL LAYOUT

2.1 INTRODUCTION

The photometer is mounted at the Cassegrain focus of the James Gregory telescope, (Figure 2.1). Optical coupling between the telescope and photometer is achieved using a Canon f/1.8, 85mm lens which converts the telescope's f/3 beam to approximately f/8. The f/8 focus coincides with an aperture slide which contains 3 matched pairs of apertures of different diameters.

Situated directly above this aperture slide is a rotating chopper wheel, which alternately masks and unmasks the apertures. Normally a star is centred into one aperture whilst the other views the sky.

The beam proceeds through a neutral density filter wheel to the collimator, which directs the radiation onto a reflection grating.

The radiation dispersed by the grating is focused by a spherical mirror to form a spectrum on a mosaic of 8 mirrors. Each of the 8 beams reflected by the mirrors pass through 4-position filter slides and Fabry lenses before striking the photocathodes.

Pulse amplifiers, discriminators, up/down counters, integration timer and a BBC microcomputer complete the measurement system.

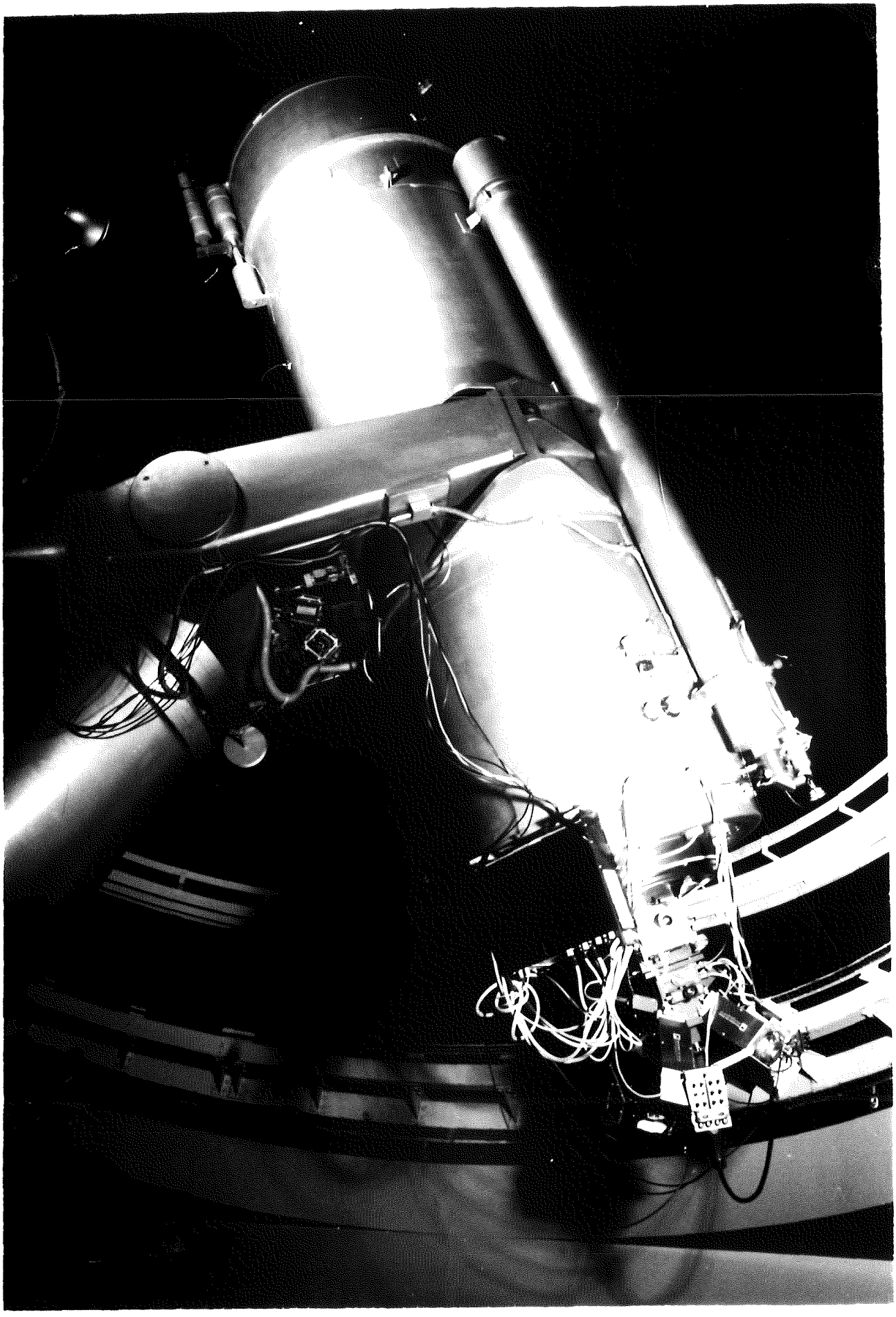

Figure 2.1

James Gregory telescope with St. Andrews - DAO 8-channel photometer.

2.2 OPTICAL DETAILS

2.2.1 James Gregory Telescope

The photometer is currently mounted on the James Gregory telescope. Built on a Cassegrain-Schmidt design, the telescope has a 0.9m spherical primary and a 0.45m spherical secondary. The effective focal length of the telescope is 2572mm (Lloyd Evans, 1967).

Under perfect observing conditions, the best attainable image diameter for a point source is about 3 arcseconds (Van Breda, 1970). For typical conditions at St.Andrews this is increased to about 4 arcseconds.

2.2.2 Optical Coupling

The photometer has been designed to work with input beams of f/3.8, f/8.0, f/13.5 and f/18.25 by choice of appropriate collimator mirrors. The James Gregory telescope has an output beam of approximately f/3.

For the purpose of commissioning the instrument it was felt that a single relay lens system would be sufficient as an optical coupling device. A Canon 85mm, f/1.8 lens has been selected. Since the lens is enclosed by the acquisition head plate, it would not have been possible to alter the focus of the telescope manually whilst observing. To overcome this difficulty a small d.c. motor coupled by a belt drive to the focussing collar of the lens is used to change the focus of the lens remotely, see Figure 2.2. The motor has a variable speed control adjustment, (Wireless World, 1972).

2.2.3 Acquisition Mirror

The acquisition mirror consists of a round optical mirror, 35mm in

diameter, located in a stainless steel cell attached to a movable cross beam,(Figure 2.3). The mirror is held in the cell using silicone rubber adhesive. The mirror can be swung into the main optical beam to divert the image to an acquisition eyepiece after a 45^{o} reflection.

2.2.4 Acquisition Eyepiece

The acquisition eyepiece, Figure 2.4, provides a means of viewing the main telescope image via the acquisition mirror with crosswires superimposed (see sec.2.3.1). The field of view is approximately 25 minutes of arc. Illumination of the crosswires is provided by a small, red, l.e.d., whose intensity can be varied. The crosswires are set such that when an object is intersected by them , then it will be centred in one of the selected aperture pairs. Each of the orthogonal wires can be moved across the field. The side illumination is reflected by the wire surfaces creating bright crosswires on a dark field.

2.2.5 Aperture Slide

The aperture slide is a mechanical construction and is described in section 2.3.5.

2.2.6 Neutral Density Filter

Three neutral density filters are available. They are constructed of evaporated metal, possibly nichrome, onto glass, with a diameter of 13mm. Silicone rubber is used to cement them into their holders.

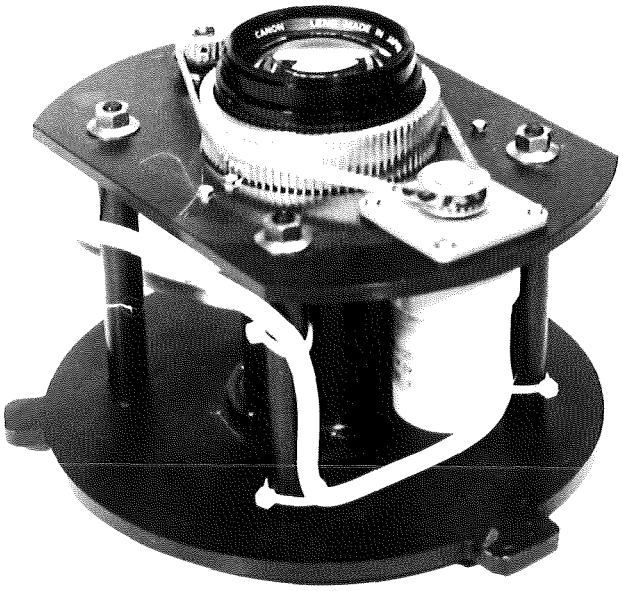

Figure 2.2 Optical coupling with remote focussing.

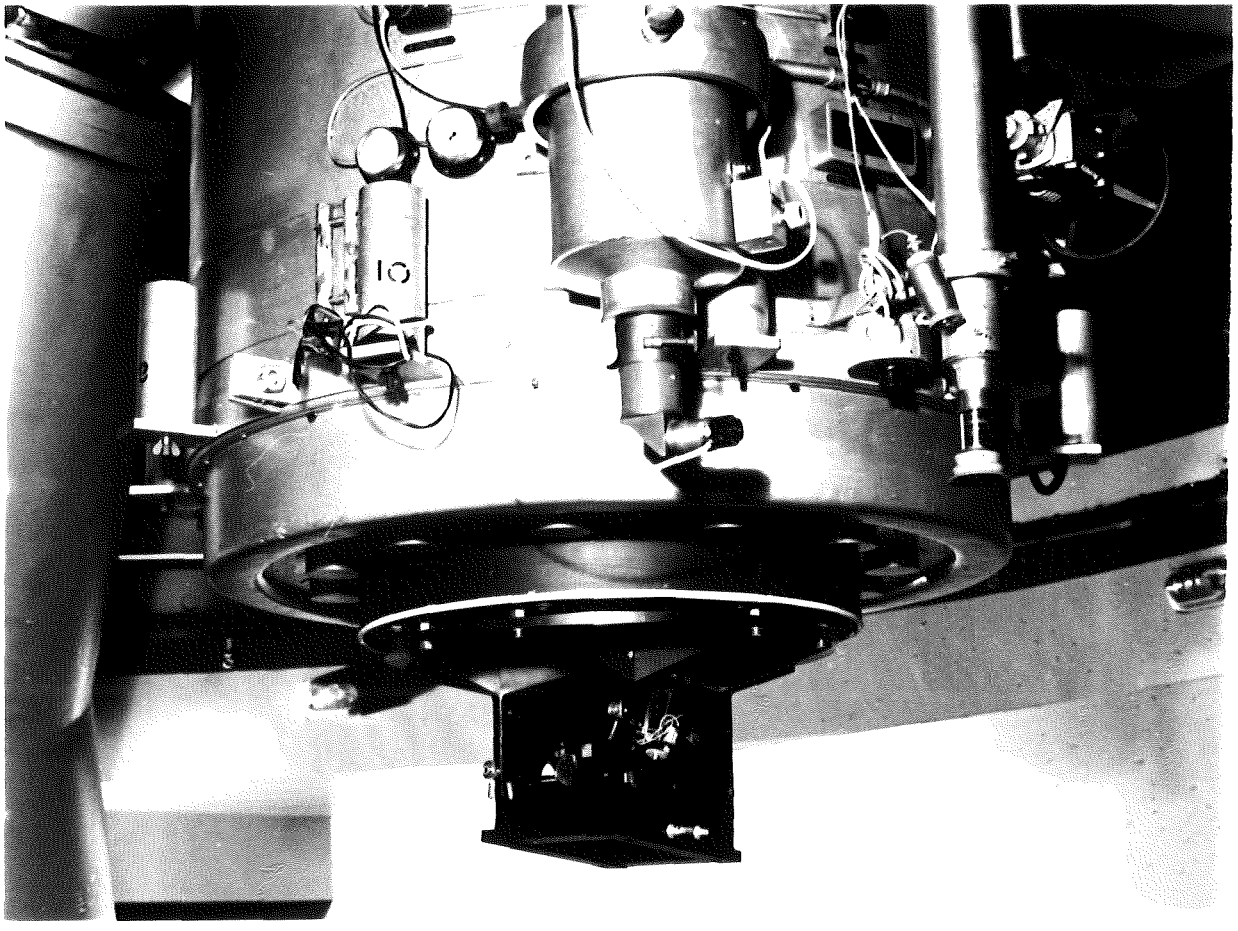

Figure 2.3 Acquisition mirror mounted in acquisition head.

Nominally, they are of 0.4, 1.0 and 2.0 density. However the scans taken using a spectrophotometer show them to have values of 0.48, 1.10 and 1.86. (See Ch.5, Figure 5.29).

2.2.7 Post-aperture Eyepiece

The post aperture eyepiece consists of a simple eyepiece which allows the observer to view the chosen aperture pair via reflection from a small mirror, which is introduced into the optical path as described in section 2.3.8.

The apertures are illuminated by a small, red, l.e.d., the intensity of which can be varied. In this case the l.e.d. brightens the whole field so that the aperture sizes and locations are readily discerned.

2.2.8 Collimator

The collimator consists of a parabolic mirror with a focal length of 133mm and aperture 40mm by 40mm. The centre of the mirror surface is 38mm off the axis of the parabola defining the mirror surface. The two entrance apertures lie at its focus. The reflected light is directed centrally onto the reflection grating.

The mirror rests in pads of PTFE in its cell and nylon strips hold the mirror in contact with the pads.

2.2.9 Grating

The grating, which measures 59x59mm, is held in a grating cell as shown in Figure 2.14. It is held secure on 3 PTFE circular pads which have an adhesive backing.

The grating pitch is 300 lines/mm and the blaze angle is 3° 38' which in a Littrow configuration corresponds to a blaze wavelength of 420 nm.

2.2.10 Camera Mirror

The camera mirror (135x44mm) is a spherical mirror of radius 1000mm. It focusses the diffracted radiation from the grating to form a spectrum on the mirror mosaic.

It rests in its cell using pads of PTFE, as for the other optics.

2.2.11 Mirror Mosaic

The mirror consists of a stack of eight mirrors, lying in the focal plane of the camera mirror. As can be seen from Figure 2.5, the mirrors are at such an angle that reflection takes place not only along the direction of dispersion, but also some 30 - 40° relative to the dispersion plane. The reflection is either to the left or to the right depending on the particular channel.

The lengths of the mirrors are chosen to match the photometric system being used and the centre of the mirror surfaces are designed to follow the spherical focal plane of the camera mirror. (Each system will require a different set of mirrors). The mirrors are clamped into the cell after their angles have been adjusted by the use of shims if necessary. The cell is then adjusted in the slide so that all the principle rays strike their photocathodes. The cell-slide pair then remain together for all time. The cell-slide pair fit into a gib which is bolted to the photometer case. A detent on each slide is adjusted for correctness and repeatability of the linear position of the mirror mosaic.

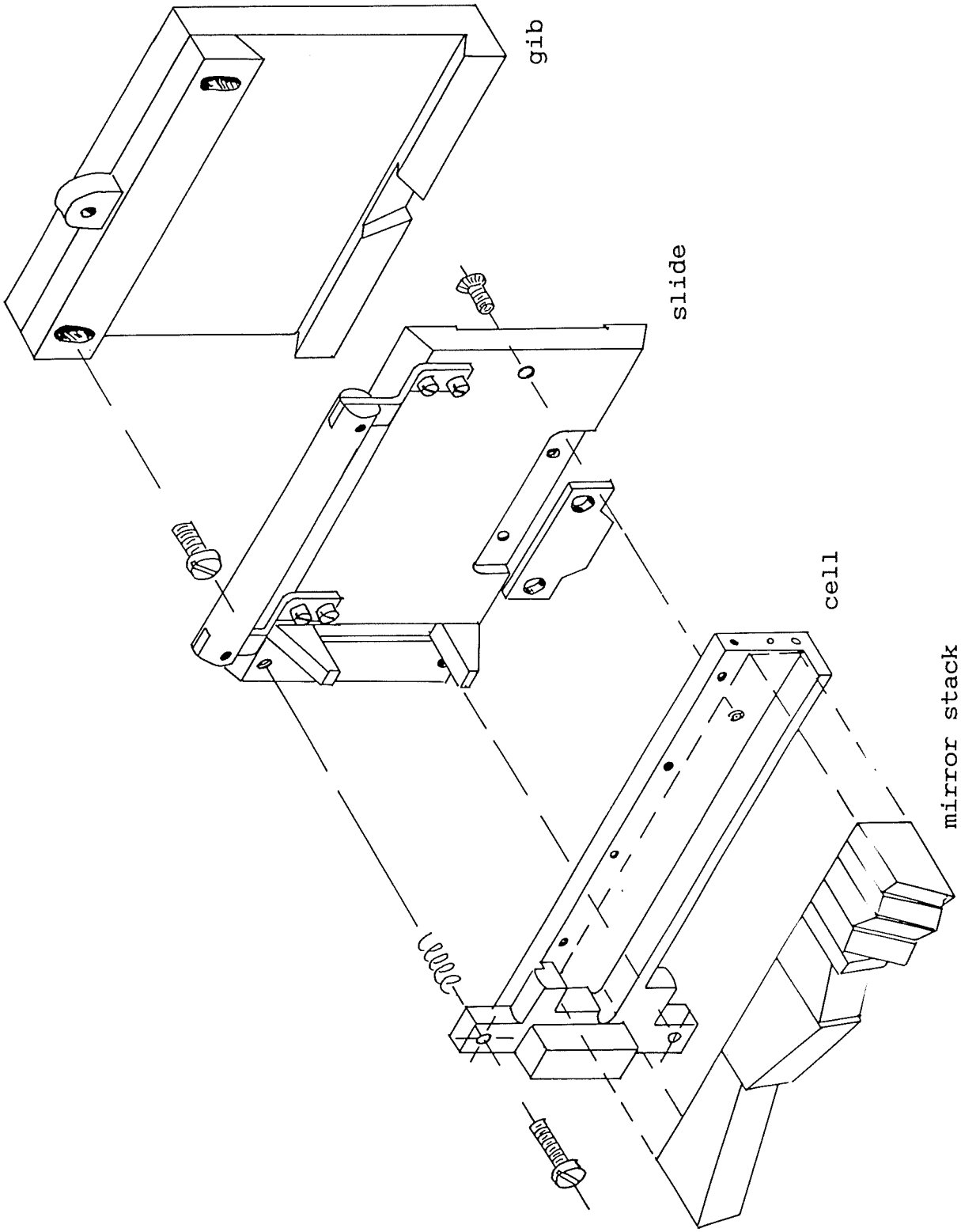

Fig.2.5 Mirror mosaic assembly.

2.2.12 Photomultiplier Filters

The photomultiplier filter units hold the filters which define the photometric bandpasses. The filters are held in position by two sprung-steel clamps. Each unit can carry up to three filters which can be interchanged automatically and one manually operated filter.

2.2.13 Window Heaters

The window heaters, constructed in-house, consist of a heating element placed within the threaded lock rings which are used to hold the Fabry lenses. Their purpose is to supply a small amount of heat energy into the immediate vicinity of the Fabry lenses to prevent them from dewing over when the photomultiplier coolers are in operation.

The heating element consist of 12, 1 Ohm resistors placed in series around the ring as shown in Figure 2.6. The resistors, rated at 0.5Watt, will dissipate 3Watt for a supply voltage of 6V. (The element capacity is 6W).

2.2.14 Fabry Lenses

The Fabry lenses are mounted in the cold boxes directly in front of the photomultiplier tubes. They are held secure by the window heater rings. Their purpose is to focus an image of the telescope's objective, illuminated by the light of the star, onto the photocathode.

All the Fabry lenses are identical in design other than the coatings, which differ for each channel. The space between the two optical elements which form the lens is hermetically sealed, so as to prevent a build up of internal condensation when the photomultiplier

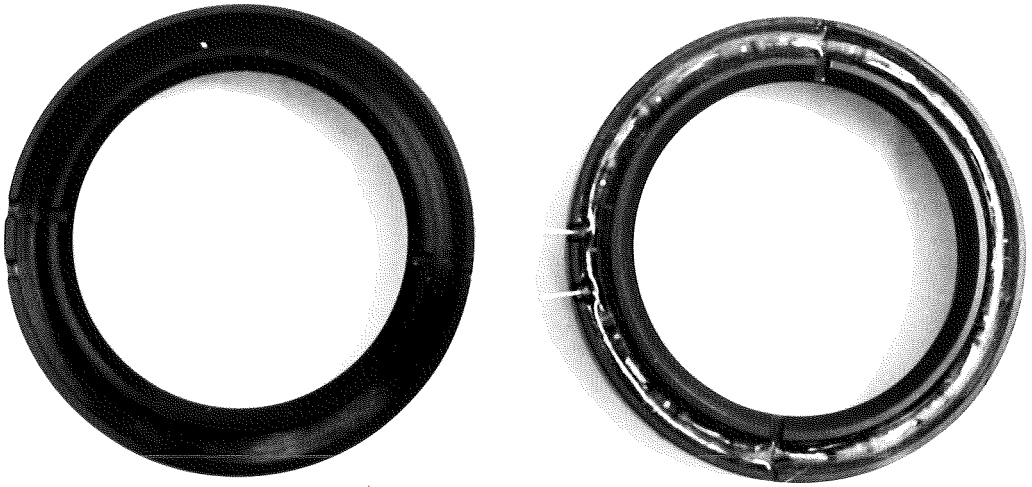

Figure 2.6 No-dew heater.

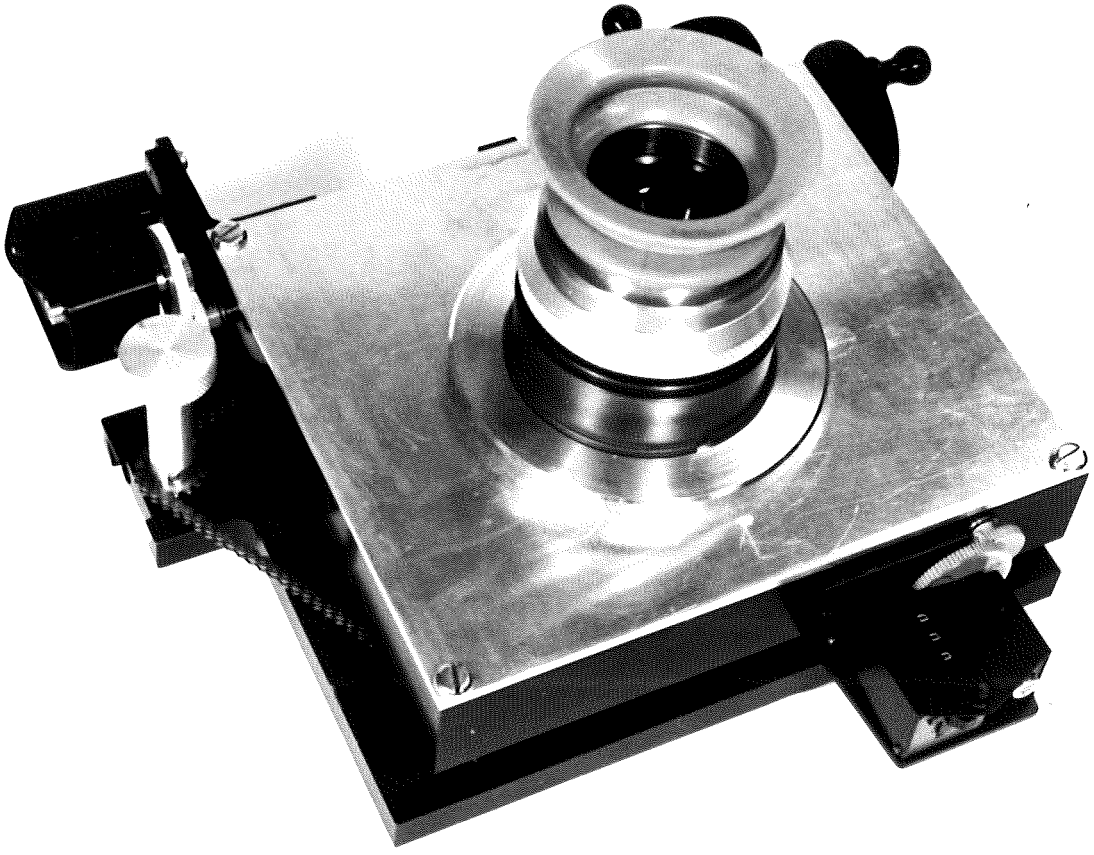

Figure 2.4 Acquisition eyepiece.

tubes are cooled. The lenses serve a dual role of Fabry imaging and cold box windows.

2.2.15 Photomultiplier Tubes

There are three types of photomultiplier tubes used in the photometer. The photomultipliers are housed in two cold boxes, which were manufactured by Products For Research Inc.. At present they are being run uncooled, but eventually the cold boxes will provide cooling by the Peltier effect, in conjunction with a recirculating cooler.

The three types of tubes used are:

a) Thorn EMI 9750B(QB).

Channels 1 and 3 use a derivative of the 9750 tube. Both have bialkali photocathodes and CsSb, high gain, 10 stage venetian blind dynodes, with a peak quantum efficiency of about 27% at 370 nm. Each has an effective cathode diameter of 45mm.

The 9750B, used in channel 3, has a borosilicate window and a wavelength range of 320 - 630nm.

Channel 1 uses a 9750QB, which has a fused silica window. The quartz window extends its wavelength range down to 175nm, (see Figure 2.7). The 9750QB is supplied graphite coated and black plastic sleeved, to minimise dark current.

b) Thorn EMI 9658R.

Channels 4, 5 and 6 all use 9658R tubes. The tube has an extended-red S20 (trialkali) photocathode and CsSb, 11 stage, venetian blind dynodes, with a peak quantum efficiency of 25% at 400nm. The effective cathode diameter is 42mm. All the tubes have

borosilicate windows and a useful sensitivity over the wavelength range of of 330 - 900nm, (see Figure 2.8).

The window of the 9658R has a prismatic surface onto which the photocathode is deposited. This results in an enhanced red response without significantly affecting the dark current. (The principle is that, light reflected back from the windows is then re-reflected by the honeycomb arrangement back onto the photocathodes).

c) Varian VPM-192M.12D.

Channels 7 and 8 both use the Varian VPM-192M.12D tube. This tube has a GaAs photocathode with 12 stage dynodes. The window material is glass and the peak quantum efficiency is around 13% at 800nm.

The usable wavelength range is 500 - 920 nm, (see Figure 2.9). The photocathode has an active area of 12.5mm and unlike the other tubes the dynode resistor network is encapsulated within the tube construction.

2.3 MECHANICAL DETAILS

2.3.1 Mechanical Overview

Mounted close to the Cassegrain focus of the telescope is the photometer top plate. This plate is the interface between the photometer and whichever telescope it is attached to.

Beneath this is the front-end upper section. This box like structure provides locating positions for the acquisition eyepiece assembly and the calibration source unit.

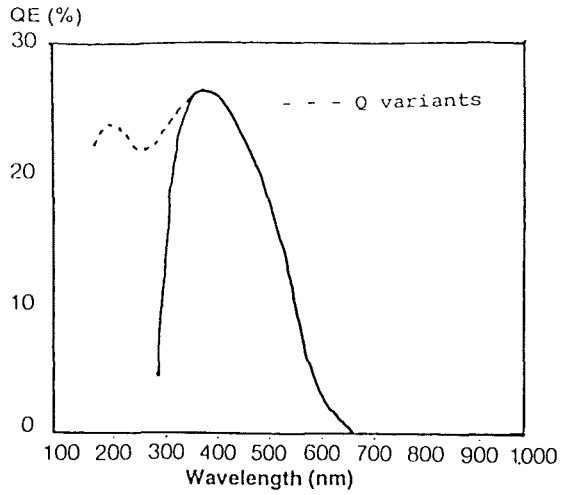

Fig.2.7 Spectral response of EMI 9750B(QB).

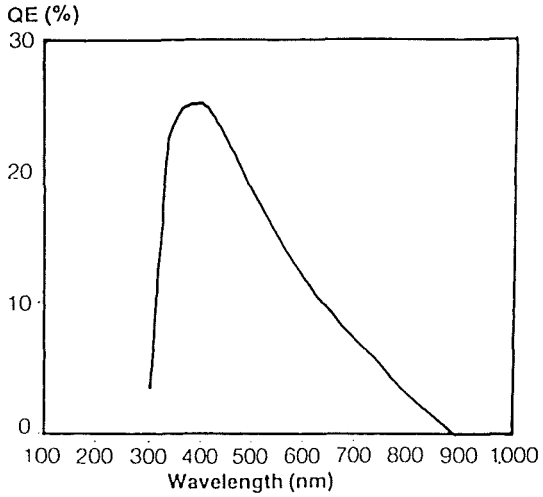

Fig.2.8 Spectral response of EMI 9658R.

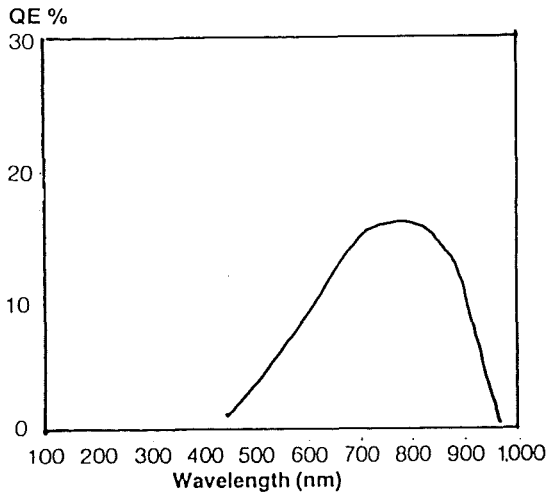

Fig.2.9 Spectral response of Varian VPM-192M.12D.

Attached to this is the upper end adaptor plate, which is chosen to match the f ratio at which the photometer is to be used and is designed to bring the centre of the appropriate collimator mirror to coincide with the telescope axis.

The main photometer head is attached to this plate. The section of the photometer base plate which contains the aperture is hinged for ease of maintenance. On the hinged portion are mounted the aperchopper, aperture slide and neutral density filter wheel.

The top cap assembly consists of two long plates (one of which is called the sawtooth plate) and 8 short plates, which form the mounting plane and register for the cold box. The other long plate, has cut in it an access port for the grating, mosaic and aperchopper.

The bottom cap is similar to the top cap, but there is no access port on the long plate. Instead, provision is made for mounting the grating components, namely the tangent gear box, encoder housing and grating base. ("Top" and "Bottom" refer to the photometer convention as pictured in Figure 2.15.)

The collimator assembly is located in the side frame and uses quick action toggle clamps for ease of removal.

The camera mirror is located in a mirror cell, which is secured by means of 3 spring catch assemblies, 2 mounted on the top plate and the other on the bottom plate.

The two end short plates project past the side of the plate and are face-to-face with similar projections on the cold boxes. Captive screws in the photometer head and fixed nuts in the cold boxes are used to secure the cold boxes to the photometer.

The two cold boxes have been manufactured by Products For Research Inc.. They house the photomultipliers and Fabry lenses. Refrigeration for the tubes is provided by Peltier coolers. The heat generated by the Peltier effect is removed using a recirculating and refrigerated water system.

2.3.2 Calibration Source Unit

The calibration source unit, Figure 2.10, is mounted on one of the side plates of the front end upper section. Its function is to introduce discharge tubes into the focal plane of the photometer for use in calibration tests (see Ch.5).

The unit consists of a rotatable hub in which up to three discharge tubes can be carried.

The hub is not allowed to rotate continuously, because of wiring constraints, but must operate between two limits. The limits are marked by microswitches, which reverse the direction of the driving motor. A further three microswitches provide positional information for the three discharge tubes.

The discharge tubes are held in racks, which in the steady state condition are retracted into the hub. As the hub rotates and the selected rack comes into position, a spring loaded d.c. motor engages with the rack. This bi-directional motor is used to insert and retract the discharge tubes. Two end-of-travel microswitches mark the "in" and "out" positions.

2.3.3 Acquisition Mirror

The acquisition mirror is mounted within the photometer head on a

bar. During an integration period the mirror would be swung out of the optical beam.

When acquiring a star the mirror is rotated through some 45°, so that the beam is reflected into the acquisition eyepiece.

The mirror is rotated by a lever on the outside of the photometer head, which is attached to the bar inside. The arm is driven by a rotating worm shaft, which is coupled to a threaded pin inserted into the arm. As the shaft rotates the pin is drawn along it. The shaft is driven by a reversible 26V d.c. motor.

On the lever is an indexing wedge which runs on a sector mounted on the photometer head. At each endpoint there is a groove. On reaching one of these endpoints the indexing wedge on the lever snaps into place. This action activates a microswitch, indicating destination and switching off the motor. The "in beam" mirror location must be precisely repeatable by the wedge position for reliable acquisition.

2.3.4 Offset Guider Counters

The acquisition eyepiece is provided with adjustable crosswires. The crosswires have separate X and Y movement, with a geared re-settable counter on each axis. The crosswire plane can be moved into focus using a screw assembly, though this is not calibrated.

2.3.5 Aperture Slide

The aperture slide is located between the entrance aperture and the aperchopper assembly.

It consists of 3 pairs of holes, plus one single hole, drilled into a rectangular diaphragm, which is mounted onto a dovetail slide. The slide has a piece of rack attached to it and is driven by a pinion, the latter carrying a detent wheel. A spring-loaded ball plunger on an adjustable bracket operates with this wheel, defining the proper positioning for placing a pair of holes in the optical path. A stop pin limits the rotation of the detent wheel to one revolution.

A handwheel, external to the casing of the photometer head, is marked, indicating the position of the slide.

The dimensions and position of the holes are shown in Figure 2.11. The choice of aperture diameters is outlined in Ch5.

2.3.6 Aperchopper Assembly

Positioned behind the aperture slide and in front of the neutral density filter wheel, the aperchopper assembly is dowel-pin-located on the bottom cap of the photometer.

The aperchopper assembly, Figure 2.12, consists of a geared disc, into which 4 slots have been cut. There is 6° of blanking between each slot. The slots lie alternately on 2 different radii. The aperchopper is driven by a precision d.c. motor, rated at 27 Volts. Its design period of rotation is 100ms and this is governed by a motor controller described in Ch3.3.1.

As the disc rotates, in a plane perpendicular to the optical axis, it masks and unmasks, twice per revolution, one of the aperture pairs described previously. Normally the star would be set into one aperture and the other would view the nearby sky.

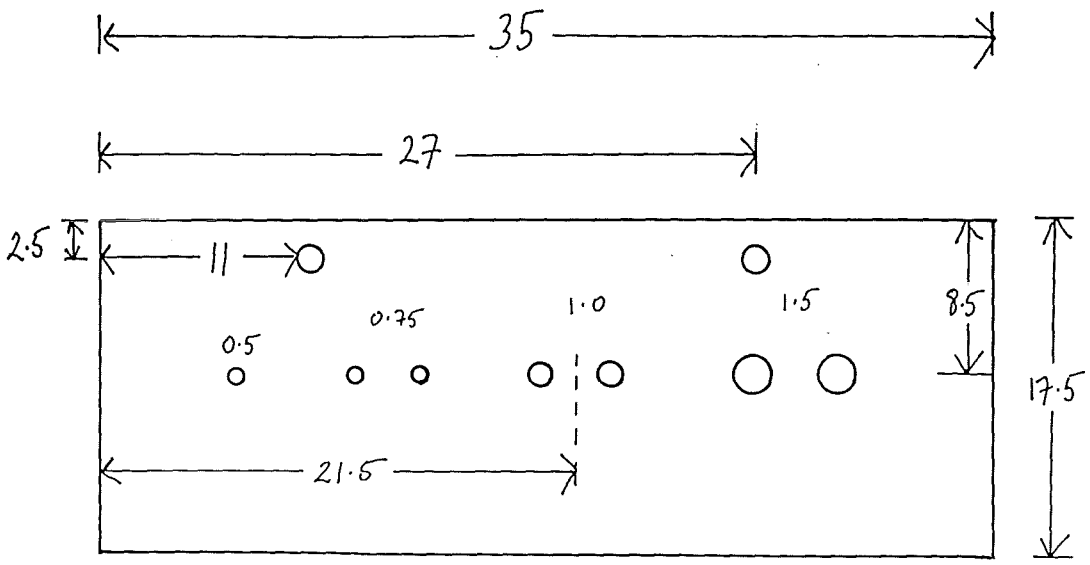

All dimensions in mm.

Spacing between holes in a pair = 2.5mm

Spacing between centres of pair = 4.4.3mm

Fig.2.11 Aperture slide.

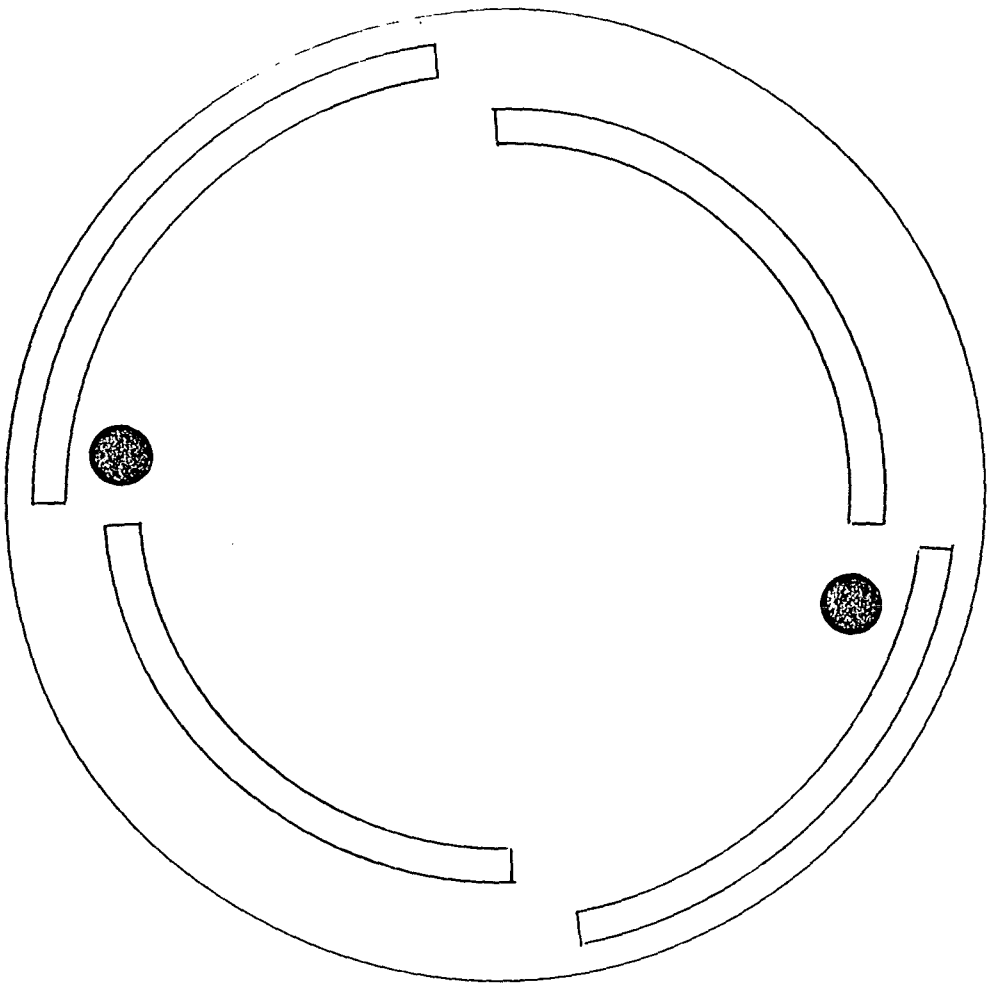

Fig.2.12 Aperchopper assembly. The dark areas show the positioning of the soft iron inserts.

Since the integrating periods have to coincide with these slots, a synchronization signal is generated twice per revolution. The signal is derived from a stationary magnet and coil which responds to two pieces of soft iron precisely located within the aluminium chopper wheel.

2.3.7 Neutral Density Filter Wheel

The neutral density filter wheel consists of a flat circular disc with filters mounted around its periphery. The filter wheel, which is situated behind the aperchopper, is aligned perpendicular to the axis of the photometer. It's rotation axis is offset from the optical axis, so that, as the wheel is rotated, each filter passes into the light beam. There are 6 filter positions placed at 60° intervals around the disc.

The filter wheel is driven by a 90° stepper motor. The stepper motor shaft is connected to a 96-tooth gear which meshes with a 144-tooth cam-gear. The cam-gear drives the filter-gear, which is of the same gearing. The reduction results in one 90° step of the stepper-motor producing a 60° rotation of the filter wheel.

The repeatability of the stepping of the filter gear is ensured by a detent arrangement. Six detent holes, at 60° intervals, have been made on top of the filter-gear cam. A ball-headed plunger, mounted on a tensioned arm, locates in these holes with sufficient pressure to overcome any backlash in the system.

Positional information is derived from 3 microswitches which ride on the cam of the filter wheel. The cam has two levels, thus the microswitches are either ON or OFF, depending on which level of the cam they are on. The output from the 3 microswitches produces a 3-bit

grey code, which means that each position has a unique address.

2.3.8 Post-Aperture Viewer

The post aperture viewing system consists of a simple tilted mirror and standard eyepiece (Figure 2.13).

The eyepiece is mounted at one end of a drawtube, with the mirror at the other. This drawtube is extended using a control rod, the amount of extension being determined by a detent and ball plunger. A control rod, with a similar detenting mechanism, is used to set the angle of tilt of the mirror.

A shutter is also provided to prevent light entering into the photometer head, via the drawtube, whilst integrating.

2.3.9 Grating Rotator

As we have seen, the grating is used to produce a spectrum on the mirror mosaic. We have also seen that there is a necessity to rotate the grating relative to the optical axis. The grating rotator assembly, Figure 2.14, allows us to do this and also provides us with information as to the angle of the grating.

The grating is held secure in its cell by plastic pads. The cell is held in a table, which is perpendicular to the optical axis, and is attached to one end of a tangent arm. The other end of the tangent arm has a section of worm-gear attached to it. This gear has a pitchline radius of 200.9mm.

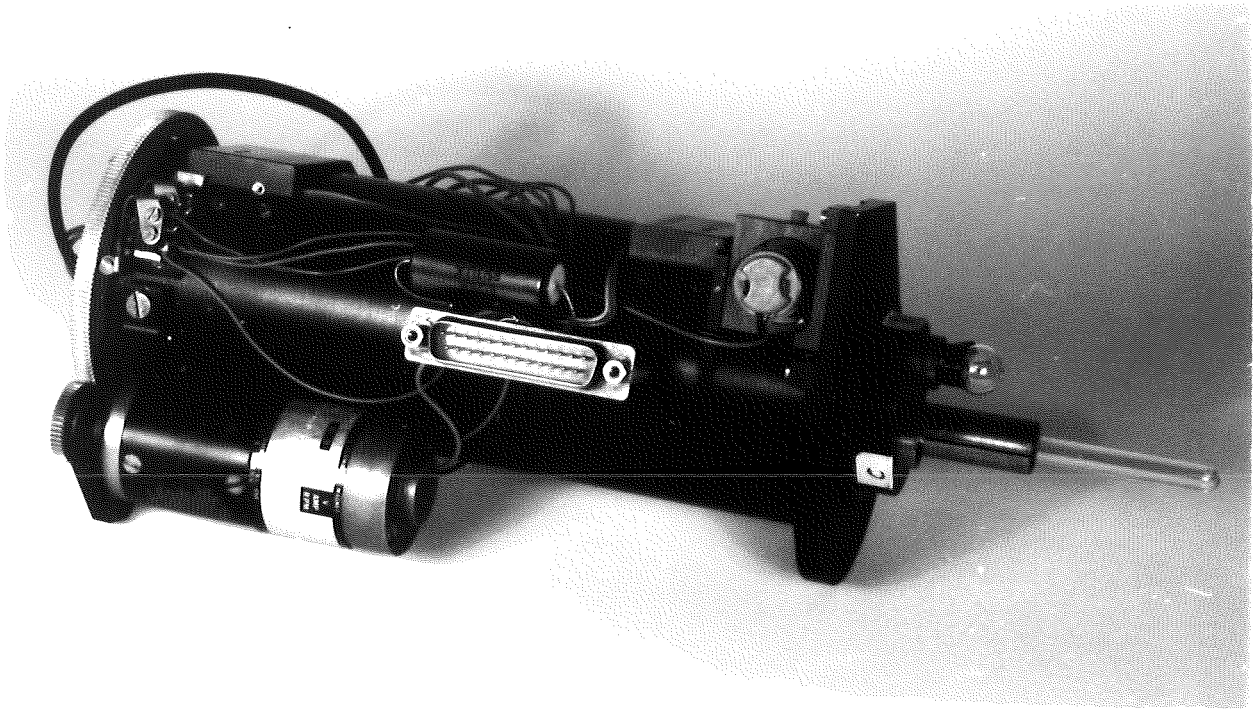

Figure 2.10 Calibration source unit.

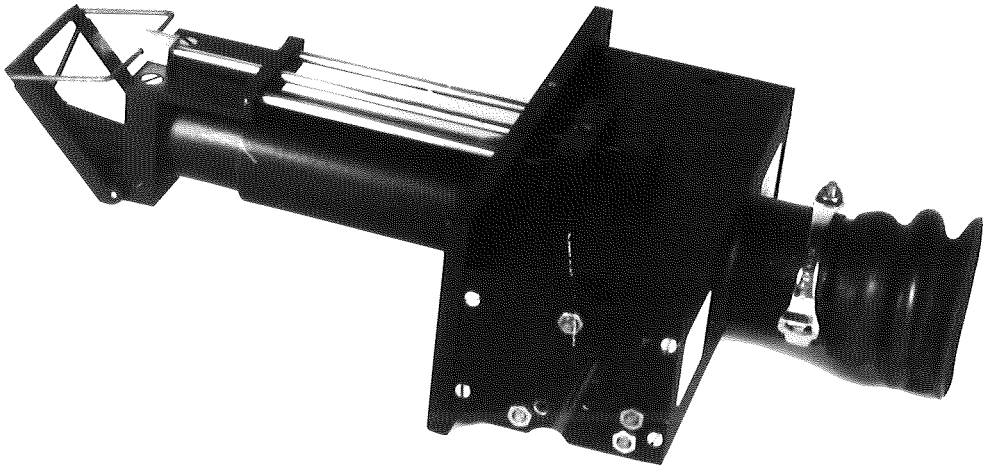

Figure 2.13 Post-aperture viewer.

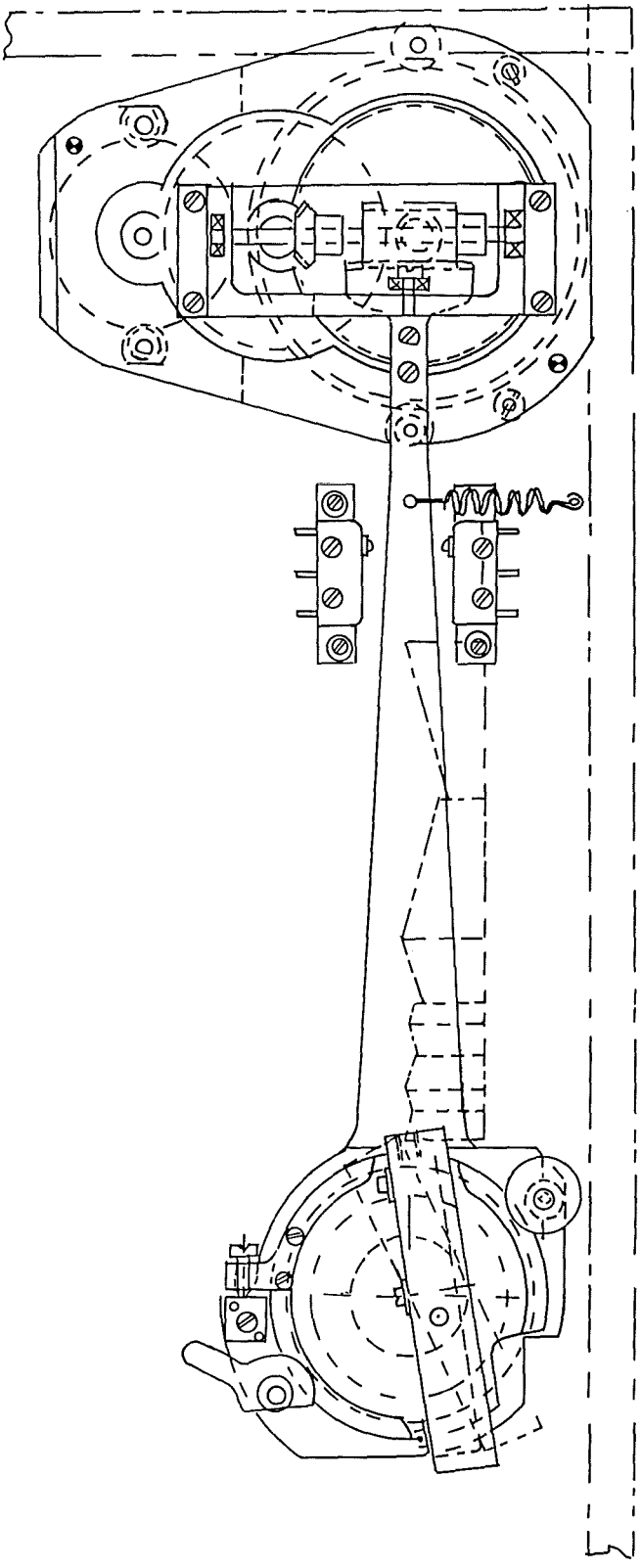

Fig.2.14 Grating rotator assembly.

A stepper motor is used to drive this gear using anti-backlash gears. The gearing is such that one 7.5^{o} step from the stepper motor rotates the grating about the optical axis by 5 arcseconds. (This corresponds to a movement of 0.153nm along the axis of the mosaic mirror). The stepper motor also drives an absolute shaft encoder, which provides information on the angle of the grating.

The degree of rotation of the grating is limited to 2^{o} and the 2 microswitches, seen in Figure 2.14, are used to define the rotation limits.

2.3.10 Photomultiplier Filter Units

The photomultiplier filter units are located in rectangular openings in the sawtooth plates, as shown in Figure 2.15. Each channel has a separate filter unit associated with it.

The filter units are used to place filters directly in front of the Fabry lenses associated with the photomutipliers. Each unit can carry up to three filters, which are selected remotely under computer control, plus an additional filter which is selected manually.

Each filter is held in a slide, which clamps it along two of its edges. The slides run on ball bearings, which are located by guide grooves cut into the side of the unit's casing.

A series of three cams are arranged around a shaft such that, as the shaft is rotated, the cams will insert each filter in succession into the optical beam. There is an additional ball bearing on the filter holder which runs on the cam, (see Figure 2.16).The filters are withdrawn, under the tension of a spring, as the cam is rotated.

The shaft is driven, (in one direction only), by a small 6Vd.c. motor, which is mounted parallel to the filters' direction of travel. The motor is coupled to the shaft with a dual bevel gear.

Positional information is derived from four microswitches. The microswitches are arranged as shown in Figure 2.17. They run on a disc which rotates with the shaft and cams. On the disc is a detent. As one of the slides is at its furthest extension, i.e. on the top of a cam, the detent activates one of the microswitches and the motor is stopped. One of the detent positions corresponds to when all of the slides are fully retracted.

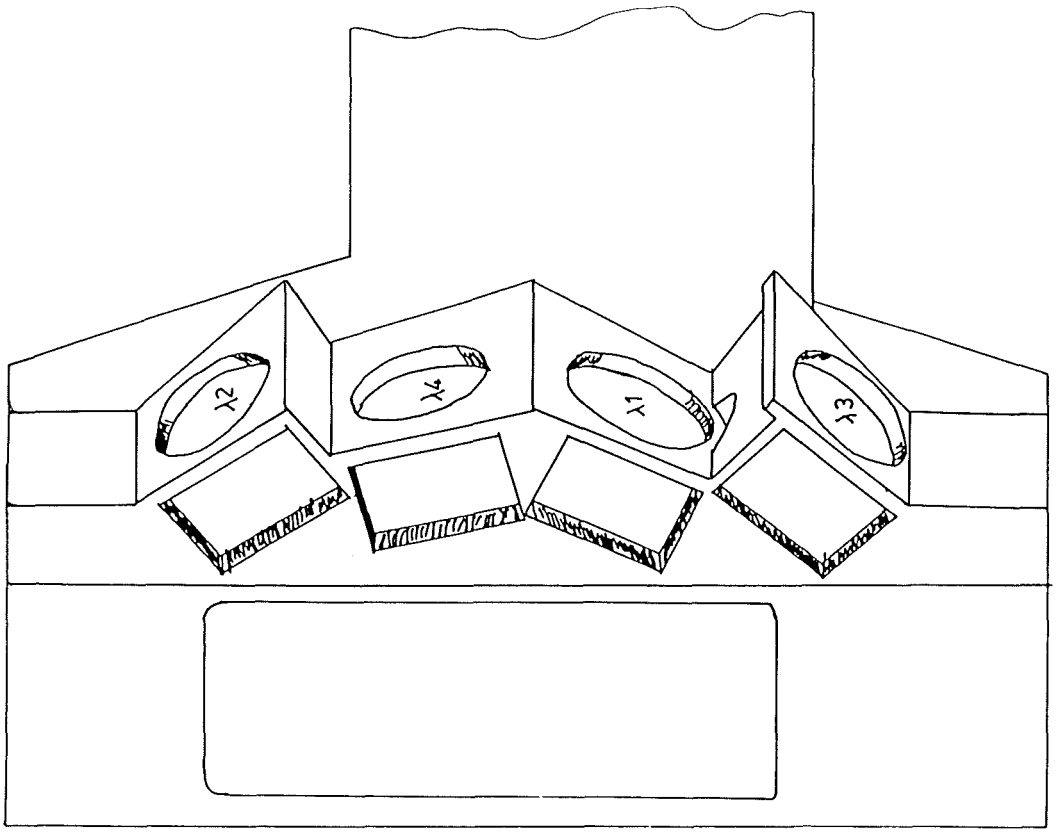

Top

Bottom

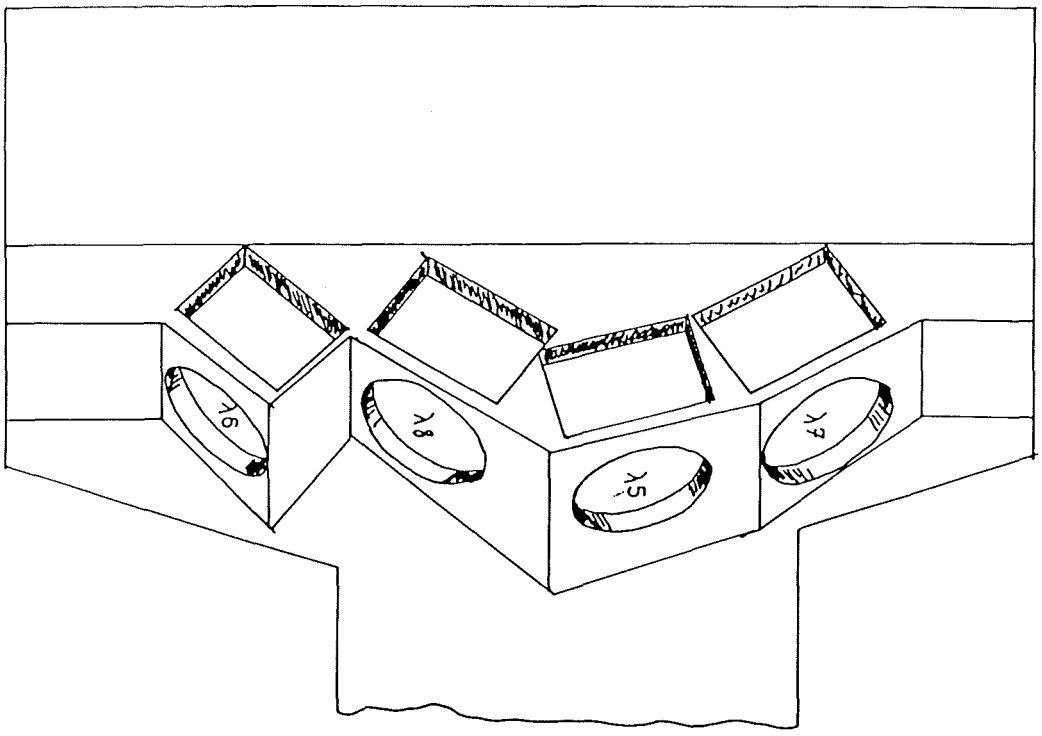

Fig.2.15 Locating positions for the photomultiplier filters.

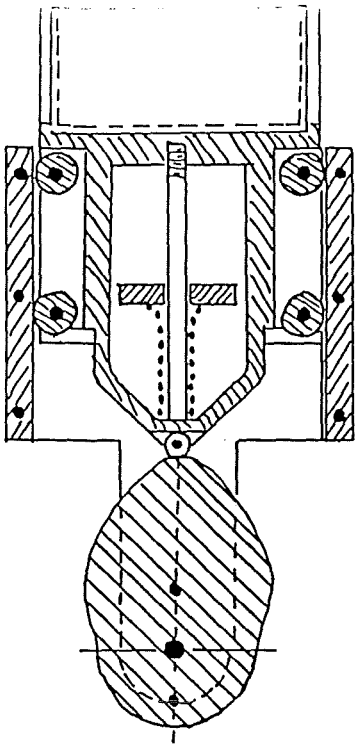

Fig.2.16 Photomultiplier filter unit showing cam detail.

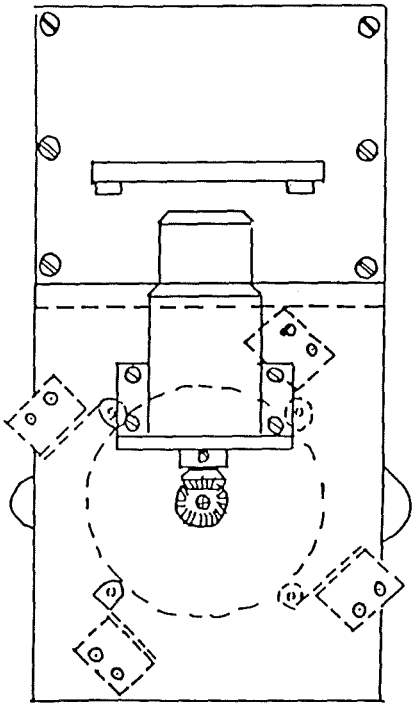

Fig.2.17 Photomultiplier filter unit showing microswitch positioning.

CHAPTER 3

SYSTEM HARDWARE

3.1 INTRODUCTION

The photometer, in its present state, has some 12 d.c.motors, 2 four-phase stepper motors and in excess of 50 microswitches associated with it. Given this degree of complexity t is clear that efficient use requires a high level of functional automation.

Automation of such routine actions as filter selection and movement of the acquisition mirror, will greatly increase the amount of time that can be spent actually collecting astronomical data. Since one of the main advantages of a multi-channel device is the reduction of observing dead-time, overall efficiency is an important consideration.

On top of the control of the instrument we also have the problem of data collection and recording. With eight photomultipliers capable of producing counts every second, automation becomes a necessity.

We can see that the two problems can be considered separately and it is along this direction that the solution to the problem evolved. A microprocessor system was developed to control the physical requirements of the instrument and a separate processing system developed for data capture.

SYSTEM HARDWARE

In the next chapter the processing power and software environment are discussed, so here we will just consider the hardware used.

The central processor and associated cards are housed in a 19" X 3U rack, complete with a backplane to allow communication between the cards. Since this processor would be required to communicate with the control electronics, it is obviously of advantage to have the two in close proximity. The electronics necessary to operate the photometer were therefore designed to be mounted on standard 3U Eurocards.

The cards were also designed to be plug compatible with the backplane. The connections in the backplane were broken at mid point and an adapter board designed that would allow the processor to communicate with the control electronics without the need for external connections. The power supply installed in the rack system was chosen so as to meet the needs of the processor and also the control electronics.

Every effort was made to design the electronics around common commercial components, so that, in the event of a failure a replacement could be easily found. To aid this ease of replacement, all ICs (integrated circuits) were mounted in socket holders, rather than being directly attached to the board. To assist in de-bugging, all connections were made using the wire-wrapping technique.

In the design of the control electronics, particular attention was given to ensuring that no damage could be done to the photometer by inadvertent use. Although, as will be seen in the next chapter, software provides such protection in the first instance, the designs have been implemented in such a way that in the event of a software failure the safety of the instrument will not be jeopardized.

So as to reduce the amount of cabling that would have to be passed from the floor of the dome up to the photometer, the rack containing the electronics and the power supply was mounted on the telescope next to the photometer.

The data capture system, principally developed by Mr.Carr, is centred around the use of the 1MHz bus on the BBC microcomputer. The eight counters, along with other pertinent electronics, are situated on the floor of the dome, with eight co-axial cables running from the amplifier/discriminators on the photometer head down to them. This system operates entirely separately from the control system.

With the independence of the two systems there is the advantage that any upgrades/modifications to one system does not affect the other.

3.2 THE CONTROL ELECTRONICS

3.2.1 Acquisition Mirror

The acquisition mirror is driven in and out of the focal beam by a 26V d.c.motor. At the two end positions are microswitches. Information from these microswitches is used to stop the motor and determine the direction of the motor. In addition they provide information on the position of the mirror (ie. ' in the beam ', ' out of the beam ' or ' inbetween ').

Figure 3.1 shows the electronics used to position the mirror. The design consists, essentially, of two D-type flip-flops — one to stop and start the motor and the other to determine its direction.

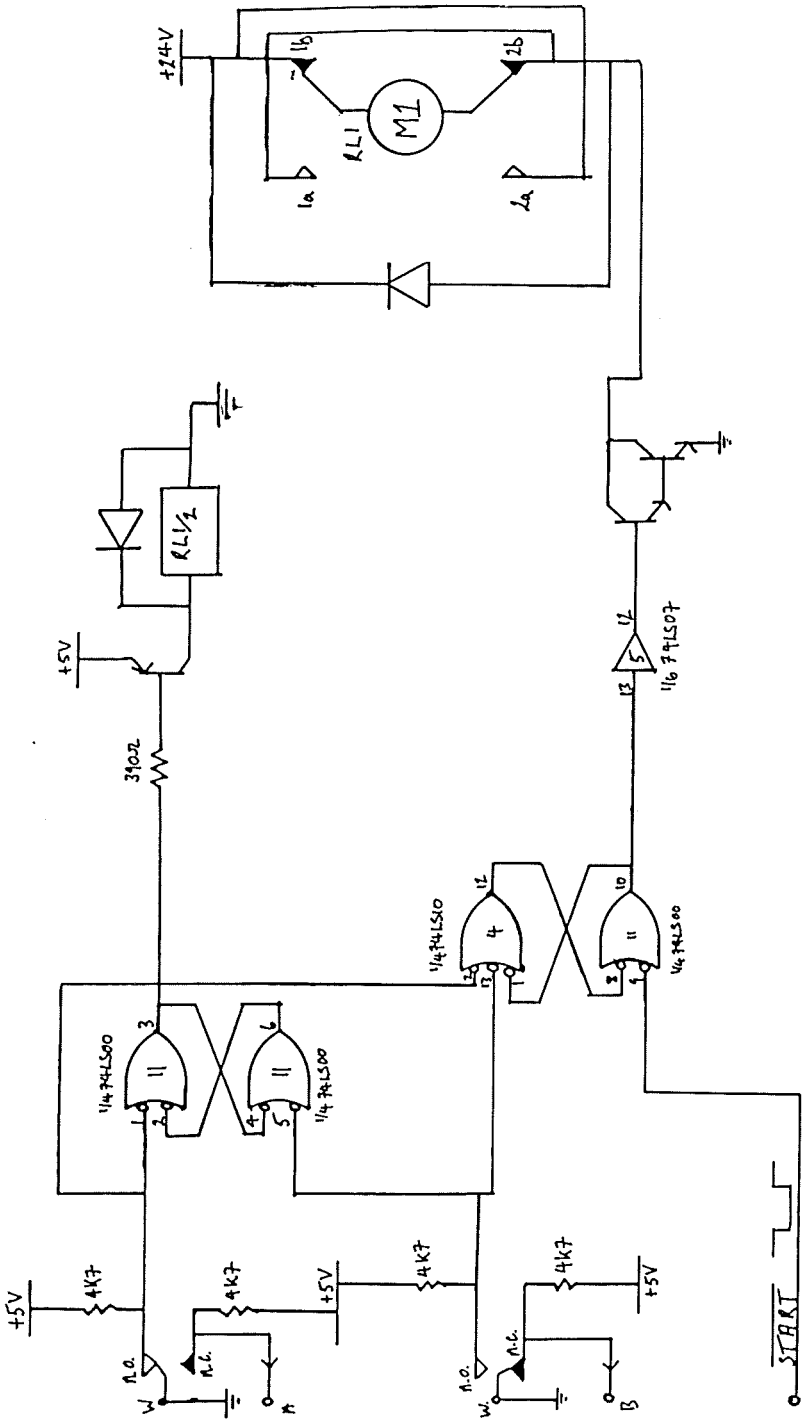

Fig.3.1 Acquisition mirror.

The motor is set in motion by software taking the processors output line, START, low. This must be held low sufficiently long for the microswitch which was activated to be de-activated and go high. START can now be taken high causing no change in the output of the flip-flop. The motor now drives until the opposite end point is reached. Now the other microswitch will be activated, changing the state of the flip-flop causing the motor to stop.

The direction of the motor is determined by the state of the normally opened contacts of the microswitch. As an end position is reached one or the other will go low causing a change in state of the output of the flip-flop. This change in state is used to energise and de-energise the relay coil and hence change the direction the motor will move in when it is started again. In the ' inbetween ' position, both inputs will be high, therefore there will be no change in state of the coil.

Only 3 control lines are necessary to implement this design, one output and two input. The output (line 45) is used for the START signal and the inputs (lines 46 and 47) read the state of the normally closed contact. This gives us sufficient information to determine the position of the mirror.

3.2.2 Calibration Source

The calibration source unit consists of a rotating hub, into which, up to a maximum of three discharge tubes can be placed. The tubes are contained within sleeves which have a rack gearing arrangement. A 6V d.c.motor engages in the rack and drives the sources in and out of position. The hub is driven by a 24V d.c.motor.

Associated with the rack system are two microswitches, marking the rear and forward positions of the sleeves.

As the hub rotates, a microswitch on the hub is activated each time a rack engages with the rack motor. Since the hub is not permitted to rotate continuously a further two microswitches define the rotation limits. This makes for a total of five microswitches on the hub.

The steady-state condition is with all discharge tubes retracted.

When a given tube is selected, if it is the one already engaged with the gear then it is driven forward until the front microswitch is activated. This then shuts off the rack drive.

This departure from the rear microswitch must prevent further rotation of the hub, otherwise damage will be done to the tube.

If the selected tube is not in position then the hub must rotate until it is.

Whilst the hub is rotating an interlock must prevent activation of the rack drive, until the desired tube is in position.

Once in position the rack drive can be activated as outlined above.

A further complication arises as there is only one rear microswitch associated with all three racks.

During the rotation of the hub, the rear microswitch will open and will remain open, until the next rack pin comes along to close it.

We have seen that we do not want to allow the hub to rotate if this microswitch opens because of rack movement, but we do require the hub to continue rotating if the rear microswitch has opened due to rotation of the hub.

Figure 3.2 shows how these various requirements were met.

First consider the rack. A D-type flip-flop determines the direction of movement of the rack. This works in the same manner as previously described for the acquisition mirror.

The initiation and termination of movement between the end points is also as per the acquisition mirror. However, to ensure that whilst the hub is rotating the rack can not be driven, the drive signal from the hub is NANDed with that from the rack, locking out rack movement if the hub is already in motion.

When the rear microswitch opens the output from the flip-flop is used to disable rotation of the hub motor.

The lockout for the hub is more complicated. A source is selected by software by taking either A, B or C low. If this tube is not already selected, the output from the triple NOR gate will go high. This is NANDed with the output from the flip-flop driven by the rear microswitch. If the rear microswitch is activated, i.e. the tube is retracted, the hub will rotate. As the hub begins to rotate though, the rear microswitch will open, which would cause the state of the flip-flop to change, inhibiting the hub motor. However, since the hub is already rotating, the OR gate on the lower input of the flip-flop locks out this change of state of the microswitch and the hub continues to rotate.

When the desired position has been reached the relevant hub microswitch will open and the motor will stop. Once the motor has stopped the lockout will no longer be operative and any departure of the tube from the rear microswitch will inhibit the hubs rotation.

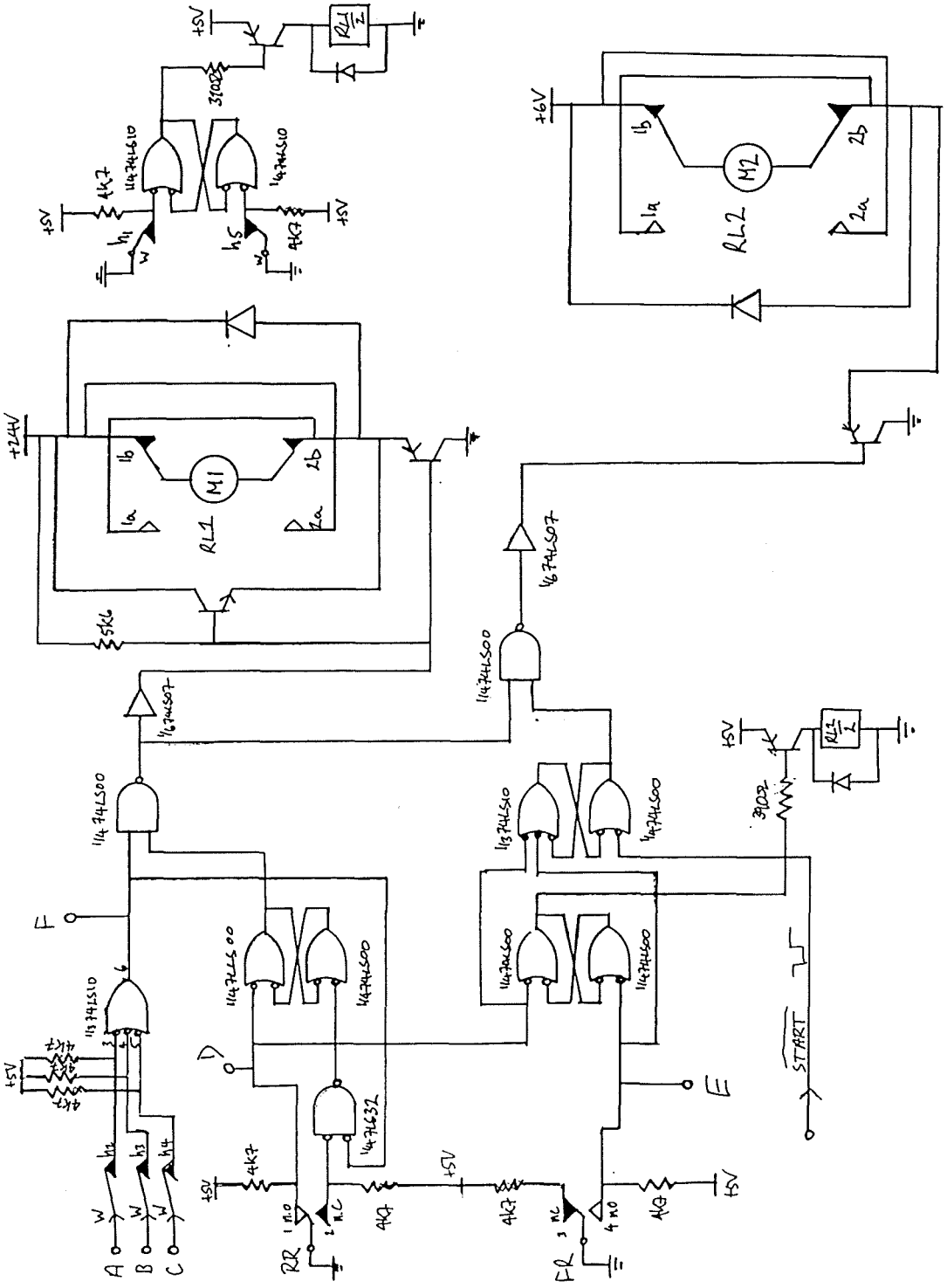

Fig.3.2 Calibration source.

Further, the hub is not allowed to rotate fully but is bound between two end-positions. On reaching one of the end-positions, a microswitch is activated which changes the state of a flip-flop. The output from this is connected to the coil of the relay driving the hub motor, so the motor automatically changes direction.

To implement this design requires a total of seven control lines, four output and three input. For the hub, three output lines are used to select a source and an input line to ascertain when the desired position has been reached. In the rack system, an output line is used to initiate the driving of the rack motor, the direction being determined automatically. An input line from the forward and rear microswitch provides information on the position of the selected rack.

3.2.3 Filter Shutter

The filter shutter has six positions. Three microswitches ride on the cam of the filter shutter wheel, which has two levels. Thus the microswitches are either ON or OFF, depending on which level of the cam they are on. The output from the microswitches produces a three bit grey code, which means that each position has a unique address.

Position	zone1	zone2	zone3
1	1	0	0
2	1	1	0
3	0	1	0
4	0	1	1
5	1	1	1
6	1	0	1

"0" = Switch normal (small cam diameter)

"1" = Switch depressed (large cam diameter)

The filter wheel is driven by a 90^{o} stepper motor which is geared to produce 60^{o} of rotation of the filter wheel for each step. (The wheel is located by means of a detenting mechanism described in the previous chapter). The electronics used are shown in Figure 3.3.

The output from the three microswitches is used as the input for one half of a four bit magnitude comparator (of which only three bits are used). To select a position, the grey code corresponding to that position is input by software into the other half of the comparator. The wheel is then stepped through the six positions until the two inputs to the comparator match (ie. until the A=B output goes high).

The stepper motor is driven by software. Although there are many stepper motor controllers cards available for use in rack systems, it was felt that this application did not warrant such a complex system. However, it was not felt to be advantageous to go to the other extreme of generating the bit pattern necessary to drive a stepper motor from software. Instead a stepper motor driver I.C. (Integrated Circuit) has been used.

The SAA 1027 is a bipolar integrated circuit intended for driving a four-phase, two stator stepper motor. It consists of a bi-directional four-state counter and a code converter to drive the four outputs in the sequence required for driving a stepper motor.

To step the motor from one position to the next, the software simply has to provide a single pulse. The stepping rate is determined by the interval separating these pulses and can therefore be controlled by software. In this application the motor is driven at a constant speed.

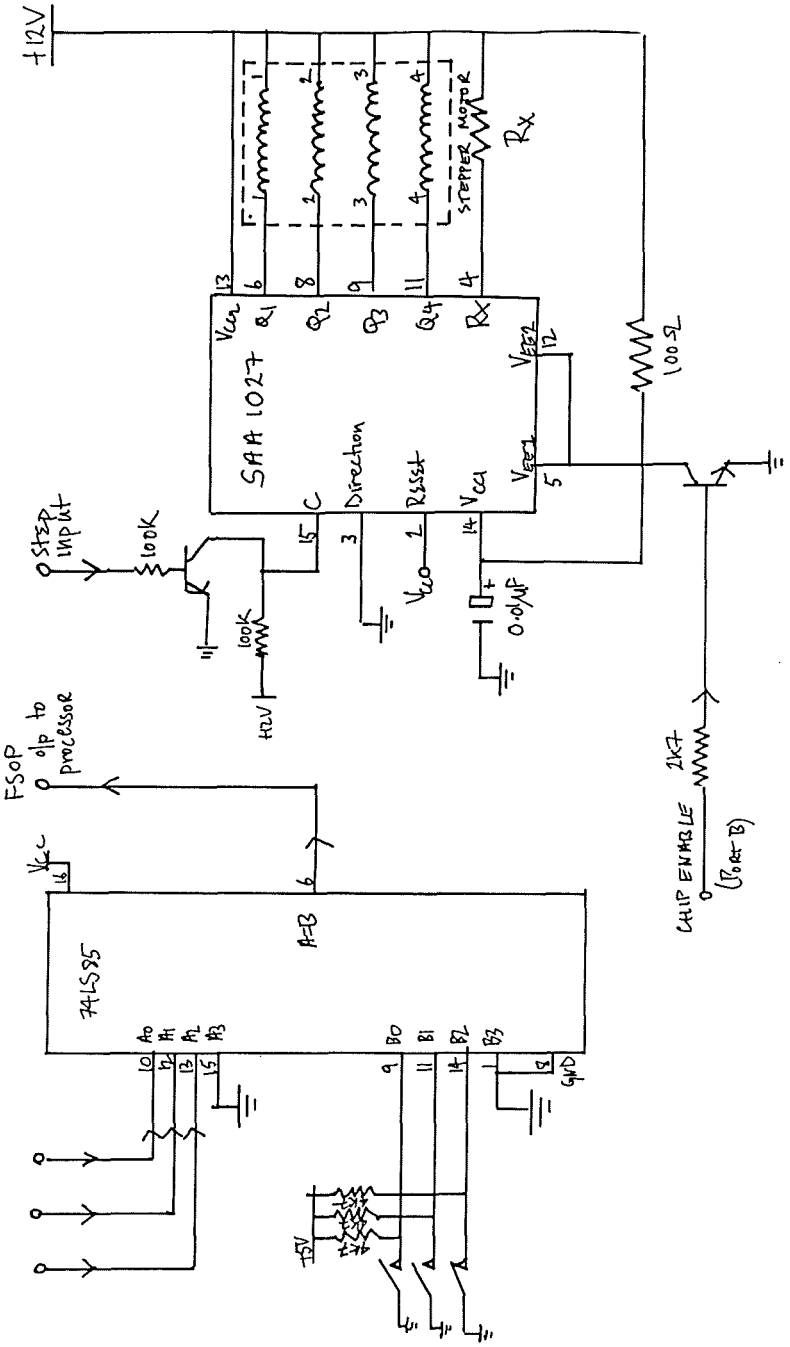

Fig.3.3 Filter shutter.

If the chip was to be left permanently enabled, the stepper motor would be left energised and would dissipate a considerable amount of heat. Since the filter shutter motor is located within the photometer head this is particularly undesirable. However, completely de-energising the coils leads to a slight shift in the position of the filter wheel. A solution is found in disabling the chip after moving, but to still supply the motor coils with sufficient current that they do not shift and yet cause negligible heating.

Lines required from the processor are five output and one input. Three of the output lines (30, 31 and 32) provide the grey code that corresponds to a filter position. The input line (33) is from the A=B output of the magnitude comparator and indicates when the desired position has been reached. The other two output lines (27 and 29) are the chip-enable and step input to the stepper motor controller I.C..

3.2.4 Grating Rotator

The grating arm is driven by a 7.5^{o} stepper motor, via a worm gear. A stepper motor controller of the same design as outlined above is used to drive the motor.

The position of the grating arm is determined by an absolute shaft encoder. This produces an eleven bit grey code output. The relationship of the encoder reading to motor step is one-to-one.

The encoder runs from 0 to 2047 giving us 2048 absolute positions. Each step of the motor produces 5" arc rotation of the grating. Therefore the encoder can encode approximately $2^{o}.8$ of grating rotation. However, since the arm limit switches only allow approximately 2^{o} of movement of the arm the entire range can be fully

resolved by the encoder.

Reading of the grey code produced by the encoder is done by the processor, which then translates it into a denary number. The shaft encoder has been set up such that moving from one arm limit to the other produces a monotonically increasing (or decreasing, depending on direction) output from the encoder. (Strictly speaking, the encoder positions are not absolute, but relational).

When moving from one position to another, either the increment, (positive or negative) or the new position can be specified. The direction bit of the controller IC is then set accordingly and the grating is then moved at its maximum speed (5 steps per second).

The motor can then be driven at a tenth of this speed if need be, to correct for any loss of positional accuracy.

As before the controller IC is disabled after movement is finished and again a small holding current supplied to the motor.

It is important that the motor should not attempt to drive the grating past its end points, which are marked by two microswitches. As can be seen from Figure 3.4, the two microswitches provide us with a lockout, preventing further movement. However, so that the arm can be moved away from the end points there has to be a way of overriding this lockout. The output line RESET provides such a means. The recovery from this position is controlled by software and is described in the next chapter.

3.2.5 Photomultiplier Filters

Each channel has associated with it a filter unit, which sits directly in front of the photomultipliers. Each filter unit is

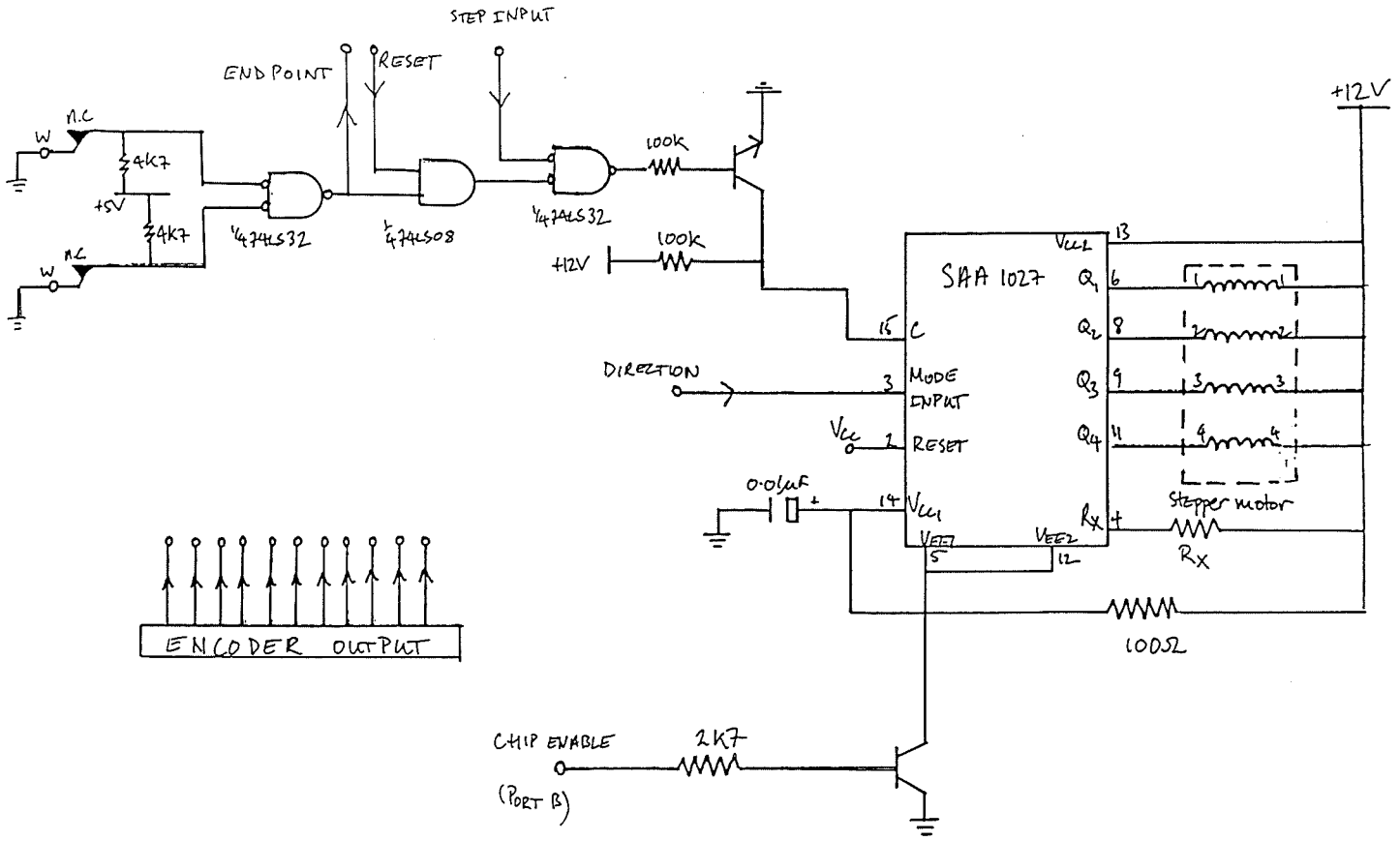

Fig.3.4 Grating rotator.

capable of holding a maximum of three filters. So there are four possible positions; one of the three filters in place, or no filter at all. The filters are driven into position by a 6V d.c.motor. Every position has a microswitch associated with it.

Consider an individual motor as shown in Figure 3.5. On selecting a filter from software, by setting a ' Filter Number ', one of the microswitches A, B, C or D will be taken low, unless that filter is already selected. Then, with ENFILTER low as well the motor will drive until the microswitch associated with the selected position opens. At this point all inputs to the LS21 will be high, therefore the motor will stop.

If this solution had been implemented for each individual filter unit then a total of 32 control lines would have been required (eight times, three output plus one input).

A considerable saving has been made not only in terms of control lines but also cabling, by multiplexing the microswitch inputs and output as shown in Figure 3.6.

The output from the ' Filter Number ' three-to-eight line decoder is commoned to all of the eight photomultiplier filter microswitches. However, the output from these microswitches is now input to the tri-state octal buffers. Which group of four is output to the quadruple OR gate is determined by the output of the ' Channel Number ' three-to-eight line decoder. (Each half of the octal buffers can be enabled separately).

Similarly, which of the eight motors to be driven is determined by the output state of the BCD-decimal decoder and this is set by the same input as for the ' Channel Number ' decoder.

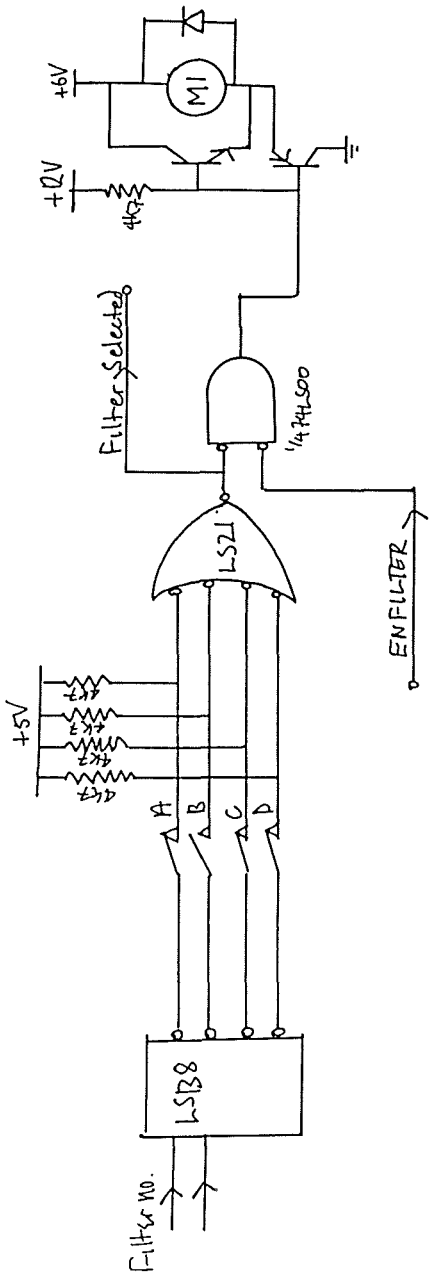

Fig.3.5 Individual photomultiplier filter electronics.

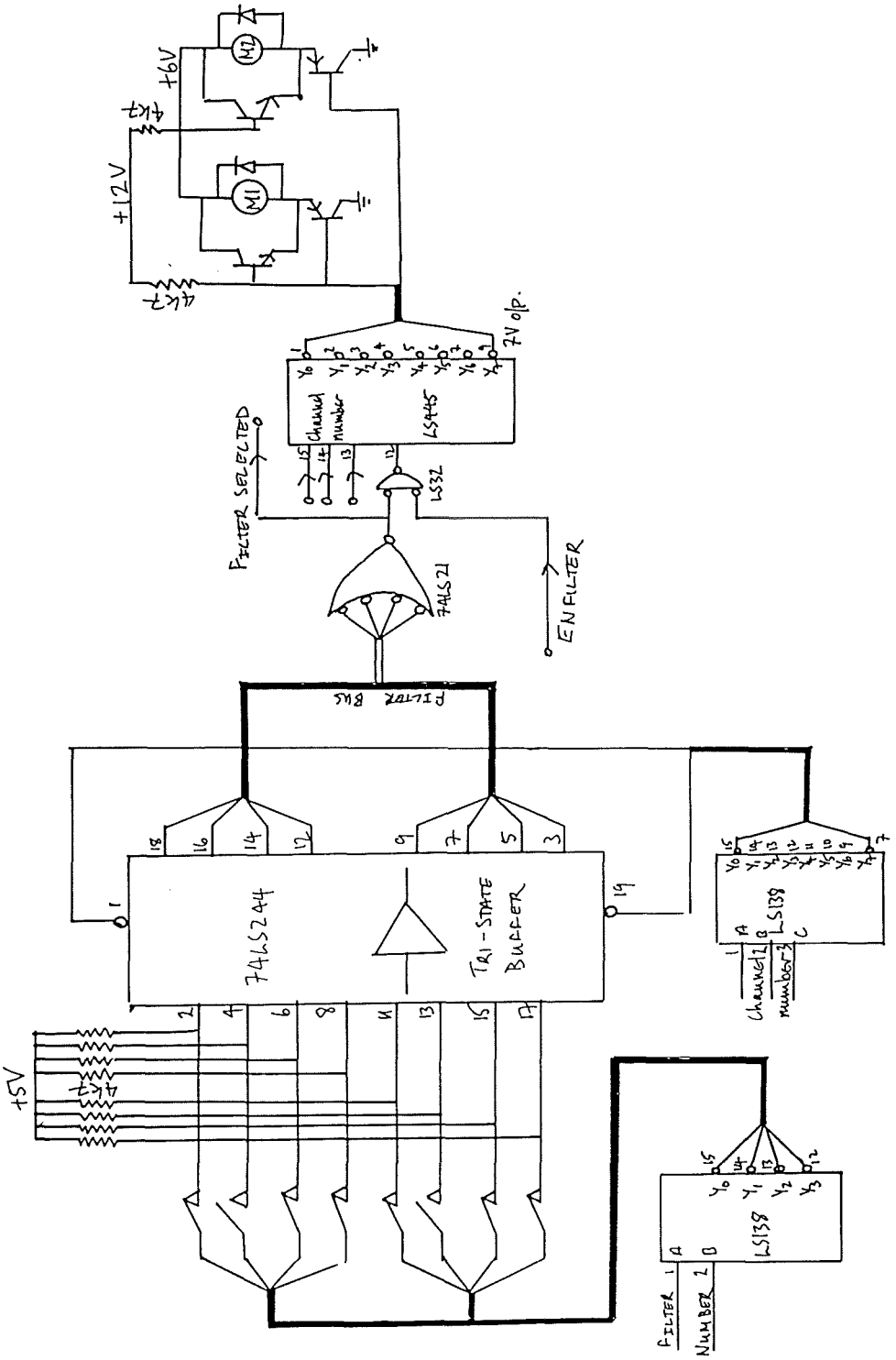

Fig.3.6 Multiplexing electronics for the eight photomultiplier filters. Only two motors are shown here.

The control ENFILTER has been introduced so that there is sufficient time to establish the channel number address before selection commences.

So now this implementation requires that the observer specifies the filter number and also the channel number as well as an enable command. The total number of control lines necessary has been reduced to six output and one input.

A significant amount of cabling has been saved also by placing the distribution box for the microswitch bus and the filter bus up on the photometer head, near to the filter units. Only eight connections need be run up to the telescope, the same number as would have been required for one unit alone if they had been treated individually.

3.3 PULSE COUNTING ELECTRONICS

The counting system consists of three main components; the aperchopper, the integration timer and the counters. The physical properties of the aperchopper have already been described in the previous chapter, but a brief overview of its function will be given. The integration timer and the counters were designed and built by Mr.Carr and only a summary review of their functioning will be given here.

3.3.1 The Aperchopper

As we have seen previously, the aperchopper consists of a rotating disc which, during the course of one half revolution opens first one and then another of a pair of apertures. Normally, one aperture would contain star+sky, and the other sky. The intention is to count up during the star plus sky period and then subtract the sky counts

during the other period. Obviously, it is a requirement that counting should only take place when the apertures are fully open.

At the beginning of each star plus sky, sky sequence the aperchopper generates a reference pulse. It was the original intention to use this reference signal to initiate the beginning of each integration cycle.

However, the rotational speed of the aperchopper, which is driven by a 27V d.c.motor, was found to drift over the interval of a half revolution. Mr.Carr designed a motor speed controller, Figure 3.7, but the motor speed was still found to vary by as much as 0.2% over a single cycle. The inability to reduce this variation is largely due to the fact that the speed can only be checked every half revolution, since only two reference pulses are generated for each revolution.

In light of this variation, the periods during which counting can take place are now determined by the integration timer.

3.3.2 Integration Timer

The reference pulse from the aperchopper is used to trigger the start of an integration cycle.

So as to ensure that the first aperture is fully open, a delay is introduced after the detection of the reference pulse, before counting commences.

Similarly, counting is inhibited before the switch over of apertures begins and there is again a delay before counting is enabled to ensure that the second aperture is fully opened.

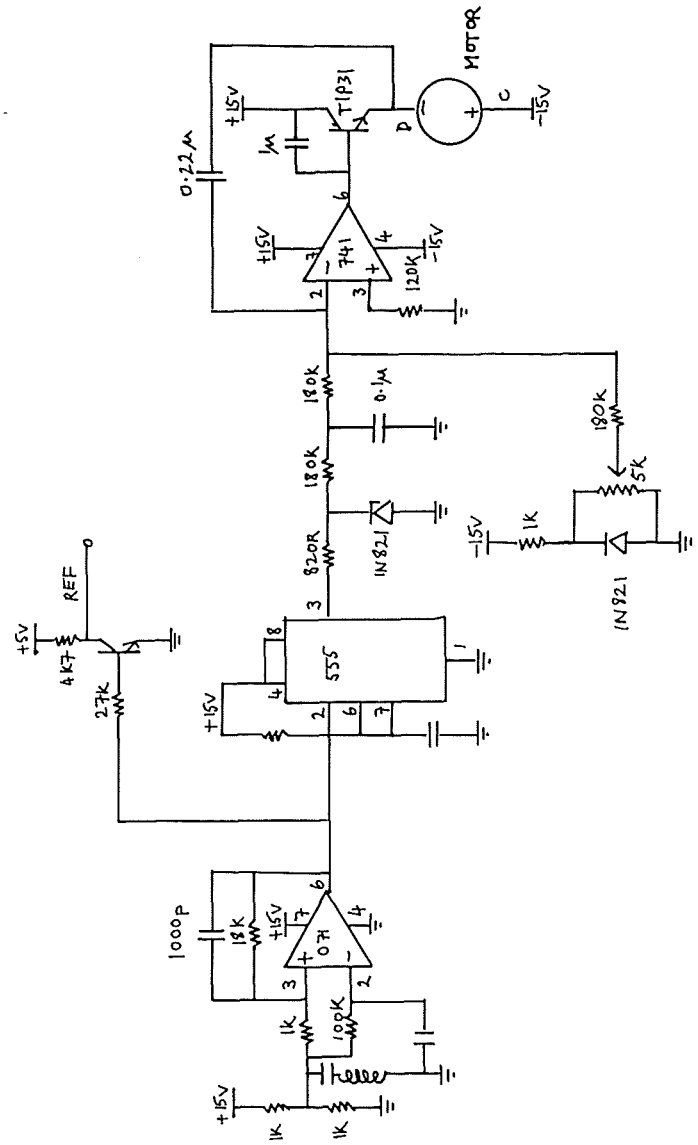

Fig.3.7 Aperchopper motor speed controller.

The safety margin introduced by these delays are sufficiently large to ensure that, even with the variation in motor speed, the apertures will always be fully open when counting is enabled. Unfortunately, these delays result in a loss of time spent counting, as the count window is effectively being shortened. The loss amounts to approximately 12% (as shown in the previous chapter).

From the timing diagram in Figure 3.8, we can see how this is implemented.

When COUNT is low, the counters are enabled. When STAR/SKY is low, the counting is incremental and when it is high, decremental.

The period from the trailing edge of the reference pulse, REF , to the first aperture being open is 9.1ms At this point STAR/SKY will be high. Q, which occurs 9.5ms after the trailing edge of REF, marks the beginning of the counting up period. After 22ms counting is disabled. This corresponds to R. The second aperture opens 34.5ms after the trailing edge of REF. Now STAR/SKY goes high. Between R and S, there is a delay of 3ms after S, counting is enabled, with the counters now counting downwards (ie subtracting the sky signal). Again this lasts for 22ms (The period counting up is exactly equal to the period counting down). The end of this cycle is marked by P. It can be seen that the next reference pulse has occurred before the counters have been inhibited. Because of this, it is not possible to use just one counter to produce the control signals P, Q, R and S.

The electronics used to produce these signals is shown in Figure 3.9.

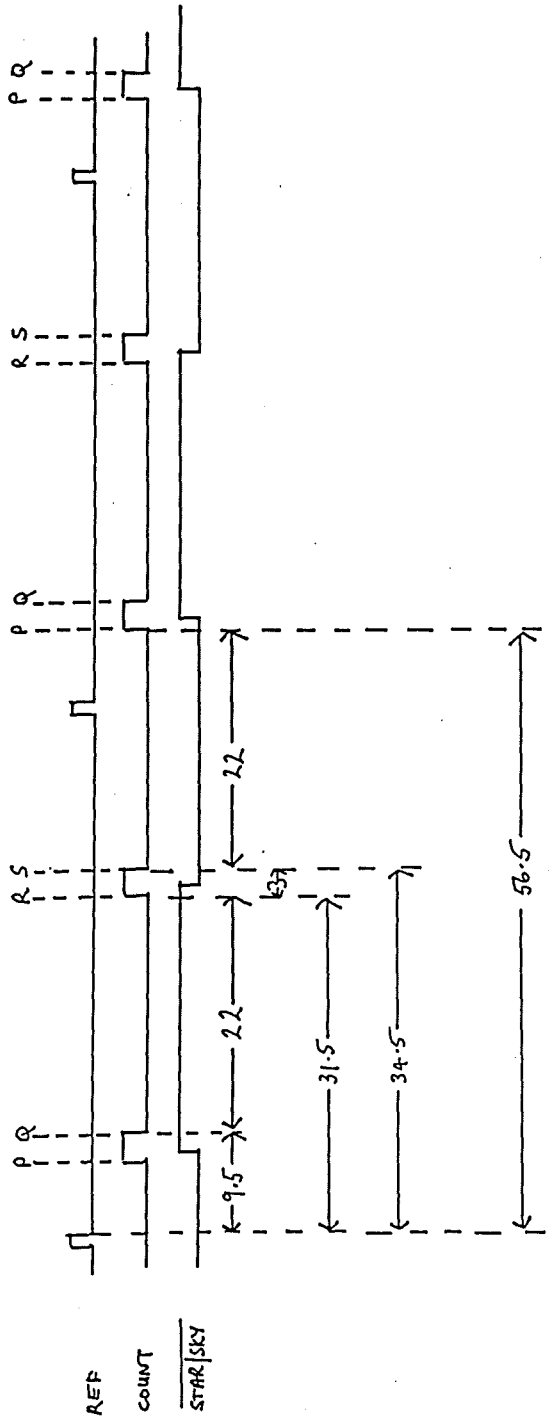

Fig.3.8 Timing diagram for integration controller.

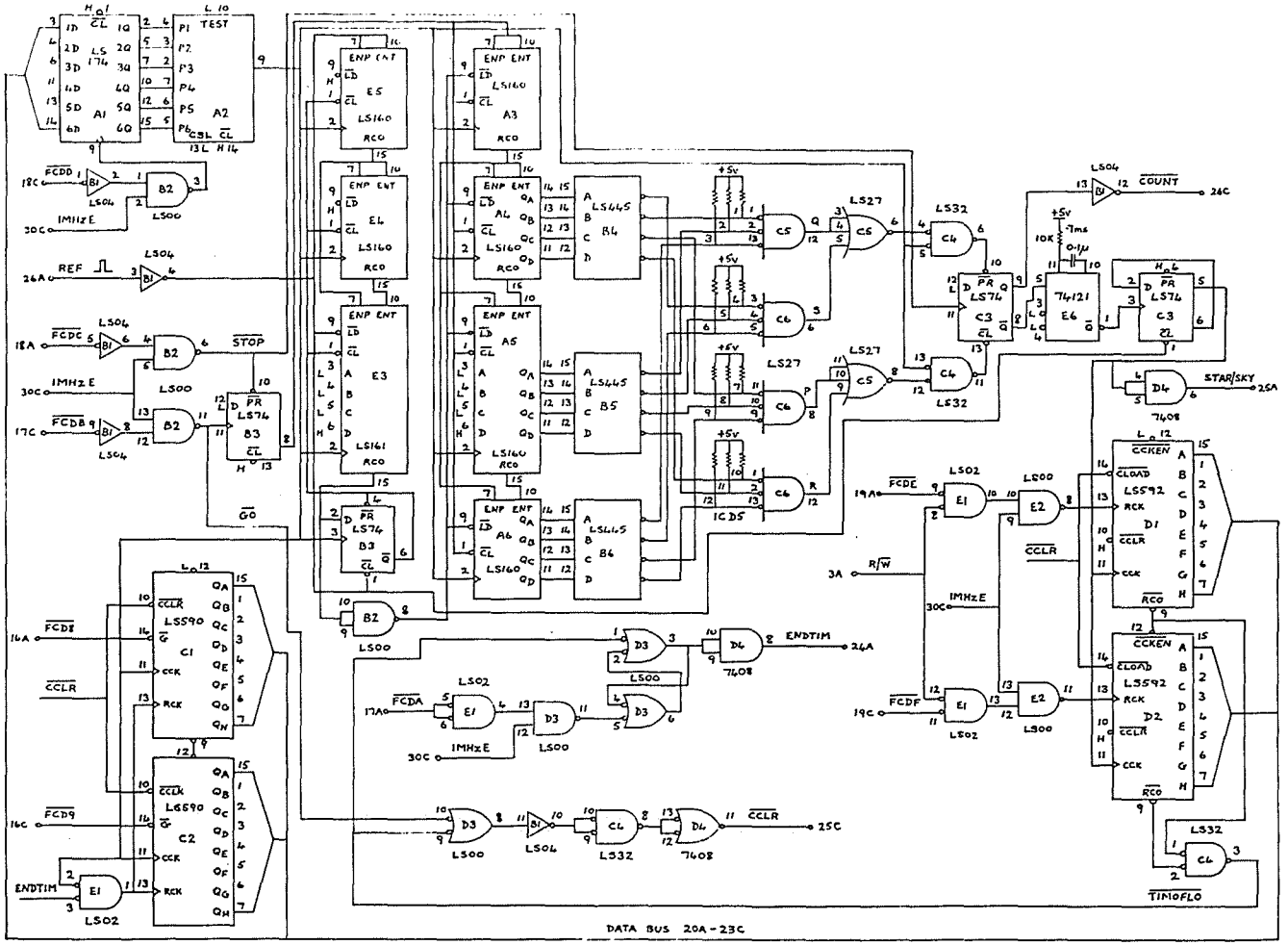

Fig.3.9 Integration timer.

The oscillator, A2, is used to drive two sets of counters. On the trailing edge of REF the first counter counts for 8ms. It then transfers its counts to the second counter which continues counting. The first counter is then disabled until the next trailing edge of REF, when it will once again count up to 8ms.

Meanwhile, the second counter continues to count and its output is decoded to produce Q,R, S and P, 9.5, 31.5, 34.5 and 56.5ms respectively, after the trailing edge of REF.

It can be seen that if only one counter were used then there would be contention at the next trailing edge of REF as this would want to re-trigger the counter, whereas the counter is still required to continue counting to produce P, approximately 3ms later. So the second counter is allowed to run on, whilst the first begins counting again. In this way, the beginning of each integration cycle can be synchronized with the trailing edge of REF.

The integration timer also controls the number of cycles in each integration period. The observer specifies the length of an integration, in units of seconds and this is converted into the corresponding number of half revolutions. Two eight bit binary counters are then loaded with &FFFF, less the number of half revolutions. The counters are then incremented by one each half revolution until they overflow, signalling the end of the integration, and disabling the pulse counters.

3.3.3 Pulse Counters

Twenty bit counters are used, constructed from five, four bit counting devices. (See Figure 3.10). The devices are capable of up/down counting. The direction of counting is determined by the

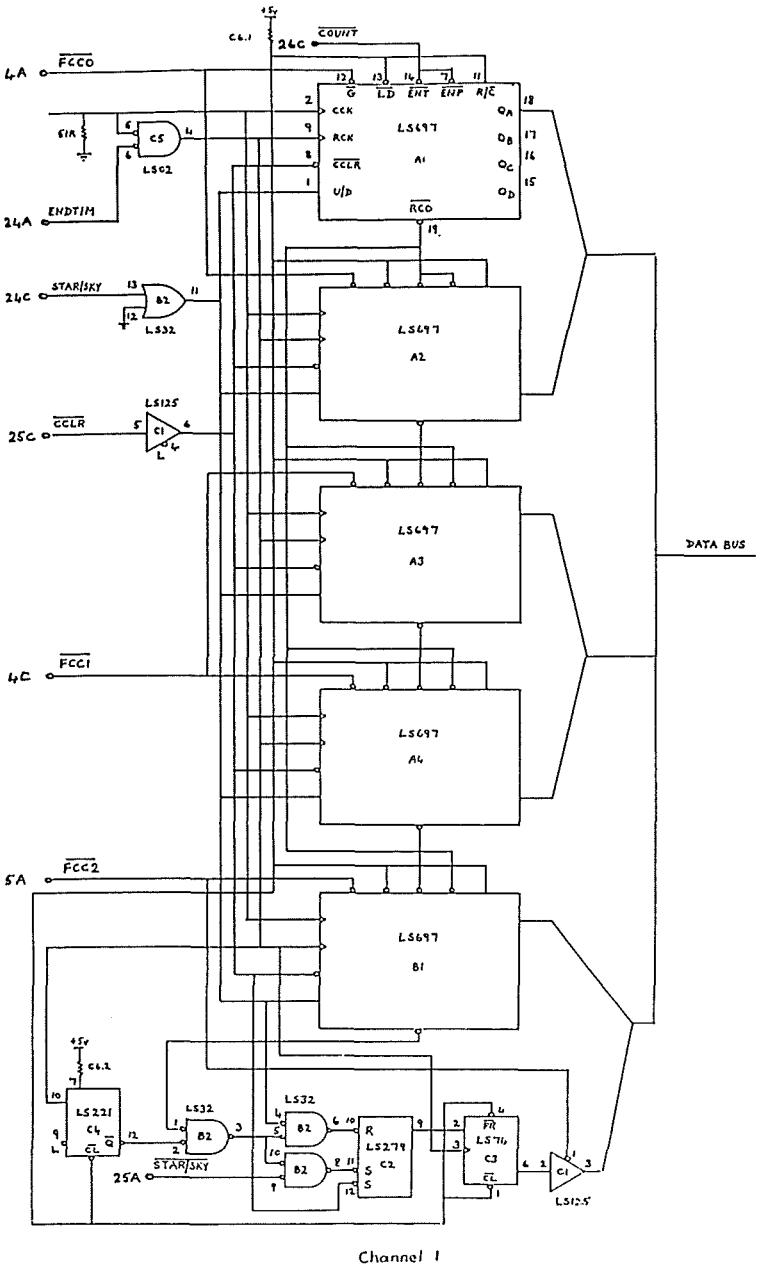

Channel 1

Fig.3.10 An individual pulse counter.

STAR/SKY line. The incoming pulses are gated through a monostable. The monostable ensures that all pulses to the counters are of the same length. It is only enabled when COUNT is low.

At the end of an integration, TIMOFLO sends ENDTIM high, which transfers the counts from the counters into the output registers. CCLR, generated by the integration timer after ENDTIM, clears the counters, so that the next integration can begin whilst the output registers are being read.

Whilst one aperture has been designated star plus sky and the other sky, it was foreseen that in some instances it could be necessary to place the object being observed in the sky channel. This would result in the counter counting more pulses ' downward ' than ' upward ', the end result being a negative number. But, due to the manner in which the counting devices work, this underflow would appear as a large positive number.

In order to differentiate between genuinely large numbers and small underflows, a flag is set when the counters underflow. By testing this flag we can verify the ' sign ' of the count and correct it if necessary.

3.4 ASSOCIATED ELECTRONICS

3.4.1 Power Supplies

There are two power supply units mounted in the rear of the 19" X 3U rack.

One is a Farnell switch mode power supply which provides the power requirements for the microprocessor as well as the control electronics and the various other motors. The +6V is derived from the 12V supply via a voltage regulator. The power is distributed to the boards via the backplane.

The other supply, provides the power requirements for the amplifier/discriminators and the EHT supply units.

The output from the EHT supply units, which are mounted on the photometer head, adjacent to the amplifier/discriminator units, is determined by the setting of the EHT controllers, Figure 3.11. The EHT supply units can supply a maximum of 3000V @ 0.5ma.

3.4.2 Connectors

A listing of all the various connections made between the individual units is given in the User Manual.

3.4.2.1 Backplane Modifications

The standard backplane provided with the rack system, which allows the processor card to talk to the other peripheral cards, was cut midway, leaving just the power rails to run the length of the backplane. An adaptor board was designed and constructed which took the output from the Synertek 6522 Versatile Interface Adaptor and placed them onto the now vacant bus lines on the backplane. In this way the control lines from the processor could be routed directly onto any of the control boards, without the need for any external connections.

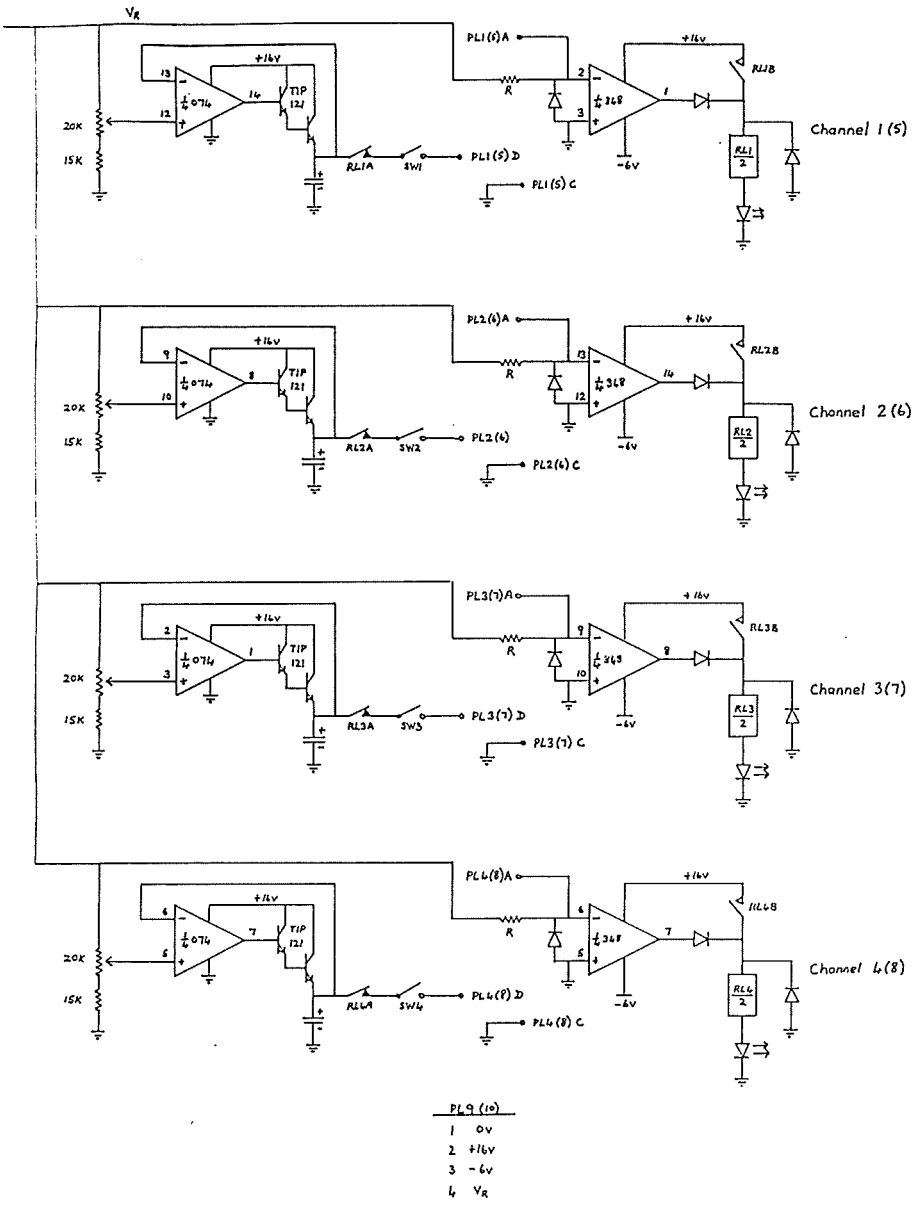

PL9 (10)
1 0V
2 +16V
3 -6V
4 V_R

Fig.3.11 EHT controllers for the photomultipliers.

CHAPTER 4

SYSTEM SOFTWARE

4.1 PHILOSOPHY BEHIND THE SYSTEM

Given the complexity of the system and the large quantity of raw data that can be generated, a high degree of automation was desirable. Also since it is envisaged that the instrument could be used abroad, there was the necessity that it should be a completely independent unit and should not rely on a fixed computer for its processing power.

Previously, data acquisition and control at St.Andrews has been largely centred around the use of LSI 11/23 computers (Bell and Hilditch 1984, Clampin 1985). Compounding the unfeasibility of transporting such hardware has been the use of FORTH as the programming language. Whilst this language has been used successfully in many astronomical applications (eg. Moore and Rather 1974) it has the disadvantage of not being easily transferable from one machine to another. Furthermore, since FORTH has a reputation of being a "write-only" language , modifications to the software, other than by the original author, can be prohibitively time consuming.

Over the last decade, there has been a growth away from using minicomputers, such as the LSI, NOVA and PDP's, and an increasing trend towards the development of inexpensive microprocessor-based systems for controlling astronomical instruments and also for data acquisition (Genet, 1983). In the past most applications have used

a computer exclusively for telescope control or exclusively for data-gathering and instrument control (Linnell, 1975). It was considered advantageous in this instance to make a further differentiation and assign individual processors to the data capture and instrument control.

The requirement was that the processing power for the photometer should be mounted on the telescope in close proximity to the instrument. This would greatly reduce the amount of cabling that would have to be run from the photometer to the floor of the dome. The processor for the data gathering would be sited on the floor of the dome, or in a central room, and so a means of communicating between the two had to be found.

4.2 PROCESSING CAPABILITIES

Given that the control processor had to be mounted on the telescope, it was a requirement that it be in a package which was robust and durable, and yet at the same time lightweight. These requirements pointed to the use of one of the many single processor systems.

The current choice in microprocessor hardware and software are overwhelming. This is especially so for those whose real interest is in the use of the tool, and not necessarily in its development. However the choice can be narrowed down by specifying certain desirable attributes.

A pre-requisite of the system was that it should be able to drive a large number of input and output lines, and that the control and reading of these lines should be readily accessible through the processor.

Another was that the programming language should be one that would be familiar to most astronomers, so that modifications could be made without recourse to assistance from the original author. The obvious choice here would be an implementation of BASIC.

Furthermore, should the need arise, the system should be easily upgradeable.

Whilst there are many single-board computers available that would fulfil the above pre-requisites (eg Intel 8052AH, Transtec 80286, NS 32000) they also have several drawbacks;

(a) With single board systems it can be very difficult to add additional features, either at the time of purchase or at a later date, due to the board being fully populated.

(b) Since the boards are provided in standard configurations, it could be difficult to find a manufacturer who provided a board from stock that would fulfil our exact requirements. There is also the likelihood of having to pay for features that would not be used. One possibility would be to order a custom board, but this would be prohibitively expensive.

The alternative approach is that of a rack system. Essentially, rack systems consist of a back-plane, or motherboard, into which individual cards can be plugged. The system would be based around a CPU Card (Central Processing Unit), which would contain the microprocessor chip. Other features, such as input/output capabilities, graphics etc., could be added to the system, on separate boards, as and when the need arose.

The advantages mainly arise out of the inherently modular approach in the assembly of such a system. It is only necessary to purchase what is required at the time, and if a standard backplane is used, boards can be purchased from different sources depending on specific requirements. Also, with boards designed for rack mounting, one invariably has ready access to the microprocessor bus. This is particularly useful if it is planned to construct in-house boards for inclusion in the system.

In early installations it was often planned that a back-up computer would be available. The rack system approach has the advantage that individual boards, rather than the whole system, could be replaced on the occasion of a failure. However, this is seldom necessary, as computers have proved to be amongst the most reliable part of the observing equipment (Robinson, 1975).

With the above criteria in mind, a survey of the available products was undertaken and a system which suited our requirements was assembled.

The system is centred around a number of cards manufactured by Control Universal. It comprises an address/data bus, which serves as an interface between the CPU card, known commercially as a 'Eurocube', and other modules. The backplane PCB is designed to accept a processor card in the leftmost position and can accommodate up to 15 more cards. The card mounts and connectors are based upon the industry-standard arrangement of rack-mounted Eurocards.

The CPU card holds the processing power, which comes from a 6502 microprocessor running at 1MHz. It also holds the operating system EPROM, a BBC BASIC interpreter ROM, two 8Kb CMOS RAMS, a Universal Asynchronous Receiver Transmitter (UART), which provides a serial

link, a Versatile Interface Adaptor (VIA), which can provide up to 20 input/output lines, a real-time calendar/clock and a battery, which acts as a back-up for the clock and CMOS memory.

The input/output capabilities of the system are served by a board equipped with 4 VIA devices (Synertek 6522's). These provide up to eighty input/output channels. Each line, or channel, represents one standard TTL load in the input mode and will drive one standard TTL load in the output mode. The configuration of these lines and their status can be controlled directly by the processor via the Eurocube address/data bus.

Finally, there is a teletext VDU interface card. This provides 1Kb of memory-mapped character storage RAM, which can be written to, or read from, by the CPU. The screen display is held in the video RAM which is mapped onto the memory of the host processor, allowing for fast direct screen access. The card allows the implementation of a dedicated console to display the control menu and the status of the photometer.

The cards and their power supply unit are housed in a standard 19" X 3U high rack system. As described in the previous chapter, the control electronics are also housed in this rack, along with the requisite power supplies. The backplane was modified halfway along its length to enable connections to be made between the processing electronics and the control electronics, which use the bus allocations differently

4.3 DESCRIPTION OF THE SOFTWARE ENVIRONMENT

Basic was considered to be the most desirable language to use to program the control processor, (for reasons mentioned earlier), so

the CPU contains a BASIC interpreter ROM. This supports a full implementation of BBC Basic.

The machine operating system on the CPU card contains a software environment similar to that of the BBC microcomputer. It holds the input and output drivers, subroutine calls and the serial filing system. In addition, the MOS contains all the peripheral drivers, (software to drive additional cards eg. the teletext card) and Control Basic.

Control Basic is an extension of BBC Basic, which provides Basic type commands for analog and digital input/output. It can be thought of as an extension of the BBC Basic interpreter. If the Basic interpreter does not recognise the word, it attempts to look it up in the variable list. If the word can not be found there, it is then passed on to the Control Basic extension.

Control Basic words work on channels, of which there are two types; those concerned with the digital access and those concerned with analog access. In this implementation we are only concerned with the former.

The digital commands relate to a Versatile Interface Adaptor, which can be positioned anywhere within the systems memory. If one or more VIAs are added, in the photometers case there are a total of four, then the VIA addressing should be contiguous. The ports on the VIAs are described as channels (on the first VIA, port A represents channels 0-7 and Port B, 8-15. On the second, Port A represents 16-31 etc.). Each channel can be defined from software as either input or output.

An input channel can be read using the statement IN;

```
microstate = IN 21.
```

The variable microstate takes the value of -1 (TRUE) if the input channel 21 is ON (ie. physically 0V on the input). Alternatively, the variable takes the value 0 (FALSE) if the input channel is in the OFF state (nominally +5V).

Output channels can similarly be defined as ON or OFF using the statements TURNON(X), TURNOFF(X). Again, +5V is defined as OFF (FALSE) and 0V is defined as ON (TRUE). Whilst this represents a logical inversion, at RESET all VIA channels default to input, and their output lines take the ' logic-high-state ' (+5V). It has therefore been implemented so that all outputs are tuned OFF at RESET.

4.4 DEVELOPMENT WORK WITH THE SYSTEM

The CPU has a serial port and communication software supplied in its operating system ROM (see 4.8 for a more detailed description). Thus development work can be performed from any suitable vdu terminal, or from a personal computer equipped with terminal emulation software (a Euro Development ROM). If a BBC microcomputer is used, then the CPU card can have access to the disc filing system, and also the printer port through the BBC.

During the development stage, software is held in the two 8Kb CMOS ROMS on the CPU card. Once the software is complete, it can then be transferred, or 'blown', into an EPROM which replaces the above ROMs.

The system can then be run as an independent unit, without a terminal. In the stand-alone mode, an autorun command line, consisting of a string of 24 bytes resident in the operating system, enables the software to be initialized when the system is powered up.

4.5 DESCRIPTION OF THE CONTROL SOFTWARE

The control software resides in two memory CROMS on the CPU board. A battery backup ensures that the software is retained even if the power to the CPU board is removed. The control program currently occupies about 10Kb of memory, leaving a further 2Kb for development.

This software is essentially a user-interface. It can be thought of as the point of physical interaction between the user and the photometer. The interface provides a means of controlling the photometer, liaising between the instrument and the user. It also provides a visual display of the current status of the photometer.

It was very desirable that the interface should isolate the observer from the complexity of the photometer. It should be able to replace complex or multiple commands with simpler commands or actions, thus minimising the chance of user errors. Through this ease of use will also come an increase in efficiency, therefore increasing the amount of time spent observing rather than setting the instrument.

One of the most popular approaches to these so-called ' user friendly ' interfaces is that of a menu system. Menu systems graphically present the available options to the user and choices are generally made by single key-strokes. The menus are typically arranged in a hierarchical order. The most frequently used and non-specific options are placed in the top menu, leading down to more specialized and less frequently used options in subsequent menus.

In the user-interface for the 8-channel photometer a two tier menu system is used, which gives the user full access to all of the instruments functions. The input to the system is centred around the use of the ten user-defined function keys on the BBC microcomputer. As each page of the menu is selected, the keys are re-defined and their new function visually displayed.

An initialization procedure first defines the base address of the four VIAs resident on the Eurocube input/output card. All channels are initially defaulted to be output channels. Then, the input channels are declared. These are mainly inputs from microswitches, except for a contiguous group of eleven, which are the input from a shaft encoder. The photometer is then set to a standard status. At the time of commissioning this consisted of; no comparison sources selected, the filter shutter set to blank, the grating-encoder position set to a pre-determined position, no photomultiplier filters selected and the acquisition mirror ' in '. The user can not alter this set-up position interactively, but can re-write the initialization routine should the need arise.

At this point the status word is set. The status word consists of a 14 character string which contains all the information the observer needs to know about the setting of the instrument. The string is built up in the following way;

1st character: This contains information about any comparison sources which may be being used. The options are N, A, B and C. N signifies no comparison source is in the beam and A B and C represent the three possible sources that could be selected. The user has to establish which sources A, B and C refer to when he inserts them into the holders.

2nd character: This bit contains information about the neutral density filters held in the filter shutter, which may be present in the beam. The options are A, C, D, E or F where,

A = blanked off

C = clear

D = neutral density 0.4

E = neutral density 1.0

F = neutral density 2.0

3rd character: These bits contain information about the interference filters directly in front of the photomultiplier tubes. Each filter has three holders, and these are referred to as 1 2 and 3. It is possible to have no filter in place and this condition is designated by a 0. It is the responsibility of the individual observer to know to which particular filter each number in the 8-channels corresponds.

Characters 11 to 14: These bits contain information on the position of the grating arm, which is derived from a shaft encoder. Under normal use, this position would not be altered by the observer, but would be determined at periodic calibrations.

A brief description of the menus will be given. Before any software alterations are undertaken the user is referred to the user manual where a more complete description of the control software can be found. A copy of the the program is given in Appendix A.

Main Menu:

From the main menu, the user cannot alter the status of the photometer. The main menu provides a pathway to other, more specific menus, which allows the setting of the photometer to be changed. There are a total of five other menus which can be accessed;

(a) Comparison Source,

(b) Acquisition Mirror,

(c) Filter Shutter,

(d) Photomultiplier Filters,

(e) Grating Rotator.

In addition, a screen giving an overall status report of the photometer can be accessed.

Comparison Source Menu:

This menu allows one of the three comparison sources to be selected and then either positioned ' in ' or ' out ' of the main optical path. A warning will be given if an attempt is made to rotate the source holder whilst a source is inserted. This acts as a backup to the electrical restraint described in the previous chapter. Power to the sources is not controlled by the software.

Acquisition Mirror Menu:

This menu allows the acquisition mirror to be remotely driven in or out of the optical path after the focal converter.

Filter Shutter Menu:

This menu allows any one of the six positions of the neutral density wheel to be selected. Software is used to drive a 90^{o} stepper motor until the desired position is attained. Three microswitches on the filter wheel generate a 3-bit grey code, which gives each position a unique address. Accurate positioning of the wheel is achieved using detents, as described in the previous chapter. The stepper motor is driven at a constant speed of 120steps/min. during filter change.

Photomultiplier Filter Menu:

This menu allows any one of four positions, for any one of the eight photomultiplier filter-units, to be selected. The filter number 0, 1, 2, or 3 is selected and the filter-unit number, 0 through 8, is selected. The ready key is hit and selection takes place. Alternatively, once the filter number has been selected, the key ' All Units ' can be hit and the chosen filter number is selected for all units.

Grating Rotator Menu:

This menu allows any one of the permitted grating positions to be selected. Movement from one position to another is achieved by specifying either incremental or decrementel intervals using the function keys. The position of the grating is determined from the 11-bit grey code output from an absolute shaft encoder attached to the arm. This grey code is read and converted to a denary number using a machine code routine.

The grating arm is driven by a 7.5^{o} stepper motor. To combine speed of operation and accuracy, the motor is driven at two speeds. Initially it is driven to the new position at the maximum driving rate. This is determined by the processors ability to turn a specified channel on and off. However, at this rate it is not possible to achieve the desired accuracy of +/- 1 step from the specified position. So, a routine is then used which drives the motor a tenth slower, correcting any error in positioning which may have occurred. An accuracy of +/- 1 step had to be imposed as it was found that, in some situations, the grating arm would oscillate about the selected position without ever reaching it because of the close match between the motor step and the resolution of the encoder.

Since the grating is only usually moved during the setting up of the instrument, and much of this procedure has been automated, (see Ch.5), a number of safety routines have been incorporated which prevent the software from attempting to drive the grating arm beyond its endpoints.

Software safety checks are incorporated into all the routines to prevent the user from damaging the photometer (eg. by the inadvertent activation of a motor). Although similar protection is built into the control electronics it was felt desirable to have a software backup.

The display is provided by a teletext vdu card driven by the processor. From this a simple and clear display can be generated, which shows the current use of the function keys and also the status display pertinent to the selected menu-page. Using this card for the display means that only a single co-axial line is required to feed a status display at any control console area.

4.6 DESCRIPTION OF DATA ACQUISITION SOFTWARE

The data acquisition software is run on a standard BBC B (64k) microcomputer equipped with a disc filing system ROM and dual disc drives. At the beginning of each observing run the data acquisition software is loaded into the BBC's memory from a 5 " floppy disc.

Briefly, the package allows us to do the following;

(a) Name a file to which the raw data will be written; The file will be created on a floppy disc, the contents of which can be later transferred to another computer for reduction (see sec4.8). The name of this file is only entered once, at the beginning of the observing run, or upon subsequent re-starting of the software.

(b) Create a header; The header will generally contain the identification of the object being observed. There is no restriction on the content of the header, but its length must not exceed 15 characters, (it will be automatically truncated if it does). A header is prompted for at the beginning of each series of integrations.

(c) Select neutral density filter; Any, or none of the neutral density filters can be selected.

(d) Select wide or narrow filter for Hb channel;

(e) Set the length of integration; The length of the integration is specified in seconds and can be any integer interval between 1 and 999 seconds.

(f) Set number of integrations on an object; This allows repeated integrations on an object without having to re-enter the header, length of integration, wide or narrow filter choice or neutral density filter. The number of repetitions can be any integer between 1 and 999.

The software checks that each input is acceptable before requesting the next. The sequence of integrations begins after RETURN is entered.

At the beginning of each integration the status word, time and date are read from the CPU card. The procedure PROCCOUNT then runs an integration for the set period of time. When the integration is finished, PROCDISC writes the header, length of integration, status word, time, date and the 8 count rates to disc. This sequence is repeated for the number of integrations specified.

The observer then has the option of

(a) keeping the same header but specifying different filters or a new integration time,

(b) re-setting all the parameters including the header,

(d) terminating the session.

The two main procedures are outlined below.

PROCCOUNT

The integration time is changed from seconds into the equivalent number of half revolutions of the aperchopper. This number is then loaded into the counters in the integration timer. The integration is started and continues until the remaining number of half-revolutions

equals zero. (the integration period is terminated by hardware, not software). The contents of each counter are then read and stored in an array. The software/hardware is now ready to begin another integration.

PROCDISC

This procedure is used to assemble a string, in a reserved section of memory, containing the information outlined previously (header, date, clock etc.). The information is assembled as an ASCII string of fixed length. The string is then written to disc, byte by byte using the Basic command BPUT.

A listing of the acquisition software is given in Appendix B.

4.7 COMMUNICATION BETWEEN THE TWO SYSTEMS

The two processing systems pass information and commands between each other using a serial link.

The serial communication channel on the control CPU card is based on a 6551 UART (Universal Asynchronous Receiver Transmitter), with RS-423 drivers and receivers, (RS-232 compatible). The BBC microcomputer also has a similar serial port.

A communication link could be accomplished by simply connecting the two serial ports back to back (ie. transmit to receive).However, to avoid loss of data, handshaking lines are added. This is effectively a BUSY signal from the receiver telling the transmitter to wait. The transmitter tests whether it is clear to send (TxENABLE or CTS) and flags whether its receiver is ready. The connections necessary for using a BBC microcomputer as a terminal for the control CPU are shown in Figure 4.1.

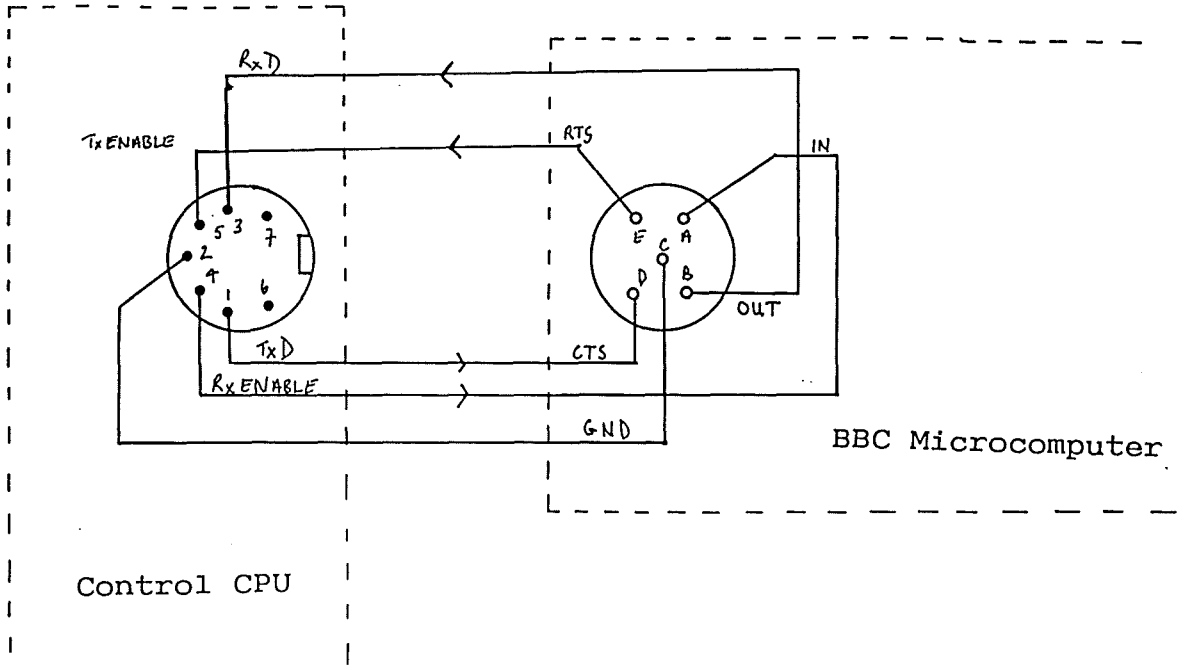

Figure 4.1 Using the BBC micro as a terminal to the Control CPU.

The baud rate of the two devices is set using the OSBYTE calls &07 and &08. Similarly, the serial link can be turned ON and OFF using OSBYTE calls &02 and &03.

Using this serial link it is possible to send commands to the control software, eg. to change filters, from within the software running on the BBC microcomputer. Also, data, such as the status bit and time from the clock, can be passed from the control CPU to the BBC microcomputer.

4.8 FILE TRANSFER PROTOCOL

At the end of each evenings observing, the data collected on the floppy disc(s) will need to be transferred to the computer on which it will be processed. In our case this is the University Observatory's Microvax.

If a dumb terminal emulator were used the data would appear on the VAX byte-for-byte as it was on the BBC microcomputer. This would create a file with extra line feeds and carriage-returns that would need laborious editing before the file could be processed. So rather than use a ' dumb capture ' program to transfer the data, a file transfer protocol system, KERMIT, has been used.

KERMIT is a system devised to permit the simple and flexible transfer of data from a microcomputer to a mainframe, (or to another microcomputer).

With KERMIT the above problem is easily avoided. The KERMIT protocols define a standard way of indicating the end of a printable line. The file sent from the BBC microcomputer has whatever ends the line of text, (LF,CR), transformed into a standard form. The

receiving end, seeing this adopted standard, will substitute for it whatever the VAX uses to indicate an end-of-line. Thus no extra characters are introduced, leaving a usable file.

The requirements that must be met for using KERMIT are that there are;

(a) a BBC KERMIT ROM in the BBC microcomputer,

(b) a KERMIT program in the targetted system,

(c) a means of linking the two machines.

CHAPTER 5

COMMISSIONING THE PHOTOMETER

5.1 INTRODUCTION

This chapter outlines the steps taken in commissioning the photometer; that is, preparing the instrument so that it can be used for a programme of astronomical observations. Some of the procedures could only be carried out with the photometer removed from the telescope, whilst others required that it be in position. The two sections to this chapter reflect, broadly speaking, this natural division.

5.2

5.2.1 Calibration Unit

The primary use of the calibration unit has been to hold a spectral discharge tube whilst either setting the grating angle or running flexure tests with the photometer mounted on the telescope.

As well as this function it has been used to introduce stable sources into the optical path beam. One of the racks has been adapted so that it will carry a tungsten-filament bulb, which was used as our standard source. To prevent any possible obstruction of the input beam from the telescope whilst observing, the calibration source can be removed in tests and the resulting aperture made light-tight with black tape.

5.2.2 Neutral Density Filter Wheel

The mechanical construction of the neutral density filter wheel has been described in Ch.3.2.3. In Ch.4, the software used to drive the system is outlined.

It was decided when assembling the neutral density system that the wheel would be limited, (mainly for mechanical reasons),to one direction of rotation. Although this means that the least number of steps will not always be taken to change from one filter to another, it does have several advantages.

Firstly, the filters can be arranged in such a way that the density progressively increases as the wheel rotates. (Naturally, if the wheel is rotated through more than 360^{o} there will come a point when the density will decrease). This means that if the count rate for a source is found to be too high, a filter with a larger density can be introduced without the risk of the photomultiplier tubes being exposed to the source through a less dense filter. Since the neutral density filters are common to all photomultipliers this precaution will safeguard all of them from possible damage.

Secondly, by always stepping in the same direction, we achieve greater repeatability in the positioning of the filters in relation to the entrance aperture. This repeatability is essential since, if there are any inhomogeneities across the filter then it is important that the same part of the filter is used in every measurement. If not, there will be no consistency in the degree of attenuation between successive measurements.

Initial tests with the unit showed that there was a large degree of backlash in the gearing system (as much as 10^{o}, measured in the six position filter wheel). In order to overcome this problem a detenting mechanism was designed and constructed.

A series of six holes were drilled into the top surface of the geared cam which houses the neutral density filters. A small mounting pillar was fixed adjacent to the filter wheel providing a securing point for a tensioned arm which has a ball-headed plunger attached to it. The plunger rides on the cam and locates in the detent holes. The tension in the arm was adjusted such that it is sufficient to overcome any backlash in the system, yet does not prevent the stepper motor from driving the wheel to the next position.

It was also noted that, when the stepper motor coil was de-energised, the shaft from the motor would turn slightly as it settled into a different position. One solution would have been to leave the motor permanently energised by 'enabling' the micro-chip that was being used to drive it. However , this would have left the motor coils energised at their working current, causing the motor to dissipate a large amount of heat energy within the photometer which is undesirable.

The problem was overcome by disabling the driving micro-chip whilst still providing the coils with a reduced current, sufficient for the motor to hold its position yet causing negligible heating.

These modifications to the original design allow the neutral density filter to achieve repeatability of positioning to within 1^{o}.

5.2.3 Aperchopper

Ch.2.3.6 describes the aperchopper as it is now installed in the photometer. The original aperchopper was similar in design but produced its reference pulse from two semi-permanent magnets which were positioned on an outer radius of the wheel. The initial intention was to use these reference pulses to signal the start of each star/sky integration period. After preliminary tests with the original wheel it became apparent that there was too much variation in the rate of rotation of the wheel for this to be feasible.

A second wheel was manufactured to high precision which produced reference pulses as outlined in Ch.2.3.6. Whilst there were improvements in regularity with the new wheel, there was still too much variation to allow direct timing of the integrations based upon the reference pulses.

A motor speed controller was then used in order to improve the stability of the aperchopper. With the motor running at 100ms/rev the degree of variablity over a single cycle is now +/- 0.2%, compared with up to 2% previously.

The reference pulse is used to trigger an integration timer, the functioning of which is described in Ch.3.3.2. The timer effectively creates "windows" during which counting may take place. Given that there is still some variability associated with the aperchopper these windows must be shorter than the physical windows produced by the slots in the aperchopper. However, with the stability of the motor improved by the motor controller, the loss of available light has been kept to 12%, (compared with a theoretical minimum loss of 6.7% as defined by the dimensions of the slots).

5.2.4 Grating Rotator

The mechanical construction of the grating assembly is outlined in Ch3.2.4. As with other sections of the photometer, the grating unit had to be dismantled, re-worked and re-assembled before it would run freely.

Reading of the encoder is achieved using a machine code routine. The encoder has been set such that a monotonically increasing/decreasing output is produced as the grating is rotated between its two limits.

Difficulties arose with the driving of the stepper motor. If too fast a stepping speed is attempted then the motor is unable to respond to the rapid changing of the state of the coils and the motor suffers from a resonance effect. By observing the performance of the motor, the maximum stepping rate was found and set.

However, this maximum stepping rate is achieved at the loss of some accuracy, eg. when stepping over some 300 steps as many as 10 steps may be gained or lost. It is therefore necessary to include a correction algorithm, with the motor stepping at a tenth of its previous rate to achieve an accuracy of +/- 1 step.

It was observed that there were certain encoder positions at which the grating arm would not settle. The unit would be either one position above or 1 position below the desired position. If a tolerance of +/- 1 step had not been allowed, then the software would have caused the stepping motor to oscillate about the position endlessly. (It will be seen later that this degree of accuracy of setting the grating arm is adequate).

5.2.5 Photomultiplier Filter Units

The mechanical construction and operation of the photomultiplier filter units have been described in Ch.3.2.5.

Upon examining the units it was found that they had been assembled in such a manner that the slides were not running freely in their guides. In some, this meant that the springs used to retract them were unable to do so, whilst, more seriously, in others the resistance was such that there was the possibility of damaging the small reduction gearboxes which were being used to drive them. Fortunately in only one gearbox were the gears stripped of teeth before this problem was discovered and this unit was subsequently repaired in the Observatory workshop.

These problems necessitated that the units be dismantled, modified and re-assembled to ensure their good running and prevent any further damage to their drive gear.

As we saw in Ch.3, the filters are held in place by two sprung-steel clamps. However, the original design of the clamps meant that pressure would have only been applied to the uppermost point of the filters with the result that they would have been liable to rest at an angle within the clamps and , more importantly, the filters would be incorrectly optically aligned.

To overcome this problem, thin aluminium strips were secured to the inside edge of the clamps using a double-sided adhesive tape. Black plastic tape was placed on the exposed metal edge to prevent damage to the filters. With these blocks in position, the springs now exert pressure along the whole of the short length of the filters and ensure that they are held parallel to the filter-slide action.

Further assembly problems were encountered when assembling the units into the photometer head. The D-type sockets on the filter units had been provided with captive nut assemblies, so that the plugs from the distribution box would be held secure. The face panel through which the sockets protruded had to be adapted so as to allow access to the captive nuts. Also, recesses around the socket exits had to be made to allow clearance for the hoods covering the plugs.

5.2.6 Photomultiplier Operating Voltage

In order to appreciate the importance of determining the voltages at which to operate the photomultipliers, it is necessary to understand the manner in which the output signal is generated and the sources of noise generated which are present within the system.

First consider the incoming light as a stream of photons. On striking the photocathode a statistically constant number of the incident photons will give rise to the emission of a single electron (photoelectron). The equivalent current produced by this single photoelectron is very small and so needs to be amplified before it can be used to drive a counter. Unlike the early photocells, which relied on a high gain external amplifier, the photomultiplier produces its own internal amplification.

In order to achieve this amplification, the initial photoelectron released by the photocathode is accelerated towards a metal surface which is maintained at a potential of a few hundred volts positive with respect to the photocathode. This metal surface is called a dynode. (The dynode is not generally a pure metal but a combination of metals forming a semiconductor. The properties of the material are generally similar to those of the photocathode ie. low electron

affinity and long photon mean free path. However since the incident radiation is now an energetic electron, as opposed to a photon, good optical absorption is no longer a problem).The photoelectron strikes the dynode with sufficient energy to release several secondary electrons. These electrons are in turn accelerated towards another dynode which is maintained at a similar potential difference from the first dynode. This process is repeated for successive dynodes until the last dynode will produce typically one million electrons for every primary electron. A further electrode, called the anode, situated close to the last dynode collects the charge pulse and passes it to external electronics.

If δ is the dynode secondary electron yield, defined as the average ratio of secondary electrons emitted per primary electron, and N represents the number of dynodes in the electron multiplier then the internal electron multiplier gain G is

$$G = \delta^N$$

The internal current amplification produced by the dynode chain is an important characteristic of the photomultiplier tube and is essentially noise free. However there are, unfortunately, noise sources present within the tube, (where noise is defined as any output current that is not the result of a photon striking the photocathode).

The noise consists of four main components.

(i) Thermionic emission by the photocathode.

This is the spontaneous emission of an electron by the photocathode in the absence of an incident photon. These signals are indistinguishable from those caused by a light source. The resultant count from these thermal electrons is called the dark current or, dark count.

In general, the dark current is an exponential function of absolute temperature, so the logarithm of the dark current is nearly a linear function of T (Young, 1974). The obvious way of reducing this contribution is to cool the tube. Also, the thermal emission from the photocathode is approximately proportional to the area of the photocathode, so that reducing the photocathode area will reduce the dark current (Eccles, 1983).

(ii) Non Thermionic Emission.

Cosmic rays and the decay of radioactive isotopes in the photomultiplier window can produce flashes of light which are seen by the photocathode. These events set the minimum photon rate detectable.

(iii) Emission from within the multiplier chain.

Thermal electrons can also originate from the early stages of the dynode multiplier chain. Electrons released from any point other than the photocathode will undergo at least one stage less than full multiplication. The resultant electron burst at the output will therefore be less than that associated with electrons released from the photocathode.

(iv) Electrical noise.

Pickup in the signal leads and noise in the amplification and associated circuitry can give rise to spurious pulses which do not originate in the photomultiplier. Whilst the number of these pulses can be kept small it is not possible to totally eliminate them.

Figure 5.1 shows the pulse height distribution in a typical situation. With the use of a discriminator it is possible to reject the small pulses arising from cases (iii) and (iv) and so improve the signal-to-noise ratio.

Figure 5.2 shows the typical count rate behaviour of a photomultiplier as the operating potential is increased. From this we can clearly see that it is desirable to operate the photomultiplier at a voltage that falls within the range of the plateau. Away from the plateau a small variation in operating voltage will cause a large change in the sensitivity of the photomultiplier.

Ideally then, if we wish to accept only those pulses belonging to a specific part of the pulse height distribution and to have a system which is relatively insensitive to drift in the applied potential, we must specify both a discriminator setting and the value of the E.H.T..

In the case of the 8-channel photometer the approach taken was as follows. The discriminators were set to a level such that the majority of noise pulses were rejected. (The discriminators in this case are not windowing devices ie. there is no upper level cut-off). With the photomultipliers illuminated by a weak source, the E.H.T. was then increased. At each voltage setting the count rate was recorded, integration times being typically 10 seconds or longer. The tube voltage was increased up to the manufacturers maximum recommended

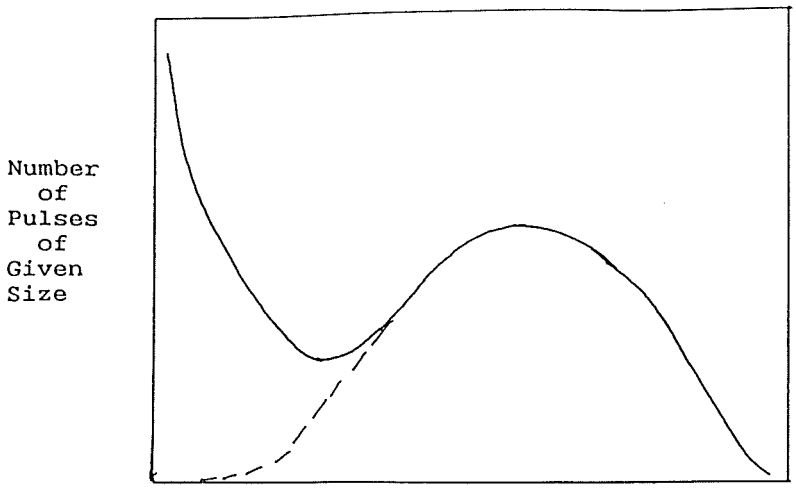

Fig.5.1 Pulse height distribution for a typical Photomultiplier. The dotted line indicates the likely distribution of small pulses from the cathode alone.

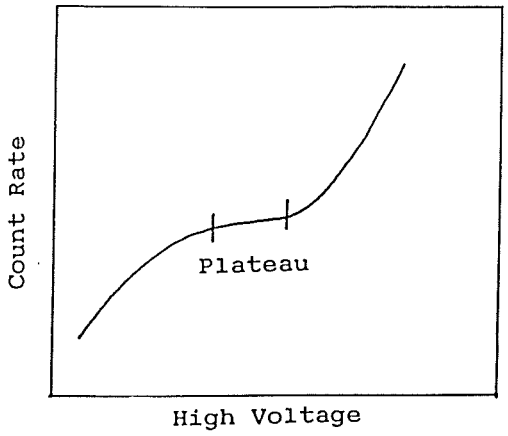

Fig.5.2 Typical count rate behaviour of a photomultiplier tube to variations in anode to photocathode voltage.

value.

A typical plot of E.H.T. with count rate is shown in Figure 5.3. From this we can establish an optimum E.H.T. value for the tube. The values used for each tube are given in Table 5.1.

Working with these E.H.T. values, the discriminator thresholds could be lowered to ensure that no counts were being missed. An optimum setting of 50mV has been used for all the discriminators. This corresponds to an average gain in the photomultiplier tube of 10^5, an order of a magnitude down on that which an electron released from the photocathode would undergo.

5.2.7 Setting Grating Angle

The design angle of incidence for the grating is 7.12°. The setting of this angle is critical as it determines the wavelength breakpoints of the mirrors. There is no facility for a direct measurement of the grating angle to be taken. All that is available is a value from the grating encoder which must be translated into a grating angle. Determination of the correct grating position was achieved in the following manner.

Consider the grating equation:

$$n\lambda = d(\sin\theta - \sin i)$$

Here we are considering the first order reflection only, so n=1. The line spacing for the grating is 300 lines mm-1, d being the number of lines per mm.

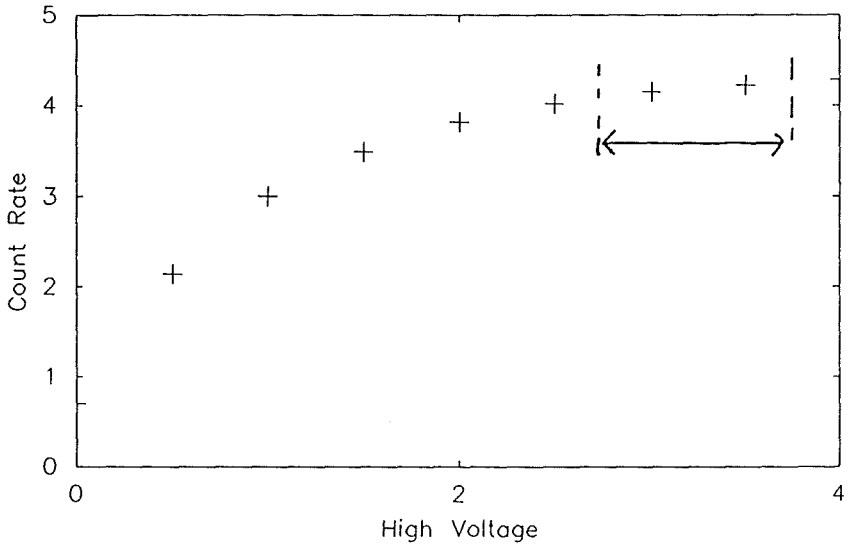

Fig.5.3 Actual plot of count rate behaviour with E.H.T. used to set operating voltage. A voltage would be chosen over the range indicated.

So for i , the angle of incidence, set to the design angle, 7.12^{o}, we can compute a value for θ , for the central wavelength, λ_c , of each mirror from the equation,

$$\theta_c = \sin^{-1}\left(\frac{\lambda_c}{d} + \sin(\text{rad}(7.12))\right)$$

Now suppose we were to rotate the grating through some angle φ . We can then form the equation,

$$\lambda_1 = d(\sin(\theta_c - \varphi) - \sin(i + \varphi))$$

λ_1 now becomes the new central wavelength.

Each step of the grating rotator motor corresponds to a rotation of the grating of 5 , or 1/720 of a degree. If we make φ equal to 1/720 of a degree, than we can calculate how many steps of the grating rotator would be necessery to replace the original central wavelength with the new wavelength λ_1 .

What we need now is to establish at what grating position a known wavelength is at the centre of a mirror.

To achieve this we use a mercury spectral lamp to produce the principal lines of mercury as follows:

nm

546.07

435.84

404.77

404.66

365.48

365.01

253.65

The grating was initially set at an angle of approximately $i=7^{o}$. The encoder was then adjusted so that its reading was halfway between its maximum and minimum output. The grating was then rotated to approximately a degree less than its design angle. With the discharge tube switched on the grating was then stepped, in 3 motor-step intervals, through 2^{o}. At each position a recording of the $counts^{-1}$ and grating position was recorded.

Initially the counts had to be recorded manually using an independent counting system. This was necessary since the aperture slide only had pairs of apertures in it. Since the counters built for the photometer are up/down counters and both apertures would be filled with the same source the nett count would be zero, (within statistical limits). The solution to this problem was to provide a single small aperture within the aperture slide for calibration purposes. The total count was now that of source plus dark counts, minus dark counts.

It was also observed that there were contributions that were not attributable to the first order. The most likely cause seemed to be that light from the zeroth order was undergoing grazing reflection on the casing supporting the camera mirror. This reflection was suppressed by placing a baffle on the mirror casing. The baffle consisted of an L shaped piece of metal which had one surface covered in black velvet to prevent further reflection of the zeroth order light within the photometer head.

COMMISSIONING THE PHOTOMETER

To supplement the measurements taken using the mercury source, a laser source was also used. A He-Ne laser was used producing the familiar red 632.8nm radiation.

A control program was subsequently written which interacted with the software in the Eurobeeb and allowed the whole procedure of data logging to be automated. Measurements were taken with the grating being rotated in both directions to avoid systematic errors.

A plotting routine, DIPSO (available in the Starlink software) , was used to display the results and to estimate the grating position which corresponded with a spectral feature being in the centre of the mirror. Had the aperture been a point source then the signal profiles produced as the spectral image entered and left the mirror aperture would have been sharp edged (limited by the Airey-type profile). Since it is not a point source the profiles are not sharply defined, but show a gradual build up and decline of count rate as the image spot enters and leaves a mirror aperture. It was this inability to precisely define either the short or long wavelength 'edge ' of the mirror that led to the centre of the mirror being used as the reference point, ie. the condition when the spectral image is centred within a mirror aperture.

By estimating the central position for several wavelengths on 5 of the mirrors it is possible to arrive at estimates for the encoder reading which will place the grating at the design angle. The results are shown in Figures 5.4, 5.5 and 5.6, with the calculated positions in Table 5.2.

Table 5.1 E.H.T. operating values.

Channel 1	1800V
Channel 3	1800V
Channel 4	1750V
Chennal 5	1700V
Channel 6	1700V
Channel 7	2350V
Channel 8	2650V

Table 5.2 Grating position for spectral feature centred on mirror mosaic. To avoid systematic errors the spectral features were centred in the mirrors from two directions. Both resultant grating positions are shown.

	Wavelength nm.	Grating Position
Channel 1	253.6	1384
	365.0	1395
	365.0	1393
	253.6	1383
Channel 3	435.8	1397
	435.8	1394
Channel 4	365.0	1387
	404.6	1385
	435.8	1394
	435.8	1385
	404.6	1387
	365.0	1388
Channel 5	435.8	1385
	546.1	1383
	546.1	1390
	435.8	1386
Channel 6	632.8	1395
	632.8	1394

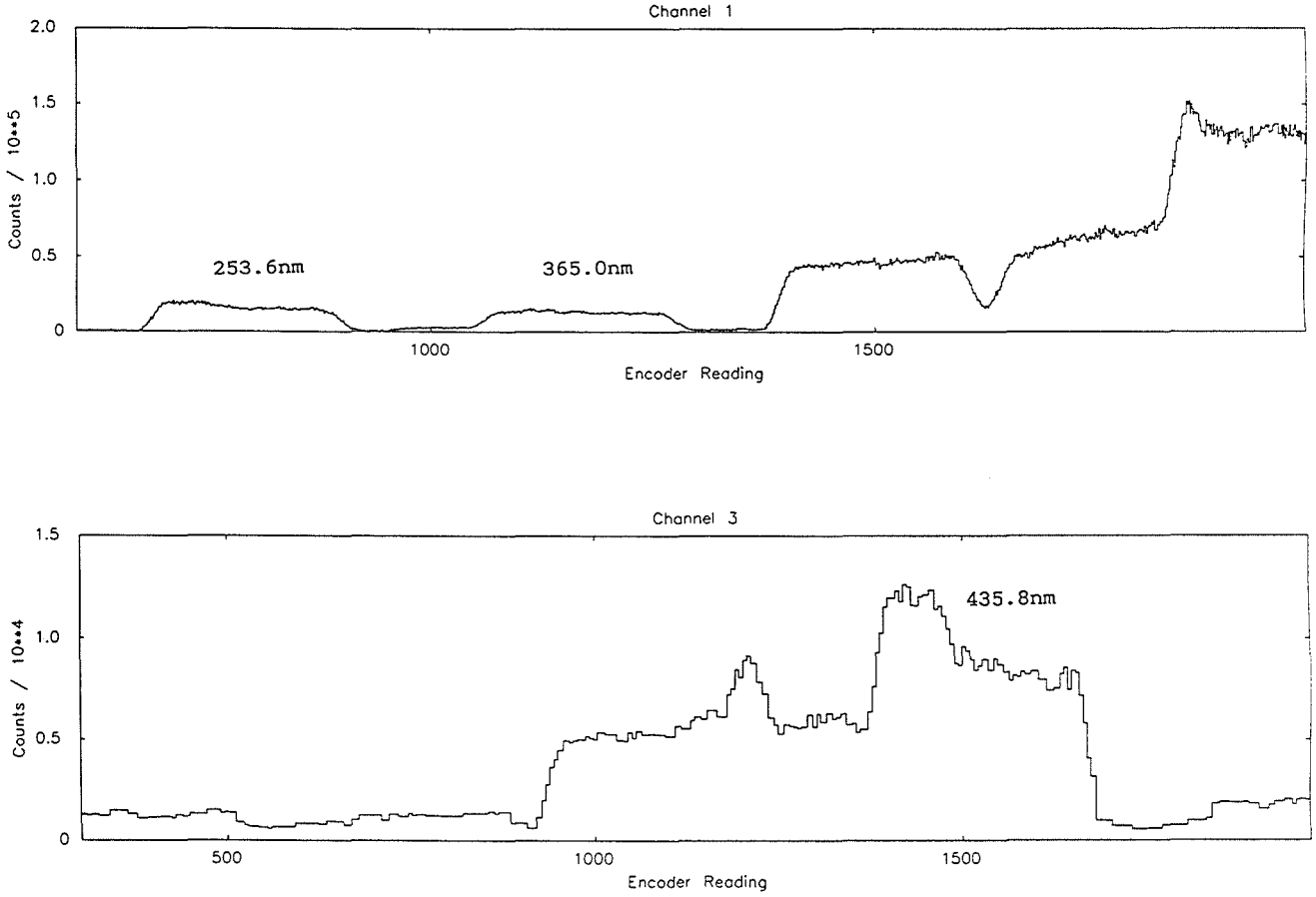
Channel 1
2.0
1.5
1.0
0.5
0
Counts / 10**5
253.6nm
365.0nm
1000
1500
Encoder Reading
Channel 3
1.5
1.0
0.5
0
Counts / 10**4
435.8nm
500
1000
1500
Encoder Reading

Fig.5.4

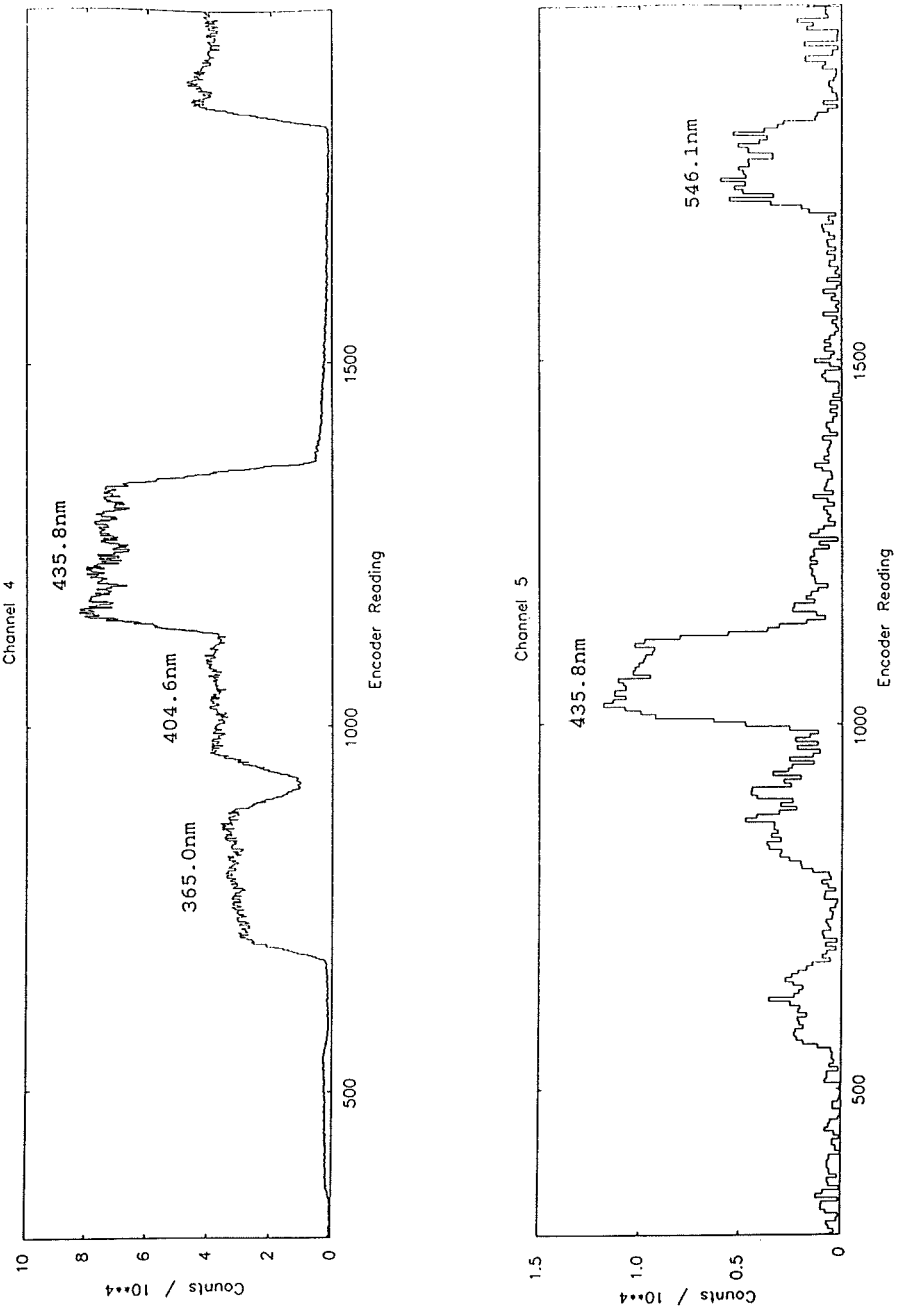
Channel 4
435.8nm
404.6nm
365.0nm
Counts / 10**4
Encoder Reading
0
2
4
6
8
10
500
1000
1500
Channel 5
435.8nm
546.1nm
Counts / 10**4
Encoder Reading
0
0.5
1.0
1.5
500
1000
1500

Fig.5.5

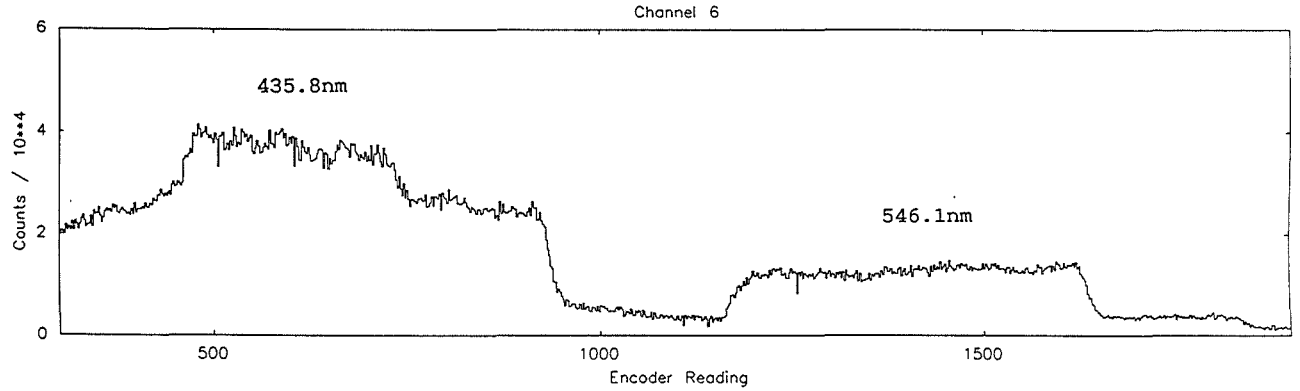
Channel 6
435.8nm
546.1nm
Counts / 10**4
Encoder Reading
0
2
4
6
500
1000
1500

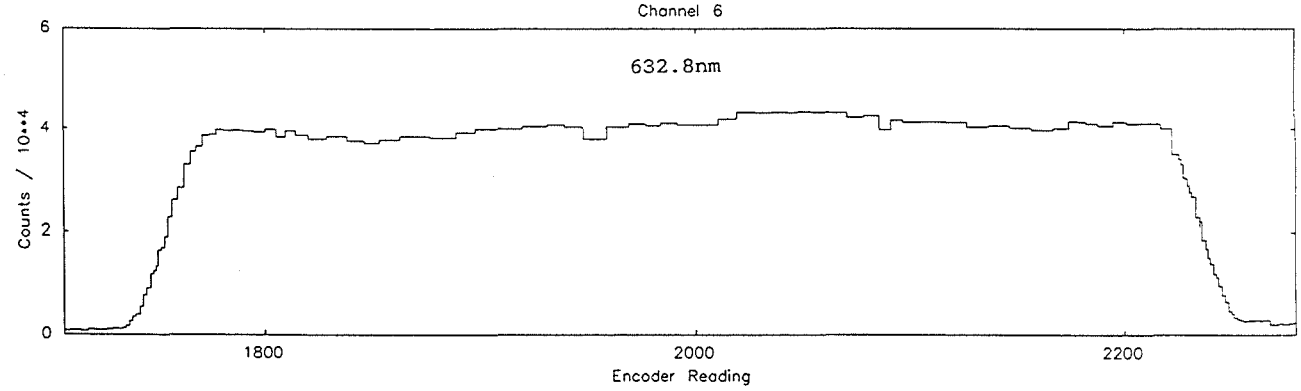
Channel 6
632.8nm
Counts / 10**4
Encoder Reading
0
2
4
6
1800
2000
2200

Figs.6

The final encoder position selected was 1385. The standard deviation being approximately 10 steps, which corresponds to less than 0.02^{o}, which corresponds to approximately 1.5nm.

5.3

5.3.1 Optical Assembly

The mounting of the optical components has already been described in Chapter 2. Since the optical alignment was primarily carried out by Dr.Edwin only a brief outline of the procedures will be given here.

For the collimator a zero order beam from the grating was viewed using a long focus telescope. The collimator focus was adjusted until a sharp image could be seen in the telescope of an illuminated target placed at the entrance aperture. The tilt of the collimator was adjusted in its cell using autocollimation onto the entrance apertures.

The camera mirror tilt was adjusted to bring the spectral images of the aperture pairs central along the line of the mirror mosaic. Checks were made that optics, including the grating, were correctly aligned. The camera focus was adjusted to produce sharp spectral images in the mosaic mirror plane.

Cardboard discs were placed in the photomultiplier exit apertures in the photometer case. Pinholes in the centre of the discs defined an optical centre. If the mosaic was now viewed via the camera mirror aperture, the central hole in each disc should be seen at the centre of its corresponding mirror. Most of the channels were observed to be out of alignment and in particular channel 2 was noted to be very much out of alignment.

Shims had to be inserted both underneath and to the side of the individual mirrors to alter their orientation within the mosaic jig. This was done for the channels that were slightly misaligned until the central pinhole was observed to be in the correct position on its mirror. However, in the case of channel 2, it was found that the angles of orientation in the X,Y plane had been transformed during manufacture and it was not possible to correct this. The result being that, with the present mirror mosaic, it is impossible to use this second channel.

5.3.2 Balancing Telescope

The James Gregory telescope was built and is primarily used for taking photographic plates. The replacement of a plate holder with a large, heavy photometer necessitated that the telescope should be rebalanced.

Initially the balancing weights located at the bottom of the telescope tube were removed and the photometer mounted. However, this one adjustment was insufficient. Additional weights had to be placed at the top of the telescope tube before the telescope could be driven in declination. Also, the main counter balancing weights had to be withdrawn to their outer limits on the arms of the telescope before driving and slewing in right ascension was satisfactory.

5.3.3 "O" Rings

The "O" rings, which act as RFI shields and optical seals, are located at the inside edge of the cold box windows. The material was supplied as a long length of hollow rubber tubing. It was cut into 8 sections to make rings of the required diameter.

Attempts to use an adhesive to join the ring ends were unsuccessful due to the porous nature of the material. Since the material was hollow, small inserts of plastic sleeving were fitted inside which allowed the two ends to be joined.

A further complication was that when the cold boxes were attached to the photometer head the "O" rings were compressed against the connectors for the no-dew heaters. Since the material used to manufacture the "O" rings is conductive, the connectors had to be covered with insulating tape.

5.3.4 Flexure Testing

It was important that instrument flexure would not alter the spectral calibration and channel bandpasses significantly. To establish whether there was any movement of the optical components within the photometer head when the telescope is in different orientations, the scanning procedure described in section 5.2.4 was used. The telescope was moved to various positions and scans were taken using the mercury discharge tube for illumination. The data were analysed to attempt to detect shifts between data taken with the telescope away from the zenith and that taken with the telescope pointing at the zenith. Comparisons were also made between scans taken when the photometer was on the telescope and when it was on the bench.

The various telescope positions in which measurements were taken are shown in Table 5.3.

Cross-correlation tests were used to determine the amount of drift. (A negative mirror image was superimposed to highlight the amount of shift and aid measurement). The results are shown in Table 5.3. The plots are shown in Figures 5.7 to 5.21. We can see that the amount of shift detected never amounted to more than approximately 10 grating positions, which is negligible and of the same order as the precision of the grating setting.

5.3.5 Testing The Counters

The operation of the counters has been described in Chapter3.

Initially the accuracy of the counters was tested in the electronics workshop using pulses from a radio-code clock. For these tests a machine code routine was written which was used to read the counters and transfer the output to disc.

When the counters were transferred to the optical workbench and fed with pulses from the photomultiplier tubes certain irregularities were noted.

The first problem was the setting of extra bits in the 4 most significant bits giving rise to very large counts. This was thought to be due to a reading error, but was eventually traced to a hardware fault in the backplane which was corrected.

The second fault occurred after transferring the counters into the dome. Again, the problem was manifest in the generation of exceptionally high counts when the true count rate was known to be low. The fault was seen to be in the incorrect generation of borrow bits. After investigation it was found that the RCO outputs of the counters were producing glitches. The RCO output from the 4

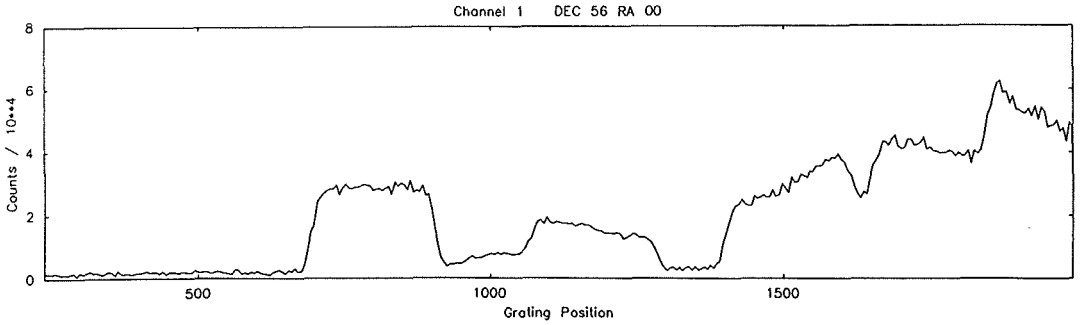
Channel 1 DEC 56 RA 00
Counts / 10**4
Grating Position

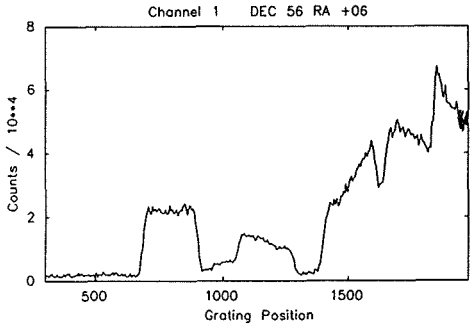
Channel 1 DEC 56 RA +06
Counts / 10**4
Grating Position

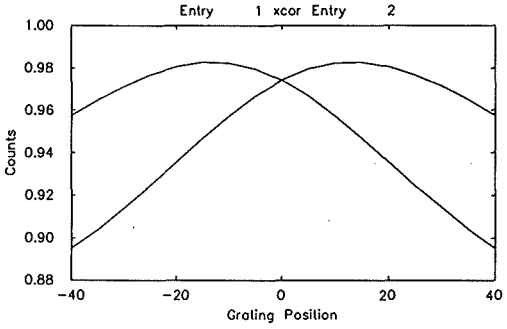
Entry 1 xcor Entry 2
Counts
Grating Position

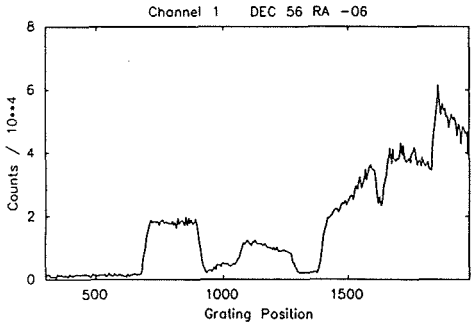
Channel 1 DEC 56 RA -06
Counts / 10**4
Grating Position

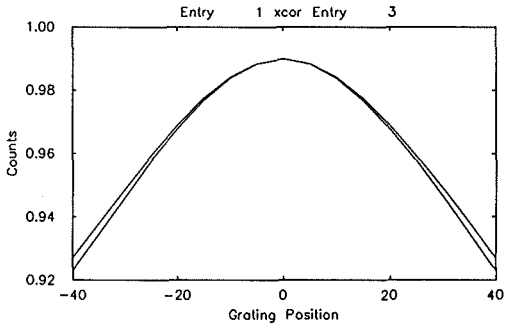
Entry 1 xcor Entry 3
Counts
Grating Position

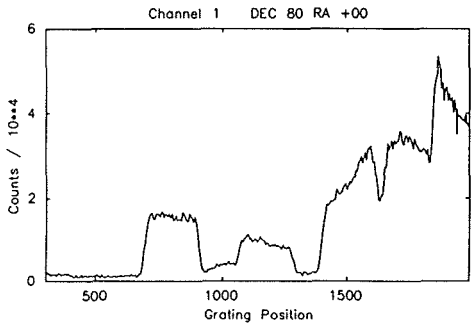
Channel 1 DEC 80 RA +00
Counts / 10**4
Grating Position

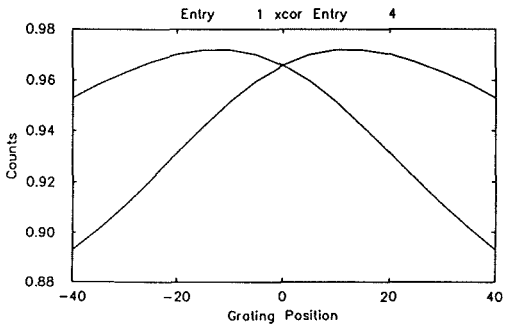
Entry 1 xcor Entry 4
Counts
Grating Position

Fig.5.7

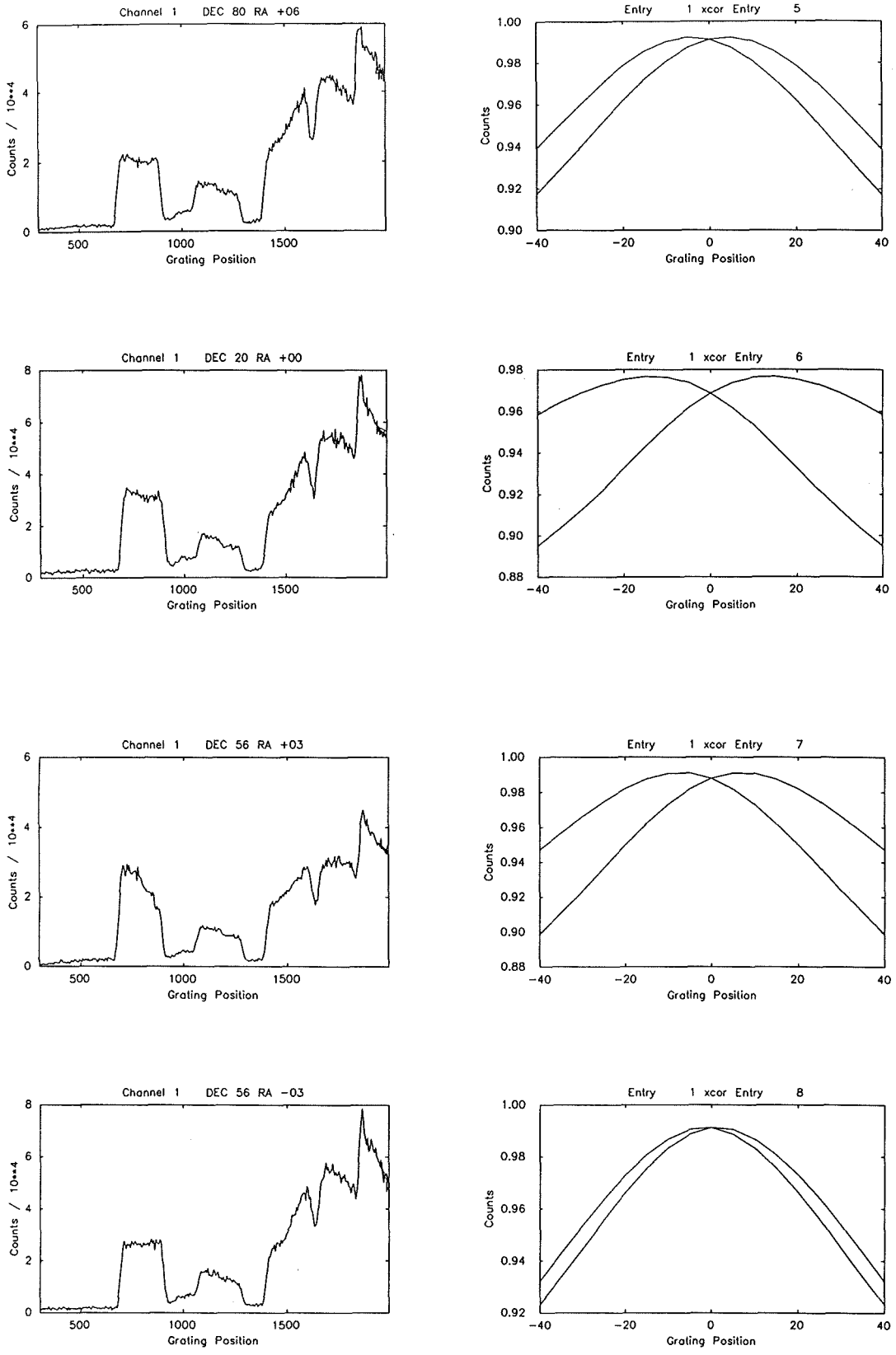
Channel 1 DEC 80 RA +06
Counts / 10**4
Grating Position
Entry 1 xcor Entry 5
Counts
Grating Position
Channel 1 DEC 20 RA +00
Counts / 10**4
Grating Position
Entry 1 xcor Entry 6
Counts
Grating Position
Channel 1 DEC 56 RA +03
Counts / 10**4
Grating Position
Entry 1 xcor Entry 7
Counts
Grating Position
Channel 1 DEC 56 RA -03
Counts / 10**4
Grating Position
Entry 1 xcor Entry 8
Counts
Grating Position

Fig.5.8

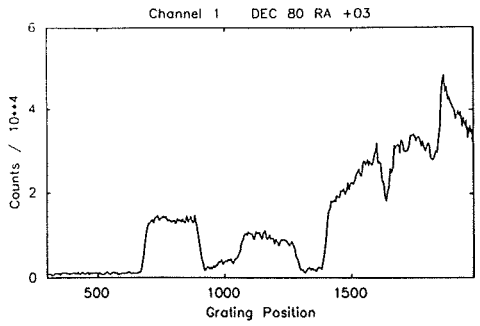
Channel 1 DEC 80 RA +03
Counts / 10**4
Grating Position

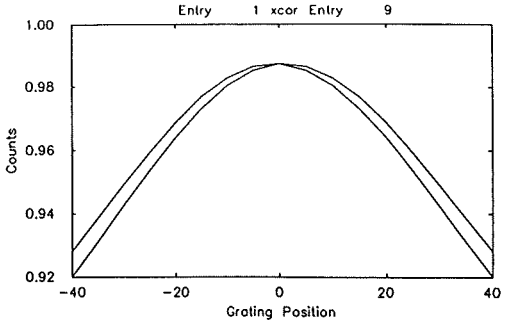
Entry 1 xcor Entry 9
Counts
Grating Position

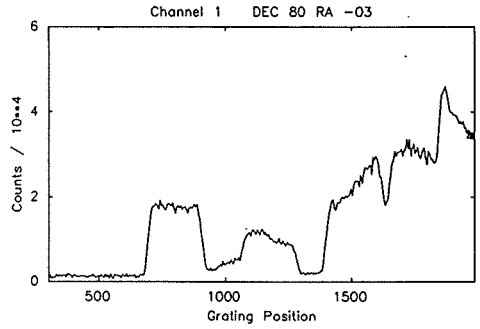
Channel 1 DEC 80 RA -03
Counts / 10**4
Grating Position

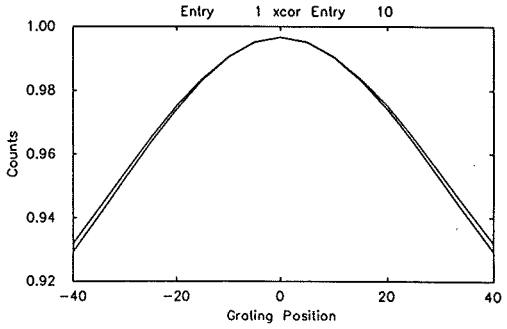
Entry 1 xcor Entry 10
Counts
Grating Position

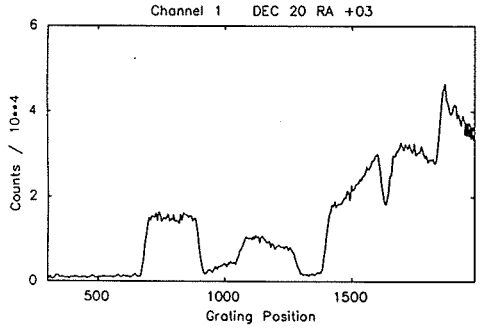
Channel 1 DEC 20 RA +03
Counts / 10**4
Grating Position

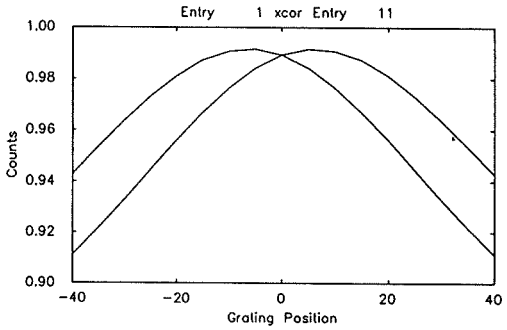
Entry 1 xcor Entry 11
Counts
Grating Position

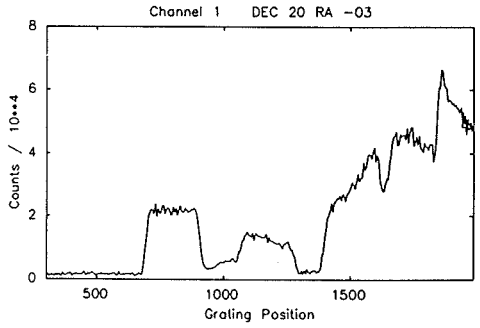
Channel 1 DEC 20 RA -03
Counts / 10**4
Grating Position

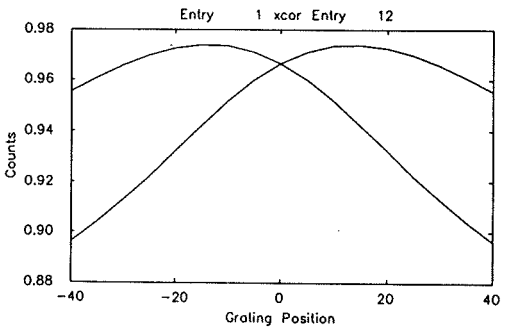
Entry 1 xcor Entry 12
Counts
Grating Position

Fig.5.9

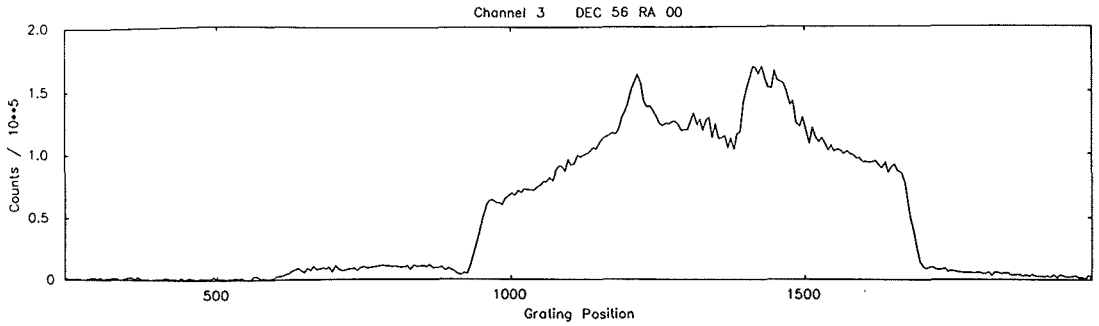
Channel 3 DEC 56 RA 00
Counts / 10**5
Grating Position

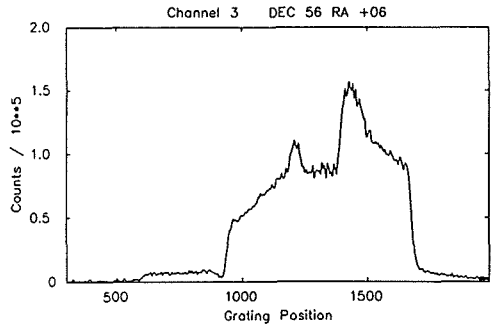
Channel 3 DEC 56 RA +06
Counts / 10**5
Grating Position

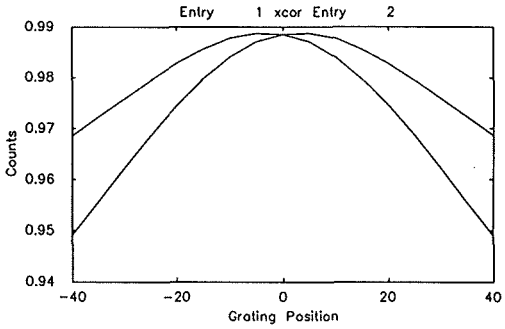
Entry 1 xcor Entry 2
Counts
Grating Position

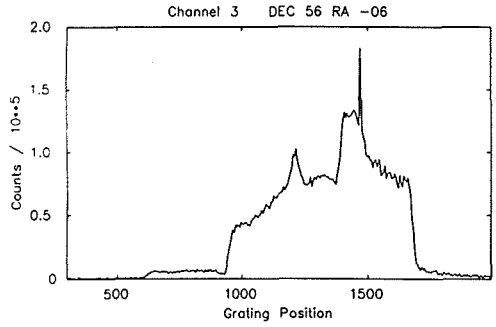
Channel 3 DEC 56 RA -06
Counts / 10**5
Grating Position

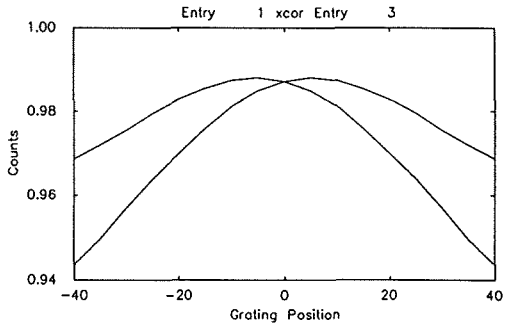
Entry 1 xcor Entry 3
Counts
Grating Position

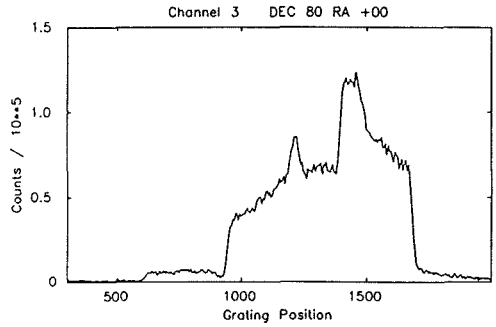
Channel 3 DEC 80 RA +00
Counts / 10**5
Grating Position

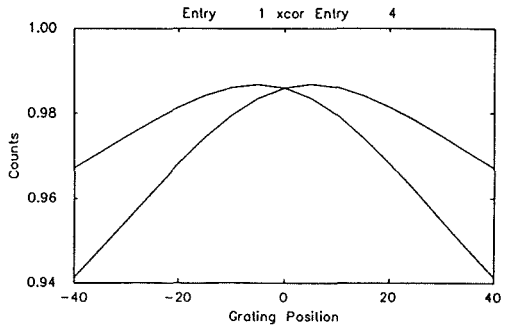
Entry 1 xcor Entry 4
Counts
Grating Position

Fig.5.10

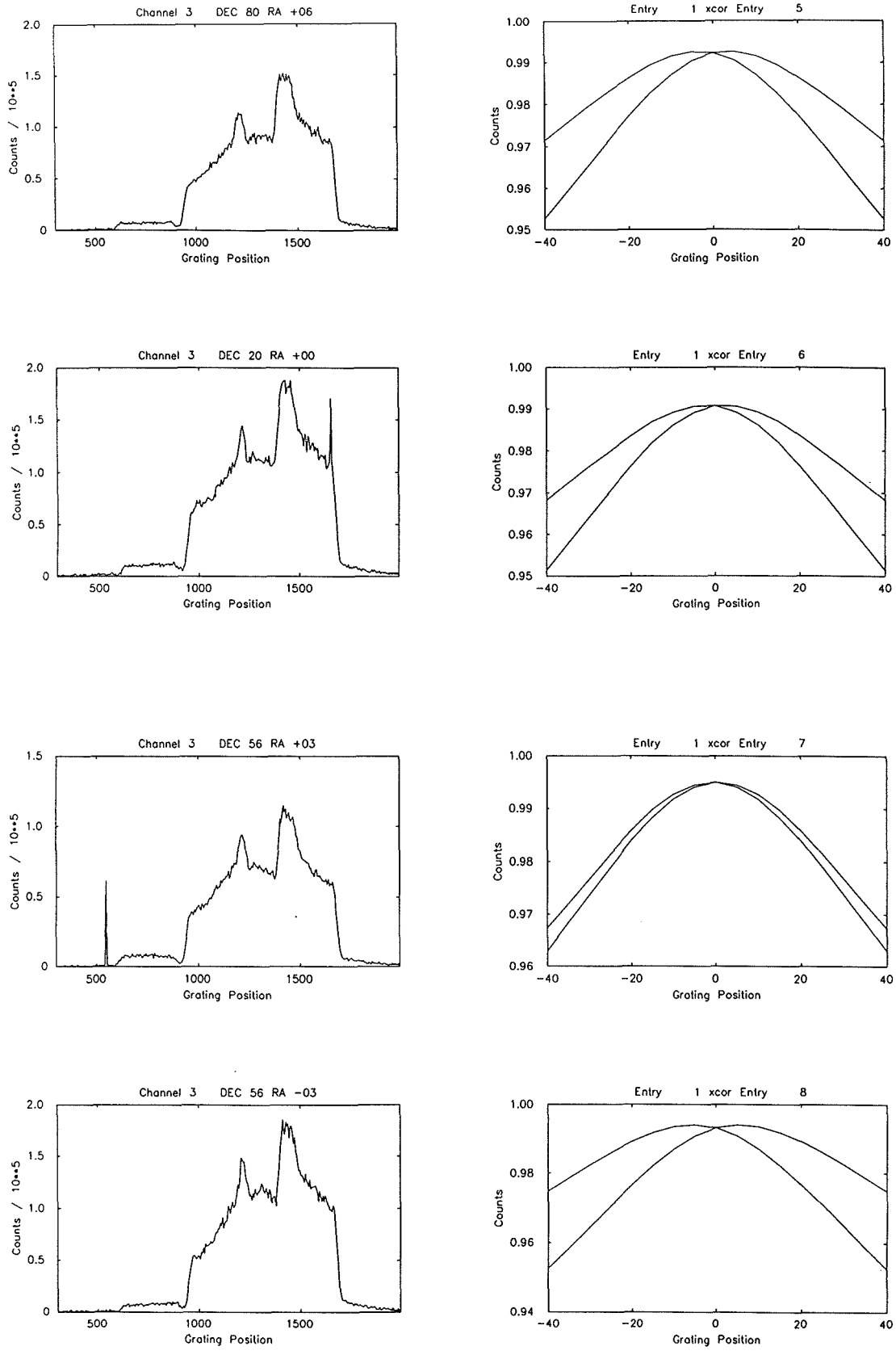
Channel 3 DEC 80 RA +06
Counts / 10**5
Grating Position
Entry 1 xcor Entry 5
Counts
Grating Position
Channel 3 DEC 20 RA +00
Counts / 10**5
Grating Position
Entry 1 xcor Entry 6
Counts
Grating Position
Channel 3 DEC 56 RA +03
Counts / 10**5
Grating Position
Entry 1 xcor Entry 7
Counts
Grating Position
Channel 3 DEC 56 RA -03
Counts / 10**5
Grating Position
Entry 1 xcor Entry 8
Counts
Grating Position

Fig.5.11

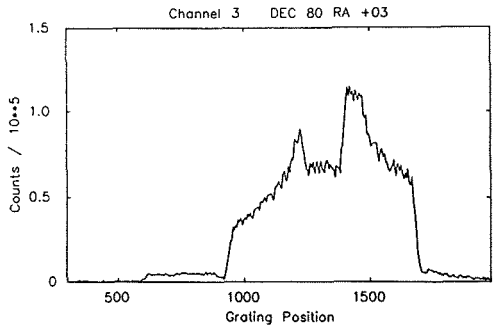
Channel 3 DEC 80 RA +03
Counts / 10**5
Grating Position

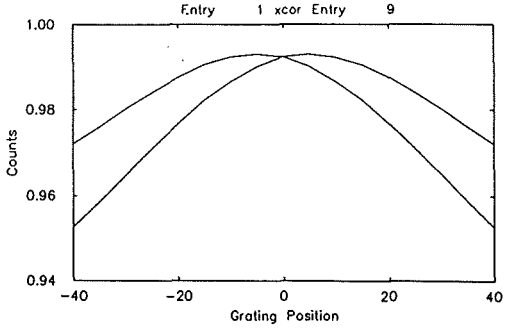
Entry 1 xcor Entry 9
Counts
Grating Position

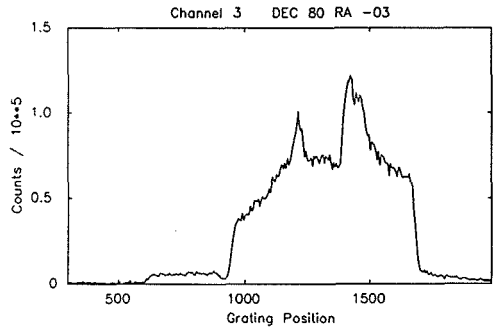
Channel 3 DEC 80 RA -03
Counts / 10**5
Grating Position

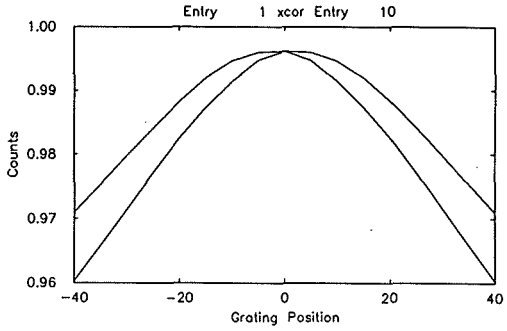
Entry 1 xcor Entry 10
Counts
Grating Position

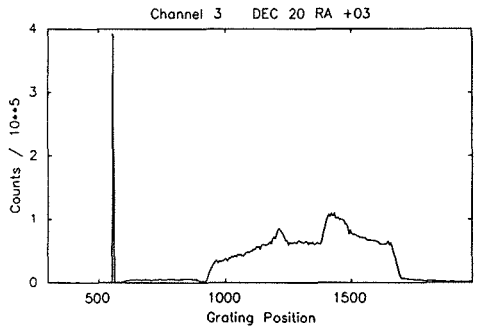
Channel 3 DEC 20 RA +03
Counts / 10**5
Grating Position

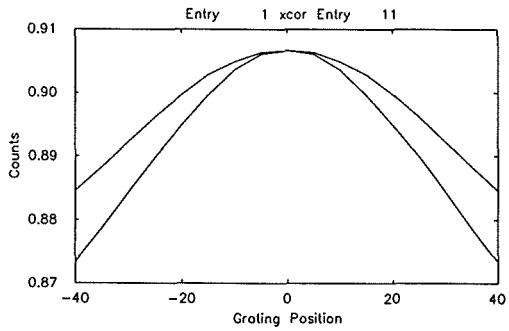
Entry 1 xcor Entry 11
Counts
Grating Position

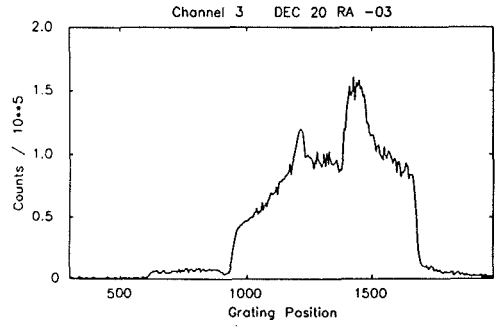
Channel 3 DEC 20 RA -03
Counts / 10**5
Grating Position

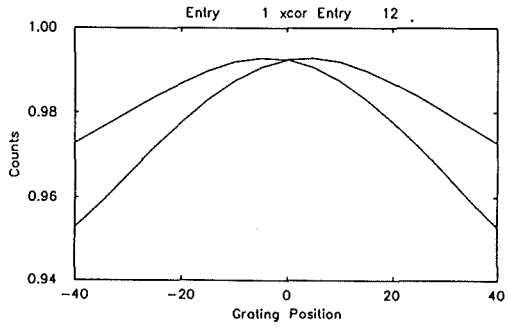
Entry 1 xcor Entry 12
Counts
Grating Position

Fig.5.12

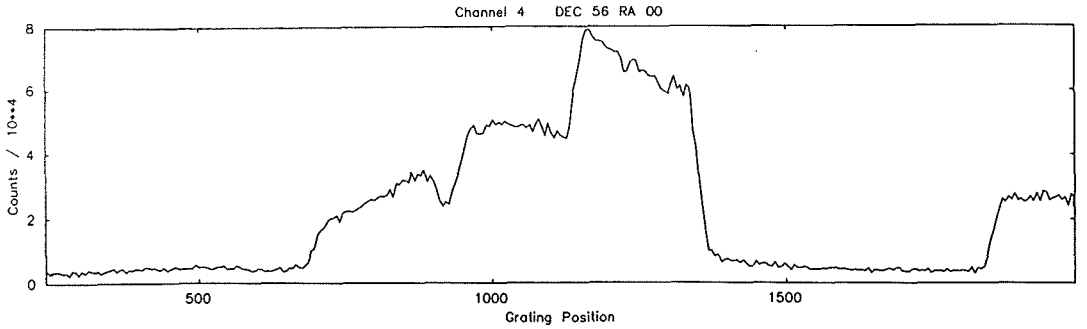
Channel 4 DEC 56 RA 00
Counts / 10**4
Grating Position

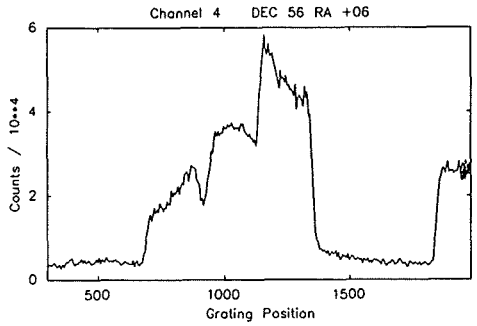
Channel 4 DEC 56 RA +06
Counts / 10**4
Grating Position

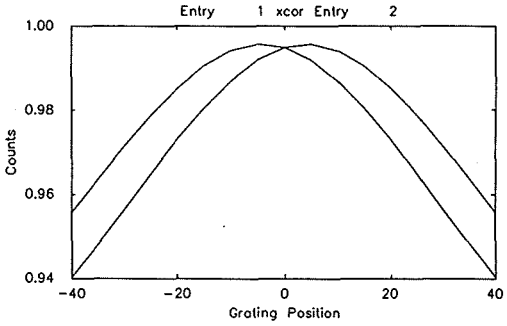
Entry 1 xcor Entry 2
Counts
Grating Position

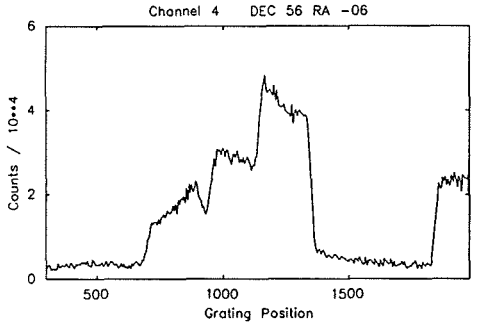
Channel 4 DEC 56 RA -06
Counts / 10**4
Grating Position

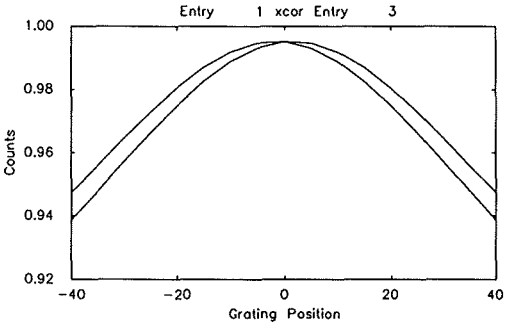
Entry 1 xcor Entry 3
Counts
Grating Position

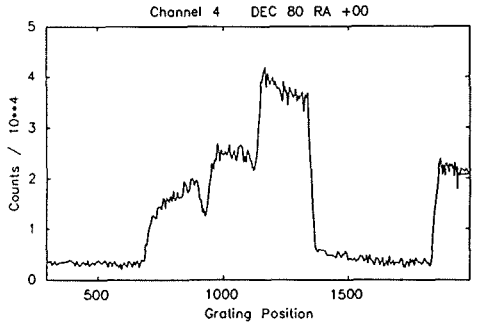
Channel 4 DEC 80 RA +00
Counts / 10**4
Grating Position

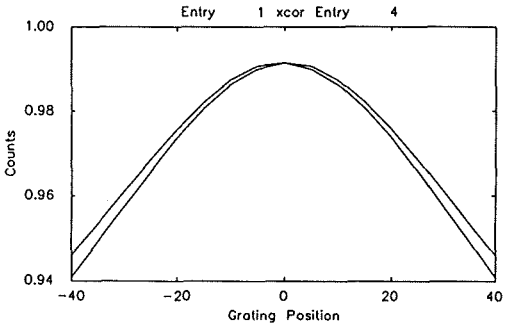
Entry 1 xcor Entry 4
Counts
Grating Position

Fig.5.13

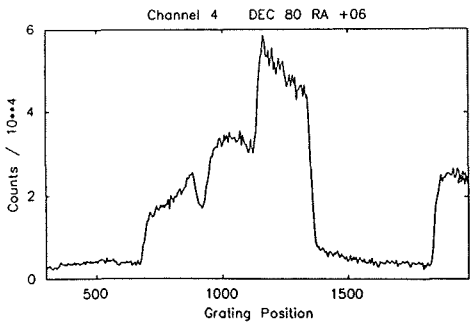
Channel 4 DEC 80 RA +06
Counts / 10**4
Grating Position

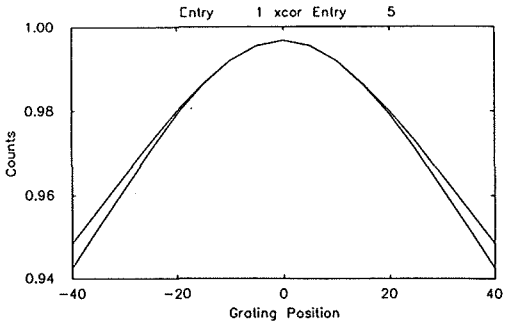
Entry 1 xcor Entry 5
Counts
Grating Position

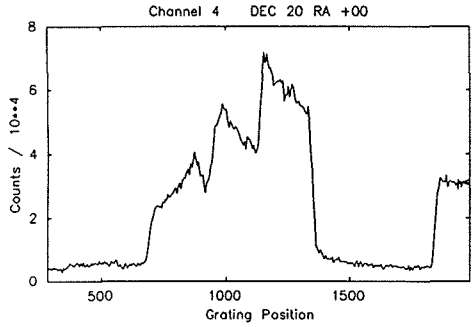
Channel 4 DEC 20 RA +00
Counts / 10**4
Grating Position

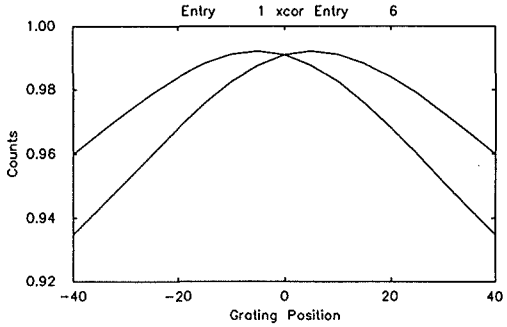
Entry 1 xcor Entry 6
Counts
Grating Position

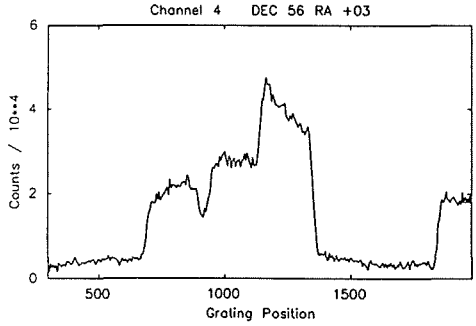
Channel 4 DEC 56 RA +03
Counts / 10**4
Grating Position

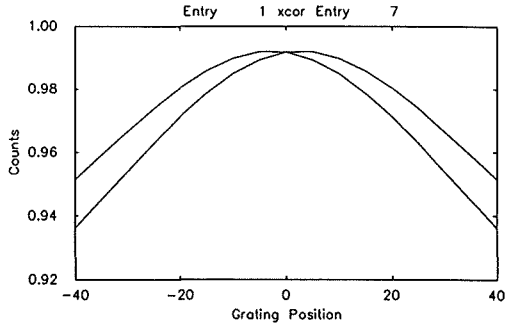
Entry 1 xcor Entry 7
Counts
Grating Position

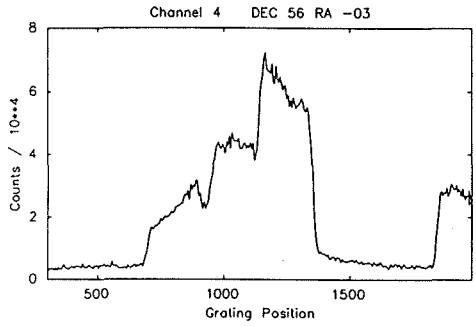
Channel 4 DEC 56 RA -03
Counts / 10**4
Grating Position

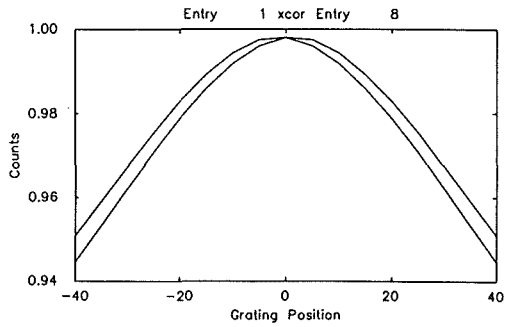
Entry 1 xcor Entry 8
Counts
Grating Position

Fig.5.14

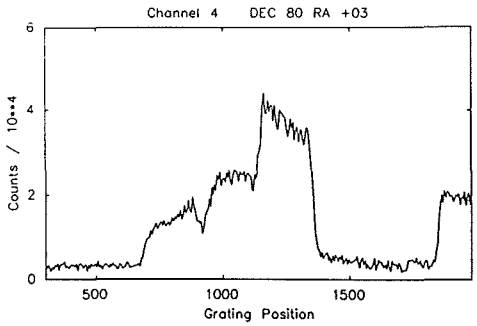
Channel 4 DEC 80 RA +03
Counts / 10**4
Grating Position

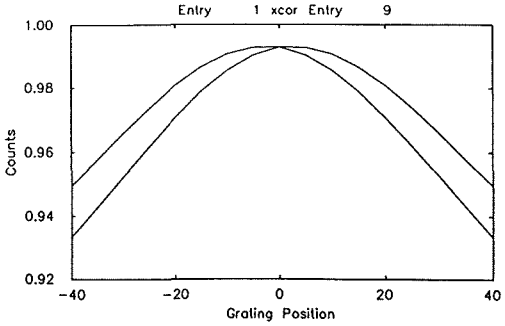
Entry 1 xcor Entry 9
Counts
Grating Position

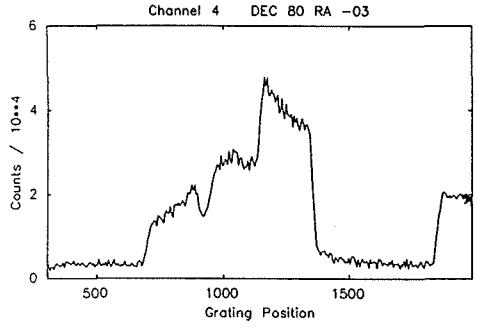
Channel 4 DEC 80 RA -03
Counts / 10**4
Grating Position

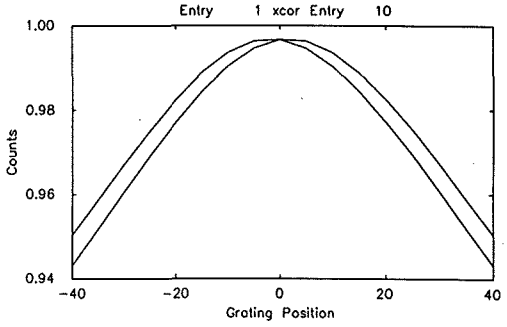
Entry 1 xcor Entry 10
Counts
Grating Position

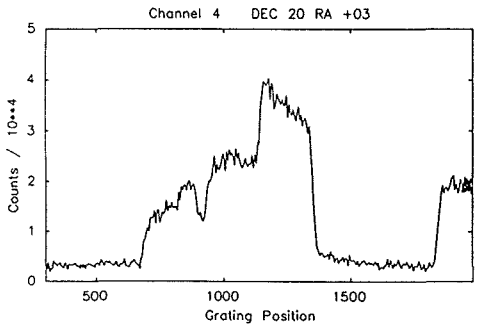
Channel 4 DEC 20 RA +03
Counts / 10**4
Grating Position

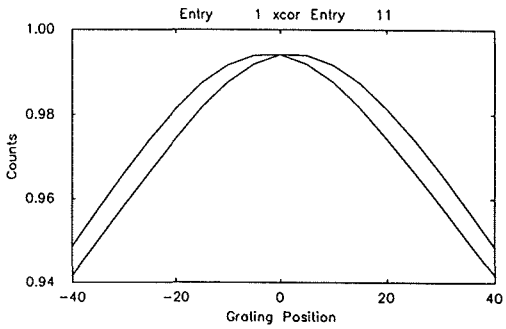
Entry 1 xcor Entry 11
Counts
Grating Position

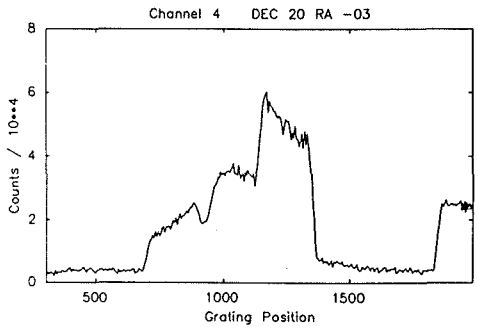
Channel 4 DEC 20 RA -03
Counts / 10**4
Grating Position

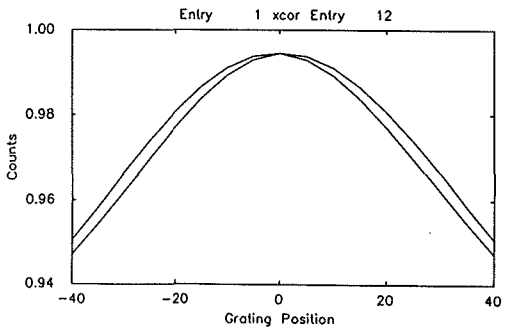
Entry 1 xcor Entry 12
Counts
Grating Position

Fig.5.15

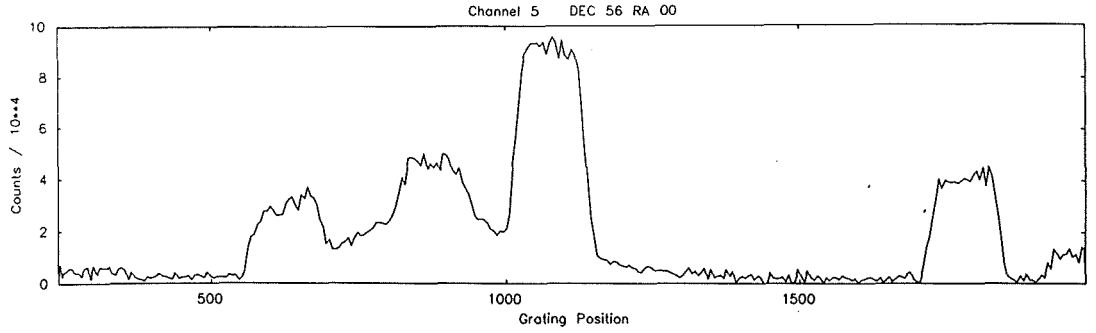
Channel 5 DEC 56 RA 00
Counts / 10**4
Grating Position

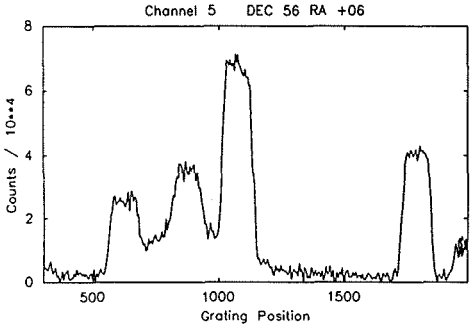
Channel 5 DEC 56 RA +06
Counts / 10**4
Grating Position

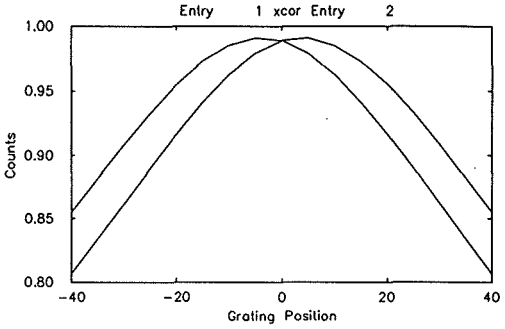
Entry 1 xcor Entry 2
Counts
Grating Position

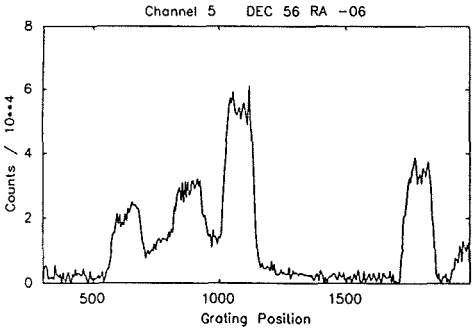
Channel 5 DEC 56 RA -06
Counts / 10**4
Grating Position

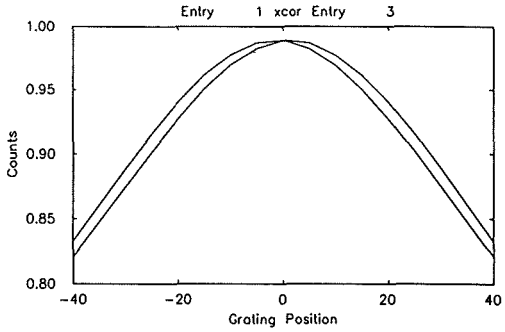
Entry 1 xcor Entry 3
Counts
Grating Position

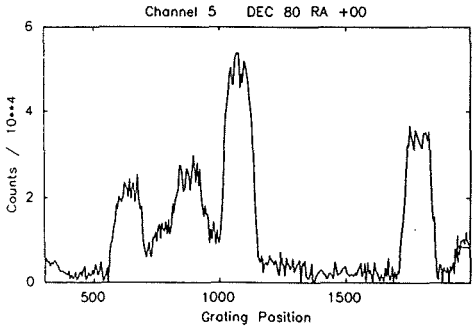
Channel 5 DEC 80 RA +00
Counts / 10**4
Grating Position

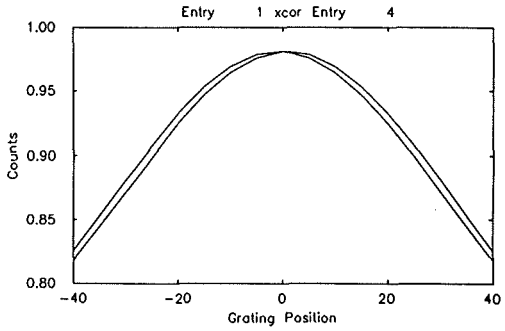
Entry 1 xcor Entry 4
Counts
Grating Position

Fig.5.16

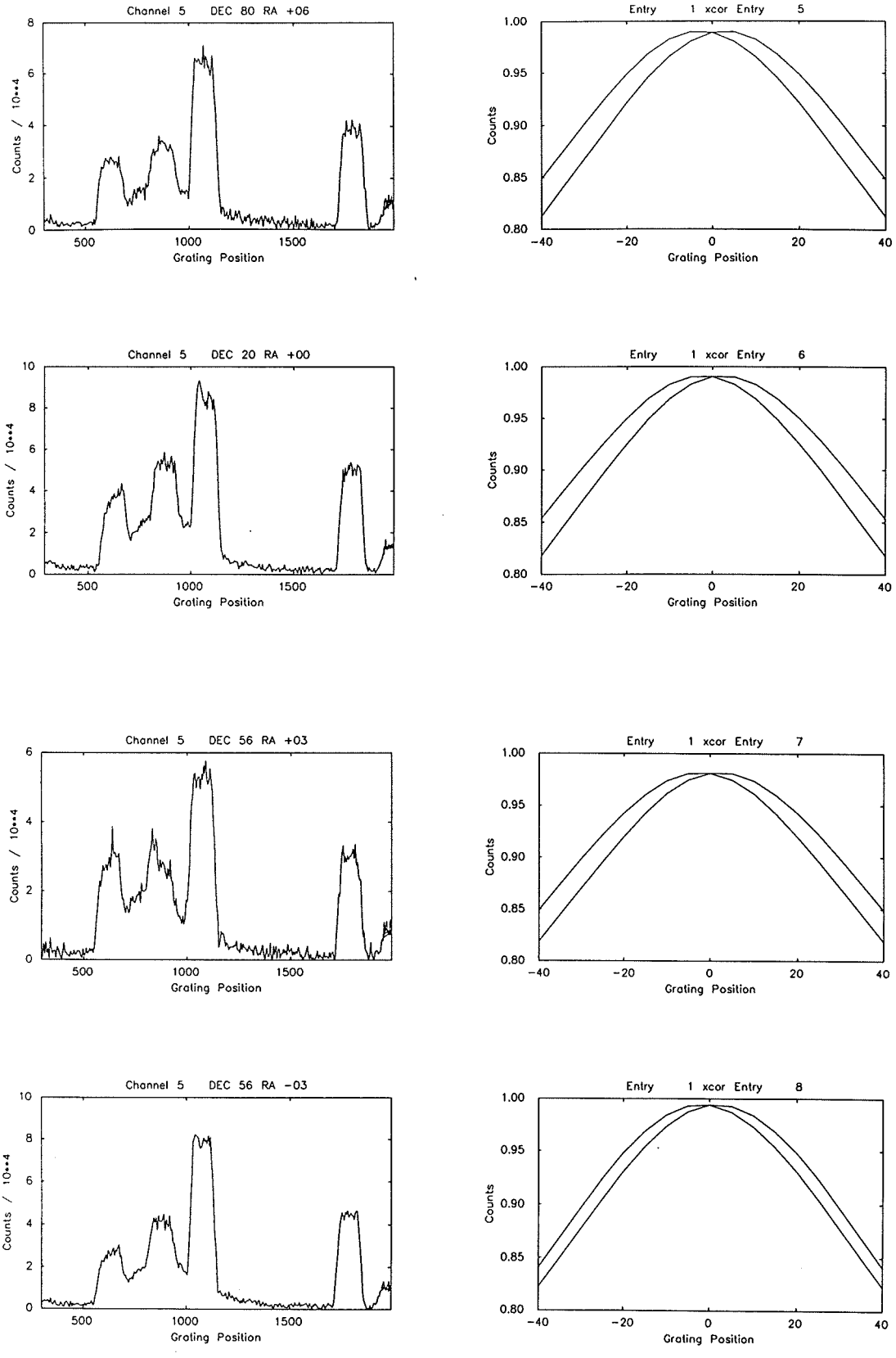
Channel 5 DEC 80 RA +06
Counts / 10**4
Grating Position
Entry 1 xcor Entry 5
Counts
Grating Position
Channel 5 DEC 20 RA +00
Counts / 10**4
Grating Position
Entry 1 xcor Entry 6
Counts
Grating Position
Channel 5 DEC 56 RA +03
Counts / 10**4
Grating Position
Entry 1 xcor Entry 7
Counts
Grating Position
Channel 5 DEC 56 RA -03
Counts / 10**4
Grating Position
Entry 1 xcor Entry 8
Counts
Grating Position

Fig.5.17

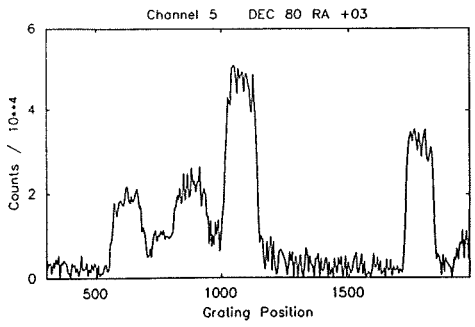
Channel 5 DEC 80 RA +03
Counts / 10**4
Grating Position

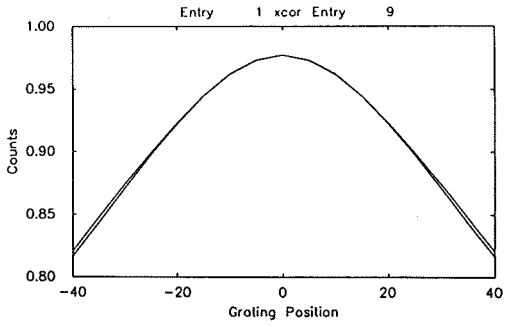
Entry 1 xcor Entry 9
Counts
Grating Position

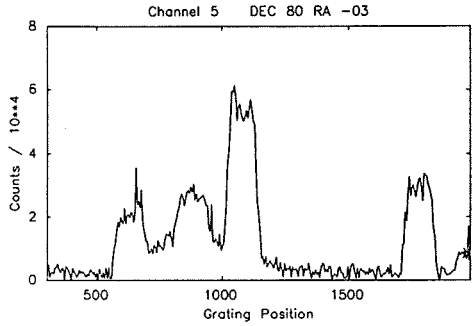
Channel 5 DEC 80 RA -03
Counts / 10**4
Grating Position

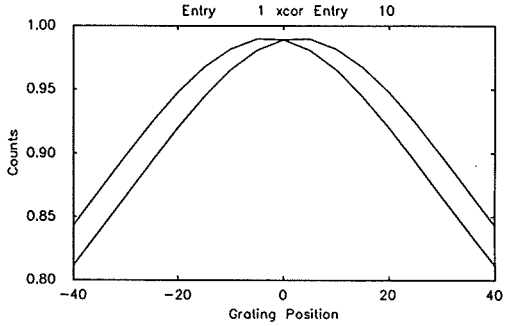
Entry 1 xcor Entry 10
Counts
Grating Position

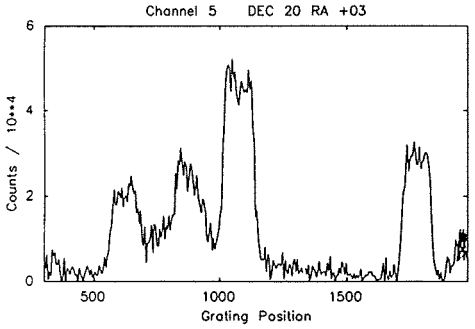
Channel 5 DEC 20 RA +03
Counts / 10**4
Grating Position

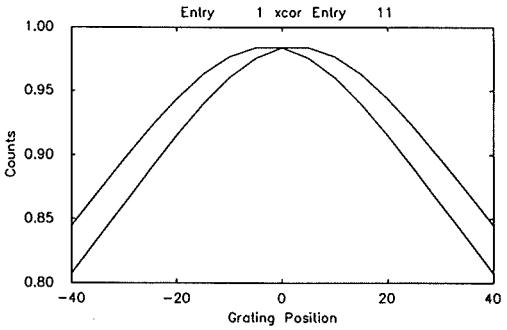
Entry 1 xcor Entry 11
Counts
Grating Position

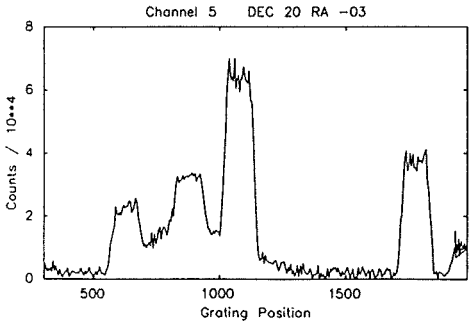
Channel 5 DEC 20 RA -03
Counts / 10**4
Grating Position

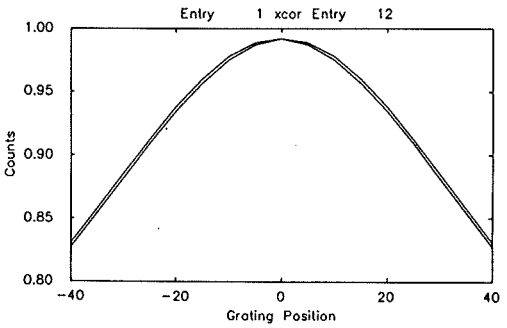
Entry 1 xcor Entry 12
Counts
Grating Position

Fig.5.18

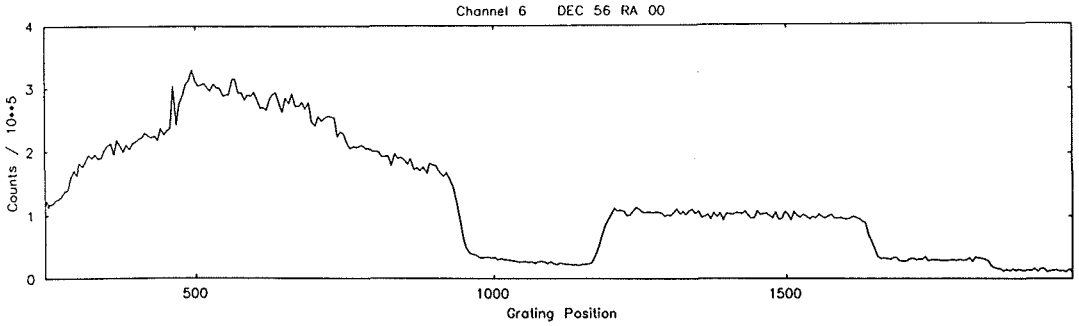
Channel 6 DEC 56 RA 00
Counts / 10**5
Grating Position

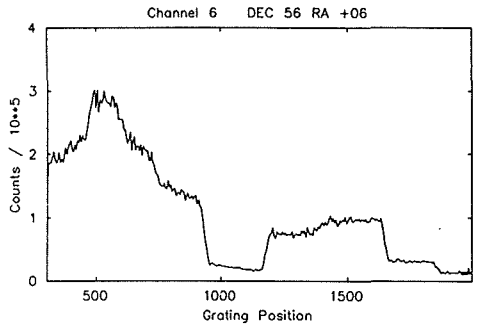
Channel 6 DEC 56 RA +06
Counts / 10**5
Grating Position

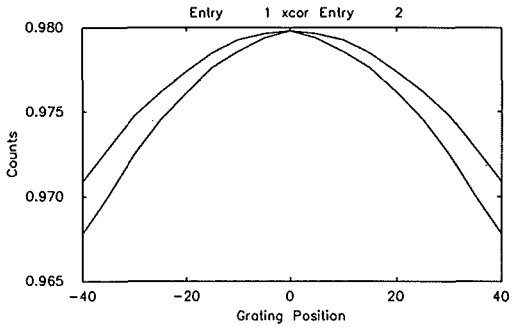
Entry 1 xcor Entry 2
Counts
Grating Position

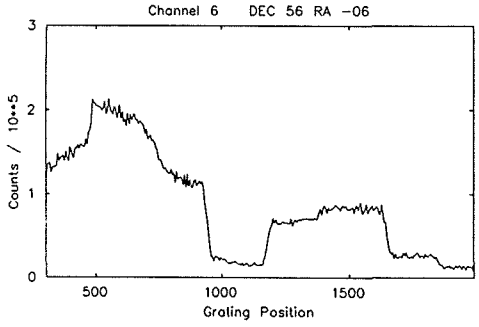
Channel 6 DEC 56 RA -06
Counts / 10**5
Grating Position

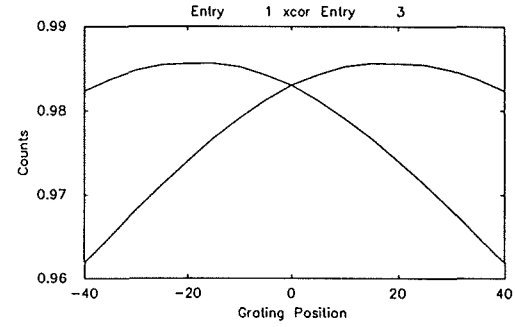
Entry 1 xcor Entry 3
Counts
Grating Position

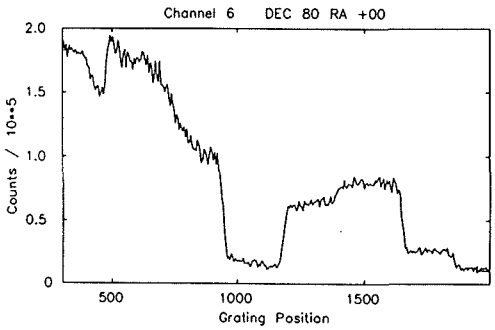
Channel 6 DEC 80 RA +00
Counts / 10**5
Grating Position

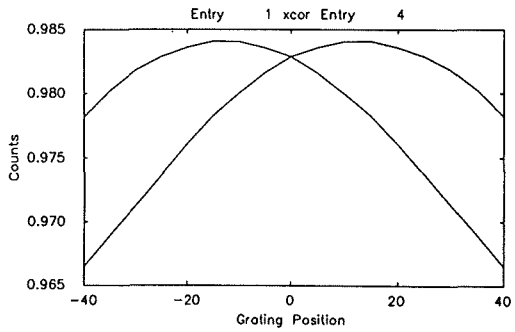
Entry 1 xcor Entry 4
Counts
Grating Position

Fig.5.19

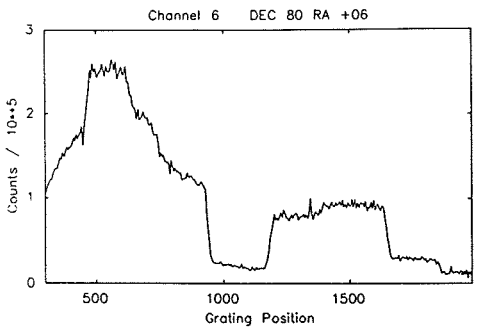
Channel 6 DEC 80 RA +06
Counts / 10**5
Grating Position

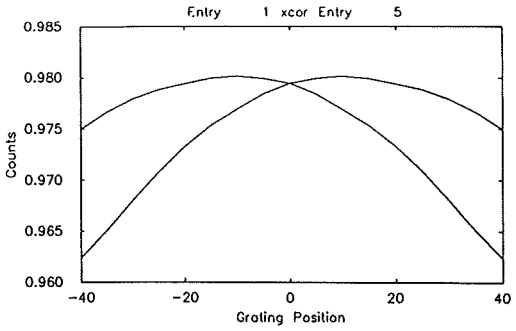
Entry 1 xcor Entry 5
Counts
Grating Position

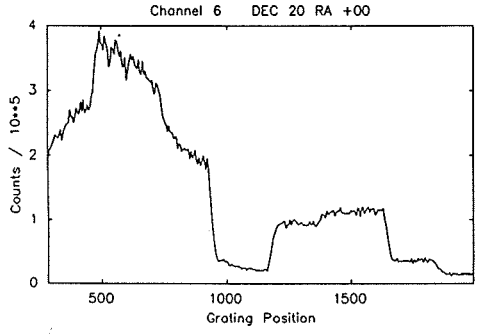
Channel 6 DEC 20 RA +00
Counts / 10**5
Grating Position

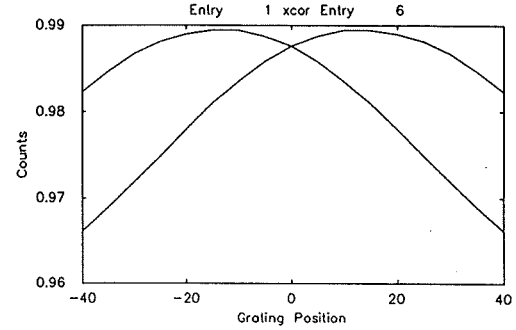
Entry 1 xcor Entry 6
Counts
Grating Position

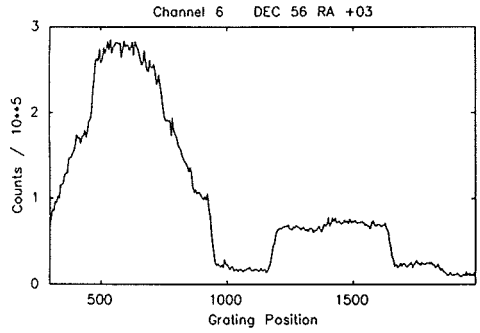
Channel 6 DEC 56 RA +03
Counts / 10**5
Grating Position

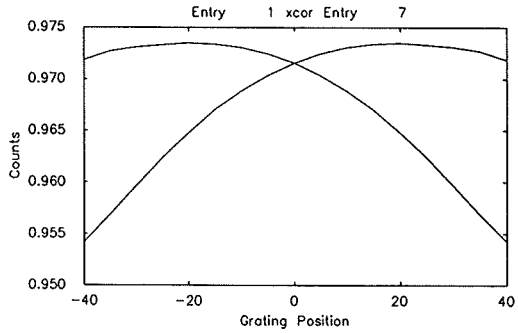
Entry 1 xcor Entry 7
Counts
Grating Position

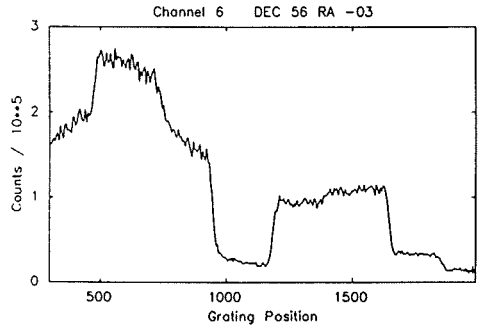
Channel 6 DEC 56 RA -03
Counts / 10**5
Grating Position

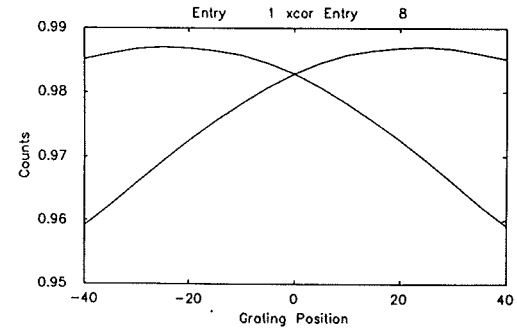
Entry 1 xcor Entry 8
Counts
Grating Position

Fig.5.20

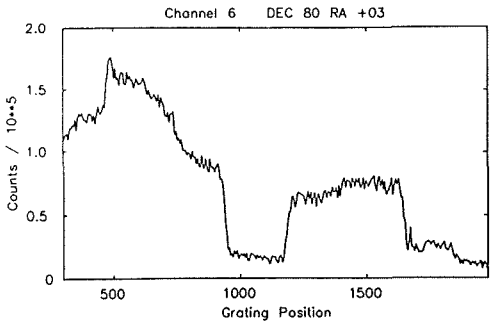
Channel 6 DEC 80 RA +03
Counts / 10**5
Grating Position

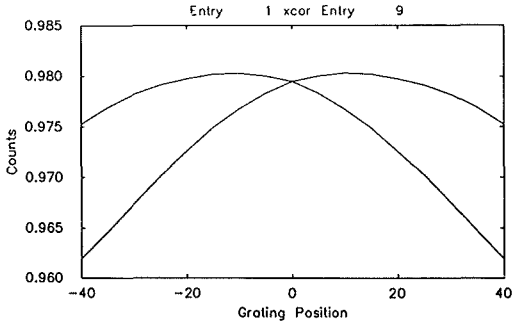
Entry 1 xcor Entry 9
Counts
Grating Position

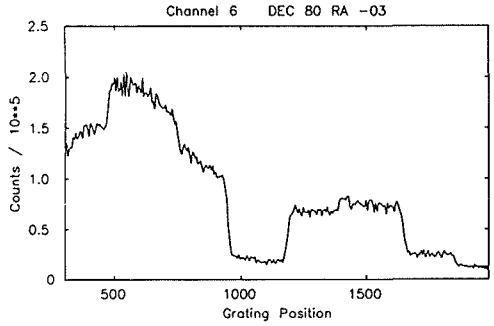
Channel 6 DEC 80 RA -03
Counts / 10**5
Grating Position

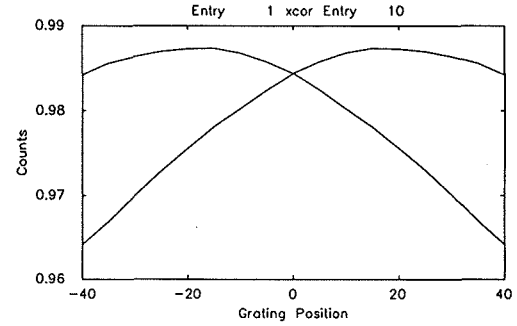
Entry 1 xcor Entry 10
Counts
Grating Position

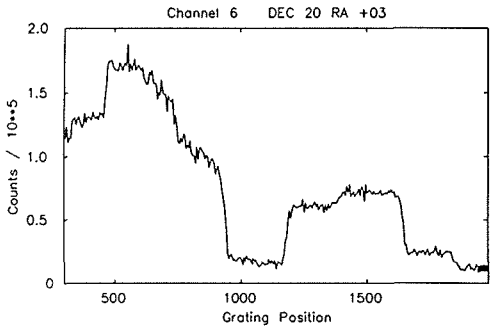
Channel 6 DEC 20 RA +03
Counts / 10**5
Grating Position

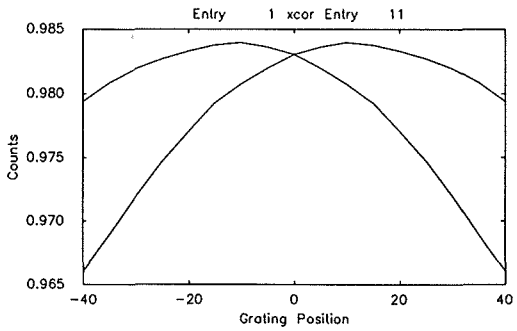
Entry 1 xcor Entry 11
Counts
Grating Position

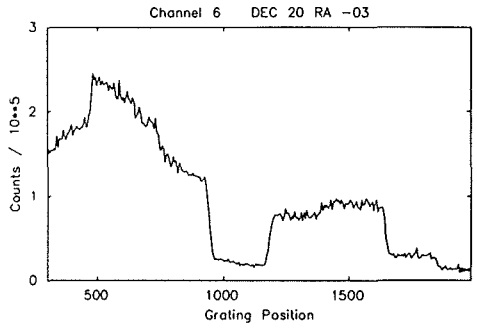
Channel 6 DEC 20 RA -03
Counts / 10**5
Grating Position

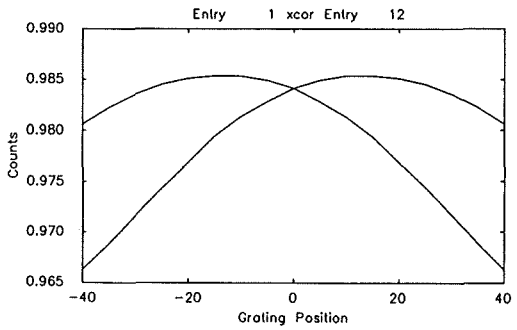
Entry 1 xcor Entry 12
Counts
Grating Position

Fig.5.21

Table 5.3 Resultant shift, in units of grating units, of the spectral features as measured for different orientations of the telescope.

DEC	RA	1	3	4	5	6
56	+6	11	7	5	6	4
56	-6	0	7	3	2	13
80	0	10	8	2	2	10
80	+6	9	8	1	5	12
20	0	12	7	5	4	13
56	+3	8	4	4	5	13
56	-3	4	9	3	4	15
80	+3	3	8	5	0	12
80	-3	1	5	3	5	13
20	+3	8	5	3	5	13
20	-3	12	7	3	0	12

Table 5.4 Amplifier pulse lengths.

Channel number	1	3	4	5	6	7	8
Pulse length (ns)	60	60	55	115	115	110	110

All measured at 2V

Table 5.5 Comparison of predicted residual counts with observed residual counts.

Channel number	1	3	4	5	6	7	8
Predicted	2	12	105	104	130	15	18
Observed	2	16	45	47	66	7	13

most-significant-bits is used to produce the borrow bit, so glitches on this line could lead to the borrow bit being set incorrectly. The glitches were removed from the line using capacitors.

After these modifications the counters were then observed to perform satisfactorily for a period of a few months. Then certain channels were seen to produce large counts again, although this time the number of erroneous counts was far less, typically 1%.

At first it was thought that the large counts may not have been real but have been produced by a reading error. It was shown that the large numbers were actually contained in the output registers of the counters. (Repeated readings of the counters produced a few large numbers and then manual enabling and reading showed the bit pattern to be consistent with the large numbers read with the software).

The accuracy of the counters was then re-examined. In theory, if the counters were driven with uniformly spaced pulses from a signal generator, then the nett output should be zero, since the counters will count up for half the integration period and down for the other half. The counters were then driven singly and in pairs from a pulse generator and the nett count was never greater than 4. No large counts were ever seen when using the pulse generator.

This was not the case when the same experiment was conducted using the photomultiplier tubes as a source. Due to the random nature of the arrival of the pulses we would not always expect to see a nett count of zero, but, if two counters were being driven by the same photomultiplier then we would expect them to be in close agreement with each other. This was often not the case. As well as this discrepancy it was seen that the counters sometimes either generated borrows when they should not have done or else failed to generate them

when they should have. (The frequency of this was again less than 1%).

In an attempt to reduce the errors the retriggerable monostable devices, which act as interfaces between the amplifier/discriminators and the counters, were replaced by non-retriggerable devices. (The required pulse length for the former being 15ns whilst that for the latter being 40ns). When the counters were driven by the same photomultiplier source the difference in nett counts between the two counters was reduced to +/- 2 counts. The problem with the generation of borrows still remained.

With the counters that were still causing problems the pulse lengths from the amplifier/discriminators were lengthened. The amplifier pulse lengths are given in Table 5.4. Since these modifications have been made no further problems have been encountered with the counters.

Recent tests, (3/2/88) using darkcounts from the photomultiplier tubes show that the counters are still performing satisfactorily, (see Table 5.5).

5.3.6 Focussing On The Apertures

It is important that the aperture eyepiece is first focussed onto the apertures before adjusting the telescopes focus to bring the stellar image into focus in the eyepiece. If the eyepiece is not focussed on the apertures then the stellar image will be focussed either in front of or behind the aperture.

The focussing of the eyepiece onto the apertures is most easily performed when the apertures are brightly illuminated by the daylight sky. The eyepiece can be moved in and out of the drawtube until a sharp image of the apertures is seen.

Whilst observing though, it was found that the eyepiece could easily be disturbed and therefore become out of focus. This problem was overcome by the fitting of a circular clamp around the drawtube which could be tightened to prevent movement of the eyepiece once it had been set.

But there are disadvantages to having the eyepiece locked in place in this manner when one needs to check the focussing of the telescope on the stellar image. The easiest way to focus the telescope is to perform a knife edge test with the aid of the aperture.

With a bright star centred in the aperture, the eyepiece is removed from the drawtube so as to view the aperture directly. An evenly illuminated image of the primary mirror should be seen with the shadow of the secondary in the middle. The star is then moved towards the edge of the aperture. If the star has been focussed in the focal plane of the apertures then the image of the primary should darken uniformly over its surface and be extinguished. If, though, the star is focussed in front of or behind the aperture plane, then one side of the image of the primary will darken before the other. With the star recentred in the aperture, the focus can be changed until uniform darkening is achieved.

We can see that the eyepiece must now be replaced and focussed onto the apertures. The standard practice is to use either the aperture illumination to see when the aperture image is sharp, or to move a bright star half way out of the aperture and then focus on the

aperture. Neither of these methods is as sensitive as using a bright sky to illuminate the apertures.

The following compromise between the two positions was used. The eyepiece would be focussed onto the apertures using a bright sky for illumination and the eyepiece would be locked in place. At the beginning of each observing session a bright star would be centred in the aperture and the telescope focussed onto it. The image was deemed to be in focus when the image was at its smallest.

To ensure that a visual estimate was sufficiently accurate, the knife edge test was performed on several nights after observations were finished. On all occasions the primary was seen to darken uniformly, thus justifying the above procedure.

5.3.7 Aperture Slide Selection

During the assembly of the photometer a new aperture plate was constructed. With the original design, too much radiation would have leaked around the edge of the plate. The opportunity was taken to include an additional single aperture in the plate for use with the calibration sources. If aperture pairs are used for this application then the subtractive nature of the up/down counting would result in a nett count of zero. By having one open aperture and one closed, there is the advantage of automatically subtracting dark counts. Table 5.6 gives the dimensions of the apertures for this mask.

When the first astronomical data acquired with the photometer were reduced, a large amount of variation, up to 20%, was seen on successive integrations taken on standard stars. The variations were seen to be monotonically increasing (or decreasing) and returned to approximately the same level at the beginning of each integration when

the star was re-centred in the aperture. Since these trends were not observed in any of the data taken when using a calibration source for illumination we could say that the fault was not with the counting system.

By taking longer runs of integrations without re-centring the star we could ascertain a period of 149 seconds (see Figure 5.22). Now, the main drive of the telescope has a period of 149 seconds, which would indicate that the problem lay with image wander within the aperture. When the star was centred in the aperture and visually observed for a period of five minutes or more, the stellar image could be seen to undergo an oscillation of some 10 - 12 " in amplitude.

Even though this is a large amount of movement within the aperture, the Fabry lenses should have ensured that the amount of movement of the primary's image on the photocathode would be negligible and therefore the count rate should be relatively independent to sensitivity variations across the cathode. If the variations had been attributable to these sensitivity variations, then defocusing the stellar image, (whilst remaining within the aperture limits), should have reduced the amplitude of the variations, but it did not. Also the trends were seen to be in the same direction in all channels, which indicates that the variation had a common source for all channels.

To try to reduce the extent of the variations, a new aperture slide was constructed with a larger pair of apertures (see Table 5.7). If the variation was being caused by loss of light due to obscuration by the aperture then we would expect to see a decrease if a larger aperture was used. Such an improvement was seen in all the channels, with the exception of channel 4. Whilst there was still a periodic

Table 5.6 Old aperture dimensions.

mm	arc. sec.
1 X 0.50	13
2 X 0.50	13
2 X 0.75	20
2 X 1.00	27

Table 5.7 New aperture dimensions.

mm	arc. sec.
1 X 0.50	13
2 X 0.75	20
2 X 1.00	27
2 X 1.50	40

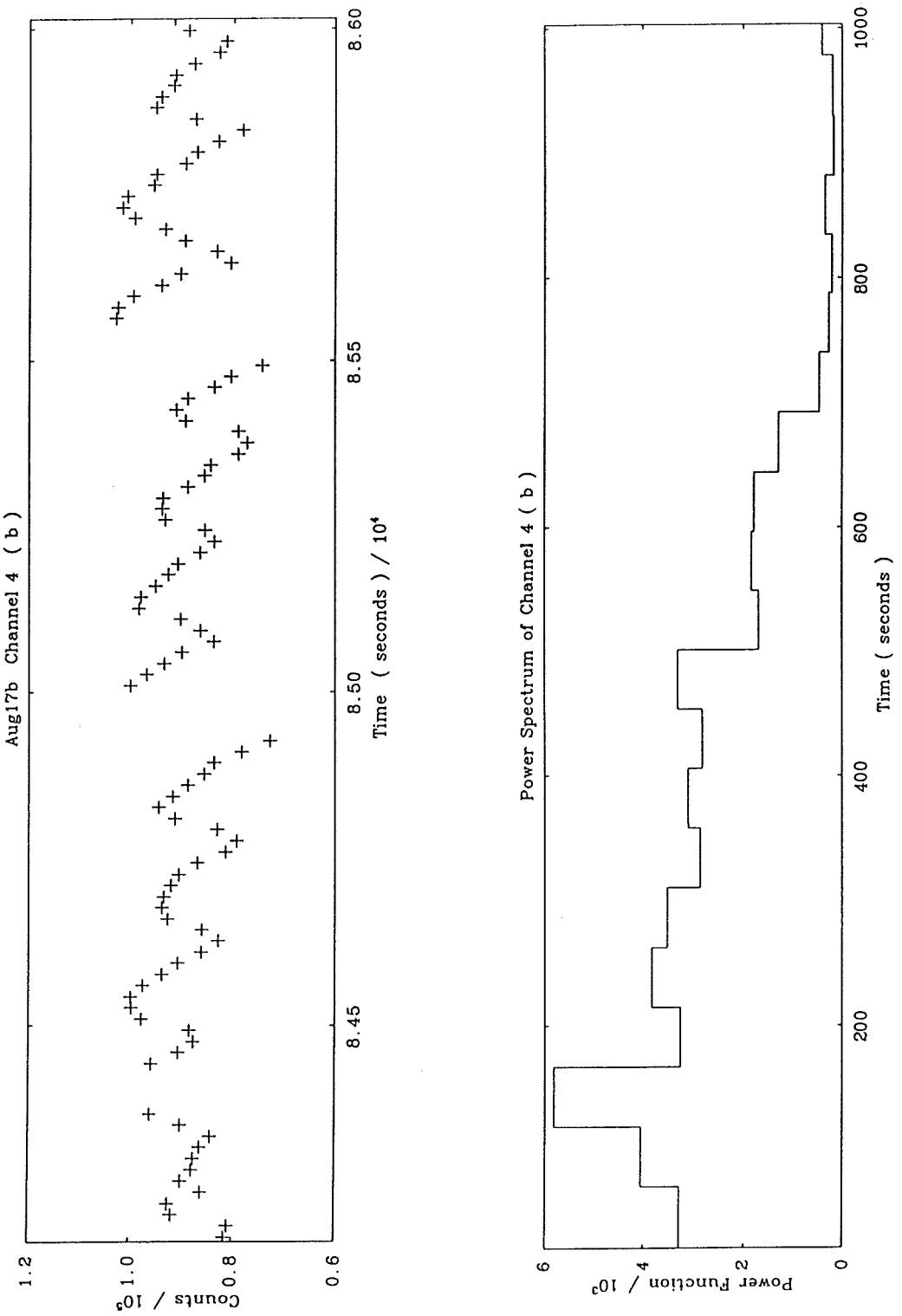

Fig.5.22 The periodic nature of the data is clearly visible. A value for the period can be found from the power spectrum.

nature to the trend the stability was now down to <2%. Channel 4 however still showed up to 15% variation.

If the interference filter in channel 4 was withdrawn whilst integrating, the variation was seen to drop to the same level as in other channels. The interference filter was replaced with another having an identical passband. The large variation was still present with the new filter in position, thus discounting the possibility that the variation may have been caused by a blemish on the filter.

The reason for the large variation was found when examining the position of the passbands of the filter in relation to the wavelength cutoffs of the mirrors in the mosaic. For channel 4 the long wavelength cutoff of the filter was seen to coincide with the long wavelength cutoff of the mirror. Therefore we are going to be very sensitive in this channel to any slight movement of the spectrum along the mirror mosaic.

If we want to reduce the variations in channel 4 we clearly need the filters passband to be more centrally located within the passband of the mirror and therefore less sensitive to any shift of the spectrum. One solution would be to alter the physical length of the mirror but this is obviously not practical. What we can do though is to re-define the break points of the mirror by rotating the grating. Whilst doing this we must bear in mind that the break points of the other mirrors will also change.

The approach taken was to introduce shifts in the mirror breakpoints from 1nm to 7nm in 1nm increments. A new grating angle was calculated at each step which would produce the new set of break points. Observations were then taken, at each new grating position, of a standard star and the amount of variation in each channel noted.

The variation in channel 4 was seen to be at a minimum for a grating position of 1430, which corresponds to the mirror mosaic passbands as shown in Table 5.8. The variations due to the movement of the stellar image in the aperture had been reduced to 3% in channel 4 (compared with less than 1.5% in the other channels). To ensure that this improvement was due to the re-defining of the mirror passbands, observations were made immediately after the above measurements with the passbands as they had been before. The variation in channel 4 reverted back to 15%, whilst remaining constant in the others.

A consequence of having to re-define the mirror passbands is that we are now unable to measure the Hβ index using channel 5, as we had been using the mirror passband to define the broad Hβ filter. (The broad Hβ filter supplied by the Dominion Astrophysical Observatory did not overlap with the narrow Hβ filter).

5.3.8 Fabry Lenses

The purpose of the Fabry lenses is to focus an image of the telescope's primary mirror onto the photomultiplier photocathodes. The photocathodes need to be positioned close to the focus of the Fabry lenses to achieve the minimum sensitivity of count rate variation due to movement of a stellar image within the aperture.

There is no facility to adjust the position of the Fabry lenses, but there is longitudinal adjustment in the photomultiplier socket holders. The photocathodes can be moved either backwards or forwards until they are at the focus of the Fabry lenses.

Table 5.8 Mosaic mirror breakpoints for the original and new grating positions. The central wavelength and bandpasses for the Stromgren filters are included for comparison. All wavelenghts in nm.

Mirror break-points for grating setting of 1385.

	Channel Number						
	1	3	4	5	6	7	8
Minimum Wavelength	330	390	440	476	496	580	750
Central Wavelength	348	416	446	476	486	665	845
Maximum Wavelength	365	440	476	496	580	750	940

Mirror break-points for grating setting of 1430.

	Channel Number						
	1	3	4	5	6	7	8
Minimum Wavelength	335	395	445	481	501	585	755
Central Wavelength	353	421	461	491	543	670	850
Maximum Wavelength	370	445	481	501	585	755	945

	Filter			
	u	v	b	y
Minimum Wavelength	330	390	460	540
Central Wavelength	350	410	470	550
Maximum Wavelength	370	420	480	560

COMMISSIONING THE PHOTOMETER

The distance between the rear of the Fabry lenses and the photocathodes vary from channel to channel. The variation is due not only to the different dimensions of the photomultiplier tubes but also to the fact that the windows of the tubes are of different thickness. For example, the Varian tubes have very thick windows, some 6.3mm, whilst the windows of the EMI tubes are only 2mm. A practical method had to be found to enable the setting of these distances.

With a blue sky to illuminate the primary mirror, with the aperchopper running and the largest aperture pair selected, the photomultiplier tubes were removed in turn from their housings. A ruler, with a piece of waxed paper mounted at its end, was inserted into the cold box housing. An image of the primary mirror could be seen on the paper. The depth of insertion was adjusted until the image was sharply focussed. the distance from the position to the mounting face of the sockets on the cold box could be read from the rule. The distance from the photocathode window to the base of the mounting bracket could now be set to this distance, and the photocathode then replaced, (allowing for the differing window thicknesses). This method of setting the photocathode distance was possible for all the channels, with the exception of channel8, where no image could be seen, because the grating could not be rotated sufficiently to bring shorter wavelength, (visible), light onto the channels mirror. The distance for this photomultiplier was set to the same distance as for the other Varian tube in channel 7.

Whilst this may seem to be a crude method of assessing the correct photocathode positioning defocussing of the image as the screen was moved about was not rapid.

5.3.9 Dark Counts

Even in the absence of any incident photons, electrons are emitted from the photocathode. These spontaneous emissions give rise to signals which are indistinguishable from those caused by a photon. The greater majority of these emissions will be thermionic. In general, the dark current is an exponential function of absolute temperature, which means that, since the photomultiplier tubes are presently being run uncooled the dark current, or dark counts, are high, as can be seen from Table 5.9. Another contributing factor is the relatively large area of the photocathode in the EMI tubes. (Thermionic emission is approximately proportional to the area of the photocathode). The ambient temperature of the dome environment was in the ranges 0 to 10^{o} C.

5.3.10 Dead-Time Calculation

A major draw back with pulse counting systems is their inability to count closely spaced pulses with accuracy. After the system (photomultipier tube, pre-amp, discriminator and counter) detects a pulse, there is a short time interval during which the system is unable to respond to any additional pulses. The minimum time interval between the detection of a pulse and the ability to respond to another is known as the dead-time. If the dead-time is known, then a correction can be made to the observed count rate to give the "true" count rate.

There are 3 main components which are going to contribute to the overall dead-time of the system, namely;

(i) the photomultiplier,

(ii) the amplifier/discriminator,

and (iii) the counter.

(i) The Photomultiplier Tube.

The dead-time of the photomultiplier tube is essentially governed by the individual electron trajectories within the tube.

The photoelectrons, generated at the photocathode, will follow individual paths to the first dynode, depending on their point of origin on the photocathode and other factors, such as emission velocities. Similarly, the secondary electrons will also follow individual paths between the dynodes and the anode.

This variation in electron transit times will determine the width of the output pulse from the tube. We can see that if two pulses were to arrive in a time interval shorter than the output pulse width, then they would not be resolved ie. they would appear as one pulse.

So the effective dead-time of the tube is given by the full width at half maximum of the output pulse.

All the tubes used in the photometer have a venetian blind structure and these typically have a f.w.h.m. spread of approximately 20ns.

(ii) Amplifier/Discriminator

The output pulse from the photomultiplier tube will be broadened by the amplifier/discriminator. Whilst this leads to a deterioration in the resolving time of the system, a certain amount of broadening of the output pulse would be necessary anyway to trigger the counters.

The width of the output pulses is readily measurable using an oscilloscope and the Table 5.4 gives the output pulse widths that are set at present. The pulse widths in channels 5 to 8 have been lengthened in an attempt to reduce the number of counting errors (see previous discussion in section 5.3.5).

(iii) The Counters

The counters provide by far the biggest contribution to the dead-time of the system. Essentially the counters are limited by the cycle time of the monostables which shape the output pulses from the amplifier/discriminators.

The monostable devices currently being used require an input pulse width of at least 40ns. Their cycle rate is set at 100ns. So the minimum dead-time we could expect from the system would be 100ns.

The individual responses of the counters is readily measured. A signal generator producing pulses 40ns wide, at 2V, is used to drive the counters. The frequency can than be increased until the counters fail, ie. we attempt to drive them at a higher frequency than their minimum cycle time. In tests carried out, the maximum response time of the counters was found to lie in the range 100-115ns.

Now, the component with the longest dead-time is going to be the major contributor to the inaccuracy of the counting. Whilst it would be convenient to adopt a figure of 115ns for the dead-time, based on the above, we must remember that, in the case of the counters, we are using evenly spaced pulses to measure the resolving time. But we know that the photons from "real" sources arrive randomly. Also, we want to have a measure of the resolving time as a whole, rather than as non-interacting, separate components. To see how we can measure the

dead-time of the complete system let us consider the equation for the dead-time correction.

$$n = Ne^{-Nt} \qquad (5.1)$$

where

n = observed count rate in counts per second

N = "true" count rate for a perfect system in counts per second

t = dead-time coefficient, defined as

$$t = 1/N$$

For which the observed count rate has fallen to 1/e of the true count rate.

We can take advantage of the fact that for low count rates the dead-time correction will be negligible. If we attenuate the light reaching the photomultiplier by a known factor, b, then only 1/b of the light will reach the photomultiplier. If we now observe a source, the observed count rate, n_L, will be low and will very nearly equal the true count rate N_L. If the attenuator is removed the true count rate, N_H, will increase b times. That is,

$$N_H = bN_L \simeq bn_L \qquad (5.2)$$

from [5.1] we have

$$n_H = N_H e^{-N_H t} \qquad (5.3)$$

and

$$n_L = N_L e^{-N_L t} \tag{5.4}$$

dividing [5.4] by [5.3]

$$\frac{n_L}{n_H} = \frac{N_L}{N_H} e^{-N_L t} e^{+N_H t} \tag{5.5}$$

substituting from [5.2] for N_H

$$\frac{n_L}{n_H} = \frac{1}{b} e^{-(1-b)N_L t} \tag{5.6}$$

If we make the substitution

$$x = b\frac{n_L}{n_H}$$

$$\ln(x) = -(1-b)N_L t$$

$$\therefore N_L = \frac{1}{(b-1)t} \ln(x) \tag{5.7}$$

substituting for N_L into [5.4]

$$n_L = \frac{1}{(b-1)t} \ln(x) \cdot x^{1/(1-b)}$$

or

$$(b-1)n_L t = \ln(x) \cdot x^{1/(1-b)}$$

$$\therefore (b-1)n_L t = \ln\left(b\frac{n_L}{n_H}\right) \cdot \left(b\frac{n_L}{n_H}\right)^{1/(1-b)} \tag{5.8}$$

This equation is correct for all count rates (assuming [5.2]) and is seen to be linear in t. So if we have a source of varying brightness, then a plot of

$$(b-1)\, n_L t = \ln\left(\frac{b n_L}{n_H}\right) \cdot \left(\frac{b n_L}{n_H}\right)^{1/(1-b)}$$

will produce a straight line with a gradient t.

Initially the measurements were taken using the darkening night sky as a light source and alternating between a clear aperture and one attenuated with a neutral density filter with an attenuation of approximately 2 magnitudes, (the precise figure is given in section 5.3.11). As the sky dimmed there would be a point at which the approximation in [5.2] would be met and from this linear part of the graph we can find t.

Several problems arose using this first method. Firstly, the large attenuation meant that too few counts were produced during the integration period. If the integration length was increased then too few points would be taken as the change in brightness of the sky between successive integrations becomes significant. Also, the tubes would have been saturated at the beginning of the run and it was felt that they would not have recovered by the end of the run, thus affecting the accuracy of the counts taken during the more critical period. The nature of the up/down counters does not allow us to see the contribution from the thermal counts, as these are subtracted out. However, for the linear part of the graph, their contribution would be negligible and will therefore not significantly affect the calculated dead time.

The measurements were repeated, this time using the brightening dawn sky, therefore the tubes would only be saturated at the end of the run. Also, by using a less dense neutral density filter (attenuation of approximately 10), the integration times would not need to be increased beyond 5 seconds, whilst still producing reasonably large count rates.

Figures 5.23 to 5.38 show the resulting plots. Once the counts rise above the background noise level we can see that the relationship is linear. The calculated values for the dead-time of each channel are given in Table 5.10, (sufficient count rates were never reached in channel 1 for a dead-time to be calculated). With the exception of channels 7 and 8, the dead-times can be see to be of the order of 150ns and this value has been adopted for all the channels.

5.3.11 Neutrality Of Neutral Density Filters

To assess the neutrality of the neutral density filters they were scanned, using a spectrophotometer, over a wavelength range of 450 - 850nm. The results, Figure 5.29, show there to be very little colour dependence. Table 5.11 gives values for the attenuation of the three filters as determined by this method.

As well as scanning the filters, their neutrality was also investigated by observing a series of standard stars with widely varying colours. The five stars observed are shown in Table 5.12, along with their spectral type and magnitude. When trying to observe a star through different neutral density filters we encounter two problems. When observing through a very dense filter the count rates will be very low and conversely, when observing with no filter the count rates are sufficiently high that dead-time corrections will not

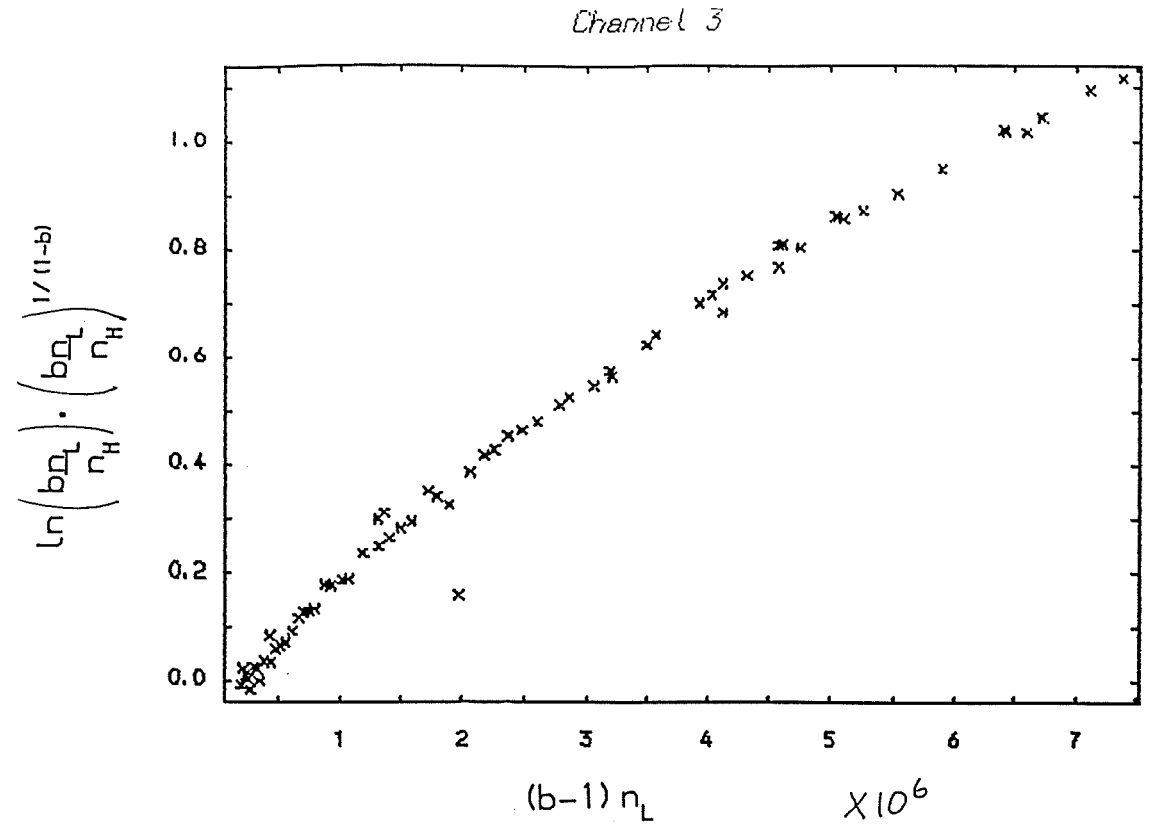

Fig.5.23

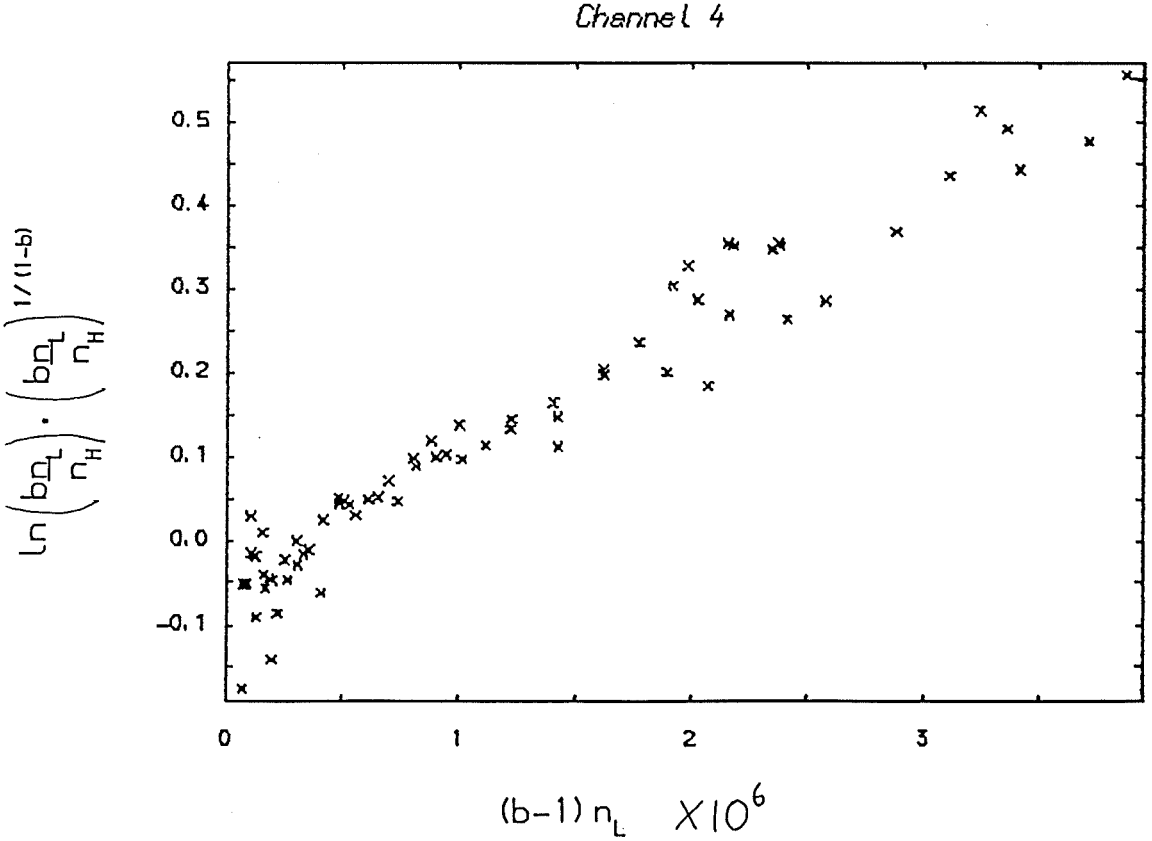

Fig.5.24

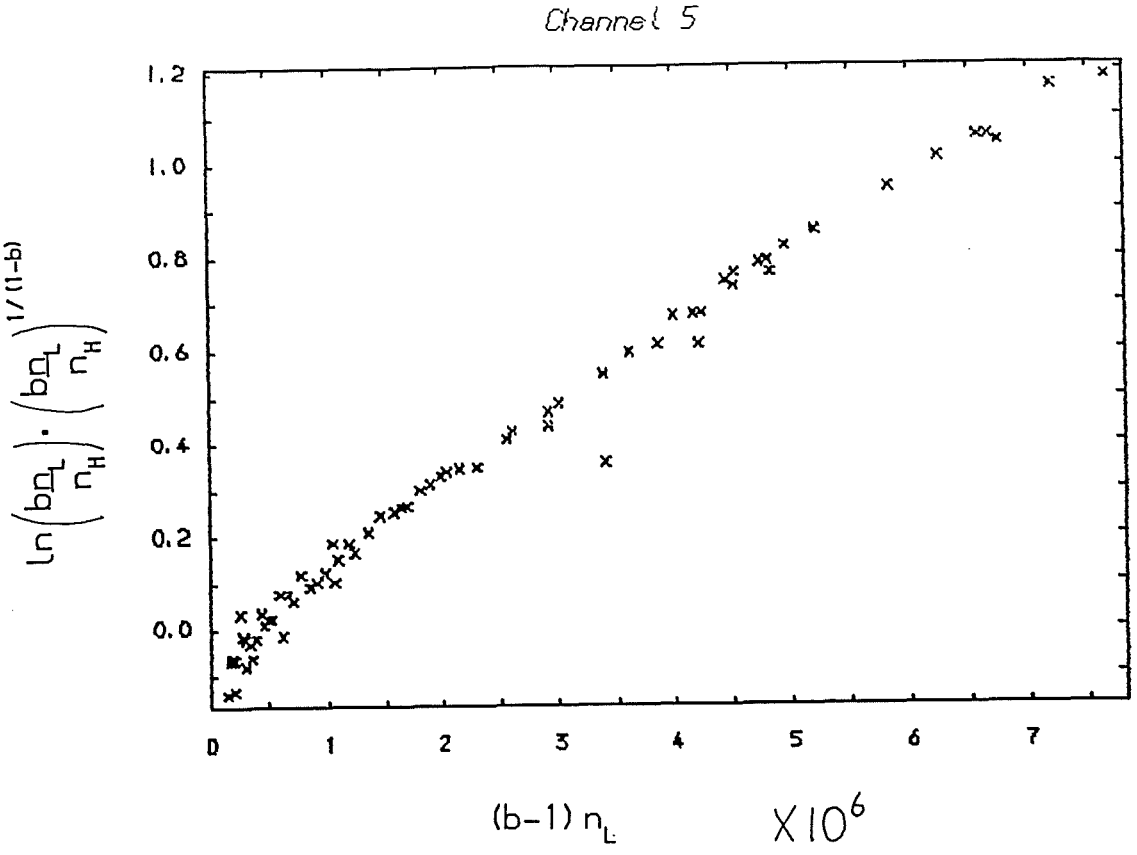

Fig.5.25

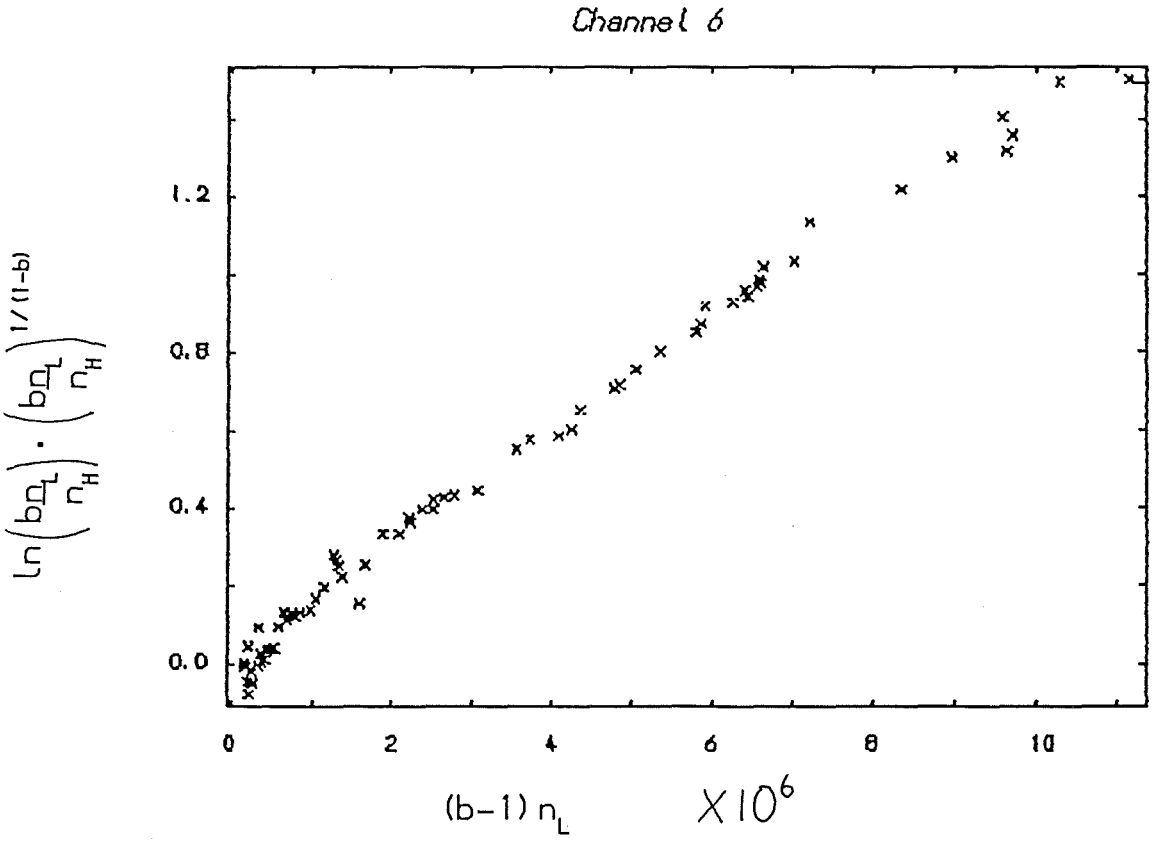

Fig.5.26

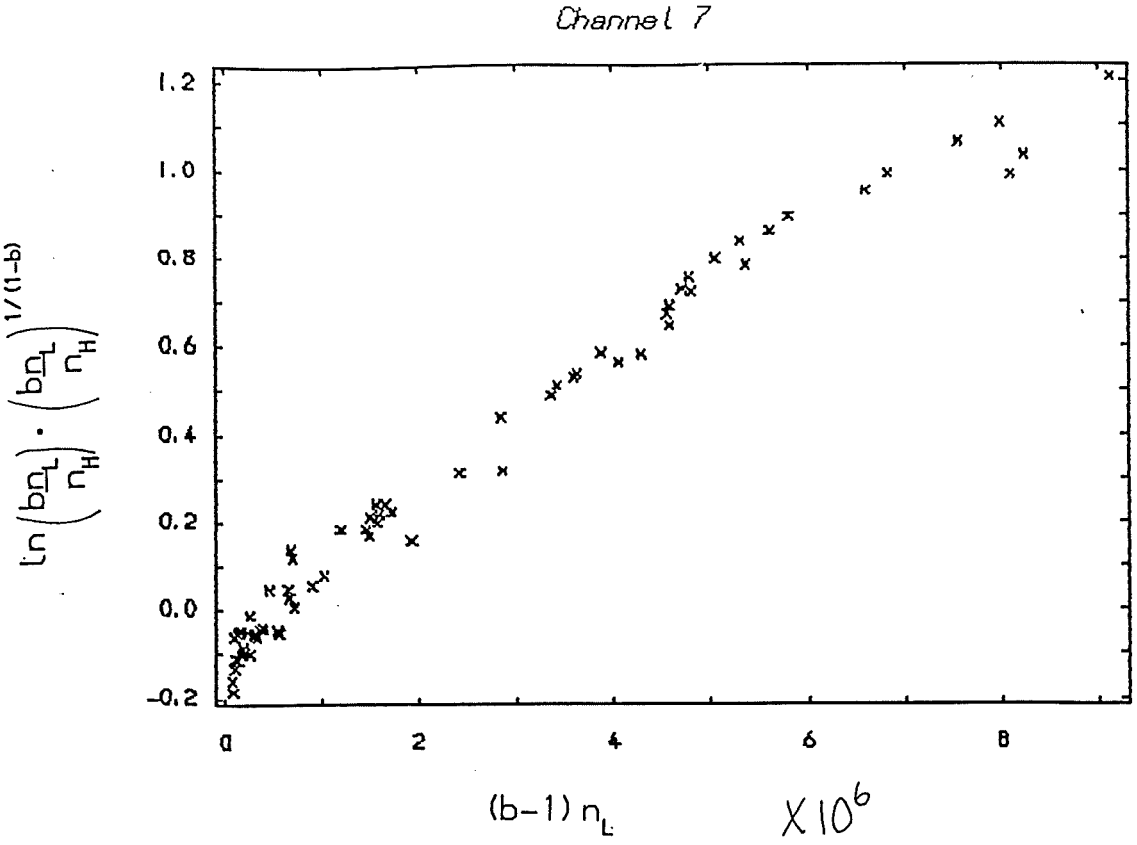

Fig.5.27

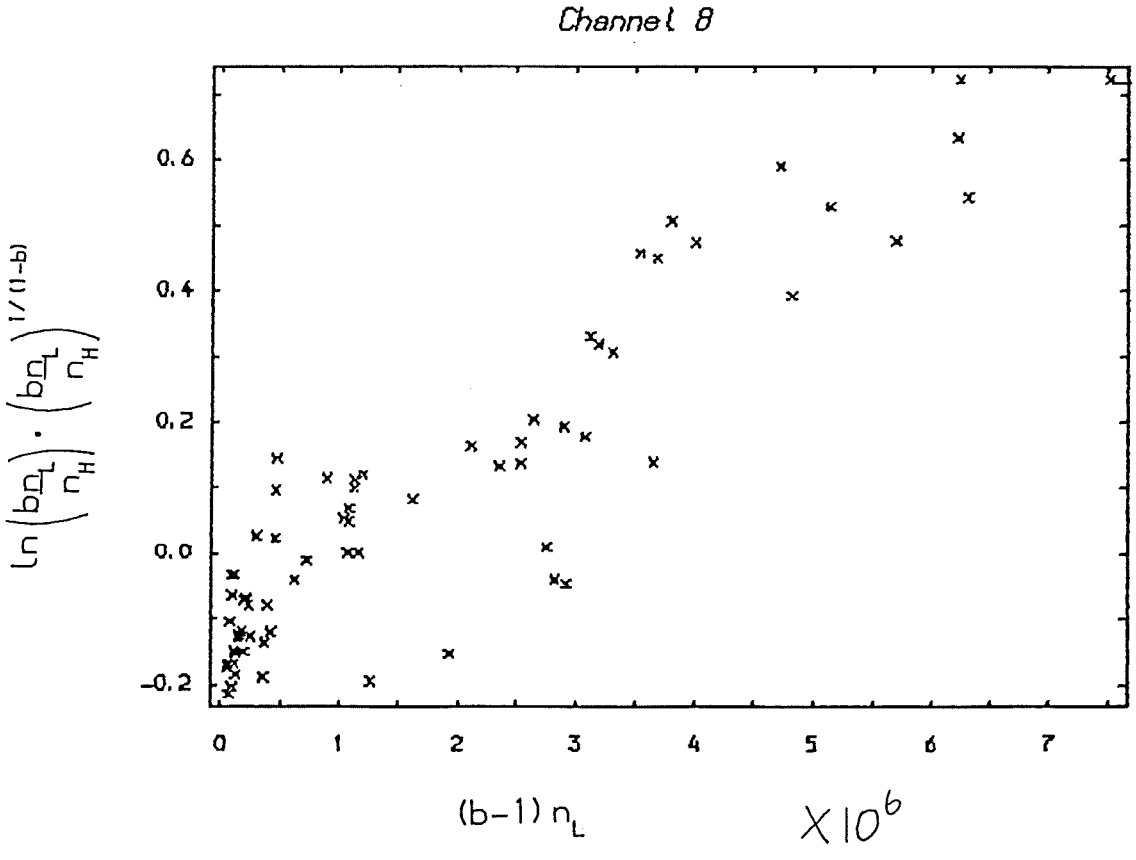

Fig.5.28

Table 5.9 Dark counts in counts per second.

Channel 1	10
Channel 3	10
Channel 4	1300
Channel 5	1700
Channel 6	2000
Channel 7	200
Channel 8	250

Table 5.10 Measured dead times.

Channel	Dead Time (ns)
3	145 +/- 2
4	151 +/- 4
5	160 +/- 1
6	143 +/- 2
7	128 +/- 3
8	113 +/- 13

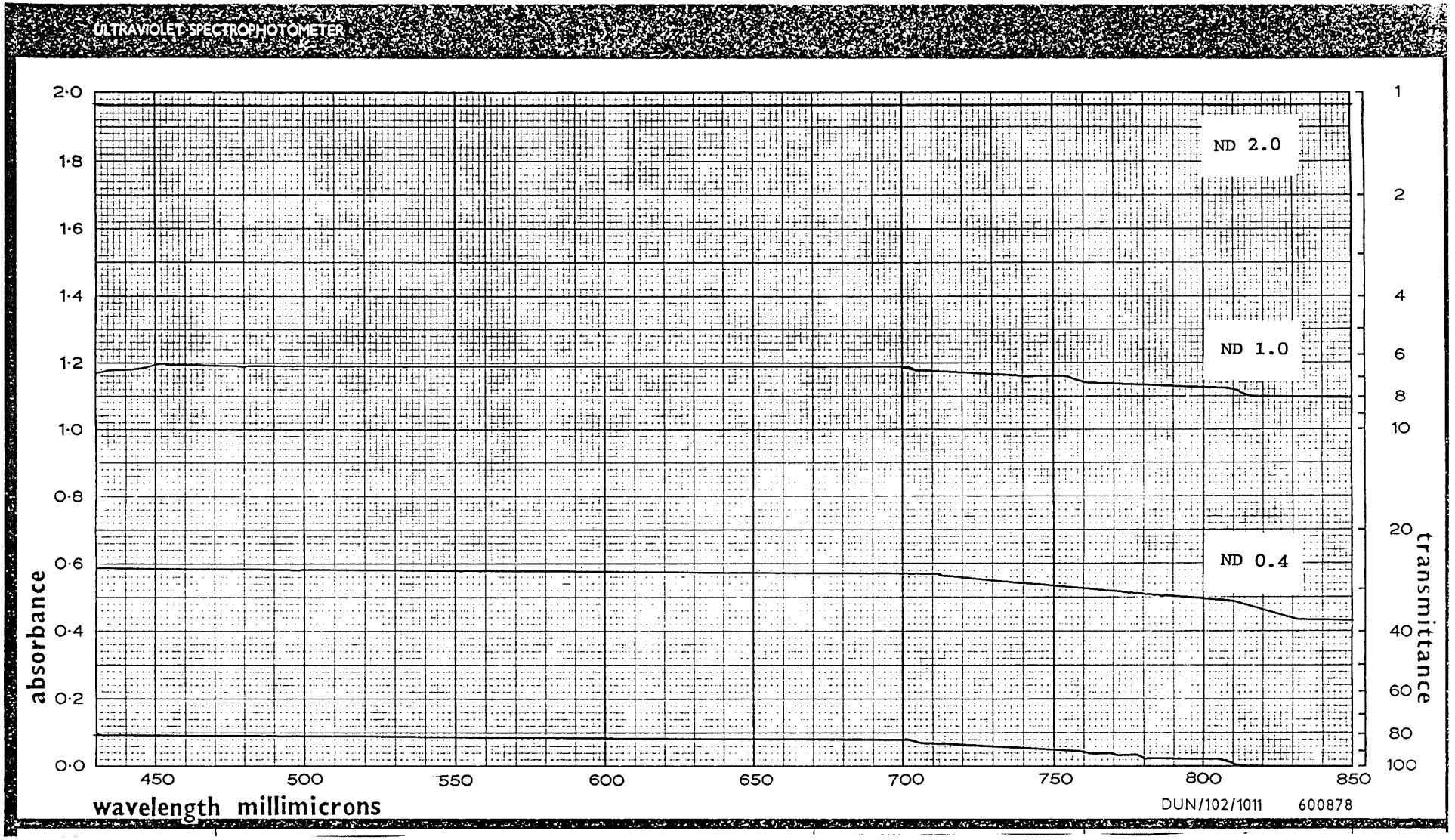
ULTRAVIOLET SPECTROPHOTOMETER
2·0
1·8
1·6
1·4
1·2
1·0
0·8
0·6
0·4
0·2
0·0
absorbance
ND 2.0
ND 1.0
ND 0.4
1
2
4
6
8
10
20
40
60
80
100
transmittance
450
500
550
600
650
700
750
800
850
wavelength millimicrons
DUN/102/1011
600878

Fig.5.29

be negligible. With these considerations in mind we can see, from the attenuation values shown in Table 5.13, that the colour dependence is again low (less than 5%). There is also good agreement between the values found by both methods.

5.3.12 Sensitivity Variation Over Apertures

Ideally we would like to be able to place a star anywhere within the aperture and record the same signal strength. Whilst the Fabry lenses, by focussing an image of the primary mirror onto the photocathodes, help considerably to eliminate these sensitivity variations within the aperture, they can not totally eliminate them, especially with the complication of possible bandpass variations mentioned previously.

To see how strong the variations are, the count rate from a standard star was recorded as it was driven across the aperture, first in Right Ascension and then Declination. (R.A. corresponds to the direction of dispersion). The results are shown in Fig 5.30 and 5.31 respectively.

From the results for motion in Right Ascension we can see that, with the exception of channel 4, the gain in variation is of the order of a few percent. The drop in sensitivity in channel 4 may be due to a blemish on the number 4 mirror in the mosaic.

For the motion in Declination the star was allowed to pass through both apertures so that a comparison could be made of the gain sensitivity from one aperture to the next. Again the variation is of the order of a few percent. (The apparent unequal size of the apertures is due to the star being trailed off-axis through the apertures. The motion in Dec. was coarser than that in R.A., hence

Table 5.11 Neutral density values taken from scan with spectrophotometer.

Nominal	Actual
0.4	0.48
1.0	1.10
2.0	1.86

Table 5.12 Spectral type and magnitude of stars used to investigate colour variation of the neutral density filters.

Name	Sp.Type	Vmag
HR 8830	A8	4.52
HR 8965	B8	4.29
HR 8976	B9	4.14
HR 27	F2	5.03
HR 63	A2	4.61

Table 5.13 Average attenuation values for the above stars observed through the 3 neutral density filters.

Channel	0.4	1.0	2.0
1	0.39 +/- 0.03	0.95 +/- 0.02	1.89 +/- 0.03
3	0.37 +/- 0.01	0.98 +/- 0.02	1.86 +/- 0.02
4	0.39 +/- 0.01	1.01 +/- 0.00	1.91 +/- 0.01
5	0.38 +/- 0.01	1.01 +/- 0.01	1.89 +/- 0.02
6	0.47 +/- 0.01	0.99 +/- 0.01	1.88 +/- 0.02
7	0.40 +/- 0.01	1.06 +/- 0.02	1.94 +/- 0.01
8	0.41 +/- 0.01	1.05 +/- 0.01	1.92 +/- 0.01
Average	0.39 +/- 0.02	1.01 +/- 0.04	1.90 +/- 0.03

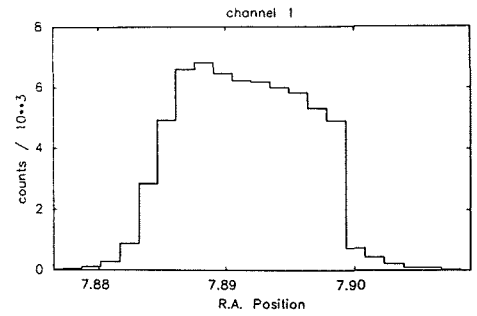

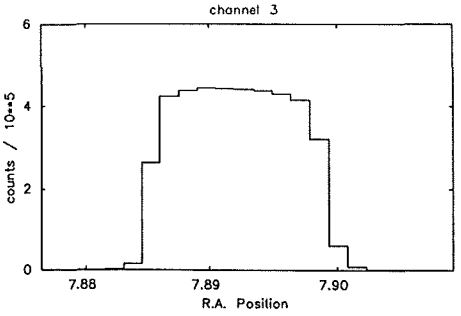

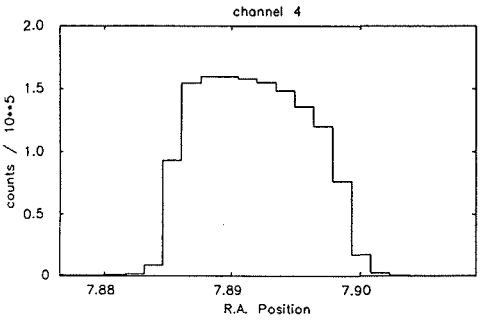

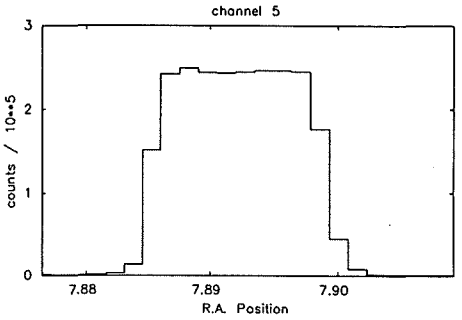

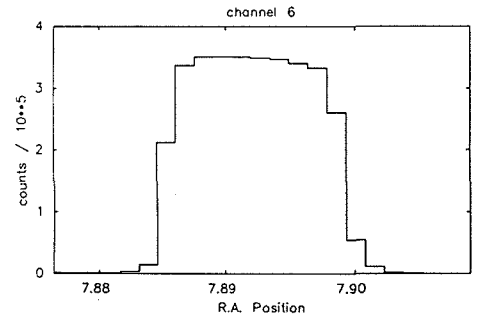

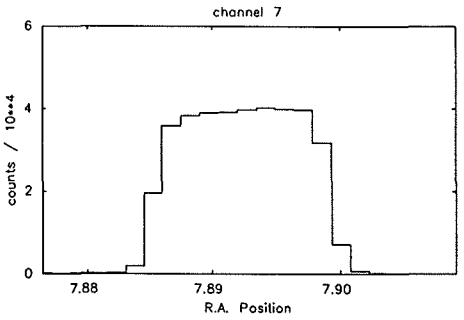

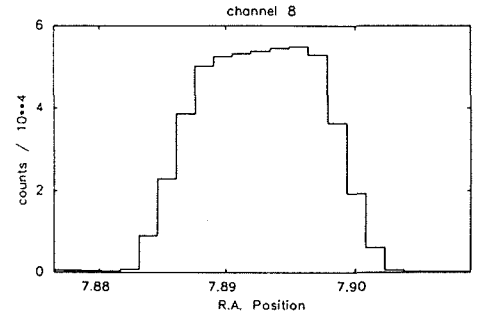

Fig.5.30 Sensitivity variation in Right Ascension.

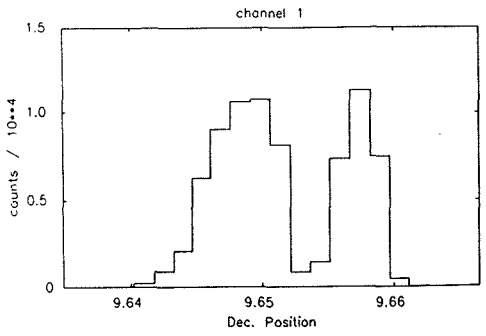

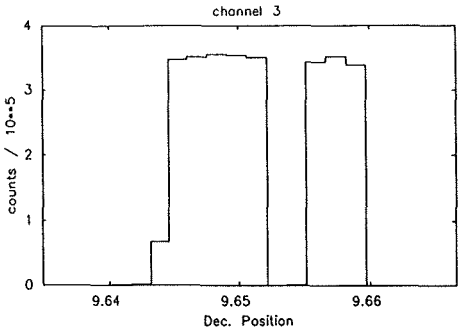

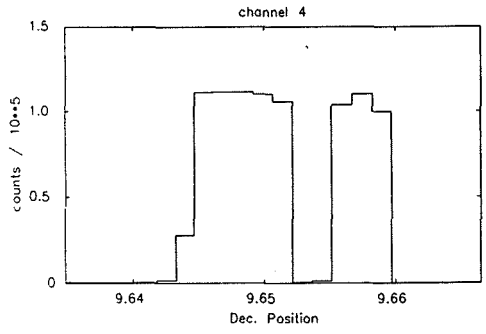

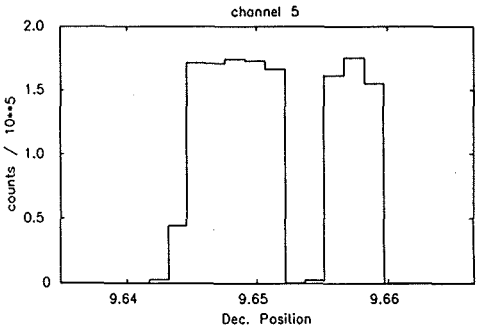

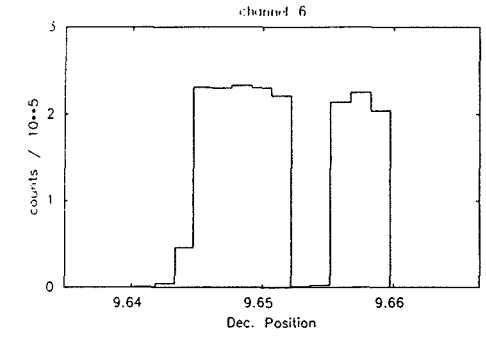

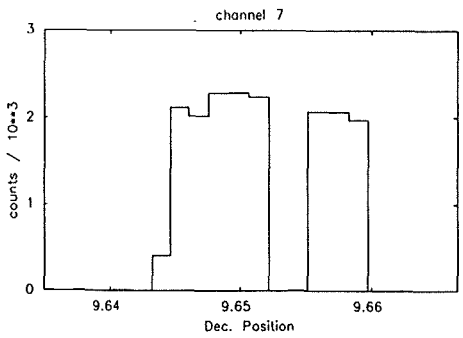

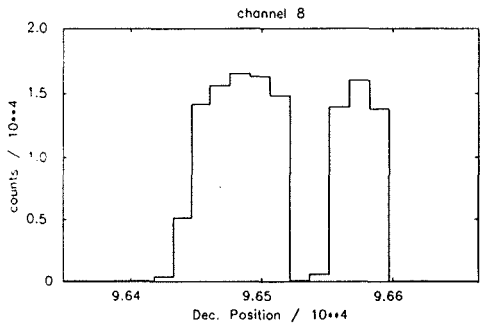

Fig.5.31 Sensitivity variation in Declination.

the larger step size).

CHAPTER 6

ASTRONOMICAL PHOTOMETRY

6.1 INTRODUCTION

The reduction of the photometric data acquired with the 8-channel photometer will primarily consist of two steps.

(i) adjustment for atmospheric extinction and

(ii) transformation to the Stromgren system.

Due to the limited amount of observing time that was available no attempt was made to provide for a transformation for the R and I magnitudes.

6.1.1 The Strömgren Four-Colour System

The Strömgren system, (Strömgren, 1966), is an intermediate-band system especially suited to the study of A, F and G-type stars. The system consists of 4 filters whose central wavelengths and halfwidths are given in Table 6.1. (The central wavelength and halfwidths of the filters used in the 8-channel photometer are also included for comparison). Figure 6.1 schematically illustrates a simplified stellar spectrum and the placement of the 4 filters.

Table 6.1 Central Wavelengths and halfwidth for Strömgren system and 8-channel photometer.

Strömgren System.

Filter	Central Wavelength (nm)	Halfwidth (nm)
u	350	40
v	410	20
b	470	10
y	550	20

8-Channel System.

Filter	Central Wavelength (nm)	Halfwidth (nm)
u	347	35
v	411	19
b	467	18
y	547	23

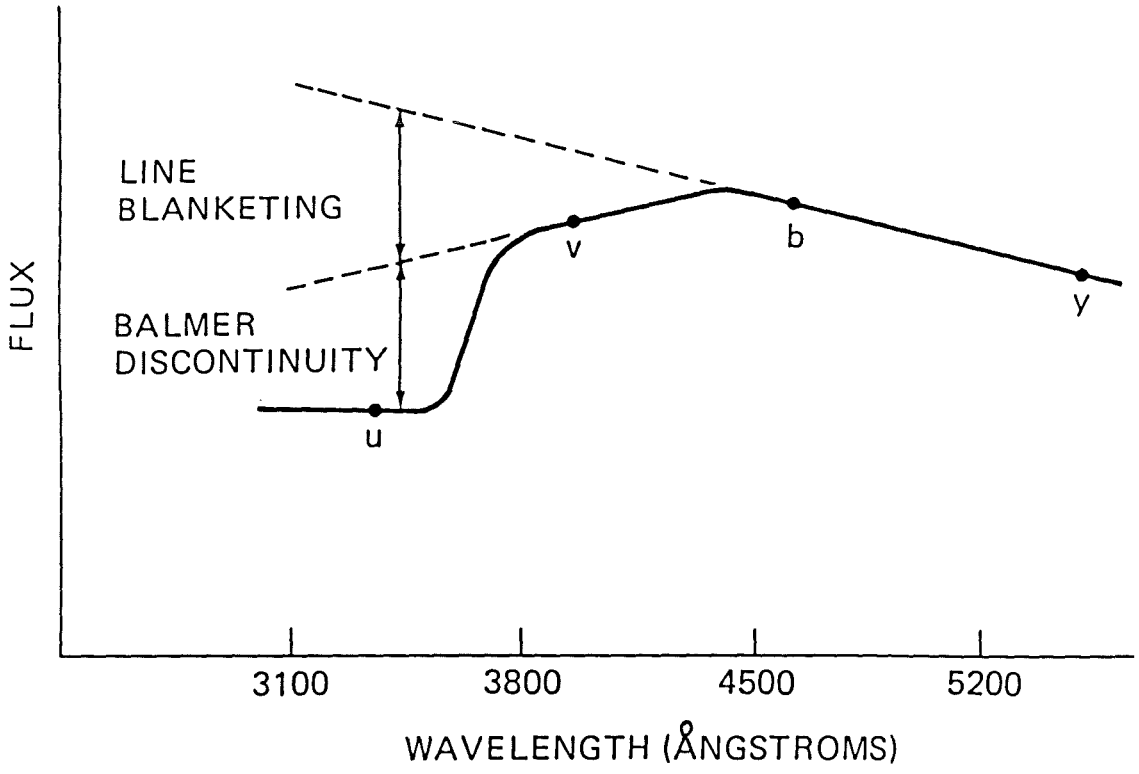

Figure 6.1 Simplified stellar spectrum showing placement of Strömgren filters.

Four main qualities can be derived from the system;

(i) The y filter provides an apparent magnitude which is equivalent to the V magnitude of the Johnson UBV system.

(ii) The (b-y) index is a good indicator of colour and a basic temperature parameter.

(iii) the colour difference

$$c_1 = (u-v) - (v-b)$$

is a measure of the size of the Balmer discontinuity and hence luminosity for a given temperature. Since the line blocking in the u filter is approximately twice that in the v filter and the b filter is relatively free from lines, the c_1 index is almost independent of chemical composition effects.

(iv) The colour difference

$$m_1 = (v-b) - (b-y)$$

provides a measure of line blocking and line metallicity.

The primary standards for the system are given by Crawford and Barnes (1970), who showed that the system was determined purely by the filters. The system is therefore independent of the telescope and photometer used.

6.1.2 Photoelectric Reduction Procedure

Photometric systems are defined with respect to the light as it was outside the Earth's atmosphere. But the atmosphere absorbs and scatters, (reddens), light as it passes through it, the effect increasing as the distance the light travels through the atmosphere

becomes greater. Thus a star at the zenith is least affected by the atmospheric extinction. The effects are expressed by Bouguer's law;

$$m_{\lambda,0} = m_{\lambda,z} - K_\lambda X$$

where $m_{\lambda,0}$ is the magnitude at λ as would be observed ouside the atmosphere

$m_{\lambda,z}$ is the magnitude at wavelength λ and at zenith distance

K_λ is the extinction coefficient at wavelength λ

and X is the path length, in units of air mass at the zenith of the observer.

As a first approximation the air mass is given by the secant of the zenith distance z,

$$X = \sec z$$

where $$\sec z = (\sin\varphi \sin\delta + \cos\varphi \cos\delta \cos H)^{-1}$$

φ Observers latitude.

δ Declination of the star.

H Hour angle in degrees.

A more accurate value for X can be found from the polynomial approximation made to the data collected by Bemporad in 1904. This is given by,

$$X = \sec z - 0.0018167(\sec z - 1) - 0.002875(\sec z - 1)^2$$

$$-0.00080803(\sec z - 1)^3$$

This is accurate to better than 0.1% up to X = 6.8 and better than 1% up to X = 10, (Hardie, 1962).

From Bouguer's law we can see that the extinction coefficient, K, is the slope of a straight line representing the graph of m with X. Therefore K could be obtained from a plot of the measured magnitude m of a single star with air mass X if observations are made for a range of zenith distances.

But on a typical night, the atmospheric transparency is likely to vary quite considerably during the time interval required for the star to move through a sufficiently large range of air mass. Also, the given amount of extinction is variable over various parts of the sky.

So it is more common to obtain several measurements throughout a night and obtain an average extinction for the night. Further, it has been shown that a mean, based on the average of several nights, can lead to a more representative value of K, particularly if the nightly averages have been determined from relatively few measurements, (Johnson and Morgan, 1951; Hiltner, 1953).

Since the atmosphere not only attenuates but scatters as well, then the extinction coefficient will be wavelength dependent. For colour indices it is usual to treat the extinction in a differential manner ie.

$$C_0 = C - K_C X$$

where K is simply the difference between the corresponding magnitude coefficients.

When using well defined, intermediate-band systems, second-order extinction coefficients can be ignored.

6.1.3 Magnitude And Colour Transformation

Each individual combination of telescope, filters and detectors will define its own set of magnitudes and colours, forming a "natural" or "instrumental" system. It is often desirable to be able to transform magnitudes and colours from this instrumental system to a standard system so that comparisons of results taken on different instruments can be made.

Considering the Strömgren system: The 4 channels associated with the u, v, b, and y filters provide us with count rates u', v', b' and y', (after dead-time corrections have been made).

If X is the air mass for the mean hour angle of the observation then the indices in the instrumental system of the photometer are written as;

$$y_{obs} = y' - K_y X$$

$$(b-y)_{obs} = (b'-y') - K_{by} X$$

$$(v-b)_{obs} = (v'-b') - K_{vb} X$$

$$(u-b)_{obs} = (u'-b') - K_{ub} X$$

where K_y, K_{by}, K_{vb} and K_{ub} are the first-order extinction coefficients.

These values may be transformed to the standard system by the formulae;

$$V = A + y_{obs} + B(b-y)$$

$$(b-y) = C + D(b-y)_{obs}$$

$$(v-b) = E + F(v-b)_{obs} + G(b-y)$$

$$(u-b) = H + I(u-b)_{obs} + J(b-y)$$

where D F and I are Scale Factors

A C E and H are Zero Points

B G J are Colour Terms

From the formulae given above we can proceed to establish a set of transformation equations.

6.1.4 Difficulties In Establishing Accurate Extinction Coefficients

In establishing the transformation coefficients one of the most difficult parameters to measure, (and control), is the zero-point term, as this is affected by sensitivity changes in the instrument. It can only be determined accurately if the extinction terms are well known.

Unfortunately, as was mentioned earlier, it is not always possible to accurately determine the extinction coefficients for every night. Indeed, Stebbins and Whitford, (1945), were of the opinion that if sufficient time was allocated for the determination of the extinction terms there would be no time left for anything else. Although this may be rather pessimistic, (see eg. Young, 1974), it is still true that the process is time-consuming. Hardie (1959) describes a method of determining extinction coefficients which is quicker and more accurate than conventional techniques. The method presupposes that the observer has already set up a system of magnitudes and colour indices outside the atmosphere for a number of standard stars, for which an accurate transformation to a standard system is known. The procedure is to then observe approximately 3 stars near the zenith with another 3 through a large air mass. This yields extinction coefficients accurate to 2 to 3%.

Clearly, when setting up a new system the above method can not be used, since an accurate transformation is not available. Further, since the scale and colour terms are best determined from stars having a wide range of colours, but located close together, and preferably near the zenith, little extinction information will be available from these data.

With the above considerations in mind, it was decided to adopt average values for the extinction coefficients and to carry out an observing programme which would result in as accurate a determination as possible of the transformation equations. This can be justified by recalling the findings of Johnson, Morgan and Hiltner discussed earlier.

6.1.5 The Observations

Due to adverse weather conditions, less than 14hrs. of observing time, spread over 3 separated nights, were available to produce a set of transformation equations. A list of the standard stars observed is shown in Table 6.2. The standards were taken from those used by Crawford and Barnes (1970). They were chosen so as to cover as wide a range as possible in spectral type.

On the two nights in October the Moon was full and observing had eventually to be stopped due to increasing cloud cover. The other night was some 12 days previous and was during the period of new Moon. This night started cloudy but gradually cleared.

On all three nights the largest pair of the apertures were used (40") and the stars were always placed in the same aperture. Where necessary neutral density filters had to be employed to attenuate the light from the brighter stars. Integration times were chosen that would result in a good Signal-to-Noise ratio (see appendix C). The total number of integrations on each star was made sufficiently large that any variations due to the movement of the star in the aperture, caused by irregularities in the telescope drive could be averaged out.

Table 6.2 Strömgren standard stars used to form transformation equations.

1 ... Observed on Sep.23rd. 1987

2 ... Observed on Oct.6th. 1987

3 ... observed on Oct.8th. 1987

Date	Name	V	b-y	m	c
1 2	HR 27	5.03	+0.273	0.123	1.082
1 2	HR 63	4.61	+0.026	0.180	1.050
1 2	HR 68	4.52	+0.026	0.187	1.040
2	HR 153	3.66	-0.090	0.087	0.134
1 2	HR 184	4.94	+0.087	0.221	0.902
1 2	HR 193	4.54	+0.007	0.076	0.479
2	HR 269	3.87	+0.068	0.194	1.056
1 2	HR 343	4.33	+0.087	0.213	0.997
1	HR 685	5.17	+0.321	-0.038	0.753
1	HR 717	5.30	+0.178	0.211	0.780
1	HR 801	4.66	-0.052	0.097	0.333
1	HR 937	4.05	+0.376	0.201	0.376
1	HR 1269	5.23	+0.226	0.159	0.588
1	HR 1303	4.14	+0.614	0.268	0.551
3	HR 5936	2.32	-0.019	0.038	-0.017
3	HR 6092	3.89	-0.056	0.089	0.440
2 3	HR 6332	5.25	+0.002	0.180	1.094
3	HR 6458	5.39	+0.409	0.182	0.309
2 3	HR 6588	3.80	-0.064	0.078	0.294
1 2 3	HR 7328	3.77	+0.579	0.390	0.430
2 3	HR 7469	4.48	+0.261	0.158	0.506
2 3	HR 7503	5.96	+0.410	0.214	0.375
2 3	HR 7504	6.20	+0.416	0.226	0.354

/continued

Table 6.2 /continued

1 ... Observed on Sep.23rd. 1987

2 ... Observed on Oct.6th. 1987

3 ... observed on Oct.8th. 1987

Date	Name	V	b-y	m	c
3	HR 7534	4.99	+0.316	0.155	0.435
1 2 3	HR 7730	4.83	+0.068	0.150	1.310
1 2 3	HR 7977	4.84	+0.356	-0.067	0.153
1 2 3	HR 7984	5.04	+0.108	0.209	0.897
2 3	HR 8085	5.21	+0.656	0.677	0.134
2 3	HR 8086	6.03	+0.791	0.676	0.067
1 2 3	HR 8494	4.19	+0.169	0.192	0.787
1 2 3	HR 8585	3.77	+0.001	0.173	1.030
1 2 3	HR 8613	4.63	+0.142	0.174	0.948
1 2 3	HR 8622	4.88	-0.070	0.042	-0.110
1 2	HR 8830	4.52	+0.181	0.172	0.723
1 2	HR 8965	4.29	-0.031	0.100	0.784
2	HR 8976	4.14	-0.035	0.131	0.831

6.1.6 Reduction Procedure

The software package STANCOL, written by Dr.S.A.Bell, was used to determine the transformation equations. The raw count rates are first dead-time corrected and then instrumental magnitudes formed. The programme 8CHANPREP, written by the author, is then used to create a file containing the instrumental and standard magnitudes and colours of the standard stars, along with the mean times of observation and airmasses.

The transformation equations are of the form shown below;

$$Cstd = \text{Zero Point} + Cext \cdot \text{Scale Factor} + \text{Colour Term} \cdot (b-y)std$$

and $$Cext = Cinst - \text{extinction coefficient} \cdot \text{airmass}$$

where Cinst, Cext and Cstd refer to the instrumental, extinction corrected and standard colours respectively. Since we know Cstd, Cinst and the airmass, then if we have n measurements for standard stars, n equations of condition for the 4 unknowns can be formed. A least squares solution may then be made to obtain the best estimates of the 4 unknowns.

The procedure used is outlined below. First extinction coefficients were adopted, based on past knowledge of the observing conditions at St.Andrews (Hilditch, 1988). Then solutions were found for the scale factors and zero points for each night. Since the colour term is usually very small this is set to zero for this preliminary analysis.

Next a mean value for the scale factor is adopted. For the same combination of telescope, filter set and detectors this should not vary much from night to night.

Using the mean scale factor, solutions are found for the zero points and colour terms for each night and a mean value for the colour term is adopted.

Finally, using the mean scale and colour terms, nightly solutions are found for the zero point.

The above procedure is carried out for the magnitude and 3 colour terms. After each solution is found, the calculated colour is plotted against the standard colour and the residuals of the standard colours from the calculated colours are plotted against the calculated colour, time and airmass to assess and detect any trends in the data. The facility exists to edit any observations which are poor, or any incorrectly identified stars.

6.1.7 The Derived Transformation Equations

Tables 6.3 to 6.30 give the results obtained, with the diagnostic plots given in Figs. 6.2 to 6.49.

For the V magnitude the residuals are greater than for the colour terms. This is to be expected, since with the colour terms any attenuation due to cloud will affect both channels equally, assuming that the clouds approximate to neutral absorbers. On the two nights in October, during which there was a full Moon and gradually increasing cloud cover, a definite trend in the residuals with time can be seen (Figs. 6.8 and 6.12). This drift confirms the observations of Warner (1971), that clouds are very much better

scatterers than absorbers. Initially the magnitudes will be overestimated due to the large amount of moonlight scattered from the clouds. Then as the cloud cover increases the magnitudes will be underestimated as absorption begins to dominate over scattering.

Transformations were made for all the stars on the 3 nights and these are shown, along with the internal errors and the standard values for comparison in Tables 6.19 to 6.30. Whilst we can see from the diagnostic plots, (Figs. 6.2, 6.6, 6.10, 6.14, 6.18, 6.22, 6.26, 6.30, 6.34, 6.38, 6.42 and 6.46) that the relationship between standard and calculated values is always very linear, there are some large errors in some of the calculated magnitudes. Some of these have arisen since the stars that were rejected during the derivation of the transformations have been included. However, no systematic trend, either with colour or magnitude, is seen in the stars which exhibit large transformation errors. If any relationship does exist it is with time, which is more a function of the observing conditions than any instrumental effect.

It must be borne in mind that the nights on which the standard stars were measured were very different in character. Furthermore, because of the low altitude of the observatory at St.Andrews, (30m above sea level), the attenuation due to the water vapour in the atmosphere is considerable in the u channel, which will affect the c1 parameter. Also the use of a camera lens as an optical coupler will greatly reduce the transmisson in the u channel.

The transformations as they stand demonstrate that the combination of filters and detectors used in the 8-channel photometer do not introduce any systematic colour effects. If better transformations are to be made then it is clear that more nights of better photometric quality are needed.

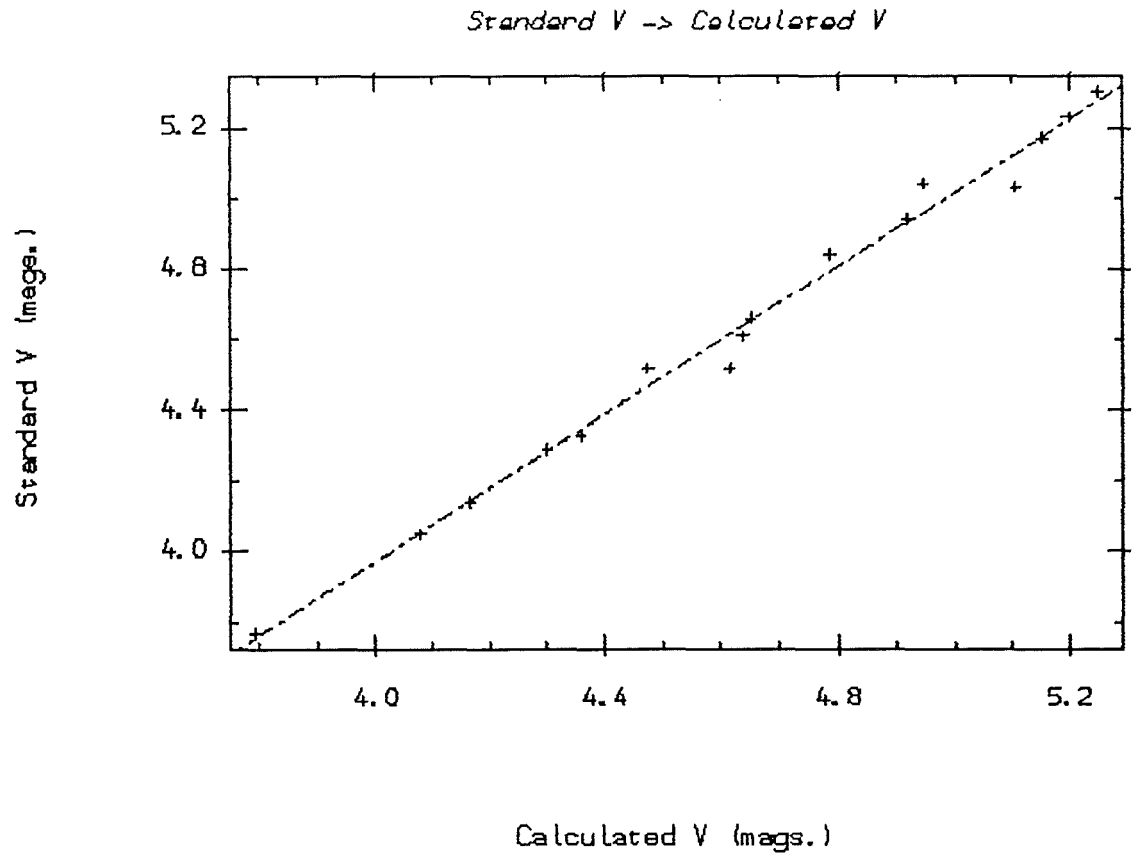

Fig.6.2 Sep.23rd V Magnitudes.

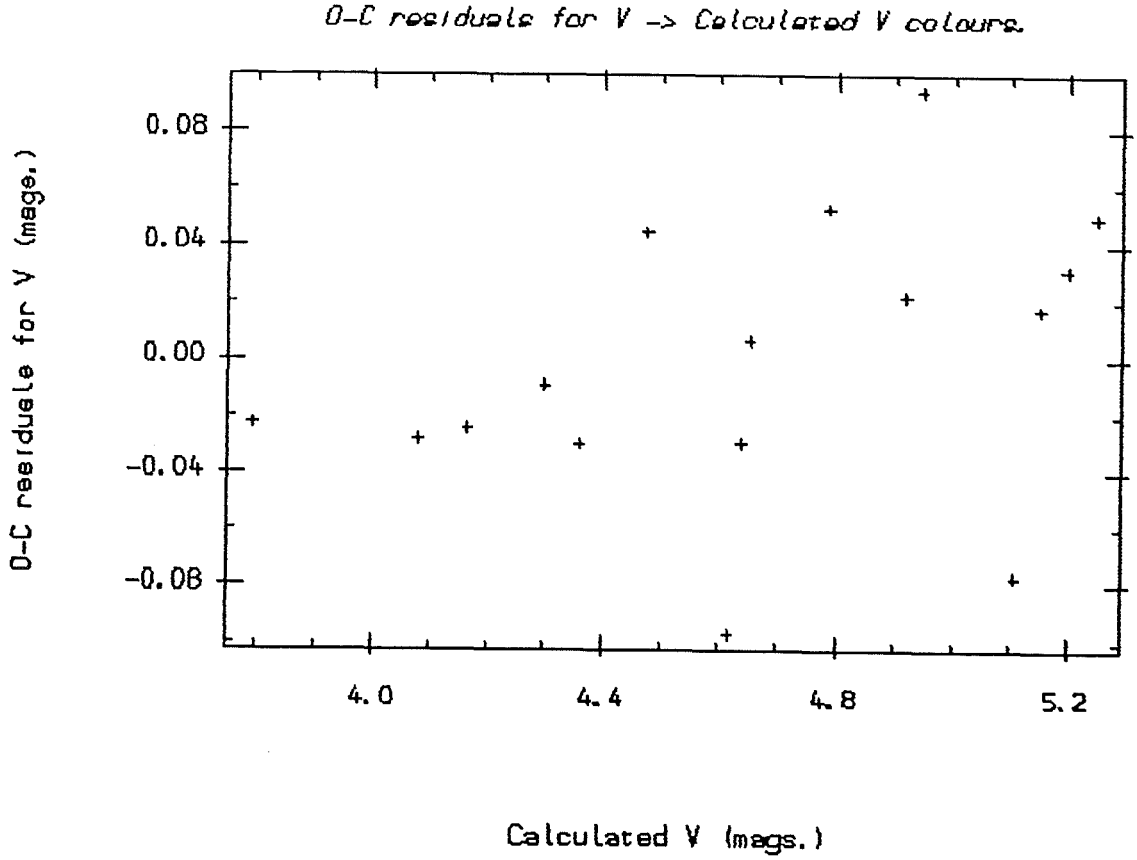

Fig.6.3 Sep.23rd V Magnitudes.

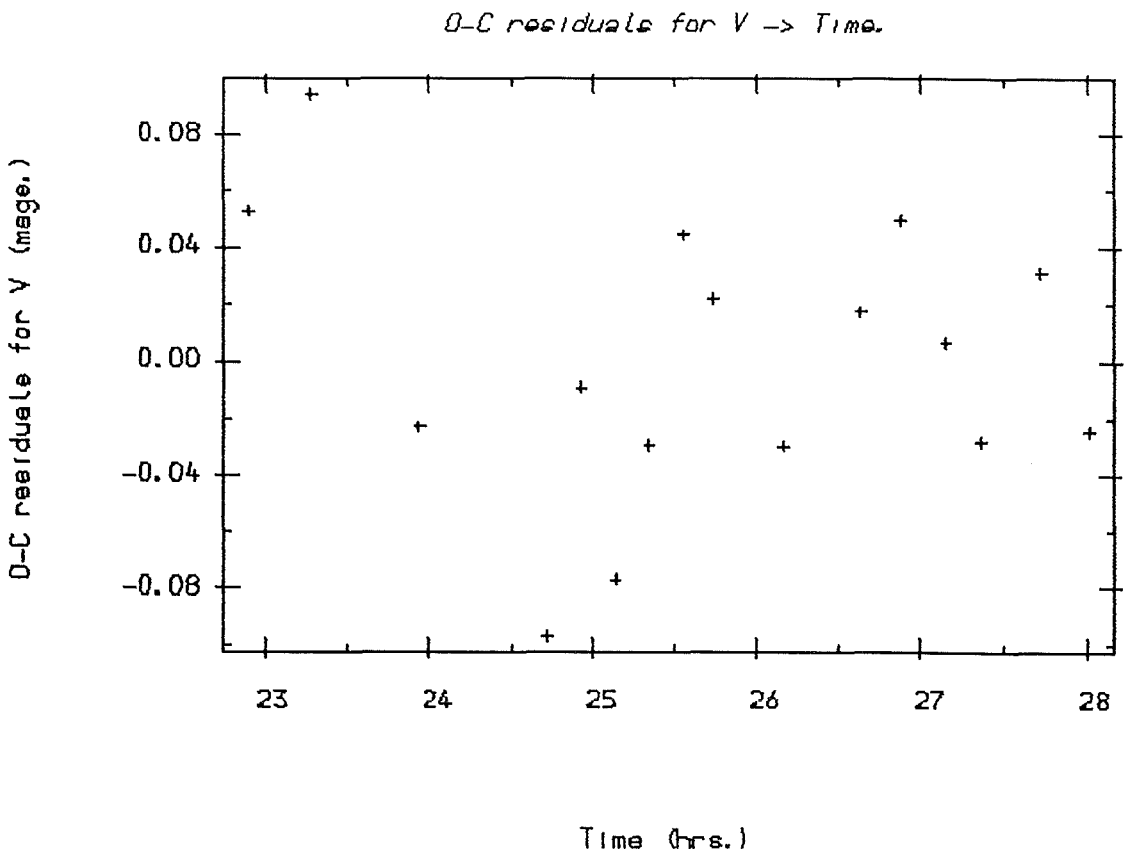

Fig.6.4 Sep.23rd V Magnitudes.

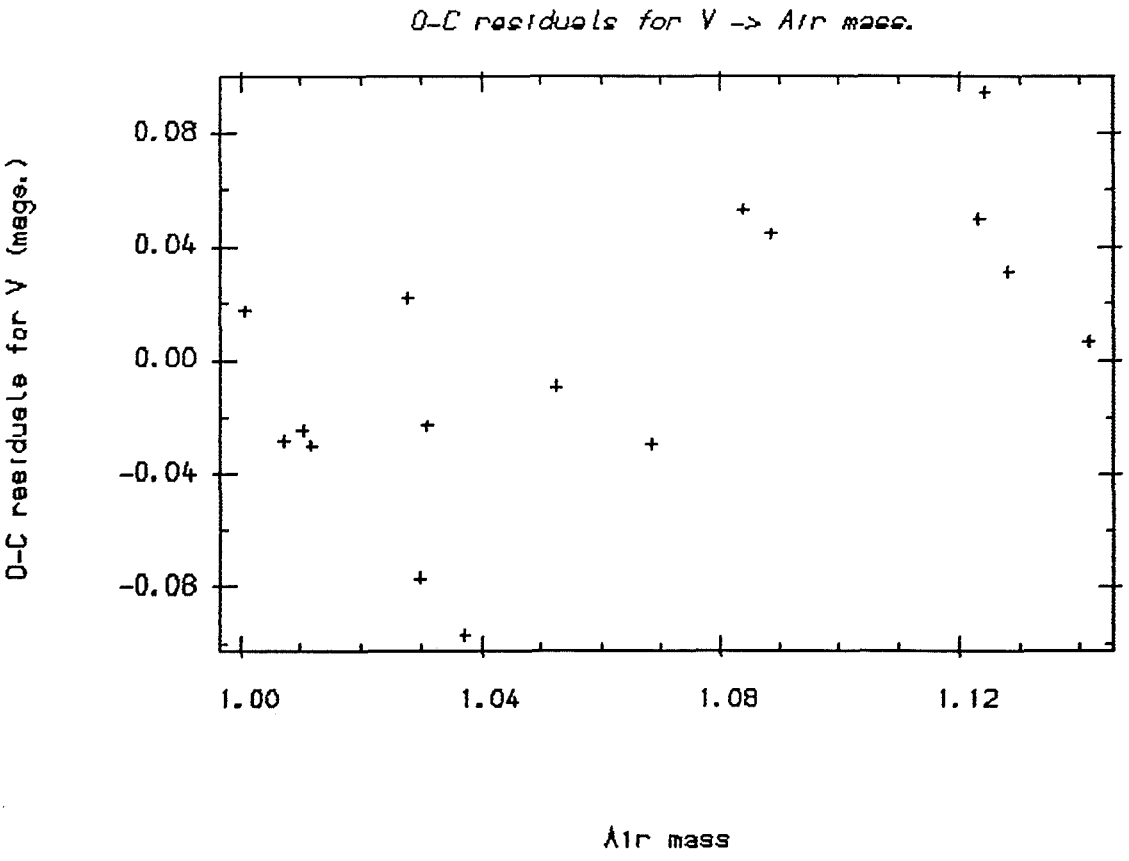

Fig.6.5 Sep.23rd V Magnitudes.

THE DEVELOPMENT AND COMMISSIONING OF AN 8-CHANNEL ASTRONOMICAL PHOTOMETER

Christopher A. Pollard

A Thesis Submitted for the Degree of PhD
at the
University of St Andrews

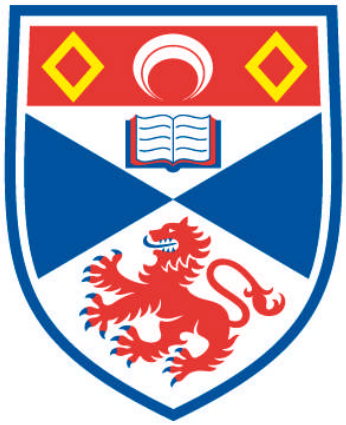

1988

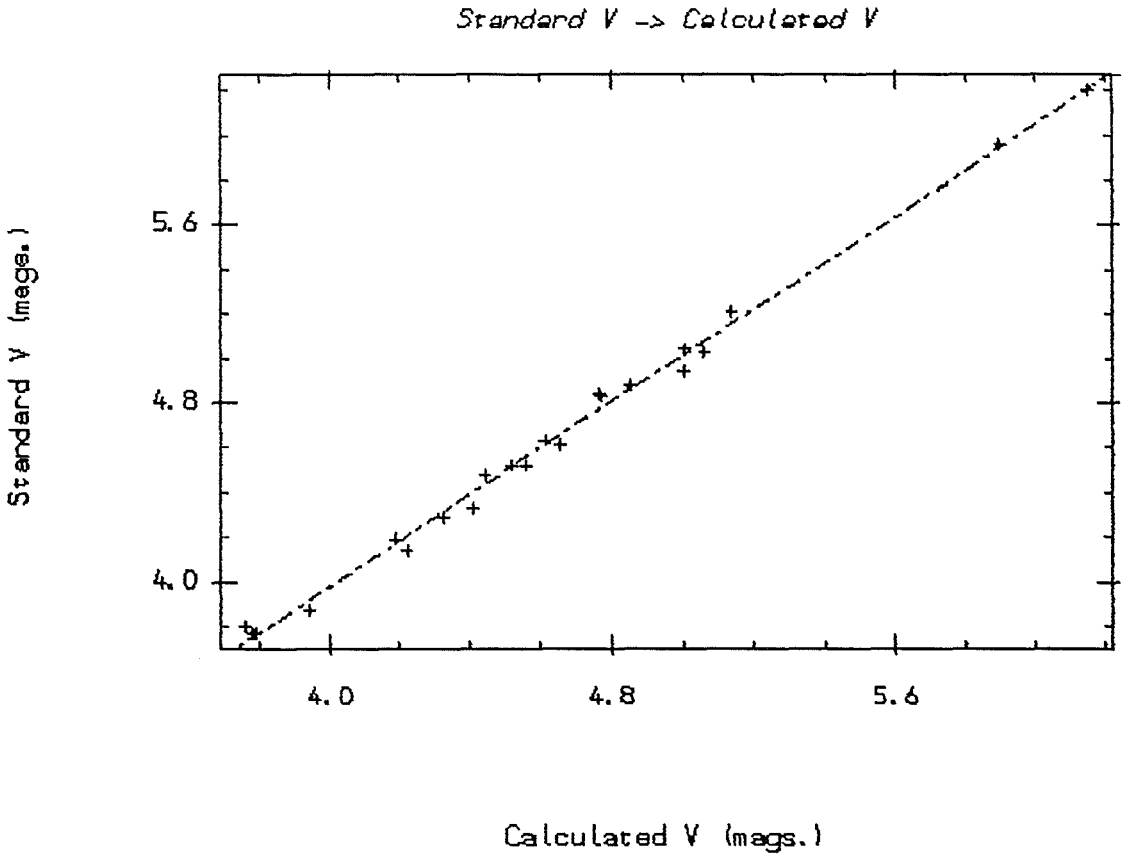

Fig.6.6 Oct.6th V Magnitudes.

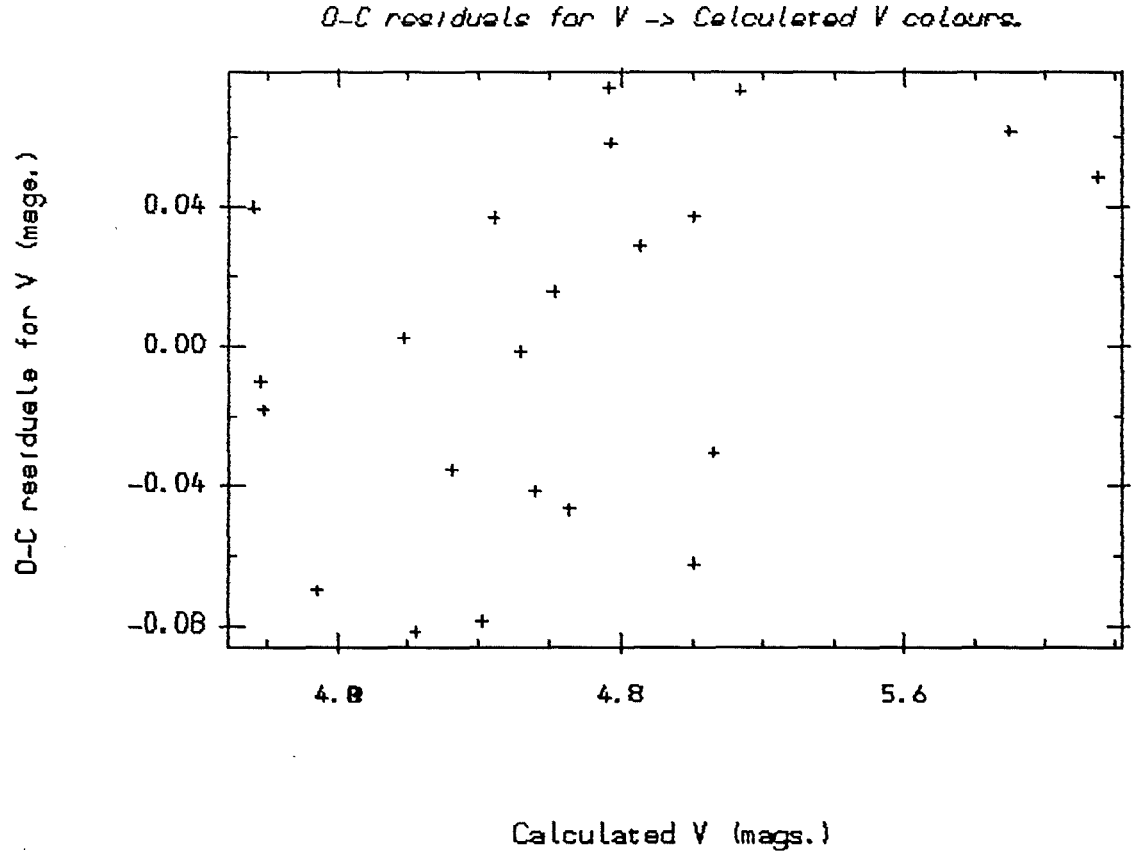

Fig.6.7 Oct.6th V Magnitudes.

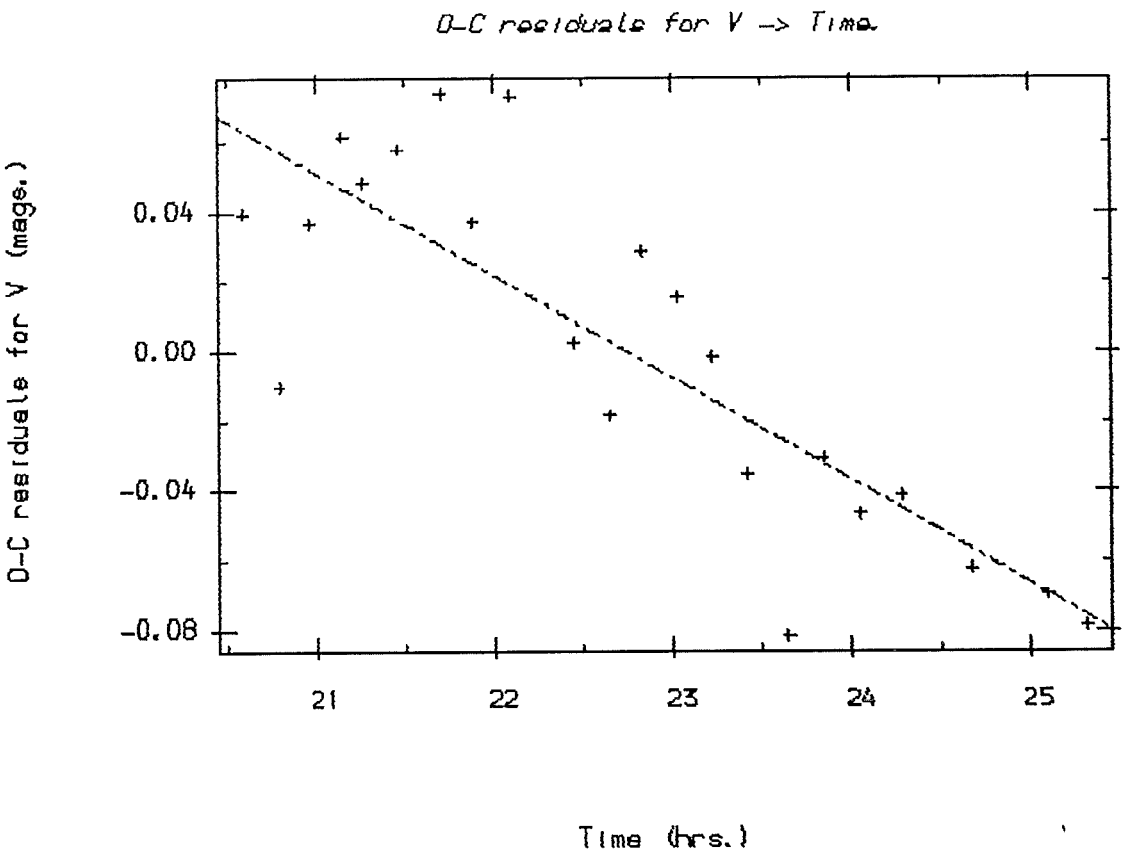

Fig.6.8 Oct.6th V Magnitudes.

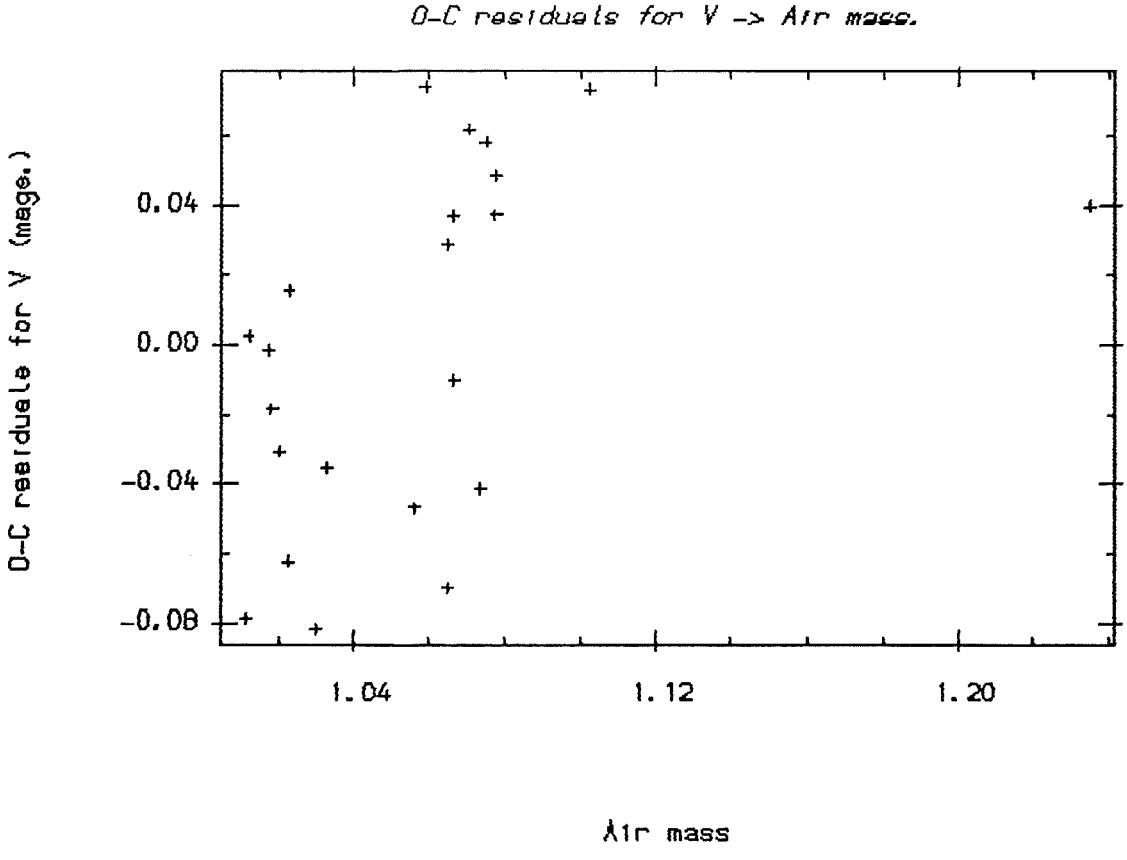

Fig.6.9 Oct.6th V Magnitudes.

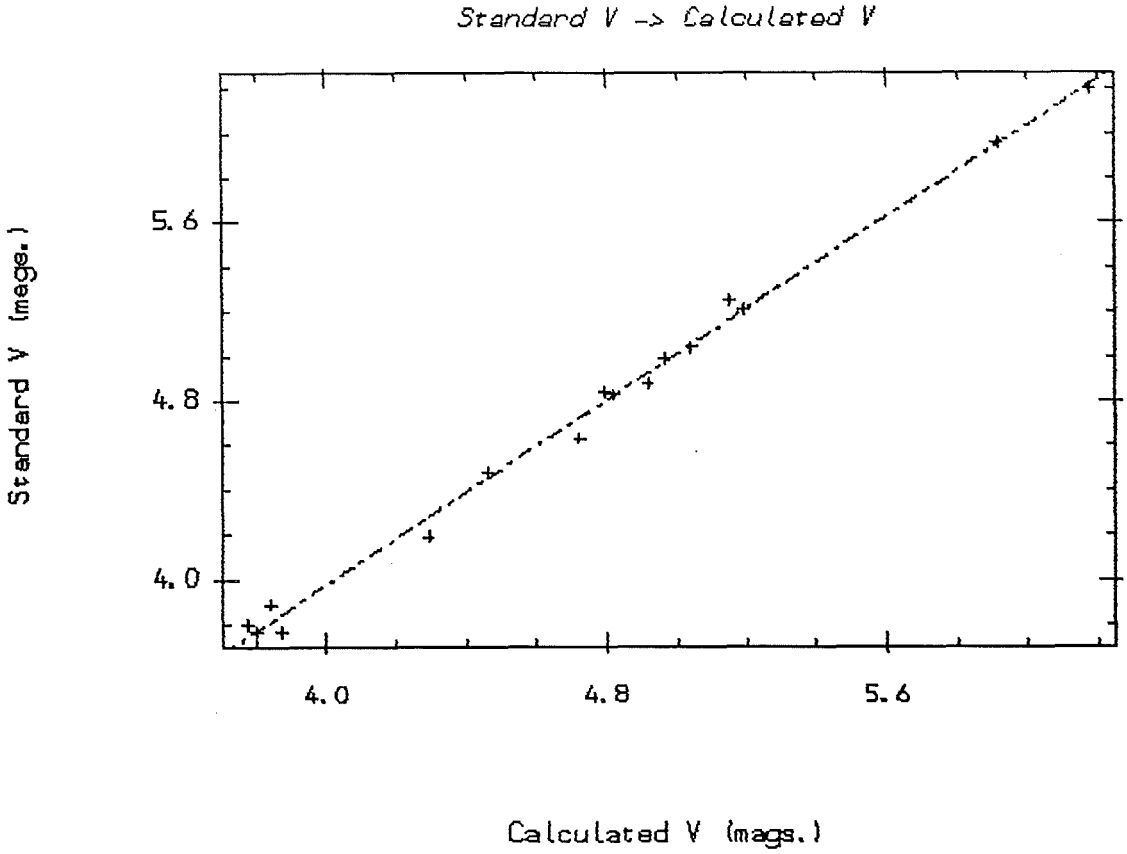

Fig.6.10 Oct.8th V Magnitudes.

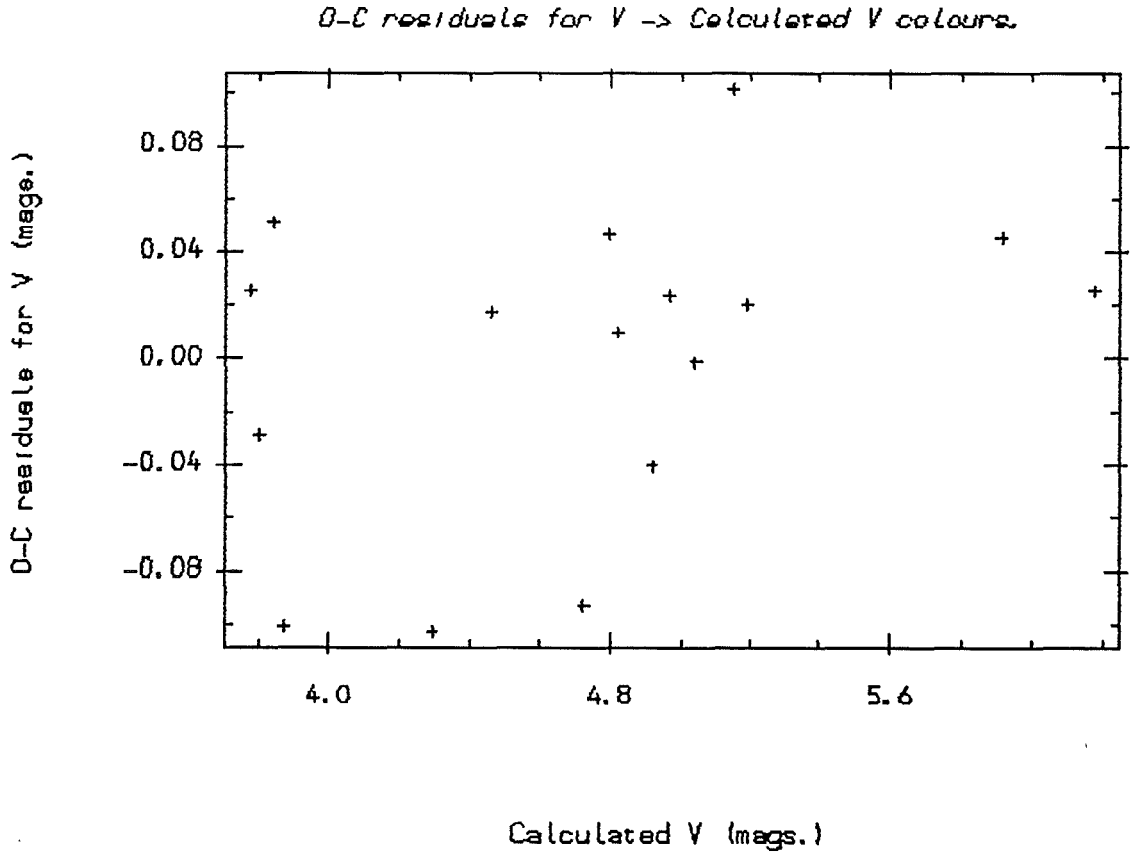

Fig.6.11 Oct.8th V Magnitudes.

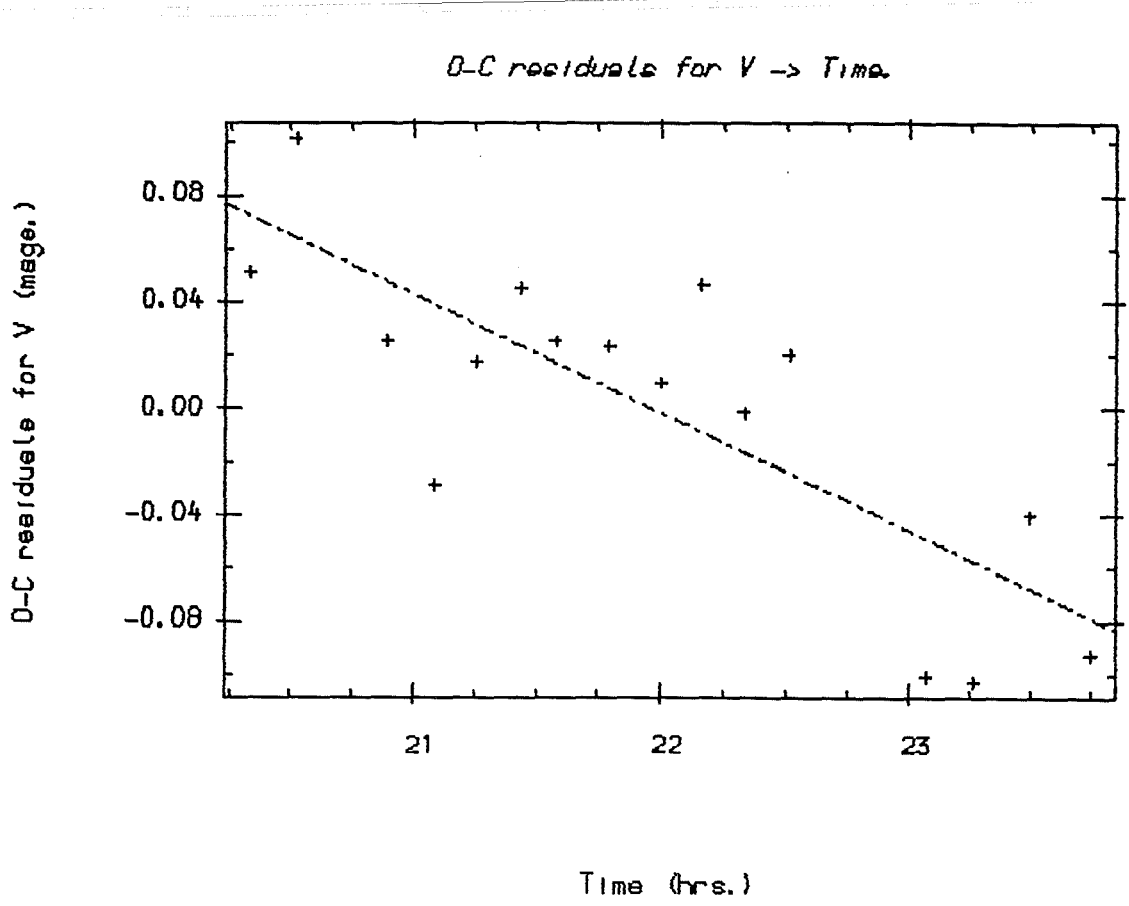

Fig.6.12 Oct.8th V Magnitudes.

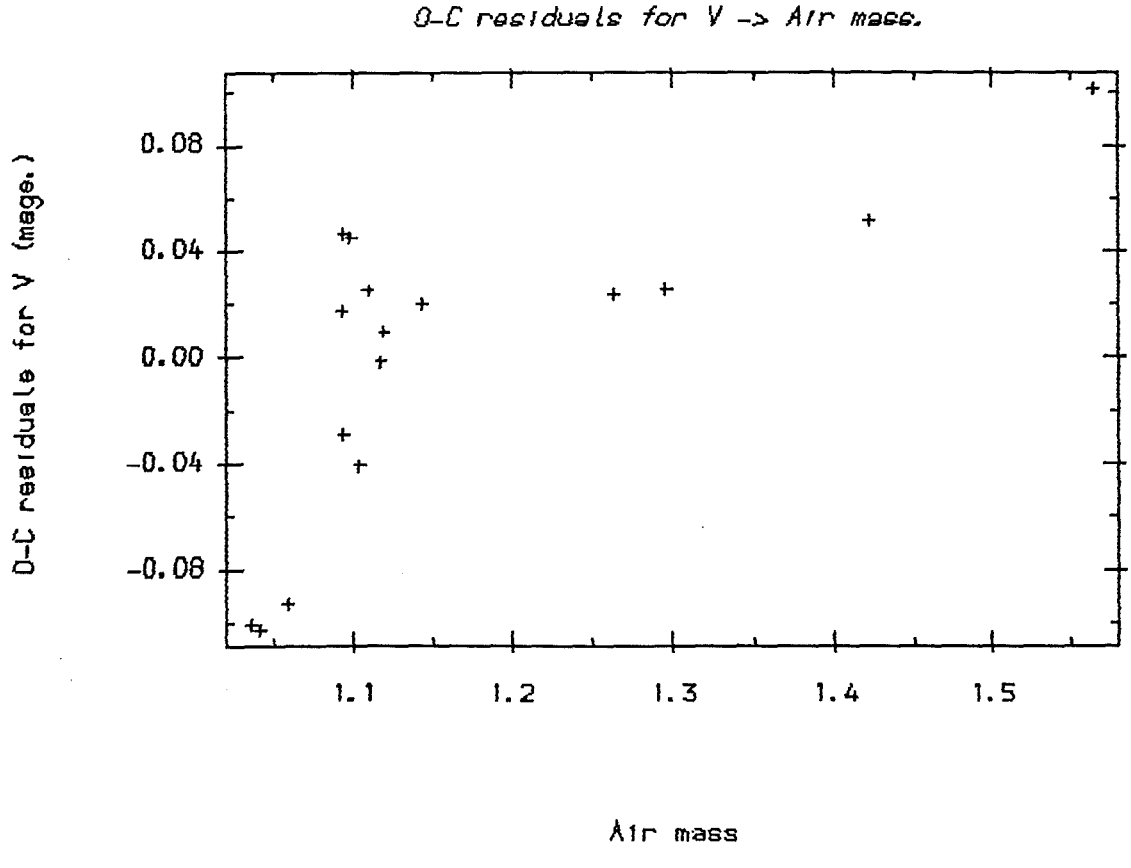

Fig.6.13 Oct.8th V Magnitudes.

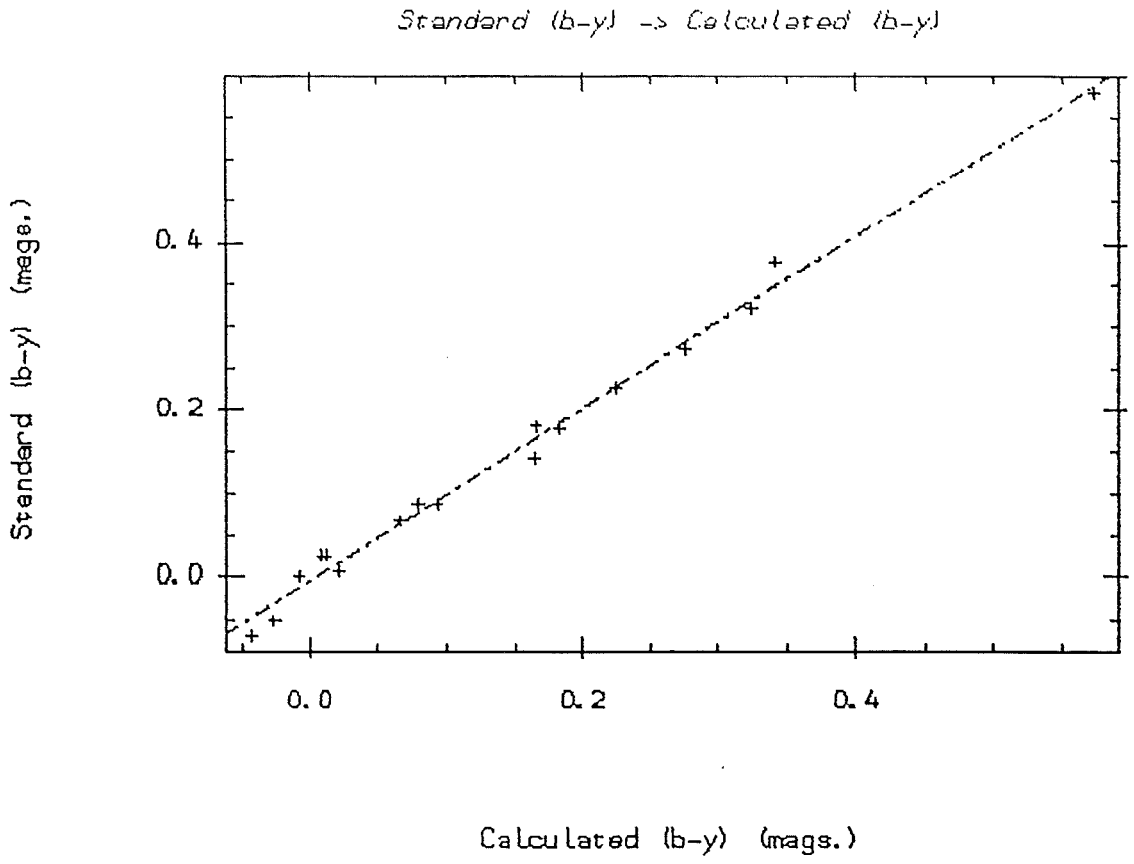

Fig.6.14 Sep.23rd (b-y) colour.

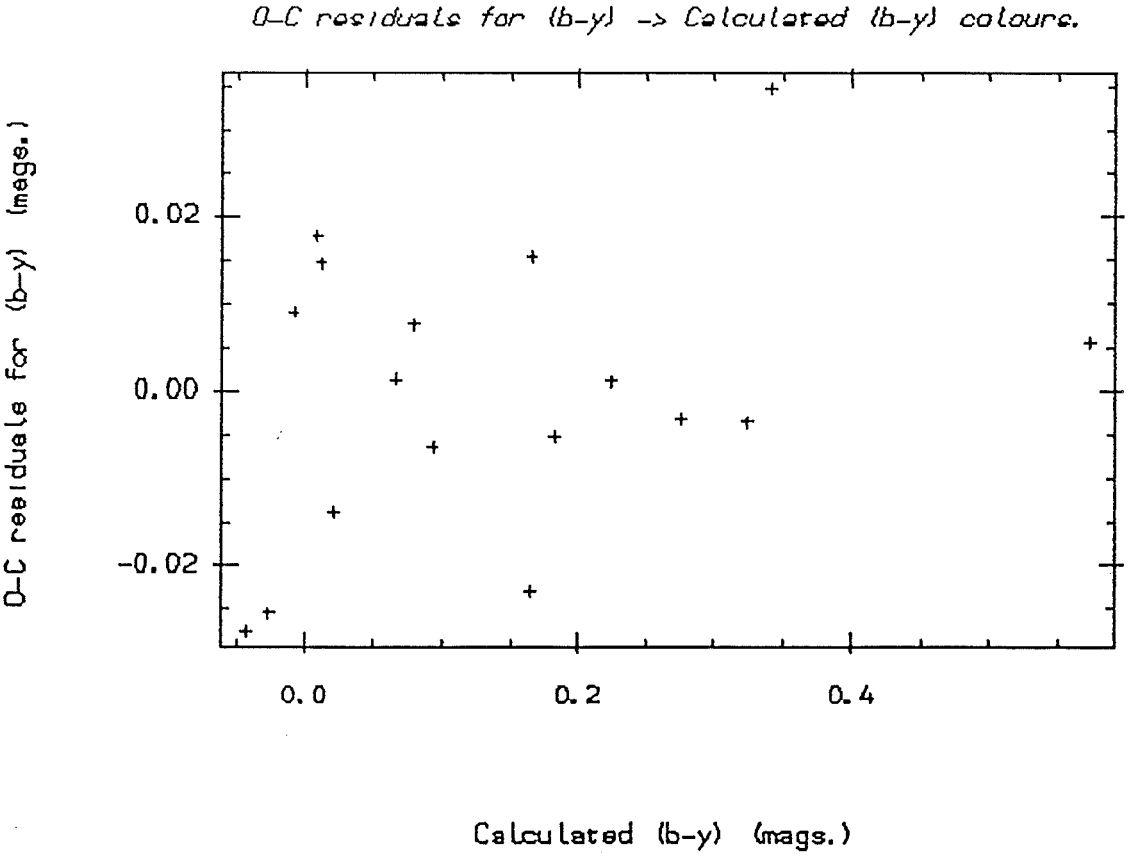

Fig.6.15 Sep.23rd (b-y) colour.

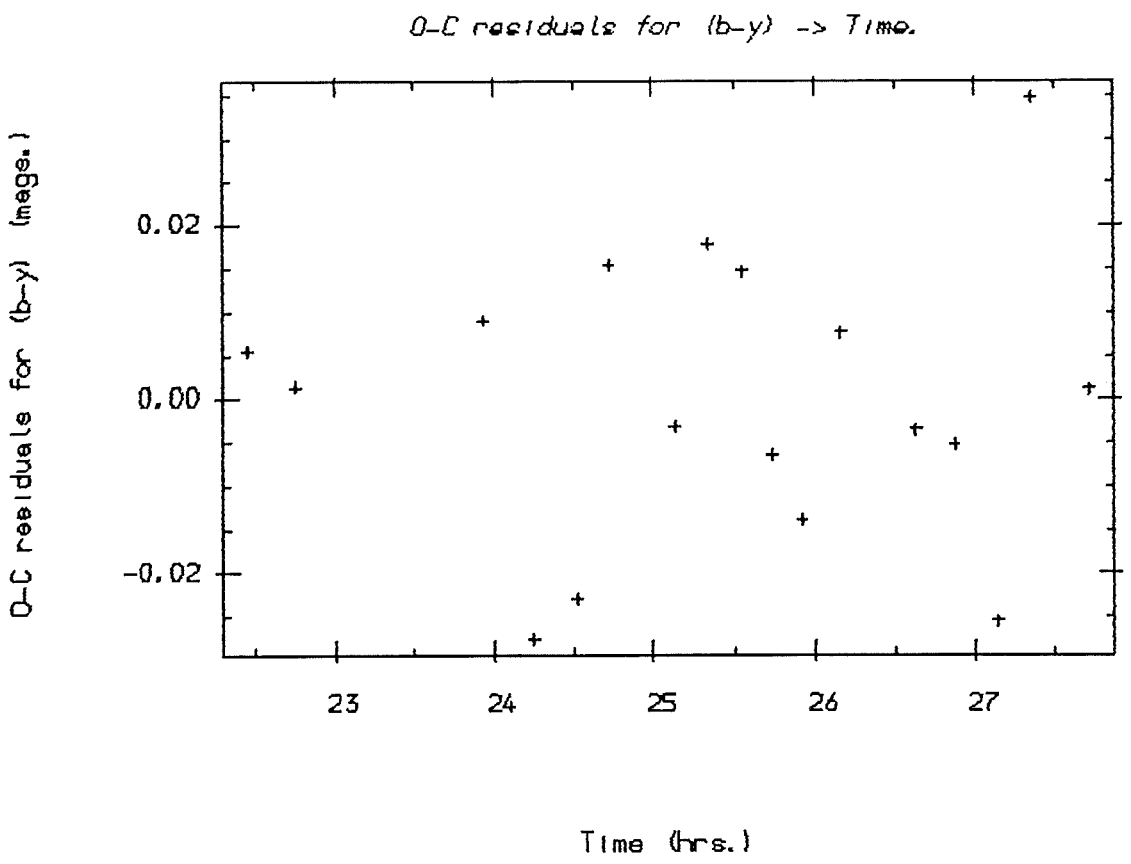

Fig.6.16 Sep.23rd (b-y) colour.

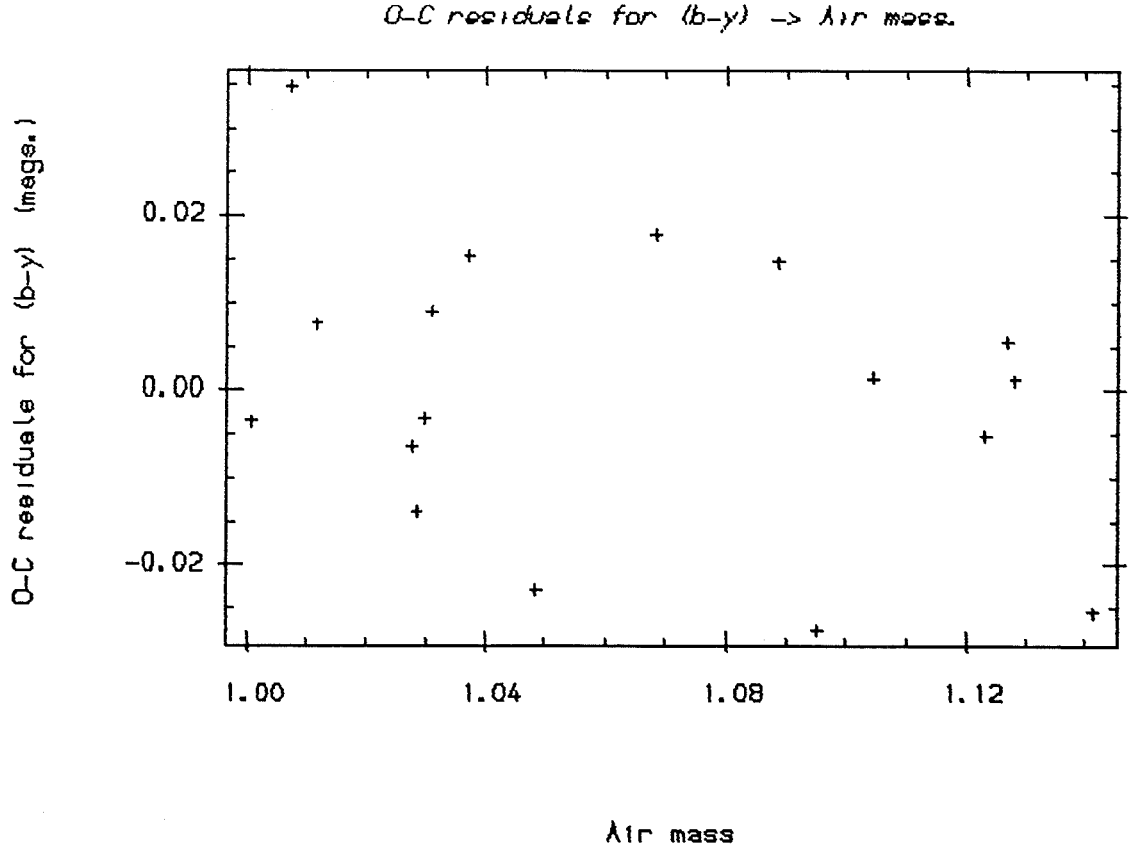

Fig.6.17 Sep.23rd (b-y) colour.

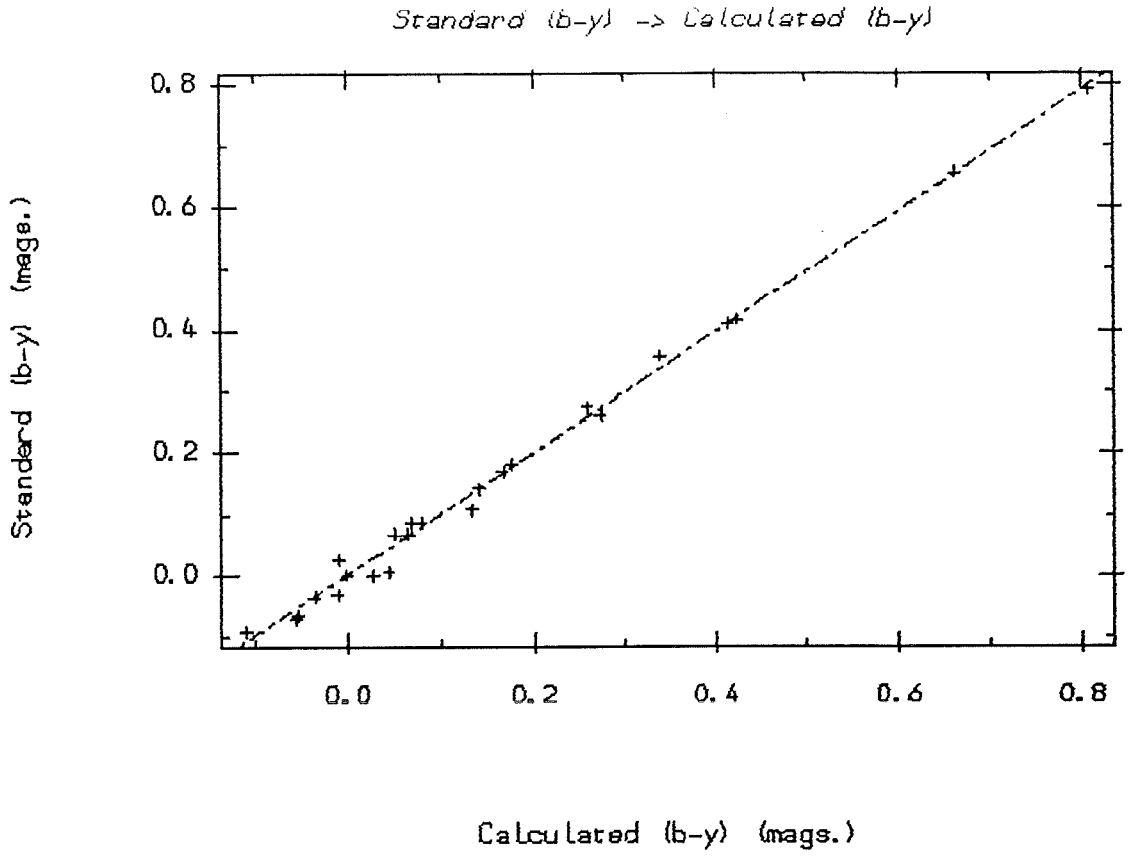

Fig.6.18 Oct.6th (b-y) colour.

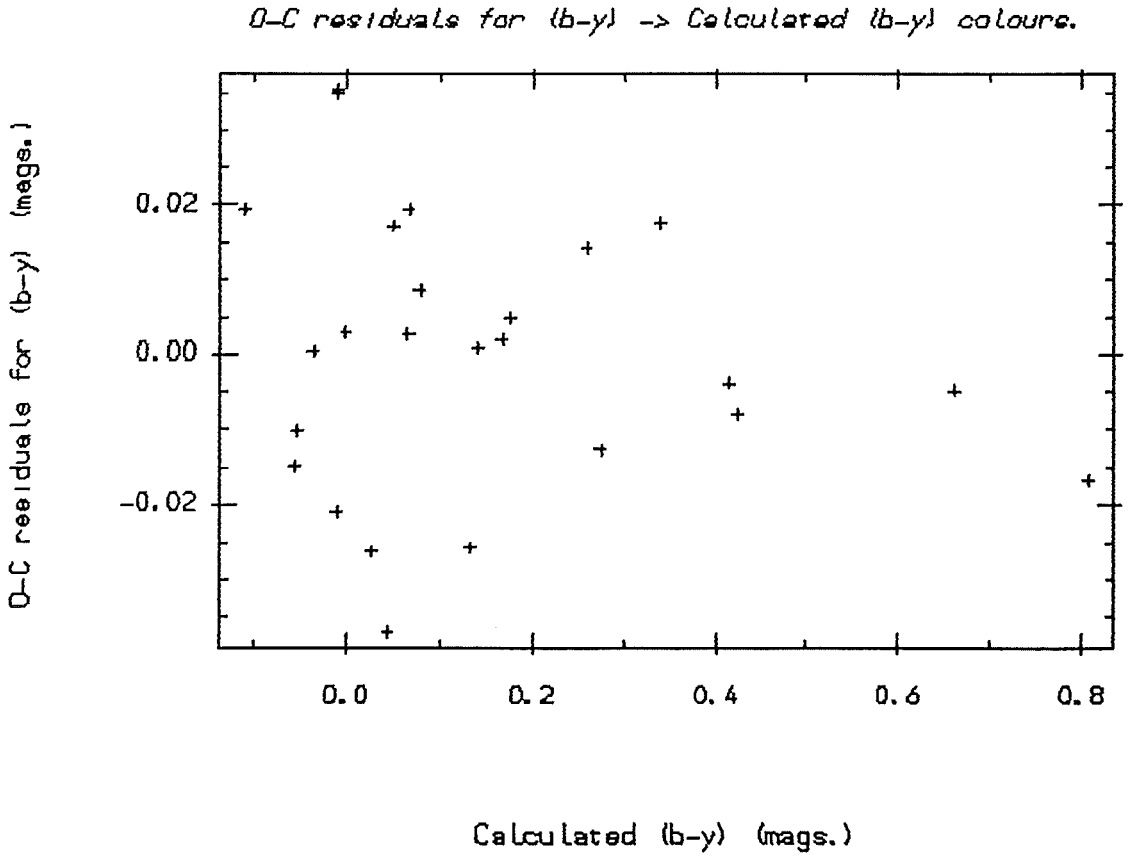

Fig.6.19 Oct.6th (b-y) colour.

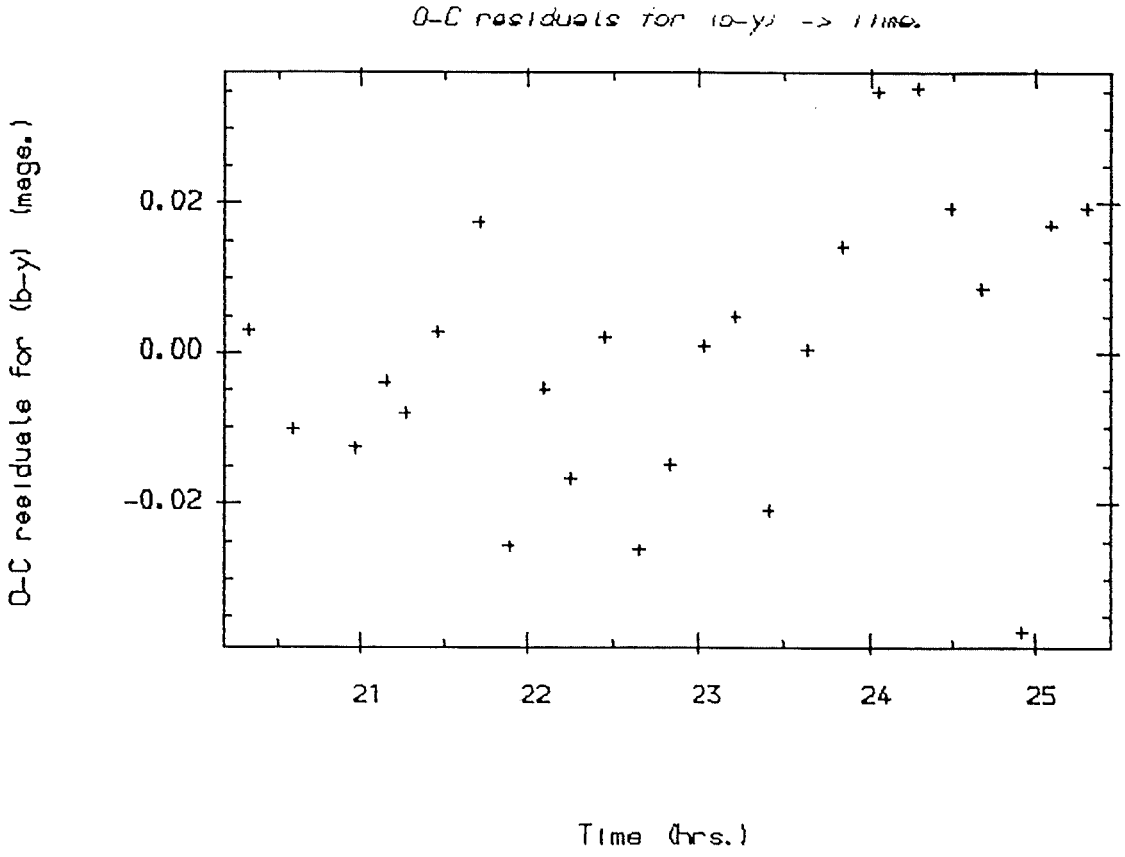

Fig.6.20 Oct.6th (b-y) colour.

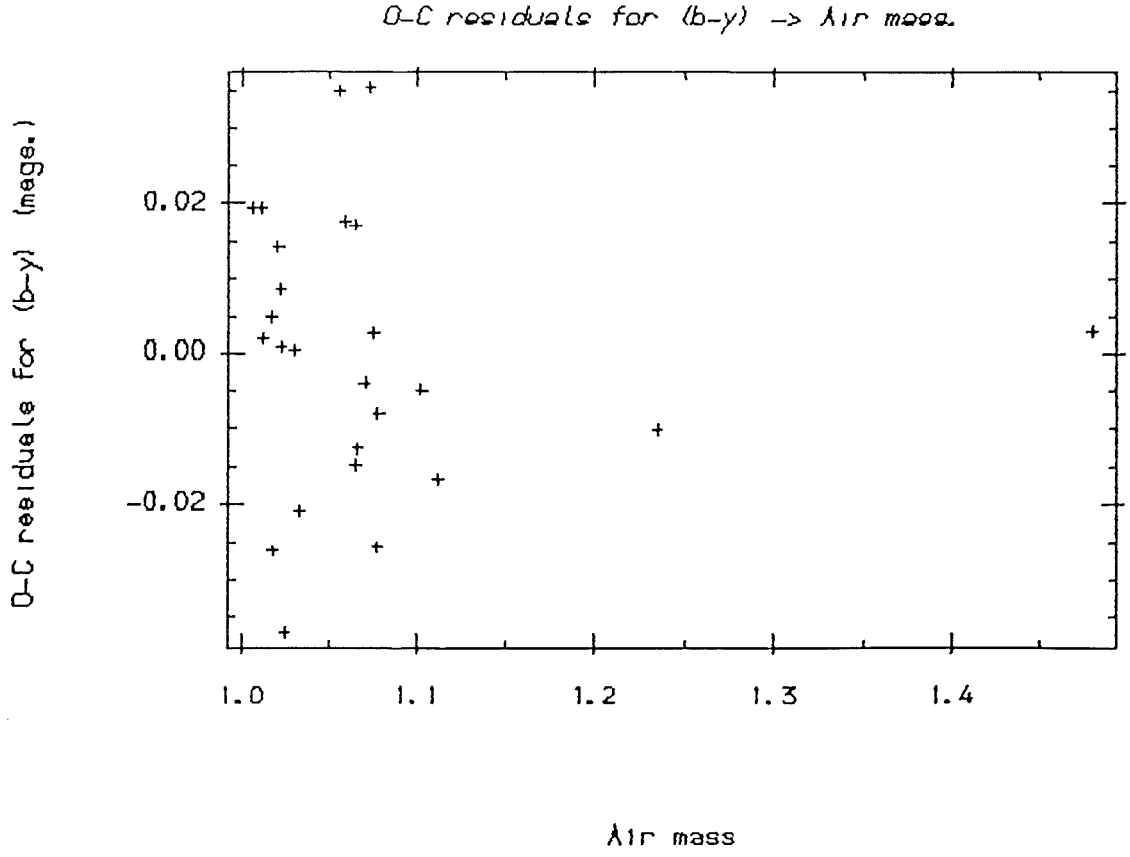

Fig.6.21 Oct.6th (b-y) colour.

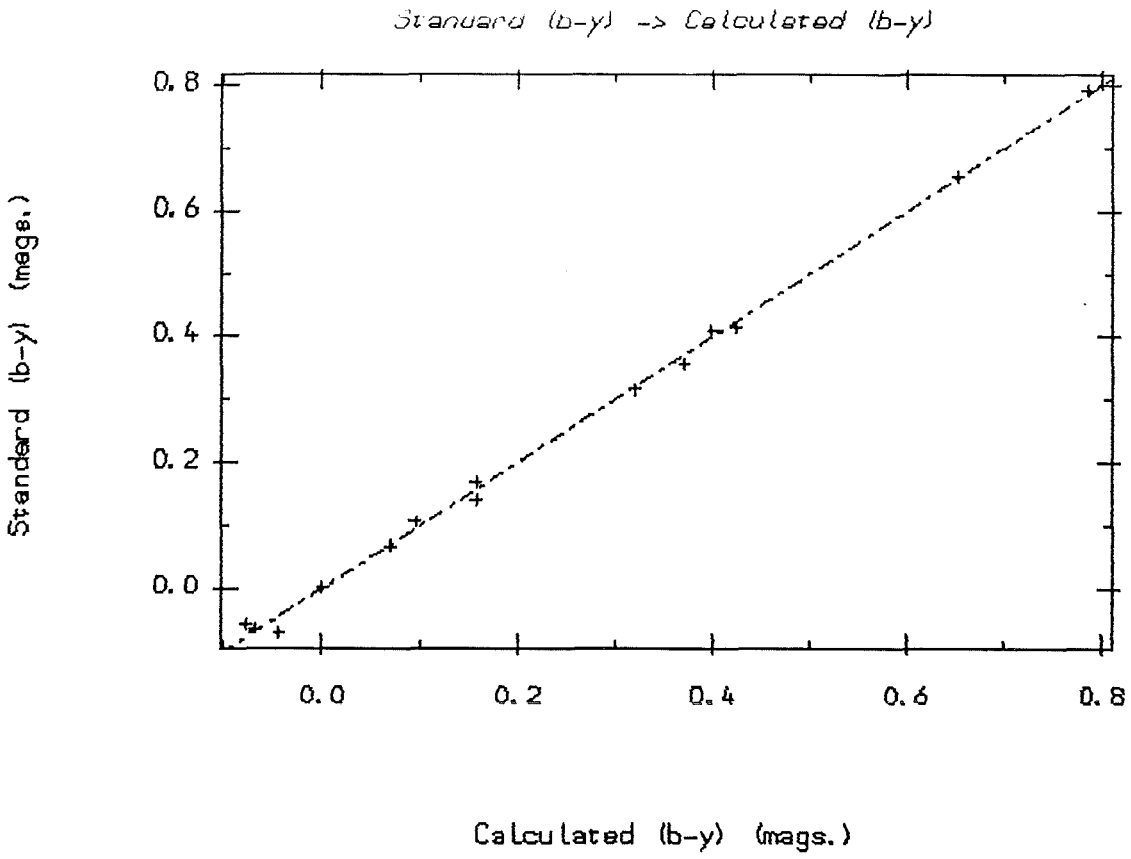

Fig.6.22 Oct.8th (b-y) colour.

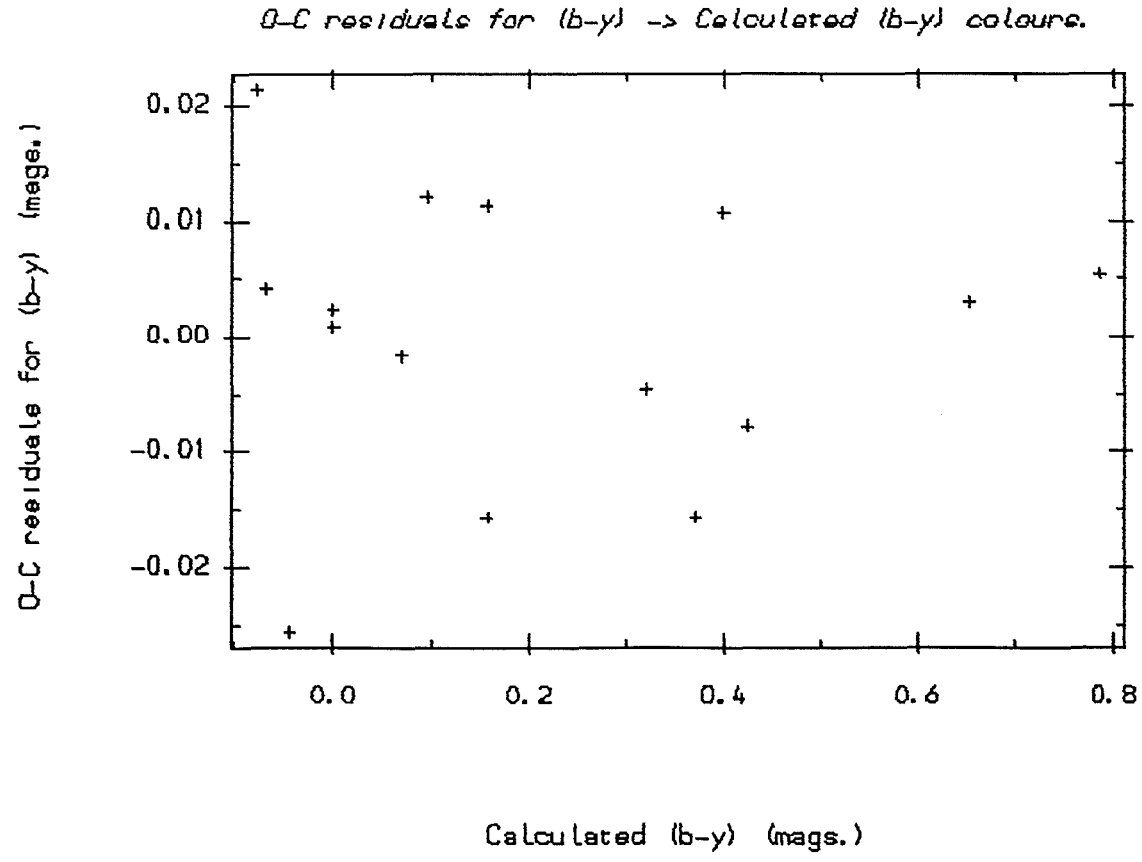

Fig.6.23 Oct.8th (b-y) colour.

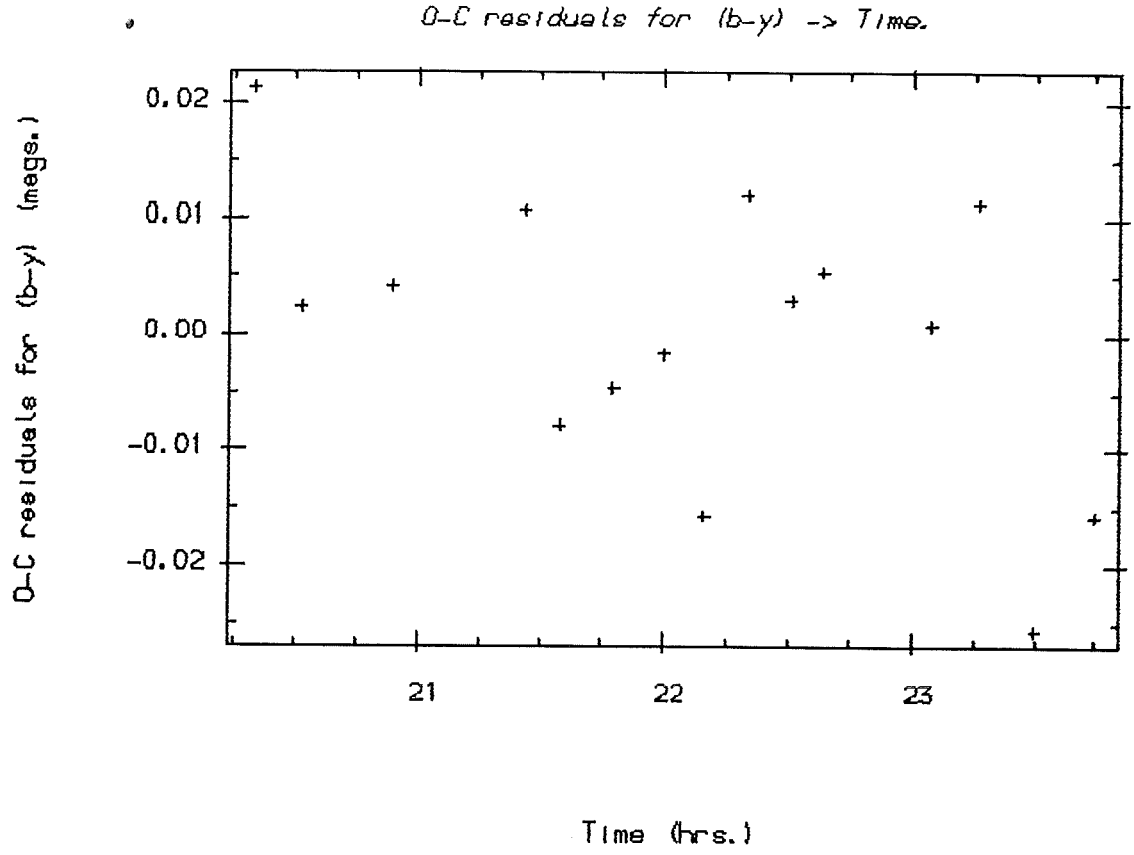

Fig.6.24 Oct.8th (b-y) colour.

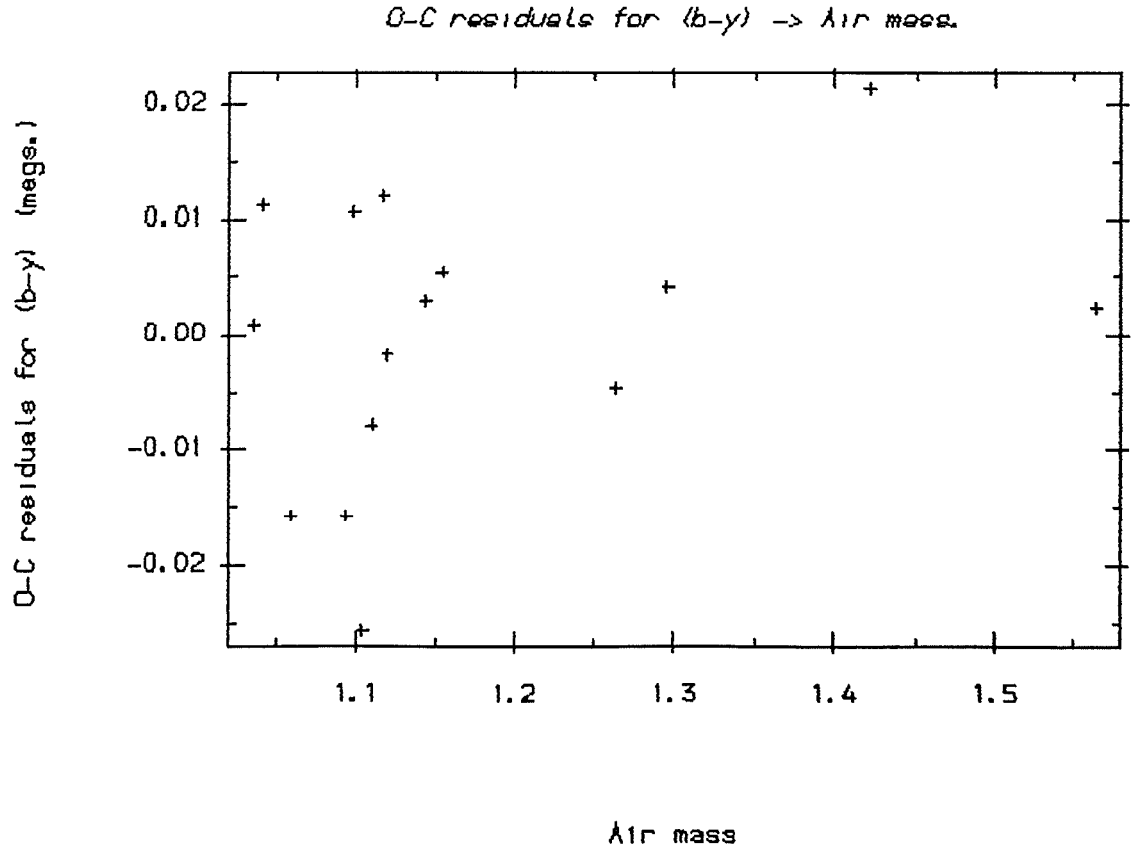

Fig.6.25 Oct.8th (b-y) colour.

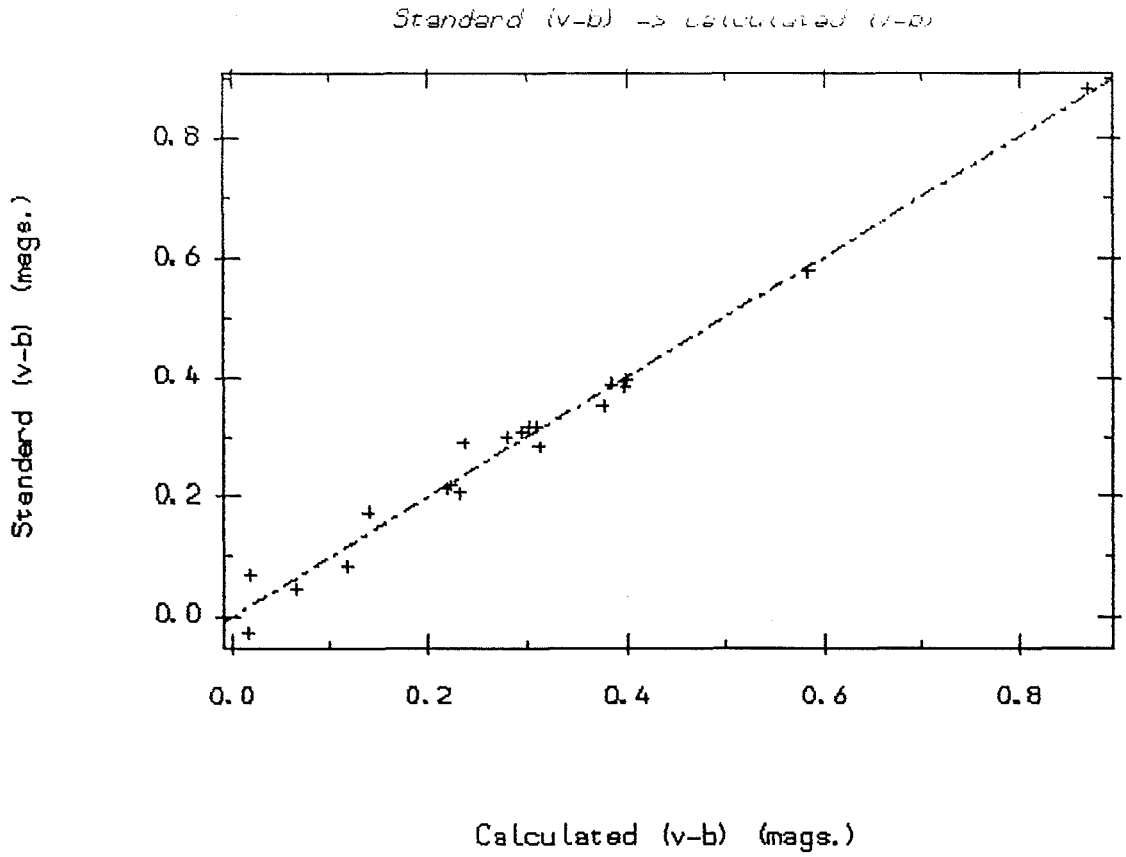

Fig.6.26 Sep.23rd (v-b) colour.

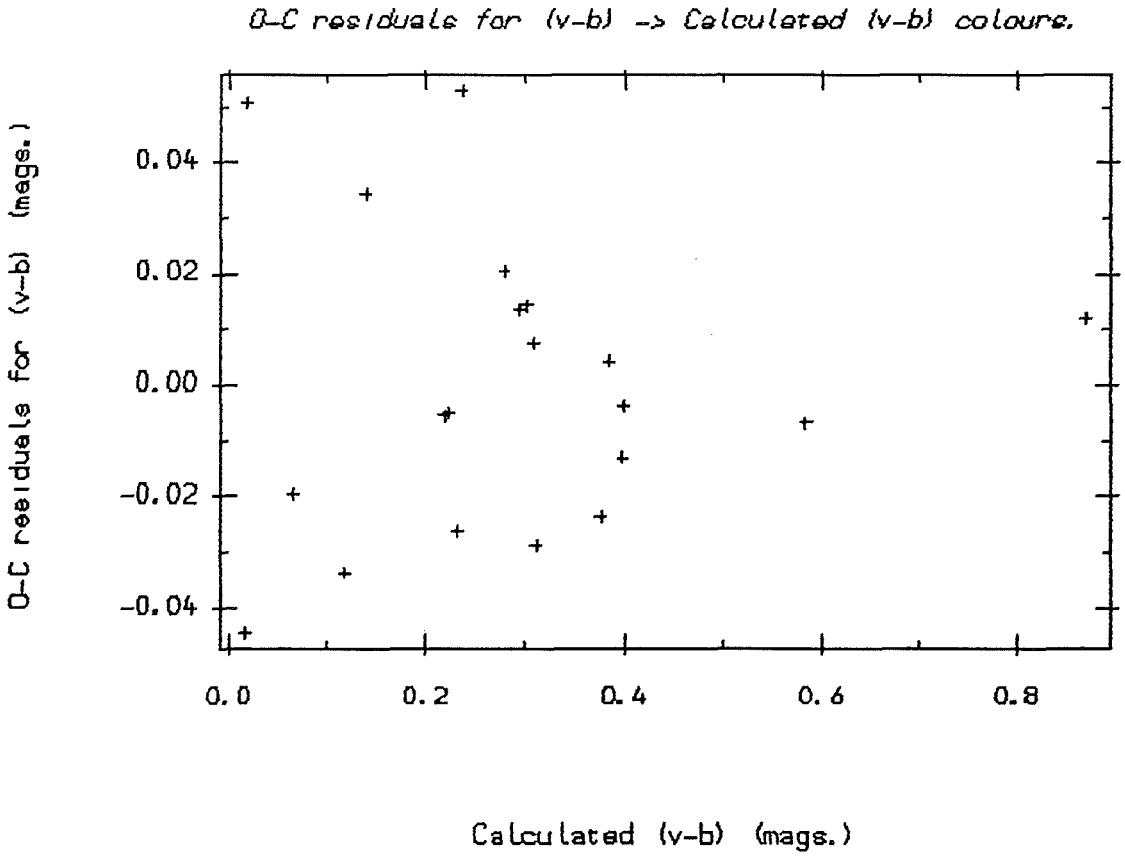

Fig.6.27 Sep.23rd (v-b) colour.

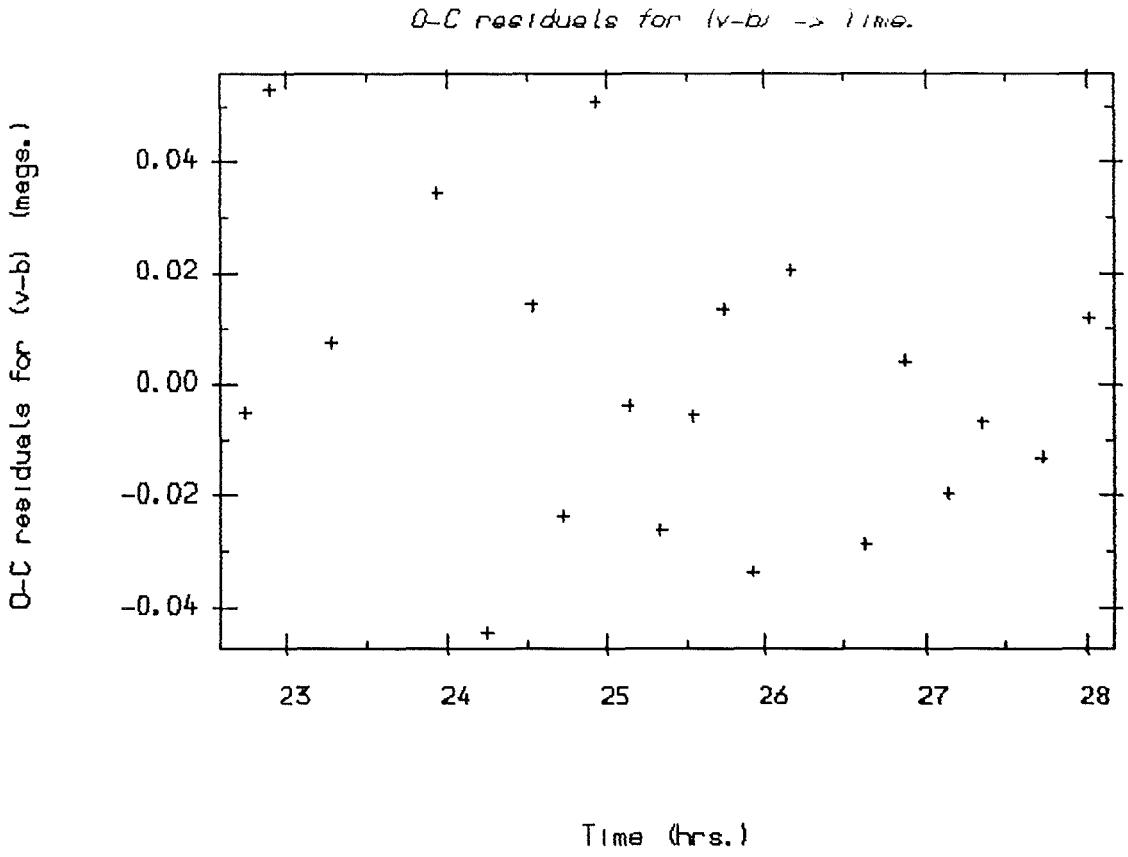

Fig.6.28 Sep.23rd (v-b) colour.

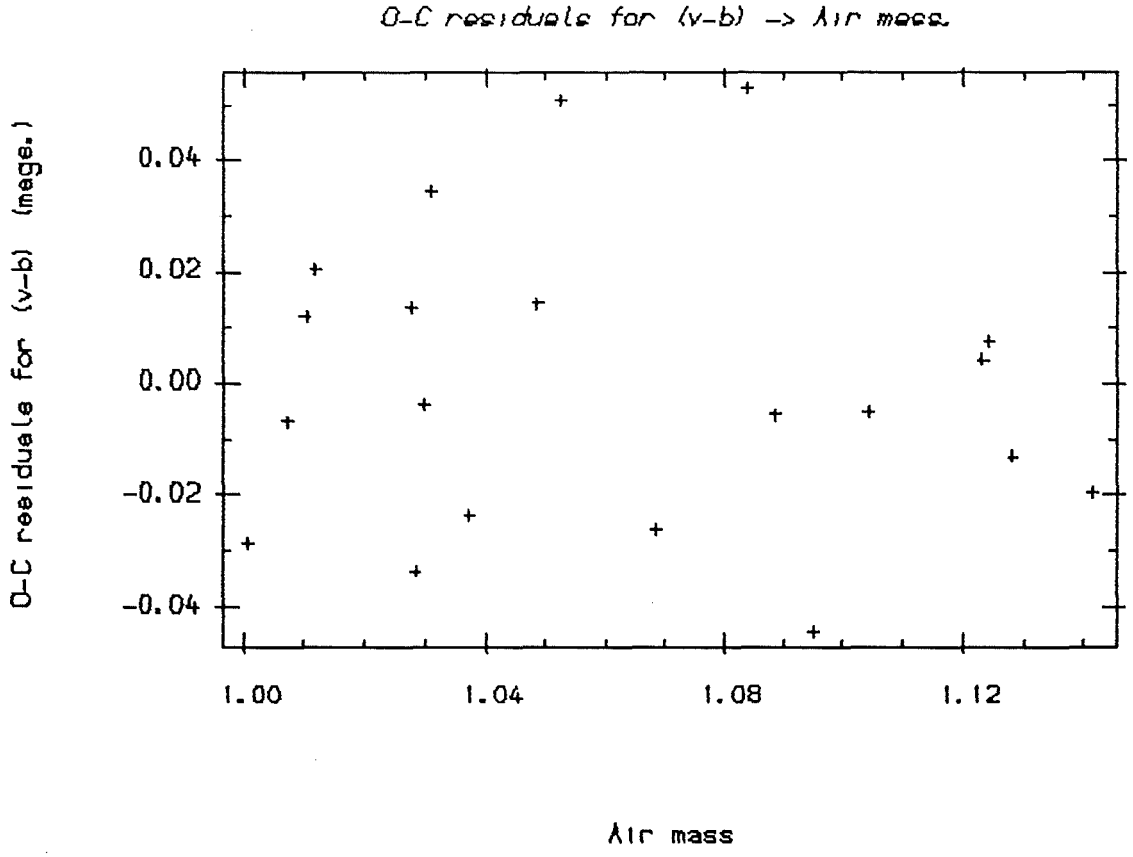

Fig.6.29 Sep.23rd (v-b) colour.

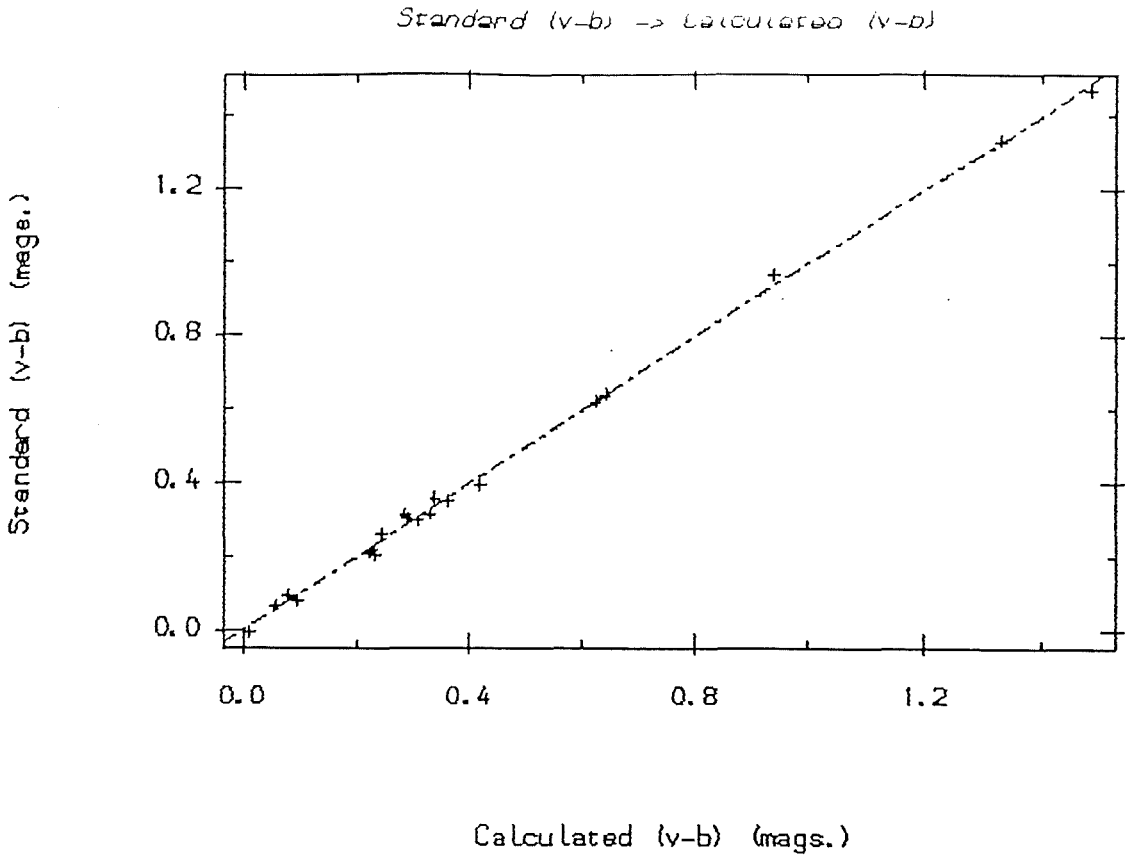

Fig.6.30 Oct.6th (v-b) colour.

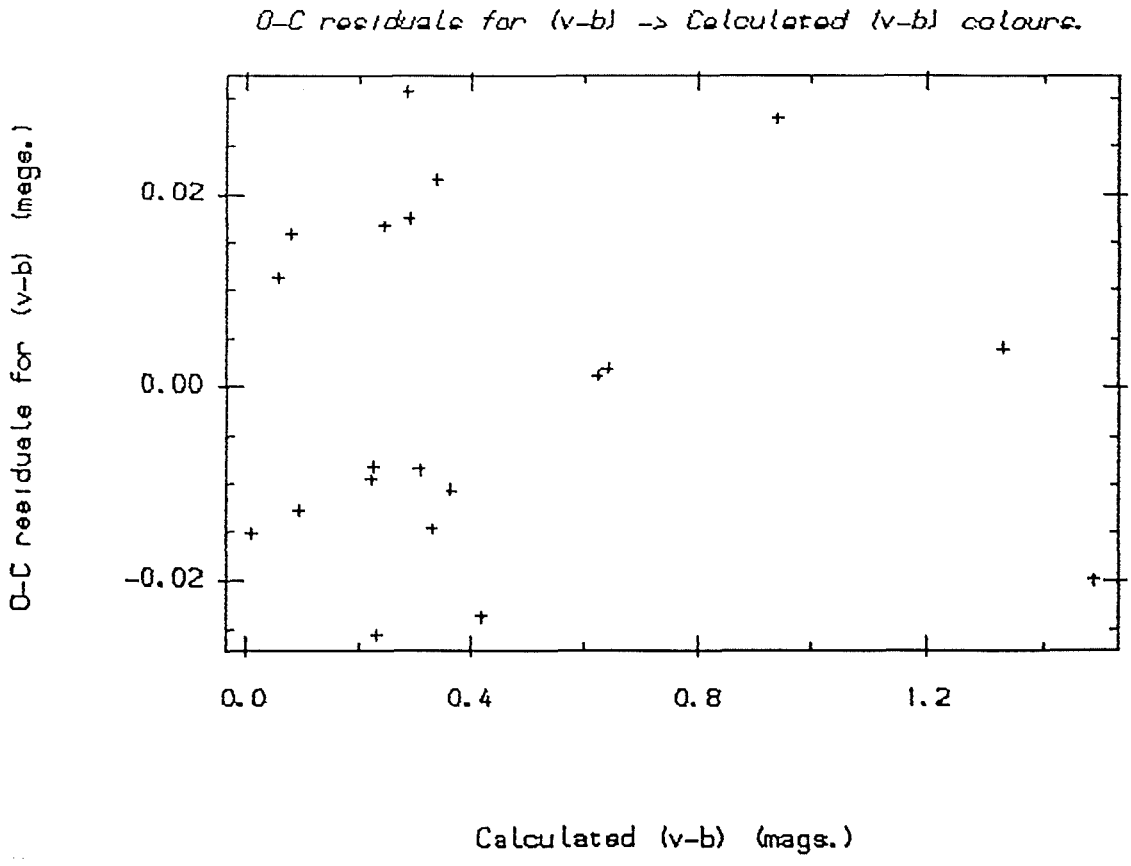

Fig.6.31 Oct.6th (v-b) colour.

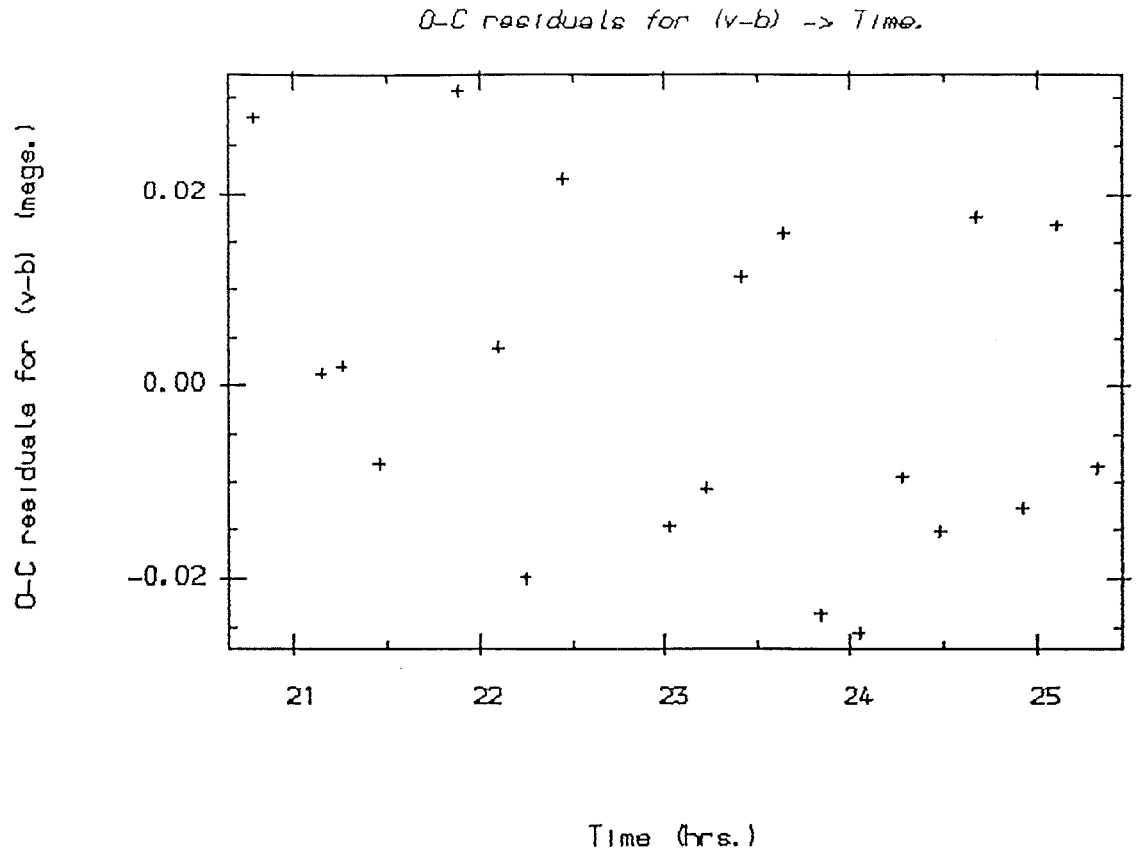

Fig.6.32 Oct.6th (v-b) colour.

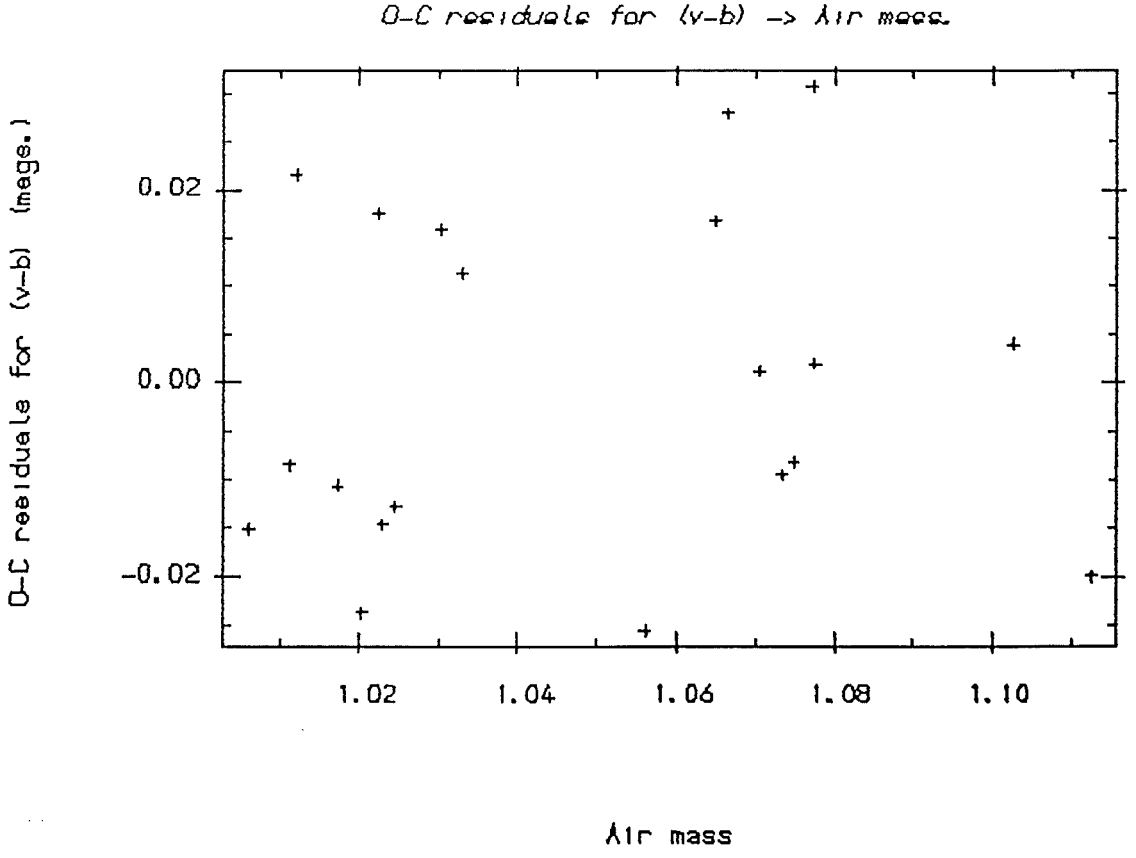

Fig.6.33 Oct.6th (v-b) colour.

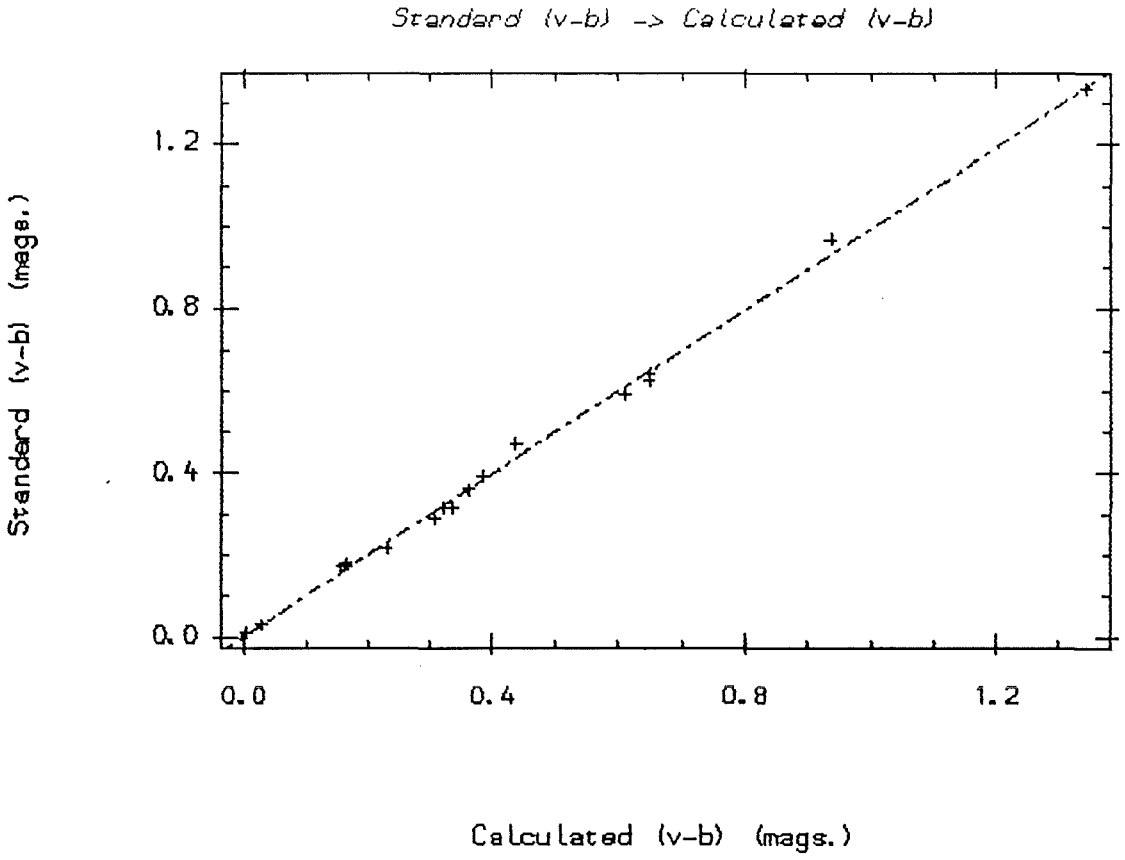

Fig.6.34 Oct.8th (v-b) colour.

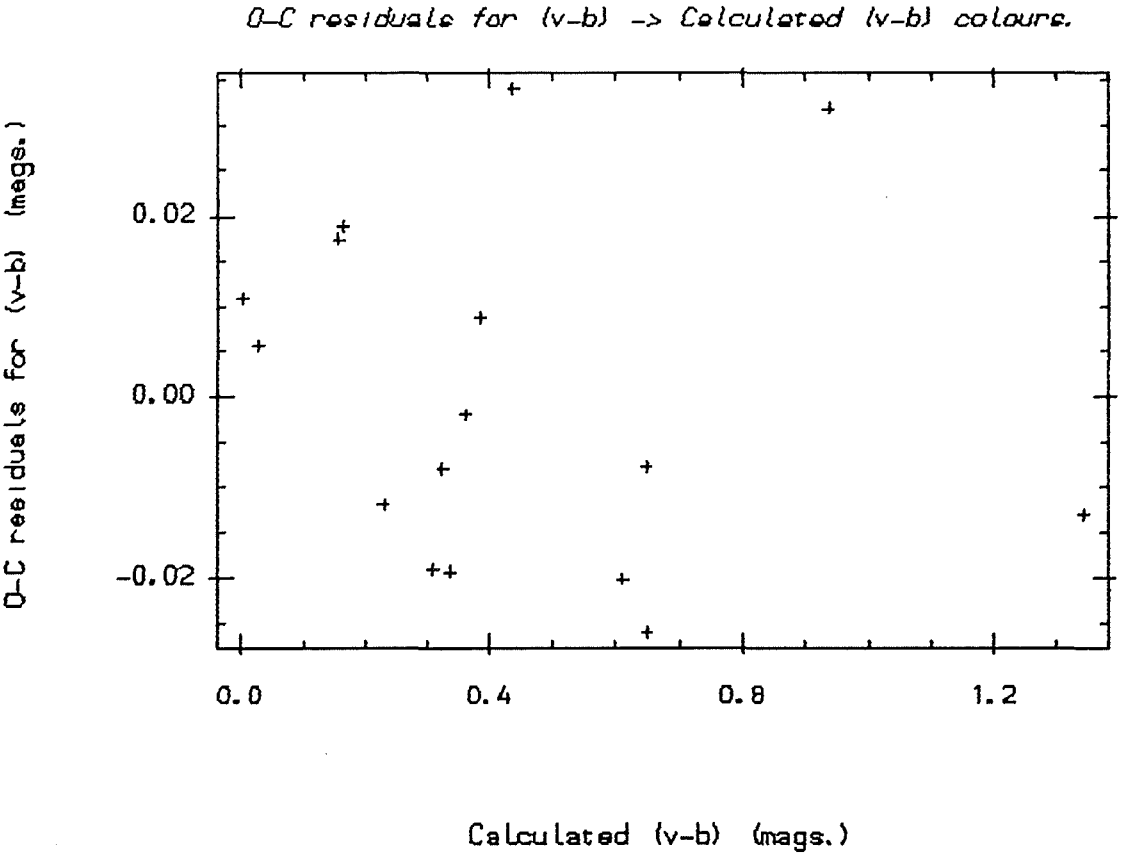

Fig.6.35 Oct.8th (v-b) colour.

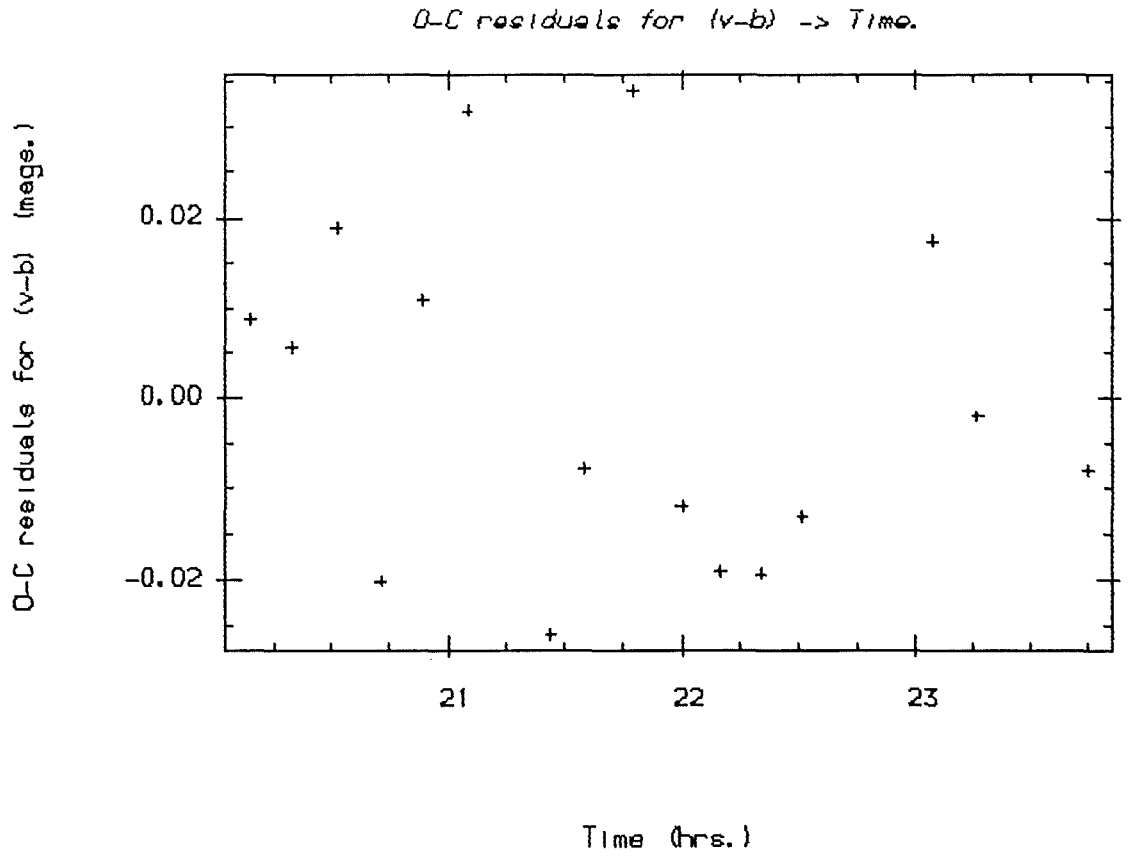

Fig.6.36 Oct.8th (v-b) colour.

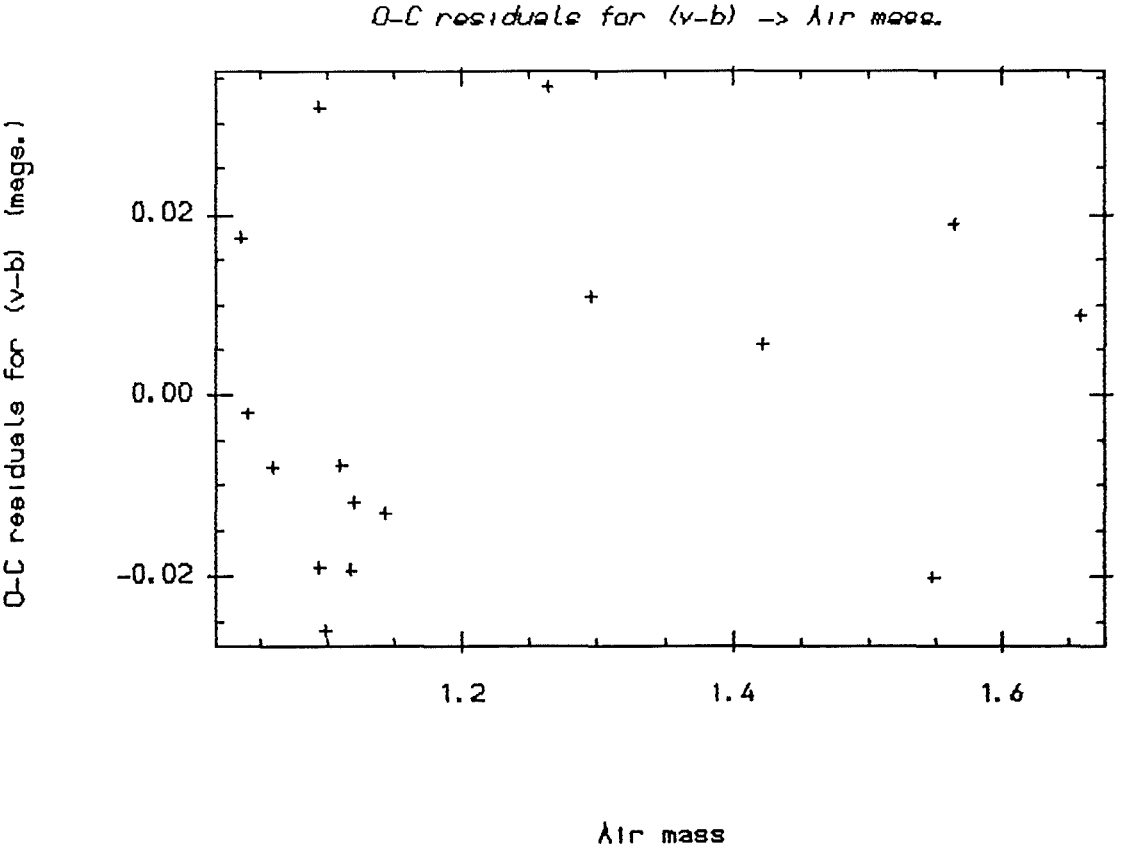

Fig.6.37 Oct.8th (v-b) colour.

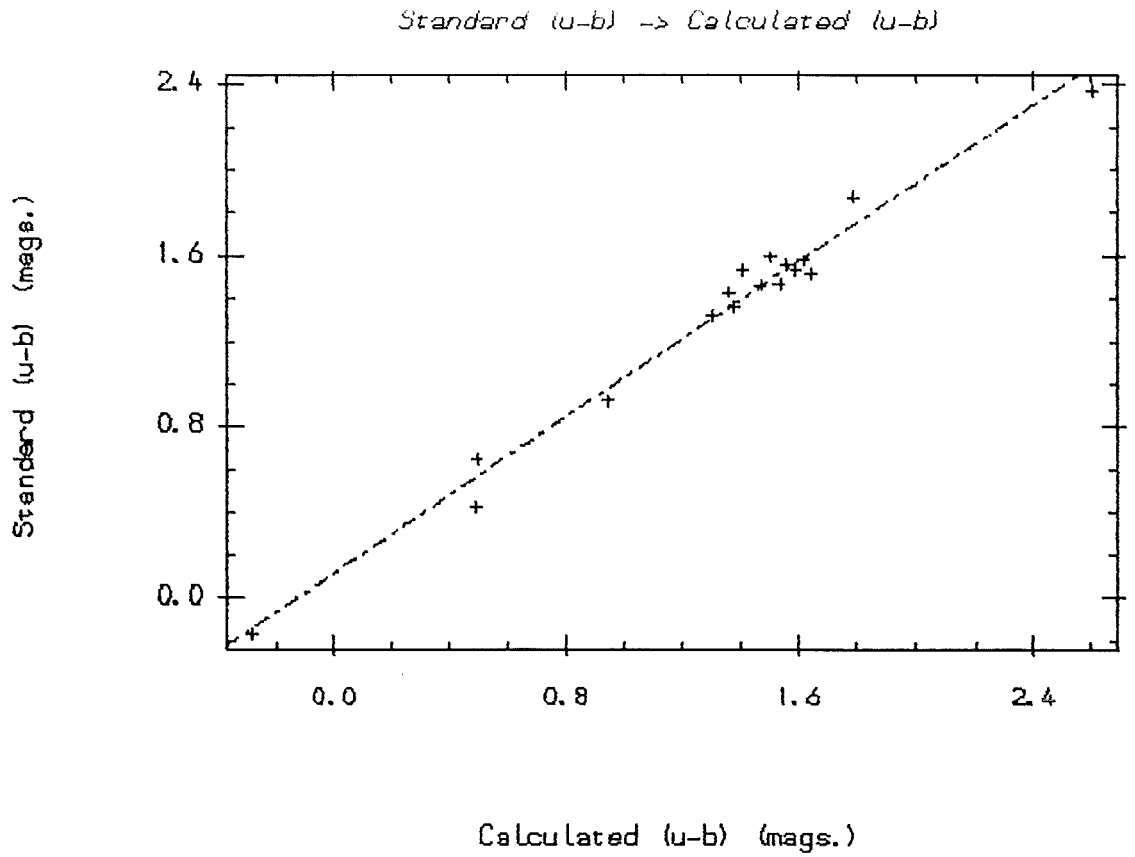

Fig.6.38 Sep.23rd (u-b) colour.

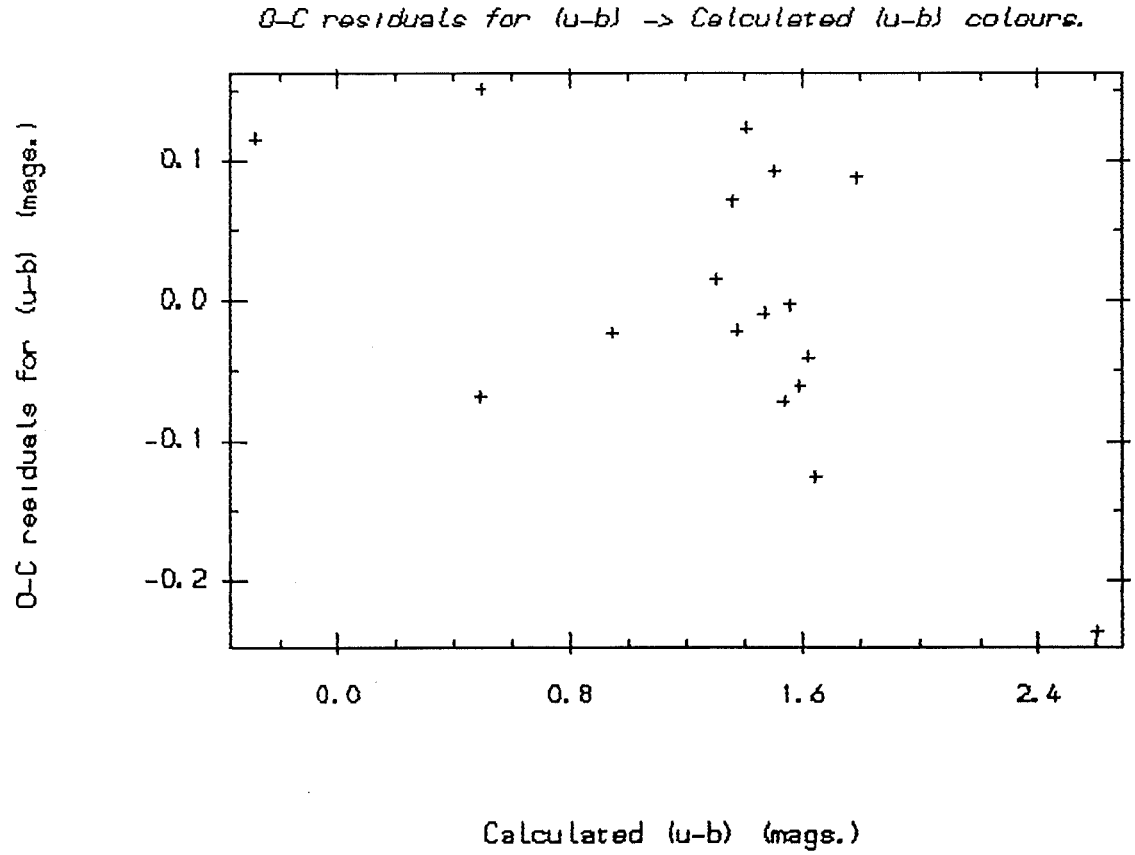

Fig.6.39 Sep.23rd (u-b) colour.

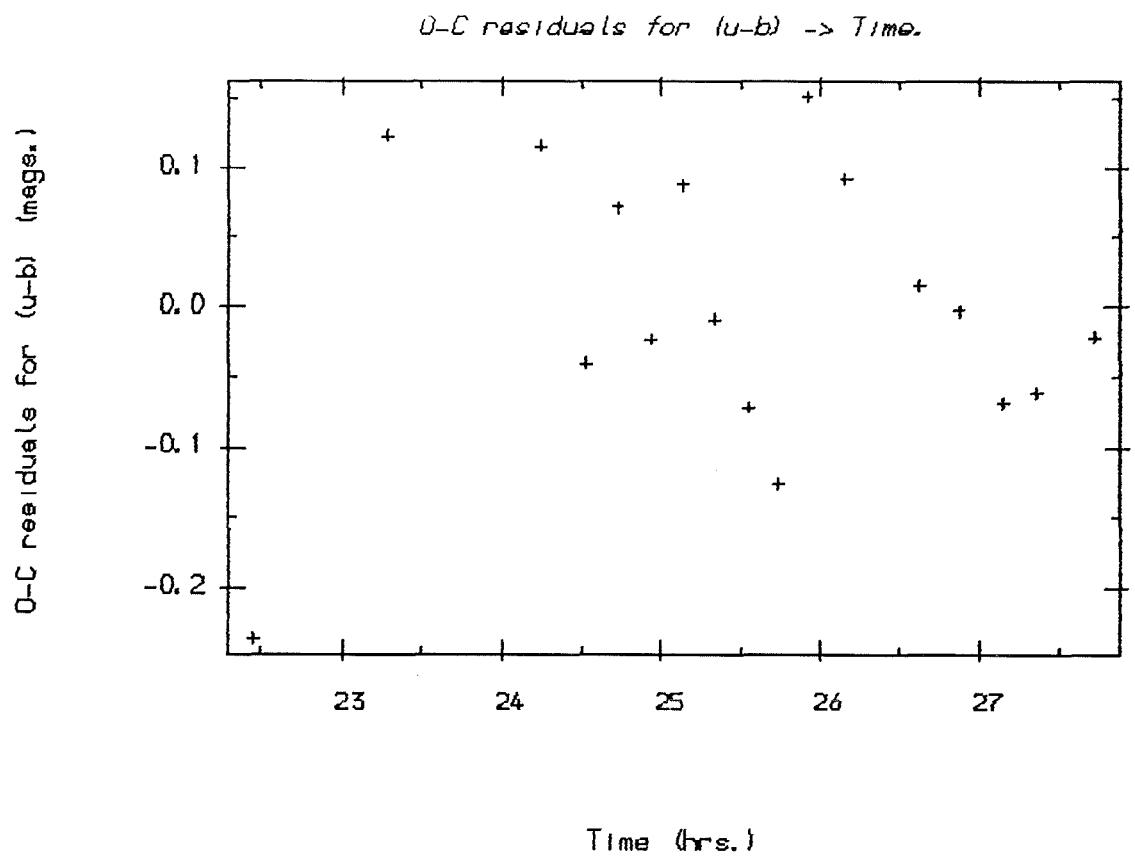

Fig.6.40 Sep.23rd (u-b) colour.

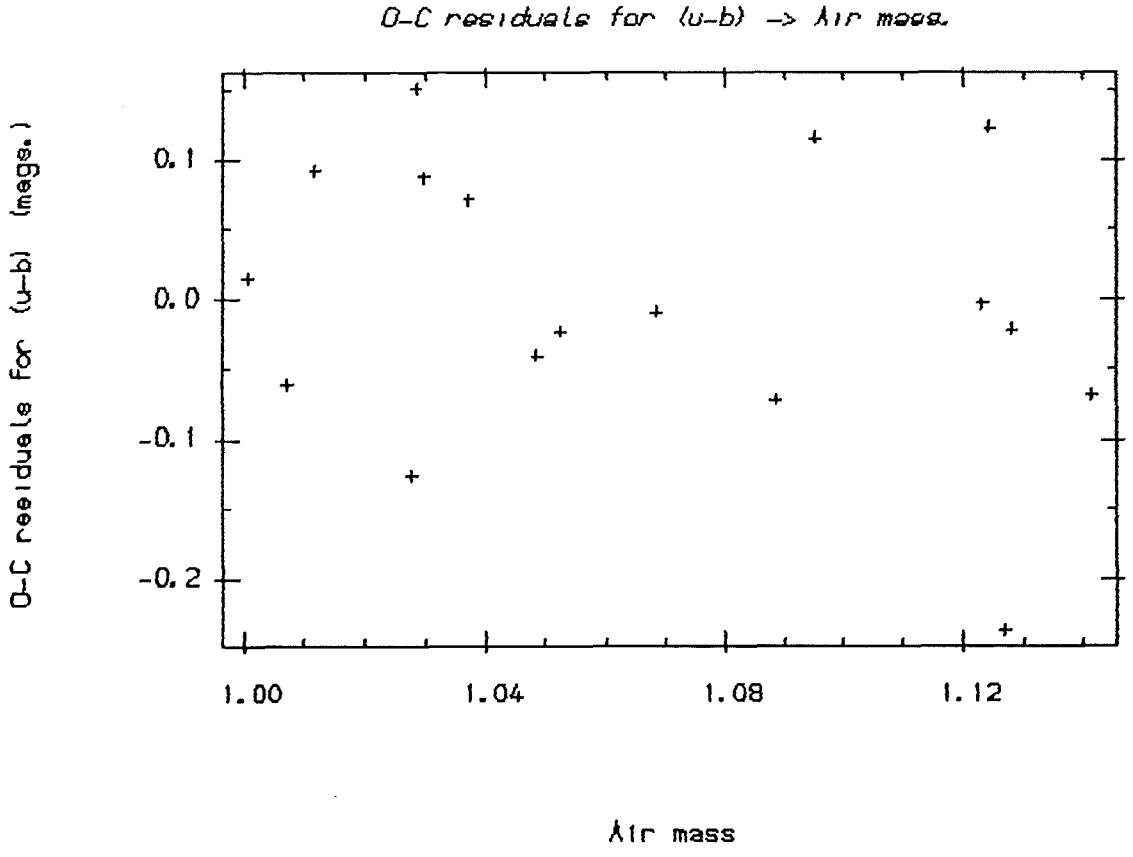

Fig.6.41 Sep.23rd (u-b) colour.

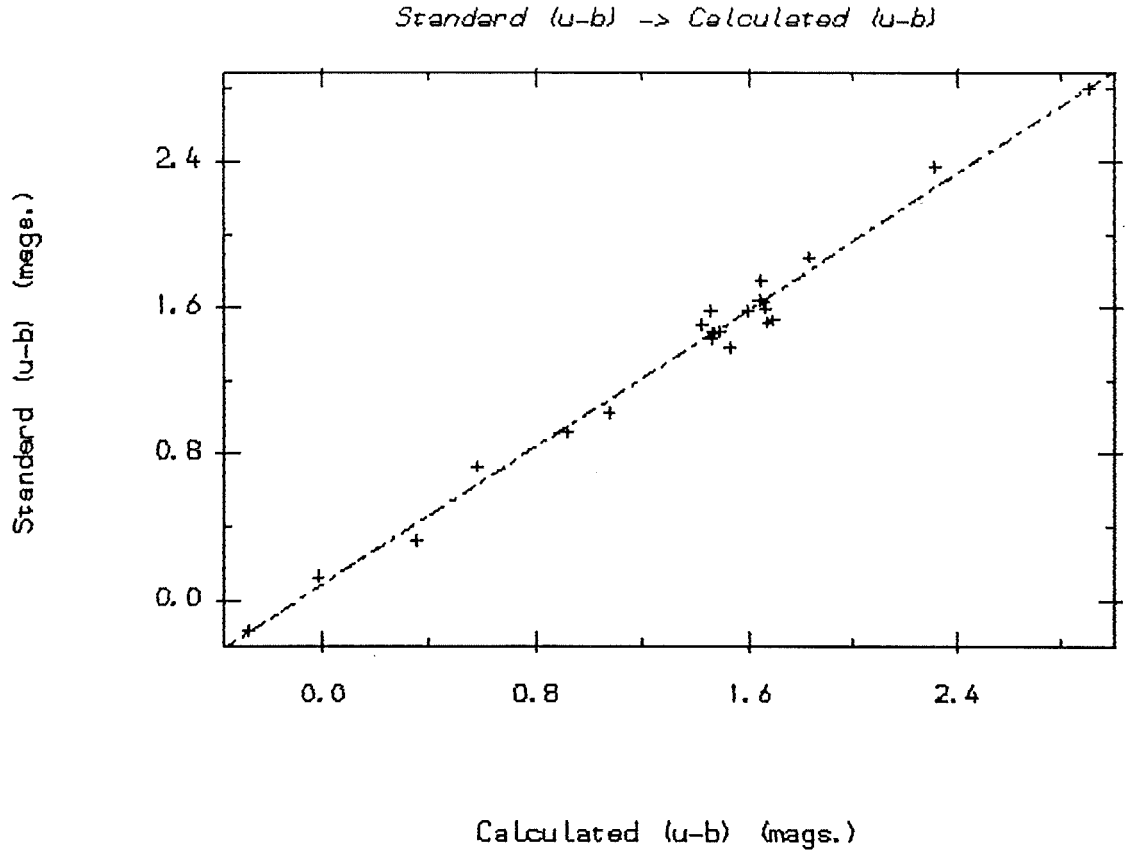

Fig.6.42 Oct.6th (u-b) colour.

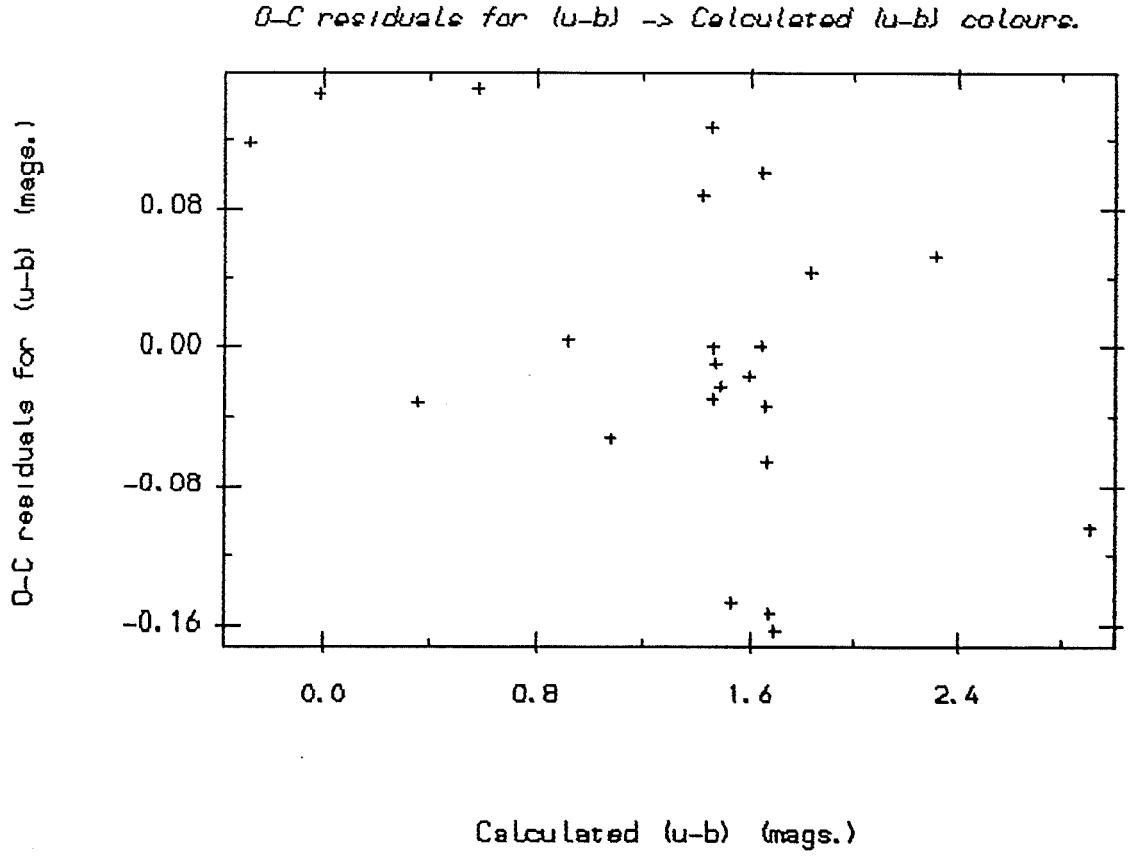

Fig.6.43 Oct.6th (u-b) colour.

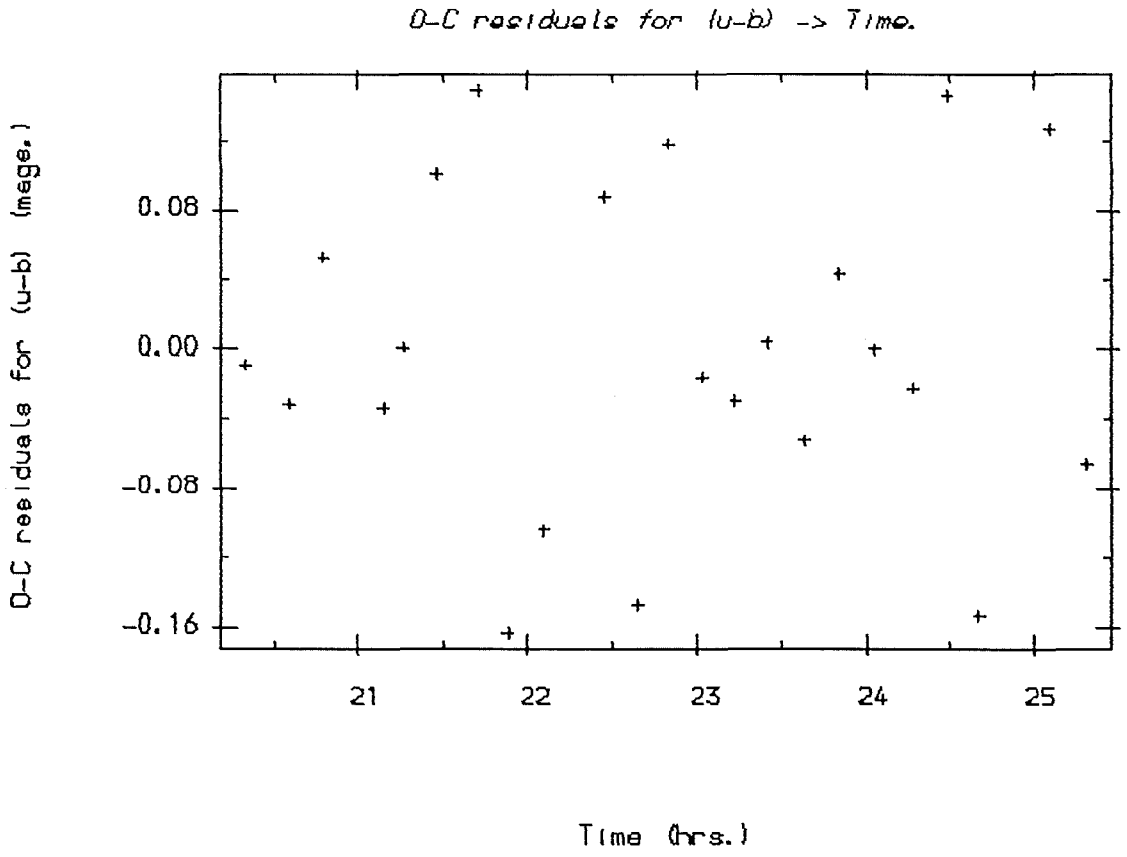

Fig.6.44 Oct.6th (u-b) colour.

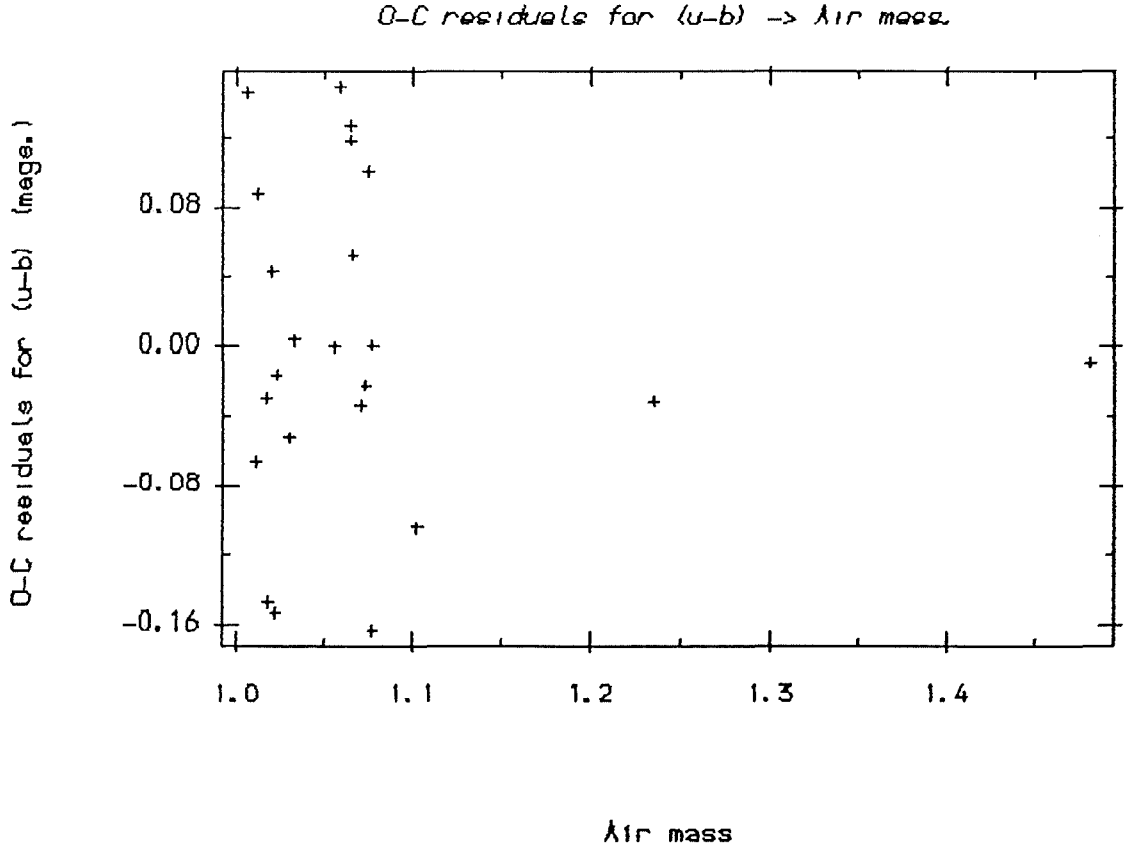

Fig.6.45 Oct.6th (u-b) colour.

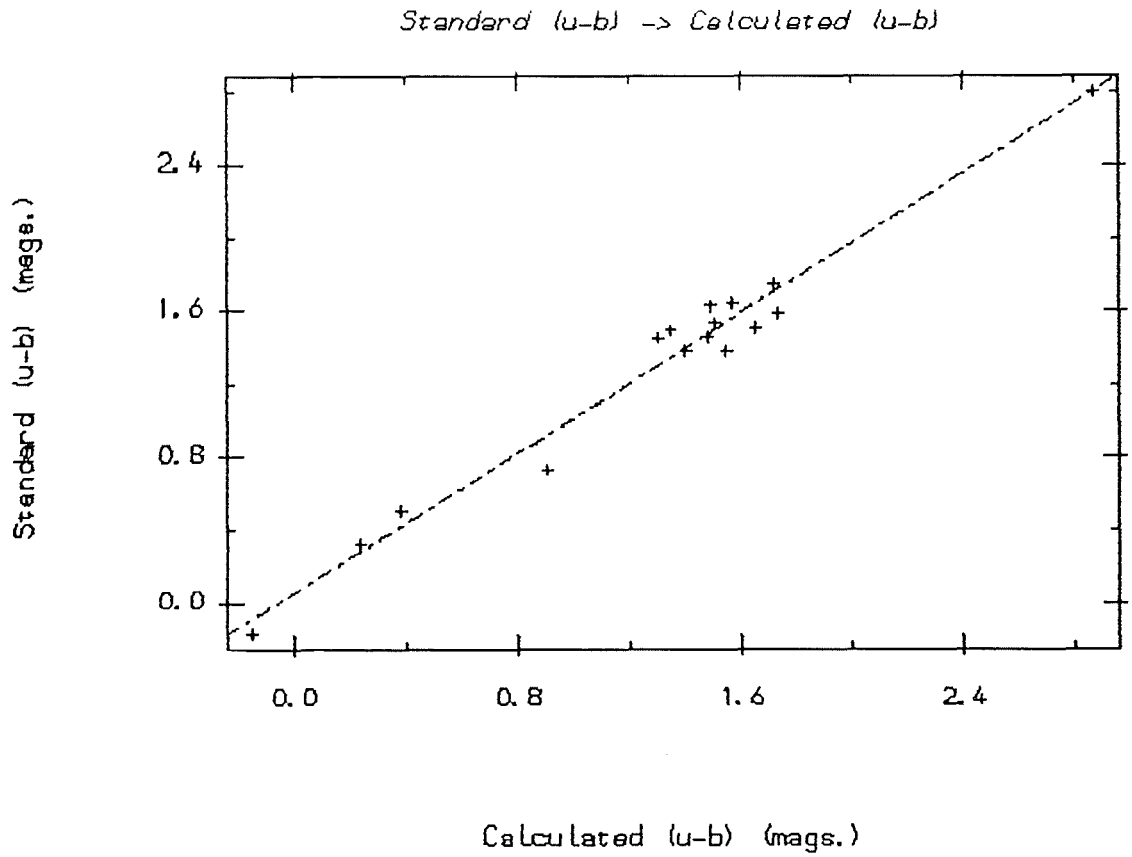

Fig.6.46 Oct.8th (u-b) colour.

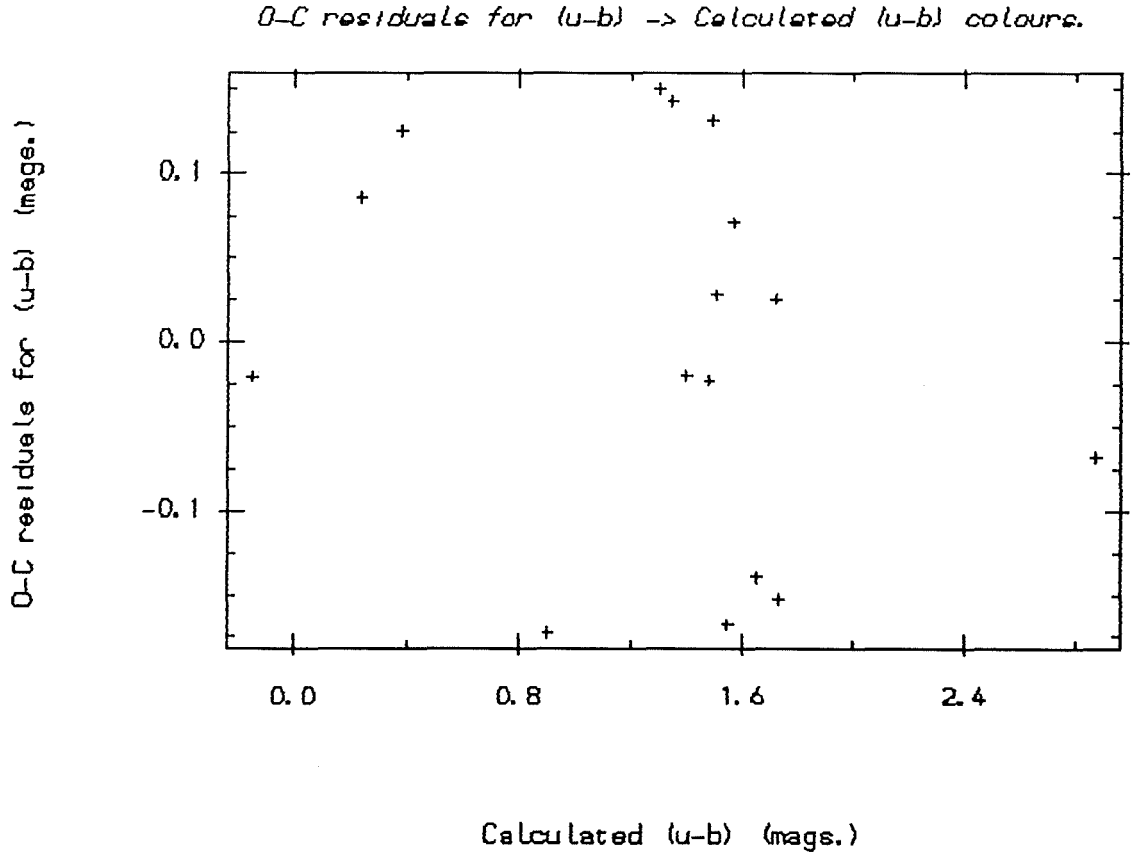

Fig.6.47 Oct.8th (u-b) colour.

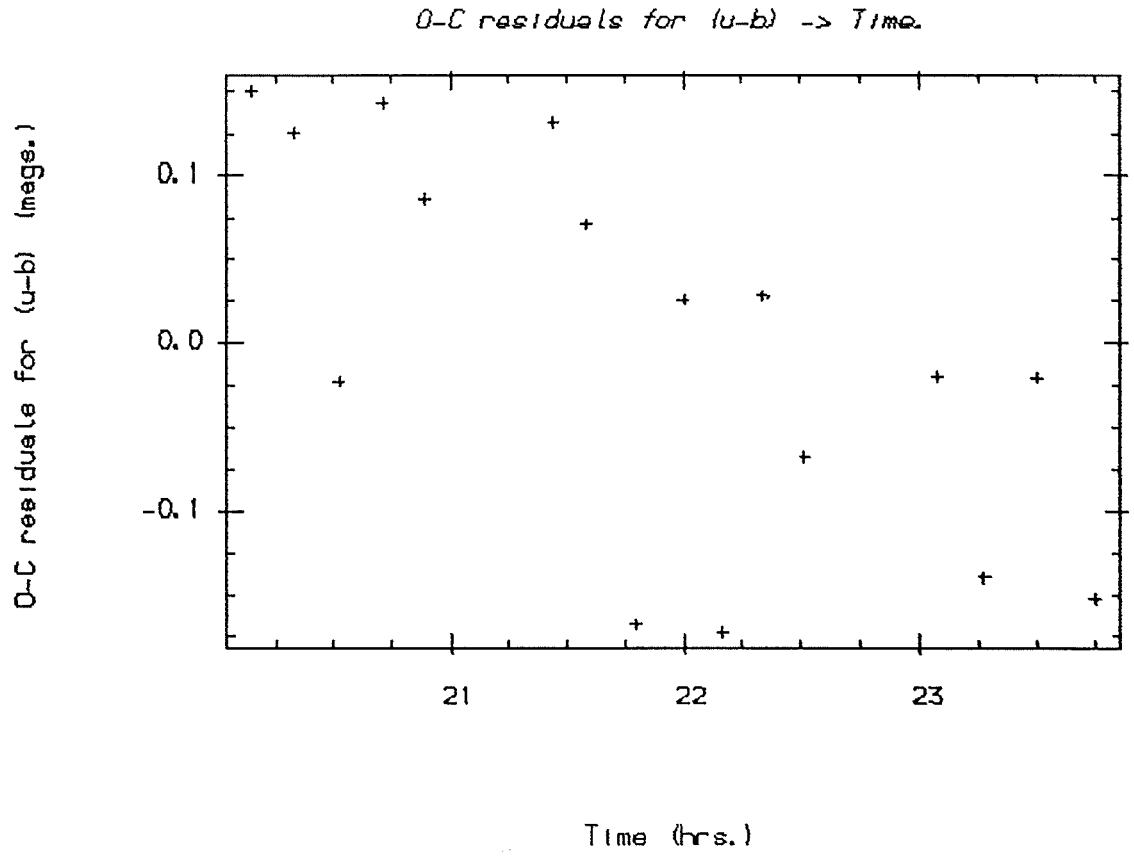

Fig.6.48 Oct.8th (u-b) colour.

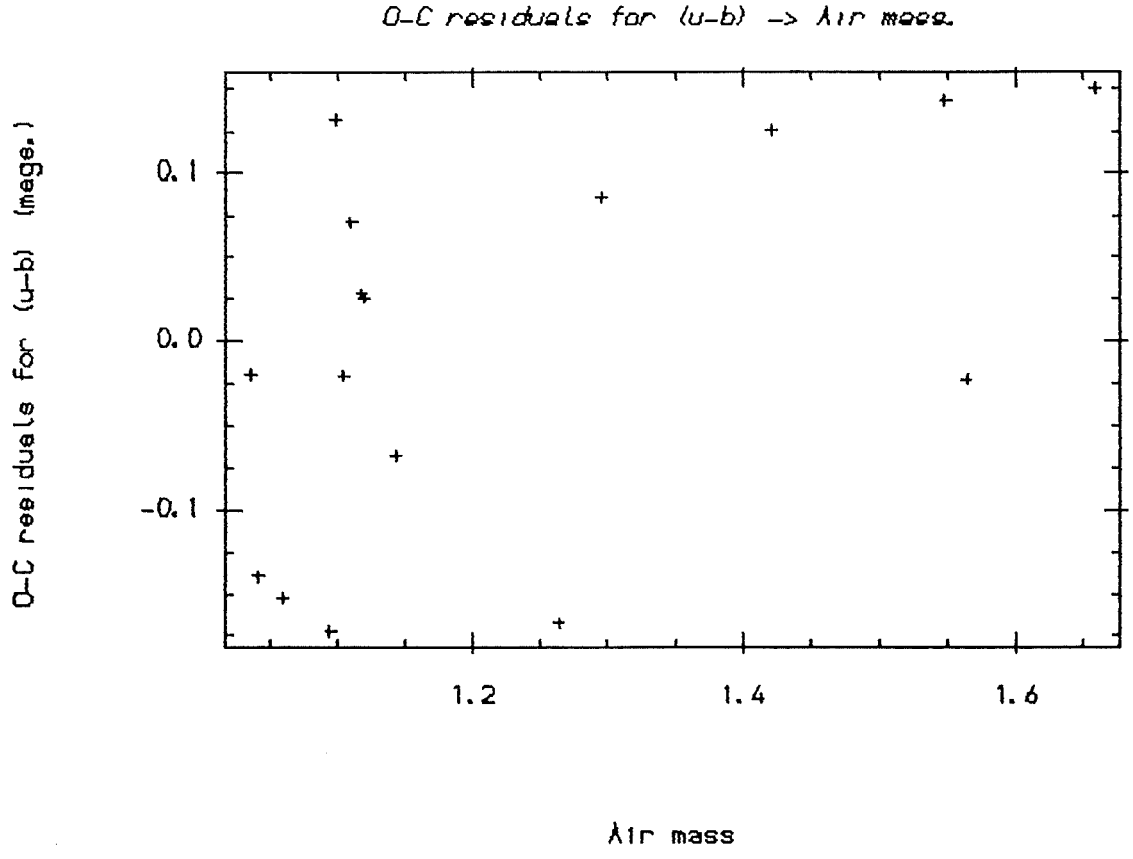

Fig.6.49 Oct.8th (u-b) colour.

Table 6.3 Residuals for V Magnitudes on Sep.23rd.

Date of observations : 23-09-1987

Name	Time	Air mass	Residual	
HR 7977	22.89990	1.0839	0.053	V
HR 7984	23.28154	1.1242	0.094	V
HR 8585	23.93861	1.0308	-0.022	V
HR 8830	24.71943	1.0372	-0.096	V
HR 8965	24.92829	1.0525	-0.009	V
HR 27	25.13843	1.0297	-0.076	V
HR 63	25.33716	1.0685	-0.029	V
HR 68	25.54746	1.0887	0.044	V
HR 184	25.73362	1.0277	0.022	V
HR 343	26.16537	1.0117	-0.029	V
HR 685	26.63168	1.0007	0.017	V
HR 717	26.87436	1.1231	0.049	V
HR 801	27.14498	1.1413	0.006	V
HR 937	27.35488	1.0071	-0.028	V
HR 1269	27.72104	1.1281	0.031	V
HR 1303	28.01537	1.0102	-0.024	V

Table 6.4 Residuals for V Magnitudes on Oct.6th.

Date of observations : 06-10-1987

Name	Time	Air mass	Residual	
HR 7328	20.79053	1.0665	-0.008	V
HR 7469	20.96566	1.0662	0.038	V
HR 7503	21.14819	1.0705	0.063	V
HR 7504	21.26419	1.0776	0.050	V
HR 7730	21.46144	1.0749	0.059	V
HR 7977	21.70678	1.0589	0.075	V
HR 7984	21.88579	1.0774	0.038	V
HR 8085	22.09598	1.1025	0.075	V
HR 8494	22.45037	1.0120	0.004	V
HR 8585	22.65001	1.0181	-0.016	V
HR 8622	22.82503	1.0649	0.030	V
HR 8613	23.02564	1.0229	0.017	V
HR 8830	23.22195	1.0172	0.000	V
HR 8965	23.41525	1.0329	-0.033	V
HR 8976	23.64108	1.0302	-0.079	V
HR 27	23.84244	1.0203	-0.028	V
HR 63	24.04770	1.0560	-0.044	V
HR 68	24.27997	1.0734	-0.039	V
HR 184	24.67344	1.0224	-0.060	V
HR 269	25.10117	1.0650	-0.067	V
HR 343	25.32076	1.0113	-0.076	V

Table 6.5 Residuals for V Magnitude on Oct.8th.

Date of observations : 08-10-1987

Name	Time	Air mass	Residual	
HR 6092	20.33231	1.4215	0.050	V
HR 6332	20.52224	1.5641	0.101	V
HR 6588	20.89050	1.2956	0.025	V
HR 7328	21.08632	1.0938	-0.028	V
HR 7469	21.25993	1.0932	0.017	V
HR 7503	21.43911	1.0983	0.045	V
HR 7504	21.57931	1.1094	0.025	V
HR 7534	21.79419	1.2634	0.023	V
HR 7730	21.99991	1.1192	0.009	V
HR 7977	22.16223	1.0938	0.046	V
HR 7984	22.33428	1.1171	-0.001	V
HR 8085	22.51375	1.1430	0.020	V
HR 8585	23.07193	1.0355	-0.100	V
HR 8494	23.26575	1.0409	-0.102	V
HR 8622	23.49794	1.1041	-0.040	V
HR 8613	23.74787	1.0587	-0.092	V

Table 6.6 Colour Terms and Zero Points for V magnitudes.

Adopted Extinction term 0.25

Night	Colour Term
Sep.23	0.045 +/- 0.047
Oct.6	0.079 +/- 0.058
Oct.8	0.072 +/- 0.036

Mean Colour Term 0.065 +/- 0.051

Night	Zero Point
Sep.23	19.000 +/- 0.012
Oct.6	19.033 +/- 0.011
Oct.8	19.049 +/- 0.015

Table 6.7 Residuals for (b-y) on Sep.23rd.

Date of observations : 23-09-1987

Name	Time	Air mass	Residual	
HR 7328	22.45092	1.1268	0.005	(b-y)
HR 7730	22.74803	1.1042	0.001	(b-y)
HR 8585	23.93861	1.0308	0.009	(b-y)
HR 8622	24.24553	1.0952	-0.027	(b-y)
HR 8613	24.52709	1.0484	-0.022	(b-y)
HR 8830	24.71943	1.0372	0.015	(b-y)
HR 27	25.13843	1.0297	-0.003	(b-y)
HR 63	25.33716	1.0685	0.017	(b-y)
HR 68	25.54746	1.0887	0.014	(b-y)
HR 184	25.73362	1.0277	-0.005	(b-y)
HR 193	25.91869	1.0284	-0.015	(b-y)
HR 343	26.16537	1.0117	0.009	(b-y)
HR 685	26.63168	1.0007	-0.004	(b-y)
HR 717	26.87436	1.1231	-0.008	(b-y)
HR 801	27.14498	1.1413	-0.021	(b-y)
HR 937	27.35488	1.0071	0.034	(b-y)
HR 1269	27.72104	1.1281	0.000	(b-y)

Table 6.8 Residual for (b-y) on Oct.6th.

Date of observations : 06-10-1987

Name	Time	Air mass	Residual	
HR 6332	20.32491	1.4810	0.002	(b-y)
HR 6588	20.58619	1.2347	-0.010	(b-y)
HR 7469	20.96566	1.0662	-0.012	(b-y)
HR 7503	21.14819	1.0705	-0.003	(b-y)
HR 7504	21.26419	1.0776	-0.008	(b-y)
HR 7730	21.46144	1.0749	0.002	(b-y)
HR 7977	21.70678	1.0589	0.017	(b-y)
HR 7984	21.88579	1.0774	-0.025	(b-y)
HR 8085	22.09598	1.1025	-0.004	(b-y)
HR 8086	22.24707	1.1124	-0.016	(b-y)
HR 8494	22.45037	1.0120	0.002	(b-y)
HR 8585	22.65001	1.0181	-0.026	(b-y)
HR 8622	22.82503	1.0649	-0.014	(b-y)
HR 8613	23.02564	1.0229	0.000	(b-y)
HR 8830	23.22195	1.0172	0.004	(b-y)
HR 8965	23.41525	1.0329	-0.020	(b-y)
HR 8976	23.64108	1.0302	0.000	(b-y)
HR 27	23.84244	1.0203	0.014	(b-y)
HR 63	24.04770	1.0560	0.034	(b-y)
HR 68	24.27997	1.0734	0.035	(b-y)
HR 153	24.48426	1.0061	0.019	(b-y)
HR 184	24.67344	1.0224	0.008	(b-y)
HR 193	24.92132	1.0246	-0.037	(b-y)
HR 269	25.10117	1.0650	0.017	(b-y)
HR 343	25.32076	1.0113	0.019	(b-y)

Table 6.9 Residuals for (b-y) on Oct.8th.

Date of observations : 08-10-1987

Name	Time	Air mass	Residual	
HR 6092	20.33231	1.4215	0.021	(b-y)
HR 6332	20.52224	1.5641	0.002	(b-y)
HR 6588	20.89050	1.2956	0.004	(b-y)
HR 7503	21.43911	1.0983	0.010	(b-y)
HR 7504	21.57931	1.1094	-0.007	(b-y)
HR 7534	21.79419	1.2634	-0.004	(b-y)
HR 7730	21.99991	1.1192	-0.001	(b-y)
HR 7977	22.16223	1.0938	-0.015	(b-y)
HR 7984	22.33428	1.1171	0.012	(b-y)
HR 8085	22.51375	1.1430	0.002	(b-y)
HR 8086	22.63977	1.1541	0.005	(b-y)
HR 8585	23.07193	1.0355	0.000	(b-y)
HR 8494	23.26575	1.0409	0.011	(b-y)
HR 8622	23.49794	1.1041	-0.025	(b-y)
HR 8613	23.74787	1.0587	-0.015	(b-y)

Table 6.10 Scale Factors and Zero Points for (b-y) colours.

Adopted Extinction term 0.10

Night	Scale Factor
Sep.23	0.983 +/- 0.016
Oct.6	0.921 +/- 0.009
Oct.8	0.924 +/- 0.009

Mean Scale Factor 0.924 +/- 0.012

Night	Zero Point
Sep.23	-0.694 +/- 0.004
Oct.6	-0.661 +/- 0.003
Oct.8	-0.653 +/- 0.003

Table 6.11 Residuals for (v-b) on Sep.23rd.

Date of observations : 23-09-1987

Name	Time	Air mass	Residual	
HR 7730	22.74803	1.1042	-0.004	(v-b)
HR 7977	22.89990	1.0839	0.052	(v-b)
HR 7984	23.28154	1.1242	0.007	(v-b)
HR 8585	23.93861	1.0308	0.034	(v-b)
HR 8622	24.24553	1.0952	-0.044	(v-b)
HR 8613	24.52709	1.0484	0.014	(v-b)
HR 8830	24.71943	1.0372	-0.023	(v-b)
HR 8965	24.92829	1.0525	0.050	(v-b)
HR 27	25.13843	1.0297	-0.003	(v-b)
HR 63	25.33716	1.0685	-0.026	(v-b)
HR 68	25.54746	1.0887	-0.005	(v-b)
HR 184	25.73362	1.0277	0.013	(v-b)
HR 193	25.91869	1.0284	-0.033	(v-b)
HR 343	26.16537	1.0117	0.020	(v-b)
HR 685	26.63168	1.0007	-0.028	(v-b)
HR 717	26.87436	1.1231	0.004	(v-b)
HR 801	27.14498	1.1413	-0.019	(v-b)
HR 937	27.35488	1.0071	-0.006	(v-b)
HR 1269	27.72104	1.1281	-0.013	(v-b)
HR 1303	28.01537	1.0102	0.012	(v-b)

Table 6.12 Residuals for (v-b) on Oct.6th.

Date of observations : 06-10-1987

Name	Time	Air mass	Residual	
HR 7328	20.79053	1.0665	0.027	(v-b)
HR 7503	21.14819	1.0705	0.001	(v-b)
HR 7504	21.26419	1.0776	0.001	(v-b)
HR 7730	21.46144	1.0749	-0.008	(v-b)
HR 7984	21.88579	1.0774	0.030	(v-b)
HR 8085	22.09598	1.1025	0.003	(v-b)
HR 8086	22.24707	1.1124	-0.019	(v-b)
HR 8494	22.45037	1.0120	0.021	(v-b)
HR 8613	23.02564	1.0229	-0.014	(v-b)
HR 8830	23.22195	1.0172	-0.010	(v-b)
HR 8965	23.41525	1.0329	0.011	(v-b)
HR 8976	23.64108	1.0302	0.015	(v-b)
HR 27	23.84244	1.0203	-0.023	(v-b)
HR 63	24.04770	1.0560	-0.025	(v-b)
HR 68	24.27997	1.0734	-0.009	(v-b)
HR 153	24.48426	1.0061	-0.015	(v-b)
HR 184	24.67344	1.0224	0.017	(v-b)
HR 193	24.92132	1.0246	-0.012	(v-b)
HR 269	25.10117	1.0650	0.016	(v-b)
HR 343	25.32076	1.0113	-0.008	(v-b)

Table 6.13 Residuals for (v-b) on Oct.8th.

Date of observations : 08-10-1987

Name	Time	Air mass	Residual	
HR 5936	20.14827	1.6589	0.008	(v-b)
HR 6092	20.33231	1.4215	0.005	(v-b)
HR 6332	20.52224	1.5641	0.018	(v-b)
HR 6458	20.71182	1.5481	-0.020	(v-b)
HR 6588	20.89050	1.2956	0.010	(v-b)
HR 7328	21.08632	1.0938	0.031	(v-b)
HR 7503	21.43911	1.0983	-0.026	(v-b)
HR 7504	21.57931	1.1094	-0.007	(v-b)
HR 7534	21.79419	1.2634	0.034	(v-b)
HR 7730	21.99991	1.1192	-0.011	(v-b)
HR 7977	22.16223	1.0938	-0.019	(v-b)
HR 7984	22.33428	1.1171	-0.019	(v-b)
HR 8085	22.51375	1.1430	-0.013	(v-b)
HR 8585	23.07193	1.0355	0.017	(v-b)
HR 8494	23.26575	1.0409	-0.002	(v-b)
HR 8613	23.74787	1.0587	-0.008	(v-b)

Table 6.14 Scale Factors, Colour Terms and Zero Points for (v-b) colours.

Adopted Extinction term 0.10

Night	Scale Factor
Sep.23	1.122 +/- 0.016
Oct.6	1.060 +/- 0.008
Oct.8	1.033 +/- 0.006

Mean Scale Factor 1.058 +/- 0.011

Night	Colour Term
Sep.23	0.048 +/- 0.025
Oct.6	0.004 +/- 0.017
Oct.8	0.004 +/- 0.016

Mean Colour Term 0.015 +/- 0.019

Night	Zero Point
Sep.23	1.680 +/- 0.006
Oct.6	1.665 +/- 0.004
Oct.8	1.679 +/- 0.005

Table 6.15 Residuals for (u-b) on Sep.23rd.

Date of observations : 23-09-1987

Name	Time	Air mass	Residual	
HR 7328	22.45092	1.1268	-0.236	(u-b)
HR 7984	23.28154	1.1242	0.123	(u-b)
HR 8622	24.24553	1.0952	0.115	(u-b)
HR 8613	24.52709	1.0484	-0.040	(u-b)
HR 8830	24.71943	1.0372	0.071	(u-b)
HR 8965	24.92829	1.0525	-0.023	(u-b)
HR 27	25.13843	1.0297	0.088	(u-b)
HR 63	25.33716	1.0685	-0.008	(u-b)
HR 68	25.54746	1.0887	-0.071	(u-b)
HR 184	25.73362	1.0277	-0.126	(u-b)
HR 193	25.91869	1.0284	0.151	(u-b)
HR 343	26.16537	1.0117	0.092	(u-b)
HR 685	26.63168	1.0007	0.016	(u-b)
HR 717	26.87436	1.1231	-0.002	(u-b)
HR 801	27.14498	1.1413	-0.067	(u-b)
HR 937	27.35488	1.0071	-0.060	(u-b)
HR 1269	27.72104	1.1281	-0.021	(u-b)

Table 6.16 Residuals for (u-b) on Oct.6th.

Date of observations : 06-10-1987

Name	Time	Air mass	Residual	
HR 6332	20.32491	1.4810	-0.009	(u-b)
HR 6588	20.58619	1.2347	-0.031	(u-b)
HR 7328	20.79053	1.0665	0.052	(u-b)
HR 7503	21.14819	1.0705	-0.034	(u-b)
HR 7504	21.26419	1.0776	0.000	(u-b)
HR 7730	21.46144	1.0749	0.100	(u-b)
HR 7977	21.70678	1.0589	0.148	(u-b)
HR 7984	21.88579	1.0774	-0.163	(u-b)
HR 8085	22.09598	1.1025	-0.104	(u-b)
HR 8494	22.45037	1.0120	0.087	(u-b)
HR 8585	22.65001	1.0181	-0.147	(u-b)
HR 8622	22.82503	1.0649	0.118	(u-b)
HR 8613	23.02564	1.0229	-0.016	(u-b)
HR 8830	23.22195	1.0172	-0.029	(u-b)
HR 8965	23.41525	1.0329	0.004	(u-b)
HR 8976	23.64108	1.0302	-0.052	(u-b)
HR 27	23.84244	1.0203	0.043	(u-b)
HR 63	24.04770	1.0560	0.000	(u-b)
HR 68	24.27997	1.0734	-0.022	(u-b)
HR 153	24.48426	1.0061	0.146	(u-b)
HR 184	24.67344	1.0224	-0.153	(u-b)
HR 269	25.10117	1.0650	0.126	(u-b)
HR 343	25.32076	1.0113	-0.066	(u-b)

Table 6.17 Residual for (u-b) on Oct.8th.

Date of observations : 08-10-1987

Name	Time	Air mass	Residual	
HR 5936	20.14827	1.6589	0.150	(u-b)
HR 6092	20.33231	1.4215	0.125	(u-b)
HR 6332	20.52224	1.5641	-0.022	(u-b)
HR 6458	20.71182	1.5481	0.143	(u-b)
HR 6588	20.89050	1.2956	0.085	(u-b)
HR 7503	21.43911	1.0983	0.131	(u-b)
HR 7504	21.57931	1.1094	0.070	(u-b)
HR 7534	21.79419	1.2634	-0.167	(u-b)
HR 7730	21.99991	1.1192	0.025	(u-b)
HR 7977	22.16223	1.0938	-0.172	(u-b)
HR 7984	22.33428	1.1171	0.028	(u-b)
HR 8085	22.51375	1.1430	-0.067	(u-b)
HR 8585	23.07193	1.0355	-0.019	(u-b)
HR 8494	23.26575	1.0409	-0.139	(u-b)
HR 8622	23.49794	1.1041	-0.020	(u-b)
HR 8613	23.74787	1.0587	-0.152	(u-b)

Table 6.18 Scale Factors, Colour Terms and Zero Points for (u-b) colours.

Adopted Extinction term 0.30

Night	Scale Factor
Sep.23	1.145 +/- 0.036
Oct.6	1.240 +/- 0.024
Oct.8	1.259 +/- 0.034

Mean Scale Factor 1.219 +/- 0.033

Night	Colour Term
Sep.23	0.088 +/- 0.135
Oct.6	0.347 +/- 0.086
Oct.8	0.560 +/- 0.106

Mean Colour Term 0.350 +/- 0.119

Night	Zero Point
Sep.23	-2.504 +/- 0.024
Oct.6	-2.468 +/- 0.019
Oct.8	-2.644 +/- 0.029

Table 6.19 Transformation from instrumental to standard system for V on Sep.23rd.

Name	Vs	Vt	error
HR 7328	3.770	3.881	0.083
HR 7730	4.830	5.026	0.055
HR 7977	4.840	4.764	0.059
HR 7984	5.040	4.939	0.064
HR 8494	4.190	4.058	0.058
HR 8585	3.770	3.793	0.050
HR 8622	4.880	5.412	0.049
HR 8613	4.630	4.803	0.060
HR 8830	4.520	4.605	0.060
HR 8965	4.290	4.301	0.051
HR 27	5.030	5.089	0.066
HR 63	4.610	4.638	0.051
HR 68	4.520	4.474	0.052
HR 184	4.940	4.912	0.056
HR 193	4.540	4.334	0.052
HR 343	4.330	4.354	0.055
HR 685	5.170	5.132	0.069
HR 717	5.300	5.238	0.061
HR 801	4.660	4.657	0.049
HR 937	4.050	4.054	0.070
HR 1269	5.230	5.184	0.064
HR 1303	4.140	4.124	0.082

Table 6.20 Transformation from instrumental to standard system for (b-y) on Sep.23rd.

Name	(b-y)s	(b-y)t	error
HR 7328	0.579	0.569	0.020
HR 7730	0.068	0.063	0.014
HR 7977	0.356	0.134	0.015
HR 7984	0.108	0.221	0.016
HR 8494	0.169	0.119	0.015
HR 8585	0.001	-0.012	0.013
HR 8622	-0.070	-0.047	0.012
HR 8613	0.142	0.161	0.015
HR 8830	0.181	0.162	0.015
HR 8965	-0.031	0.004	0.013
HR 27	0.273	0.272	0.017
HR 63	0.026	0.004	0.013
HR 68	0.026	0.007	0.013
HR 184	0.087	0.089	0.014
HR 193	0.007	0.017	0.013
HR 343	0.087	0.075	0.014
HR 685	0.321	0.320	0.017
HR 717	0.178	0.179	0.015
HR 801	-0.052	-0.031	0.013
HR 937	0.376	0.337	0.017
HR 1269	0.226	0.221	0.016
HR 1303	0.614	0.557	0.020

Table 6.21 Transformations from instrumental to standard system for m1 on Sep.23rd.

Name	m1s	m1t	error
HR 7328	0.390	0.298	0.044
HR 7730	0.150	0.160	0.020
HR 7977	-0.067	0.097	0.023
HR 7984	0.209	0.088	0.027
HR 8494	0.192	0.122	0.023
HR 8585	0.173	0.152	0.017
HR 8622	0.042	0.064	0.015
HR 8613	0.174	0.139	0.025
HR 8830	0.172	0.213	0.025
HR 8965	0.100	0.015	0.016
HR 27	0.123	0.124	0.029
HR 63	0.180	0.228	0.019
HR 68	0.187	0.211	0.019
HR 184	0.221	0.204	0.022
HR 193	0.076	0.100	0.018
HR 343	0.213	0.203	0.021
HR 685	-0.038	-0.013	0.030
HR 717	0.211	0.203	0.026
HR 801	0.097	0.096	0.016
HR 937	0.201	0.241	0.033
HR 1269	0.159	0.174	0.028
HR 1303	0.268	0.304	0.044

Table 6.22 Transformation from instrumental to standard system for c1 on Sep.23rd.

Name	c1s	c1t	error
HR 7328	0.430	0.668	0.456
HR 7730	1.310	1.501	0.315
HR 7977	0.153	1.336	0.328
HR 7984	0.897	0.754	0.337
HR 8494	0.787	1.315	0.324
HR 8585	1.030	1.354	0.288
HR 8622	-0.110	-0.292	0.227
HR 8613	0.948	0.971	0.329
HR 8830	0.723	0.546	0.323
HR 8965	0.784	0.918	0.271
HR 27	1.082	0.899	0.359
HR 63	1.050	0.998	0.289
HR 68	1.040	1.092	0.291
HR 184	0.902	1.027	0.314
HR 193	0.479	0.258	0.263
HR 343	0.997	0.917	0.307
HR 685	0.753	0.576	0.355
HR 717	0.780	0.734	0.333
HR 801	0.333	0.378	0.252
HR 937	0.376	0.302	0.372
HR 1269	0.588	0.510	0.337
HR 1303	0.551	0.344	0.444

Table 6.23 Transformations from instrumental to standard system for V on Oct.6th.

Name	Vs	Vt	error
HR 6332	5.250	5.134	0.049
HR 6588	3.800	3.764	0.046
HR 7328	3.770	3.742	0.078
HR 7469	4.480	4.426	0.064
HR 7503	5.960	5.872	0.072
HR 7504	6.200	6.124	0.073
HR 7730	4.830	4.767	0.053
HR 7977	4.840	4.743	0.068
HR 7984	5.040	4.996	0.057
HR 8085	5.210	5.094	0.086
HR 8086	6.030	6.112	0.094
HR 8494	4.190	4.176	0.058
HR 8585	3.770	3.788	0.051
HR 8622	4.880	4.856	0.046
HR 8613	4.630	4.605	0.057
HR 8830	4.520	4.510	0.059
HR 8965	4.290	4.327	0.049
HR 8976	4.140	4.224	0.047
HR 27	5.030	5.043	0.064
HR 63	4.610	4.655	0.049
HR 68	4.520	4.560	0.049
HR 153	3.660	3.796	0.043
HR 184	4.940	4.996	0.054
HR 193	4.540	4.435	0.052
HR 269	3.870	3.935	0.052
HR 343	4.330	4.403	0.053

Table 6.24 Transformations from instrumental to standard system for (b-y) on Oct.6th.

Name	(b-y)s	(b-y)t	error
HR 6332	0.002	-0.004	0.013
HR 6588	-0.064	-0.057	0.012
HR 7328	0.579	0.505	0.019
HR 7469	0.261	0.271	0.016
HR 7503	0.410	0.411	0.018
HR 7504	0.416	0.421	0.018
HR 7730	0.068	0.062	0.013
HR 7977	0.356	0.335	0.017
HR 7984	0.108	0.131	0.014
HR 8085	0.656	0.658	0.021
HR 8086	0.791	0.805	0.023
HR 8494	0.169	0.164	0.015
HR 8585	0.001	0.024	0.013
HR 8622	-0.070	-0.058	0.012
HR 8613	0.142	0.138	0.014
HR 8830	0.181	0.173	0.015
HR 8965	-0.031	-0.013	0.012
HR 8976	-0.035	-0.038	0.012
HR 27	0.273	0.256	0.016
HR 63	0.026	-0.012	0.012
HR 68	0.026	-0.012	0.012
HR 153	-0.090	-0.112	0.011
HR 184	0.087	0.075	0.014
HR 193	0.007	0.041	0.013
HR 269	0.068	0.048	0.013
HR 343	0.087	0.065	0.013

Table 6.25 Transformations from instrumental to standard system for m1 on Oct.6th.

Name	m1s	m1t	error
HR 6332	0.180	0.152	0.016
HR 6588	0.078	0.033	0.013
HR 7328	0.390	0.427	0.042
HR 7469	0.158	0.093	0.028
HR 7503	0.214	0.206	0.035
HR 7504	0.226	0.213	0.036
HR 7730	0.150	0.163	0.019
HR 7977	-0.067	-0.002	0.030
HR 7984	0.209	0.154	0.022
HR 8085	0.677	0.661	0.051
HR 8086	0.676	0.670	0.058
HR 8494	0.192	0.173	0.024
HR 8585	0.173	0.097	0.017
HR 8622	0.042	0.087	0.013
HR 8613	0.174	0.190	0.023
HR 8830	0.172	0.188	0.025
HR 8965	0.100	0.071	0.015
HR 8976	0.131	0.119	0.015
HR 27	0.123	0.160	0.028
HR 63	0.180	0.243	0.017
HR 68	0.187	0.234	0.017
HR 153	0.087	0.126	0.011
HR 184	0.221	0.214	0.021
HR 193	0.076	0.055	0.017
HR 269	0.194	0.196	0.019
HR 343	0.213	0.243	0.020

Table 6.26 Transformations from instrumental to standard system for c1 on Oct.6th.

Name	c1s	c1t	error
HR 6332	1.094	1.171	0.278
HR 6588	0.294	0.423	0.232
HR 7328	0.430	0.248	0.427
HR 7469	0.506	0.772	0.345
HR 7503	0.375	0.281	0.383
HR 7504	0.354	0.224	0.385
HR 7730	1.310	1.172	0.298
HR 7977	0.153	-0.210	0.331
HR 7984	0.897	1.087	0.316
HR 8085	0.134	0.037	0.485
HR 8086	0.067	-0.545	0.514
HR 8494	0.787	0.689	0.317
HR 8585	1.030	1.283	0.285
HR 8622	-0.110	-0.317	0.216
HR 8613	0.948	0.890	0.316
HR 8830	0.723	0.674	0.320
HR 8965	0.784	0.813	0.259
HR 8976	0.831	0.927	0.258
HR 27	1.082	0.904	0.349
HR 63	1.050	0.991	0.277
HR 68	1.040	1.036	0.278
HR 153	0.134	-0.013	0.211
HR 184	0.902	1.063	0.303
HR 193	0.479	0.225	0.258
HR 269	1.056	0.941	0.290
HR 343	0.997	1.019	0.301

Table 6.27 Transformations from instrumental to standard system for V on Oct.8th.

Name	Vs	Vt	error
HR 5936	5.450	5.277	0.060
HR 6092	3.890	3.842	0.044
HR 6332	5.250	5.148	0.049
HR 6458	5.390	5.235	0.069
HR 6588	3.800	3.778	0.045
HR 7328	3.770	3.761	0.079
HR 7469	4.480	4.445	0.066
HR 7503	5.960	5.888	0.071
HR 7504	6.200	6.147	0.073
HR 7534	4.990	4.946	0.067
HT 7730	4.830	4.815	0.053
HR 7977	4.840	4.770	0.070
HR 7984	5.040	5.034	0.054
HR 8085	5.210	5.147	0.085
HR 8086	6.030	6.174	0.093
HR 8585	3.770	3.870	0.049
HE 8494	4.190	4.281	0.058
HR 8622	4.880	4.924	0.046
HR 8613	4.630	4.713	0.058

Table 6.28 Transformations from instrumental to standard system for (b-y) on Oct.6th.

Name	(b-y)s	(b-y)t	error
HR 5936	0.233	0.191	0.015
HR 6092	-0.056	-0.079	0.011
HR 6332	0.002	-0.002	0.012
HR 6458	0.409	0.357	0.017
HR 6588	-0.064	-0.070	0.012
HR 7328	0.579	0.537	0.019
HR 7469	0.261	0.302	0.016
HR 7503	0.410	0.398	0.018
HR 7504	0.416	0.422	0.018
HR 7534	0.316	0.319	0.017
HT 7730	0.068	0.068	0.013
HR 7977	0.356	0.370	0.017
HR 7984	0.108	0.094	0.014
HR 8085	0.656	0.651	0.021
HR 8086	0.791	0.784	0.023
HR 8585	0.001	-0.002	0.012
HE 8494	0.169	0.156	0.015
HR 8622	-0.070	-0.046	0.012
HR 8613	0.142	0.156	0.015

Table 6.29 Transformations from instrumental to standard system for m1 on Oct.8th.

Name	m1s	m1t	error
HR 5936	0.233	0.191	0.015
HR 6092	-0.056	-0.079	0.011
HR 6332	0.002	-0.002	0.012
HR 6458	0.409	0.357	0.017
HR 6588	-0.064	-0.070	0.012
HR 7328	0.579	0.537	0.019
HR 7469	0.261	0.302	0.016
HR 7503	0.410	0.398	0.018
HR 7504	0.416	0.422	0.018
HR 7534	0.316	0.319	0.017
HT 7730	0.068	0.068	0.013
HR 7977	0.356	0.370	0.017
HR 7984	0.108	0.094	0.014
HR 8085	0.656	0.651	0.021
HR 8086	0.791	0.784	0.023
HR 8585	0.001	-0.002	0.012
HE 8494	0.169	0.156	0.015
HR 8622	-0.070	-0.046	0.012
HR 8613	0.142	0.156	0.015

Table 6.30 Transformations from instrumental to standard system for c1 on Oct.8th.

Name	c1s	c1t	error
HR 5936	0.662	0.427	0.322
HR 6092	0.440	0.316	0.231
HR 6332	1.094	1.126	0.281
HR 6458	0.309	-0.034	0.364
HR 6588	0.294	0.223	0.229
HR 7328	0.430	0.044	0.431
HR 7469	0.506	0.870	0.356
HR 7503	0.375	0.032	0.378
HR 7504	0.354	0.107	0.385
HR 7534	0.435	0.542	0.358
HT 7730	1.310	1.211	0.304
HR 7977	0.153	0.145	0.349
HR 7984	0.897	0.768	0.306
HR 8085	0.134	-0.062	0.484
HR 8086	0.067	-0.602	0.513
HR 8585	1.030	1.057	0.278
HE 8494	0.787	0.841	0.323
HR 8622	-0.110	-0.188	0.224
HR 8613	0.948	1.011	0.325

6.2 PHOTOMETRIC OBSERVATIONS OF SV CAMELOPARDIS

6.2.1 Introduction

SV Camelopardis (BD+82^{o}174) is a short period (P=0^{d}.593) eclipsing binary. It was discovered by Guthnick (1929) and has been observed extensively since its discovery. From the oldest photoelectric observations van Woerden (1957) reports variations in the shape of the light curve amounting to as much as 0.1 mag.. Wood (1946) has also reported variation and asymmetry in the light curve. Since then further light curves have been obtained by Nelson (1963a, b), Nelson and Duckworth (1968), Hilditch et al (1979), Patkos (1982a, b) and Cellino et al (1985) confirming the out-of-eclipse variations.

From DDO photometry, Hilditch et al (1979) concluded that the primary component was of spectral type G2-3V and the secondary of K4V. Hall (1976) classified SV Cam as a short-period RS CVn-type binary on the basis of these earlier light curve observations, whilst Hilditch et al (1979) have attributed the out-of-eclipse changes to BY Draconis-type variability (Kunkel, 1975; Bopp and Fekel, 1977) of the cooler component.

From an analysis of the published times of the minima for the system, Friboes-Coude and Herczeg (1973) concluded that the cyclic variations seen were probably a light-time effect due to the presence of a third body. This has further been substantiated by the work of Hilditch et al (1979) and Cullino et al (1985), who find a period ranging from 57.5 to 72.75 yrs. for the 3rd component.

6.2.2 The Observations

Observations were made of SV Cam on 2 separate nights using the 0.9m James Gregory Telescope with the St.Andrews-DAO 8-channel photometer mounted at the f/8 Cassegrain focus. The details of the photometer and associated hardware/software are discussed elsewhere in this thesis.

The comparison star used (BD+82^{o}168;G0) is the same as that used by van Woerden (1957), Hilditch et al (1979), Patkos (1982a) and Cellino et al (1984). Since no variation in this star has been previously reported the check star, (BD+82^{o}176;K0), was not observed.

Simultaneous observations were made in the Strömgren uvby system and Johnson VRI. On each night a number of standard stars were observed to determine the zero points, which were seen to vary by less than 5% over a period of 5 months. The uvby observations were then transformed to the standard Strömgren system, but the VRI data was left in instrumental magnitudes.

The observations were reduced using a suite of programmes, written by the author, which incorporates the fitting of a cubic spline function (Willingale, 1988) to the comparison data. Thus, by interpolating in time in the appropriate spline function, differential magnitudes in the sense (variable minus comparison) can be made. The smoothing of the comparison star observations results in a reduction of observational error; typically the rms error of the comparison-star observations about the spline function was +/- 0.01mag for these data.

The observations of the secondary minimum were made on Oct. 23/24 1987 and those of the primary minimum on Feb. 10/11 1988. Table 6.32 provides a list of the Julian date, phase and transformed uvby magnitudes. Table 6.33 lists the VRI instrumental magnitudes.

6.2.3 Time Of Minimum and Revised Orbital Period

The time of minimum was found for the primary eclipse using the technique described by Hertzsprung (1928). The primary minimum is shown in Figure 6.50. The eclipse is slightly asymmetric, the descending branch being steeper than the ascending branch and this, coupled with the fact that there are no measurements during the time of minimum, introduce a degree of uncertainty as to the precise time of the minimum. The following time of minimum was found;

JD 2447203.3790

+/- 17

Using the latest available ephemeris, derived by Cellino et al (1985) and with E=34151 we can calculate the time when the eclipse should have occurred. This is found to be;

JD 2447203.3729

From this we derive an (O - C) of $0^d.0061$, which corresponds to a change in period of 0.02 sec. Therefore we have a revised ephemeris of;

$$Pr.Min(JD) = 2447203.3790 + 0.59307115.E$$

$$+/- 17 \qquad +/- 5$$

Table 6.32 /continued

2447091.6500	0.6381	0.115	0.582	0.471	9.549
2447091.6507	0.6394	0.138	0.607	0.458	9.541
2447091.6515	0.6407	0.140	0.600	0.476	9.535
2447091.6523	0.6420	0.190	0.628	0.448	9.528
2447091.6531	0.6434	0.235	0.596	0.465	9.540
2447091.6539	0.6447	0.185	0.600	0.492	9.515
2447091.6631	0.6602	0.136	0.642	0.425	9.521
2447091.6639	0.6615	0.202	0.631	0.452	9.502
2447091.6647	0.6629	0.130	0.630	0.454	9.505
2447091.6655	0.6642	0.240	0.619	0.466	9.496
2447091.6663	0.6656	0.187	0.637	0.462	9.489
2447091.6671	0.6669	0.207	0.634	0.449	9.490
2447091.6679	0.6683	0.196	0.653	0.447	9.486
2447091.6687	0.6696	0.286	0.598	0.472	9.490
2447091.6770	0.6837	0.169	0.643	0.440	9.477
2447091.6778	0.6850	0.133	0.635	0.462	9.469
2447091.6786	0.6864	0.124	0.639	0.454	9.477
2447091.6794	0.6877	0.188	0.636	0.463	9.479
2447091.6802	0.6891	0.255	0.660	0.444	9.474
2447091.6810	0.6904	0.103	0.617	0.471	9.482
2447091.6818	0.6917	0.189	0.623	0.472	9.477
2447091.6826	0.6931	0.213	0.626	0.473	9.473
2447091.6834	0.6944	0.217	0.615	0.491	9.470
2447091.6929	0.7105	0.200	0.635	0.470	9.485
2447091.6937	0.7119	0.176	0.639	0.456	9.484
2447091.6945	0.7132	0.260	0.643	0.457	9.481
2447091.6953	0.7145	0.334	0.642	0.469	9.474
2447091.6961	0.7159	0.331	0.628	0.480	9.466
2447091.6969	0.7172	0.266	0.607	0.483	9.488
2447091.6977	0.7186	0.300	0.620	0.474	9.476
2447091.6985	0.7200	0.373	0.612	0.496	9.468
2447091.7078	0.7356	0.096	0.623	0.470	9.506
2447091.7086	0.7369	0.175	0.650	0.446	9.509
2447091.7100	0.7393	0.213	0.626	0.472	9.505
2447091.7108	0.7407	0.223	0.640	0.453	9.520
2447091.7116	0.7420	0.214	0.604	0.489	9.515
2447091.7124	0.7433	0.227	0.626	0.469	9.518
2447091.7132	0.7447	0.271	0.626	0.471	9.513
2447091.7140	0.7461	0.338	0.607	0.492	9.519
2447091.7227	0.7608	0.134	0.639	0.466	9.519
2447091.7235	0.7621	0.205	0.645	0.456	9.519
2447091.7243	0.7635	0.186	0.612	0.482	9.523
2447091.7339	0.7796	0.155	0.645	0.450	9.510
2447091.7347	0.7809	0.232	0.640	0.450	9.513
2447091.7355	0.7823	0.156	0.614	0.474	9.516
2447091.7363	0.7837	0.157	0.636	0.467	9.508
2447091.7371	0.7850	0.315	0.612	0.469	9.513
2447091.7464	0.8007	0.178	0.629	0.455	9.508
2447091.7472	0.8021	0.146	0.641	0.449	9.511
2447091.7480	0.8034	0.196	0.638	0.441	9.514
2447091.7488	0.8047	0.135	0.603	0.486	9.508
2447091.7496	0.8061	0.250	0.606	0.483	9.502
2447091.7504	0.8074	0.247	0.595	0.473	9.521
2447091.7512	0.8088	0.270	0.610	0.474	9.520
2447091.7520	0.8101	0.358	0.598	0.474	9.529

continued.....

Table 6.32 /continued

1988 Feb 11/12

H.J.D.	Phase	u-b	v-b	b-y	y
2447203.3258	0.9393	1.467	0.654	0.462	9.497
2447203.3265	0.9405	1.614	0.676	0.436	9.512
2447203.3272	0.9417	1.566	0.660	0.460	9.505
2447203.3279	0.9429	1.693	0.676	0.435	9.515
2447203.3286	0.9441	1.604	0.680	0.444	9.521
2447203.3294	0.9454	1.769	0.668	0.450	9.525
2447203.3301	0.9465	1.540	0.646	0.461	9.529
2447203.3384	0.9605	1.539	0.701	0.424	9.598
2447203.3391	0.9617	1.606	0.675	0.438	9.608
2447203.3398	0.9629	1.542	0.686	0.433	9.618
2447203.3405	0.9641	1.542	0.683	0.434	9.631
2447203.3412	0.9653	1.657	0.673	0.444	9.634
2447203.3419	0.9665	1.563	0.676	0.431	9.652
2447203.3426	0.9678	1.520	0.664	0.440	9.670
2447203.3434	0.9690	1.573	0.653	0.469	9.663
2447203.3523	0.9841	1.614	0.661	0.447	9.832
2447203.3530	0.9853	1.659	0.679	0.431	9.842
2447203.3538	0.9865	1.644	0.631	0.472	9.859
2447203.3545	0.9877	1.637	0.656	0.456	9.872
2447203.3552	0.9889	1.840	0.625	0.480	9.886
2447203.3559	0.9901	1.678	0.670	0.456	9.894
2447203.3566	0.9913	1.758	0.651	0.463	9.915
2447203.3573	0.9925	1.744	0.654	0.474	9.922
2447203.3657	0.0066	1.600	0.705	0.455	10.067
2447203.3664	0.0078	1.576	0.691	0.468	10.092
2447203.3671	0.0090	1.841	0.699	0.450	10.108
2447203.3678	0.0102	1.542	0.682	0.464	10.116
2447203.3685	0.0114	1.689	0.686	0.475	10.105
2447203.3692	0.0126	1.730	0.717	0.455	10.122
2447203.3700	0.0138	1.758	0.663	0.482	10.132
2447203.3707	0.0150	1.675	0.686	0.506	10.110
2447203.3813	0.0330	1.791	0.654	0.515	10.161
2447203.3820	0.0342	1.697	0.708	0.451	10.143
2447203.3828	0.0354	1.921	0.693	0.464	10.132
2447203.3835	0.0366	1.990	0.719	0.455	10.109
2447203.3842	0.0378	1.577	0.660	0.501	10.111
2447203.3849	0.0390	1.788	0.678	0.485	10.116
2447203.3856	0.0402	1.718	0.638	0.505	10.111
2447203.3863	0.0414	1.625	0.625	0.526	10.110
2447203.3958	0.0574	1.560	0.671	0.439	10.016
2447203.3965	0.0586	1.636	0.686	0.437	9.992
2447203.3972	0.0598	1.631	0.701	0.429	9.979
2447203.3979	0.0610	1.493	0.672	0.464	9.950
2447203.3986	0.0622	1.599	0.669	0.449	9.954
2447203.3994	0.0634	1.578	0.683	0.426	9.991
2447203.4001	0.0646	1.654	0.657	0.446	10.107
2447203.4008	0.0658	1.606	0.687	0.418	10.074
2447203.4089	0.0795	1.616	0.651	0.443	9.778
2447203.4096	0.0807	1.622	0.661	0.434	9.761
2447203.4103	0.0819	1.726	0.675	0.424	9.755
2447203.4110	0.0831	1.700	0.655	0.448	9.739
2447203.4117	0.0843	1.707	0.633	0.458	9.731

continued.....

Table 6.32 /continued

2447203.4125	0.0855	1.793	0.628	0.458	9.722
2447203.4132	0.0867	1.953	0.667	0.435	9.715
2447203.4139	0.0879	1.724	0.632	0.458	9.711
2447203.4223	0.1020	1.483	0.652	0.419	9.616
2447203.4230	0.1032	1.543	0.623	0.438	9.620
2447203.4237	0.1044	1.592	0.643	0.425	9.608
2447203.4244	0.1056	1.490	0.635	0.445	9.600
2447203.4251	0.1068	1.654	0.628	0.432	9.611
2447203.4258	0.1080	1.637	0.641	0.412	9.616
2447203.4265	0.1092	1.782	0.651	0.426	9.589
2447203.4273	0.1104	1.764	0.622	0.448	9.597
2447203.4352	0.1238	1.544	0.662	0.411	9.557
2447203.4359	0.1250	1.676	0.634	0.420	9.568
2447203.4366	0.1262	1.667	0.631	0.438	9.552
2447203.4373	0.1274	1.612	0.638	0.428	9.556
2447203.4380	0.1286	1.688	0.630	0.427	9.561
2447203.4387	0.1298	1.787	0.631	0.425	9.564
2447203.4394	0.1310	1.703	0.648	0.421	9.564
2447203.4401	0.1322	1.703	0.639	0.416	9.567
2447203.4509	0.1504	1.466	0.612	0.457	9.562
2447203.4517	0.1516	1.572	0.664	0.413	9.561
2447203.4524	0.1528	1.710	0.622	0.437	9.572
2447203.4531	0.1540	1.664	0.609	0.448	9.574
2447203.4538	0.1552	1.747	0.653	0.428	9.568
2447203.4545	0.1564	1.843	0.609	0.463	9.568
2447203.4552	0.1576	1.761	0.613	0.442	9.576
2447203.4559	0.1588	1.812	0.621	0.463	9.560
2447203.4643	0.1729	1.666	0.658	0.409	9.599
2447203.4650	0.1741	1.593	0.659	0.407	9.602
2447203.4657	0.1753	1.490	0.645	0.425	9.605
2447203.4665	0.1765	1.713	0.658	0.413	9.618
2447203.4672	0.1777	1.624	0.637	0.422	9.620
2447203.4679	0.1789	1.724	0.626	0.427	9.635
2447203.4686	0.1801	1.737	0.630	0.429	9.632
2447203.4693	0.1813	1.785	0.606	0.447	9.632
2447203.4860	0.2095	1.568	0.658	0.404	9.653
2447203.4867	0.2107	1.684	0.646	0.409	9.661
2447203.4881	0.2131	1.610	0.636	0.425	9.650
2447203.4889	0.2143	1.593	0.629	0.416	9.660
2447203.4896	0.2155	1.599	0.634	0.420	9.648
2447203.4903	0.2167	1.616	0.627	0.430	9.654
2447203.4910	0.2179	1.730	0.643	0.428	9.647

Table 6.33 VRI Observations of SV Cam.

1987 Oct 23/24

H.J.D.	Phase	V	R	I
2447091.53379	0.4422	-9.2828	-8.3171	-8.2152
2447091.53490	0.4441	-9.3001	-8.3168	-8.2162
2447091.53611	0.4461	-9.2973	-8.3189	-8.2044
2447091.53725	0.4480	-9.2976	-8.3119	-8.2039
2447091.53845	0.4500	-9.2852	-8.3012	-8.2021
2447091.53952	0.4519	-9.2923	-8.3130	-8.2078
2447091.54062	0.4537	-9.2896	-8.3097	-8.2067
2447091.54172	0.4556	-9.3112	-8.3118	-8.2133
2447091.55450	0.4771	-9.2433	-8.3218	-8.1574
2447091.55614	0.4799	-9.2428	-8.2990	-8.1469
2447091.55731	0.4819	-9.2301	-8.2941	-8.1332
2447091.55845	0.4838	-9.2340	-8.2655	-8.1264
2447091.55953	0.4856	-9.2254	-8.2776	-8.1341
2447091.56065	0.4875	-9.2116	-8.2575	-8.1310
2447091.56179	0.4894	-9.1809	-8.2369	-8.0957
2447091.56290	0.4913	-9.1909	-8.2325	-8.1021
2447091.57560	0.5127	-9.1180	-8.1666	-8.0216
2447091.57640	0.5140	-9.1942	-8.2413	-8.1022
2447091.57780	0.5164	-9.1972	-8.2279	-8.0738
2447091.57930	0.5189	-9.2000	-8.2340	-8.0919
2447091.58009	0.5203	-9.2034	-8.2425	-8.1032
2447091.58232	0.5240	-9.2230	-8.2588	-8.1250
2447091.58351	0.5260	-9.2229	-8.2630	-8.1316
2447091.58472	0.5281	-9.2196	-8.2458	-8.1120
2447091.59623	0.5475	-9.1882	-8.2030	-8.0747
2447091.59701	0.5488	-9.1780	-8.2064	-8.0580
2447091.59787	0.5502	-9.1771	-8.2093	-8.0607
2447091.59925	0.5526	-9.1866	-8.2164	-8.0699
2447091.60005	0.5539	-9.1833	-8.2101	-8.0767
2447091.60083	0.5552	-9.1798	-8.2058	-8.0823
2447091.60167	0.5566	-9.1689	-8.2028	-8.0807
2447091.60248	0.5580	-9.1755	-8.2006	-8.0637
2447091.61516	0.5794	-9.1525	-8.1524	-8.0108
2447091.61597	0.5808	-9.1345	-8.1536	-8.0079
2447091.61678	0.5821	-9.1297	-8.1567	-8.0202
2447091.61757	0.5835	-9.1358	-8.1584	-8.0082
2447091.61836	0.5848	-9.1265	-8.1523	-8.0095
2447091.61916	0.5861	-9.1293	-8.1500	-8.0187
2447091.61995	0.5875	-9.1356	-8.1569	-8.0198
2447091.62074	0.5888	-9.1402	-8.1582	-8.0261
2447091.63322	0.6098	-9.1483	-8.1481	-8.0029
2447091.63402	0.6112	-9.1463	-8.1596	-8.0067
2447091.63480	0.6125	-9.1526	-8.1526	-8.0093
2447091.63559	0.6138	-9.1335	-8.1474	-8.0137
2447091.63639	0.6152	-9.1423	-8.1495	-8.0115
2447091.63718	0.6165	-9.1482	-8.1528	-8.0151
2447091.63802	0.6179	-9.1333	-8.1459	-8.0087
2447091.64836	0.6354	-9.1487	-8.1539	-8.0321
2447091.64916	0.6367	-9.1600	-8.1659	-8.0374

continued.....

Table 6.33 /continued

2447091.64996	0.6381	-9.1527	-8.1676	-8.0538
2447091.65074	0.6394	-9.1609	-8.1656	-8.0435
2447091.65153	0.6407	-9.1671	-8.1723	-8.0517
2447091.65232	0.6420	-9.1746	-8.1696	-8.0547
2447091.65310	0.6434	-9.1621	-8.1693	-8.0742
2447091.65390	0.6447	-9.1868	-8.1869	-8.0665
2447091.66308	0.6602	-9.1811	-8.2021	-8.1028
2447091.66387	0.6615	-9.2004	-8.2096	-8.1069
2447091.66467	0.6629	-9.1976	-8.2209	-8.1130
2447091.66547	0.6642	-9.2070	-8.2235	-8.1194
2447091.66626	0.6656	-9.2134	-8.2311	-8.1213
2447091.66705	0.6669	-9.2126	-8.2450	-8.1340
2447091.66787	0.6683	-9.2168	-8.2398	-8.1279
2447091.66866	0.6696	-9.2124	-8.2399	-8.1373
2447091.67703	0.6837	-9.2262	-8.2423	-8.1399
2447091.67782	0.6850	-9.2342	-8.2450	-8.1395
2447091.67860	0.6864	-9.2257	-8.2481	-8.1486
2447091.67940	0.6877	-9.2238	-8.2305	-8.1443
2447091.68020	0.6891	-9.2285	-8.2327	-8.1467
2447091.68099	0.6904	-9.2206	-8.2390	-8.1521
2447091.68177	0.6917	-9.2259	-8.2384	-8.1531
2447091.68257	0.6931	-9.2304	-8.2432	-8.1532
2447091.68336	0.6944	-9.2327	-8.2462	-8.1498
2447091.69294	0.7105	-9.2183	-8.2269	-8.1382
2447091.69374	0.7119	-9.2192	-8.2293	-8.1470
2447091.69453	0.7132	-9.2219	-8.2476	-8.1541
2447091.69532	0.7145	-9.2296	-8.2309	-8.1562
2447091.69610	0.7159	-9.2374	-8.2378	-8.1754
2447091.69690	0.7172	-9.2153	-8.2375	-8.1664
2447091.69770	0.7186	-9.2274	-8.2371	-8.1663
2447091.69852	0.7200	-9.2348	-8.2450	-8.1801
2447091.70778	0.7356	-9.1975	-8.2049	-8.1114
2447091.70859	0.7369	-9.1944	-8.2143	-8.1260
2447091.71002	0.7393	-9.1982	-8.2024	-8.1267
2447091.71080	0.7407	-9.1827	-8.2026	-8.1323
2447091.71160	0.7420	-9.1877	-8.2026	-8.1294
2447091.71238	0.7433	-9.1851	-8.2039	-8.1328
2447091.71318	0.7447	-9.1896	-8.2005	-8.1286
2447091.71401	0.7461	-9.1839	-8.1960	-8.1307
2447091.72272	0.7608	-9.1836	-8.1583	-8.0928
2447091.72354	0.7621	-9.1839	-8.1491	-8.0735
2447091.72433	0.7635	-9.1793	-8.1475	-8.0992
2447091.73391	0.7796	-9.1925	-8.1676	-8.1031
2447091.73469	0.7809	-9.1896	-8.1577	-8.1117
2447091.73549	0.7823	-9.1868	-8.1637	-8.1081
2447091.73631	0.7837	-9.1942	-8.1680	-8.1102
2447091.73711	0.7850	-9.1893	-8.1592	-8.1105
2447091.74644	0.8007	-9.1938	-8.1724	-8.1113
2447091.74723	0.8021	-9.1907	-8.1699	-8.1189
2447091.74802	0.8034	-9.1878	-8.1709	-8.1193
2447091.74880	0.8047	-9.1938	-8.1744	-8.1103
2447091.74960	0.8061	-9.1999	-8.1742	-8.1178
2447091.75039	0.8074	-9.1812	-8.1696	-8.1324
2447091.75119	0.8088	-9.1816	-8.1798	-8.1251
2447091.75196	0.8101	-9.1724	-8.1785	-8.1246

continued.....

Table 6.33 /continued

1988 Feb 11/12

H.J.D.	Phase	V	R	I
2447203.32507	0.9381	-9.1802	-5.9202	-7.8243
2447203.32578	0.9393	-9.2040	-6.1577	-7.9275
2447203.32649	0.9405	-9.1890	-6.1523	-7.9062
2447203.32720	0.9417	-9.1955	-6.1620	-7.9184
2447203.32792	0.9429	-9.1861	-6.1360	-7.9188
2447203.32864	0.9441	-9.1802	-6.1541	-7.9101
2447203.32935	0.9454	-9.1765	-6.1458	-7.9129
2447203.33006	0.9465	-9.1722	-6.1405	-7.8978
2447203.33836	0.9605	-9.1035	-6.0780	-7.8232
2447203.33907	0.9617	-9.0938	-6.0838	-7.8107
2447203.33978	0.9629	-9.0840	-6.0699	-7.7936
2447203.34050	0.9641	-9.0708	-6.0603	-7.7916
2447203.34120	0.9653	-9.0677	-6.0367	-7.7954
2447203.34192	0.9665	-9.0499	-6.0441	-7.7899
2447203.34264	0.9678	-9.0324	-6.0449	-7.7652
2447203.34336	0.9690	-9.0385	-6.0325	-7.7827
2447203.35233	0.9841	-8.8706	-5.4571	-7.4734
2447203.35303	0.9853	-8.8599	-5.4375	-7.4798
2447203.35375	0.9865	-8.8434	-5.4528	-7.4690
2447203.35447	0.9877	-8.8300	-5.3995	-7.4598
2447203.35519	0.9889	-8.8163	-5.4549	-7.4438
2447203.35589	0.9901	-8.8082	-5.4234	-7.4272
2447203.35661	0.9913	-8.7878	-5.4270	-7.4370
2447203.35731	0.9925	-8.7804	-5.4212	-7.4181
2447203.36567	0.0066	-8.6359	-5.2804	-7.2607
2447203.36639	0.0078	-8.6106	-5.2400	-7.2587
2447203.36709	0.0090	-8.5950	-5.2304	-7.2401
2447203.36781	0.0102	-8.5869	-5.2479	-7.2557
2447203.36852	0.0114	-8.5973	-5.2654	-7.2480
2447203.36924	0.0126	-8.5810	-5.1911	-7.2513
2447203.36995	0.0138	-8.5713	-5.2683	-7.2468
2447203.37067	0.0150	-8.5930	-5.2606	-7.2476
2447203.38134	0.0330	-8.5424	-5.1578	-7.1763
2447203.38205	0.0342	-8.5600	-5.2075	-7.2125
2447203.38277	0.0354	-8.5711	-5.2452	-7.2458
2447203.38347	0.0366	-8.5938	-5.2959	-7.2670
2447203.38419	0.0378	-8.5919	-5.2521	-7.2747
2447203.38491	0.0390	-8.5872	-5.2738	-7.2626
2447203.38561	0.0402	-8.5922	-5.3024	-7.2739
2447203.38633	0.0414	-8.5934	-5.3003	-7.2840
2447203.39580	0.0574	-8.6869	-5.3854	-7.2897
2447203.39651	0.0586	-8.7110	-5.3559	-7.3299
2447203.39722	0.0598	-8.7237	-5.3860	-7.3366
2447203.39794	0.0610	-8.7534	-5.3894	-7.3430
2447203.39864	0.0622	-8.7488	-5.4119	-7.3423
2447203.39937	0.0634	-8.7116	-5.3677	-7.3198
2447203.40008	0.0646	-8.5957	-5.2580	-7.2199
2447203.40080	0.0658	-8.6292	-5.2753	-7.2228
2447203.40890	0.0795	-8.9255	-5.5975	-7.5045
2447203.40960	0.0807	-8.9421	-5.5635	-7.5267
2447203.41032	0.0819	-8.9477	-5.5894	-7.5243
2447203.41103	0.0831	-8.9641	-5.6090	-7.5318
2447203.41175	0.0843	-8.9723	-5.5841	-7.5538

continued.....

Table 6.33 /continued

2447203.41245	0.0855	-8.9806	-5.6405	-7.5547
2447203.41317	0.0867	-8.9881	-5.6097	-7.5591
2447203.41389	0.0879	-8.9918	-5.6090	-7.5645
2447203.42227	0.1020	-9.0871	-5.7243	-7.6301
2447203.42297	0.1032	-9.0826	-5.6657	-7.6117
2447203.42369	0.1044	-9.0947	-5.7017	-7.6190
2447203.42441	0.1056	-9.1030	-5.6967	-7.6223
2447203.42511	0.1068	-9.0913	-5.5633	-7.5647
2447203.42583	0.1080	-9.0861	-5.5482	-7.5640
2447203.42654	0.1092	-9.1137	-5.6812	-7.6208
2447203.42725	0.1104	-9.1055	-5.6644	-7.6277
2447203.43517	0.1238	-9.1451	-5.5815	-7.5960
2447203.43588	0.1250	-9.1346	-5.4843	-7.5498
2447203.43659	0.1262	-9.1503	-5.6552	-7.6363
2447203.43730	0.1274	-9.1459	-5.6462	-7.6282
2447203.43802	0.1286	-9.1416	-5.6832	-7.6251
2447203.43872	0.1298	-9.1379	-5.6010	-7.6186
2447203.43944	0.1310	-9.1380	-5.5652	-7.6134
2447203.44015	0.1322	-9.1356	-5.5259	-7.5768
2447203.45093	0.1504	-9.1400	-5.7920	-7.6543
2447203.45165	0.1516	-9.1408	-5.6017	-7.5972
2447203.45236	0.1528	-9.1298	-5.6034	-7.5867
2447203.45308	0.1540	-9.1274	-5.7253	-7.6294
2447203.45379	0.1552	-9.1338	-5.8044	-7.6614
2447203.45450	0.1564	-9.1334	-5.8140	-7.6701
2447203.45522	0.1576	-9.1258	-5.7728	-7.6776
2447203.45593	0.1588	-9.1416	-5.7608	-7.6654
2447203.46431	0.1729	-9.1015	-5.6525	-7.5729
2447203.46502	0.1741	-9.0990	-5.6548	-7.5742
2447203.46574	0.1753	-9.0960	-5.6518	-7.5712
2447203.46645	0.1765	-9.0829	-5.6735	-7.5513
2447203.46716	0.1777	-9.0803	-5.6306	-7.5496
2447203.46788	0.1789	-9.0661	-5.6325	-7.5437
2447203.46858	0.1801	-9.0688	-5.6020	-7.5314
2447203.46930	0.1813	-9.0681	-5.5946	-7.5305
2447203.48600	0.2095	-9.0460	-5.5566	-7.4866
2447203.48671	0.2107	-9.0379	-5.5532	-7.4997
2447203.48814	0.2131	-9.0495	-5.5241	-7.5091
2447203.48886	0.2143	-9.0393	-5.5322	-7.5017
2447203.48957	0.2155	-9.0507	-5.5701	-7.4905
2447203.49028	0.2167	-9.0452	-5.5858	-7.5009
2447203.49099	0.2179	-9.0522	-5.5299	-7.4935

6.2.4 Results Of Observations

In Figure 6.51 the whole of the data obtained on SV Cam is shown for differential V magnitudes. Figures 6.52 and 6.53 show the primary and secondary minimum in detail. Figures 6.54 to 6.58 show the Strömgren colours and instrumental (V-R) and (V-I) colours for the primary minimum, with the corresponding colours for the secondary in Figures 6.59 to 6.63. That the light curve is incomplete reflects the exceptionally poor observing conditions over the past 6 months.

Even so, it is surprising that no variations in colour are observed during the primary eclipse in the (V-I) and (V-R) colours. There is a possible variation occurring just after the primary minimum, but, given the fluctuations observed in the comparison star, which is known to be of constant magnitude, it would be unwise to attempt to read too much into these apparent out-of-eclipse variations.

The depth of the primary minimum is found to be deeper than that observed by Hilditch et al in 1979, by about $0^m.15$. Cellino et al (1985) attribute this variation in depth to the varying number of cool spots covering the photosphere of the active component. If we accept the 10 yearly cycle in sunspot activity proposed by Busso (1984) and that the last maximum was in the interval 1975.5-1978.5 (Busso et al, 1985) then we would expect the primary minimum to be deeper than that observed by Hilditch, which it is. By comparison observations taken by Nelson in 1951 and 1963 (Nelson 1951; 1963a) have a minimum some $0^m.2$ deeper than that of the minimum presented here. Since Nelson's data would have been taken during a minimum of the spot cycle, this would seem to verify Cellino's assumption that irregular changes and variations occur caused by phenomena other than the spot activity, (Cellino et al 1984).

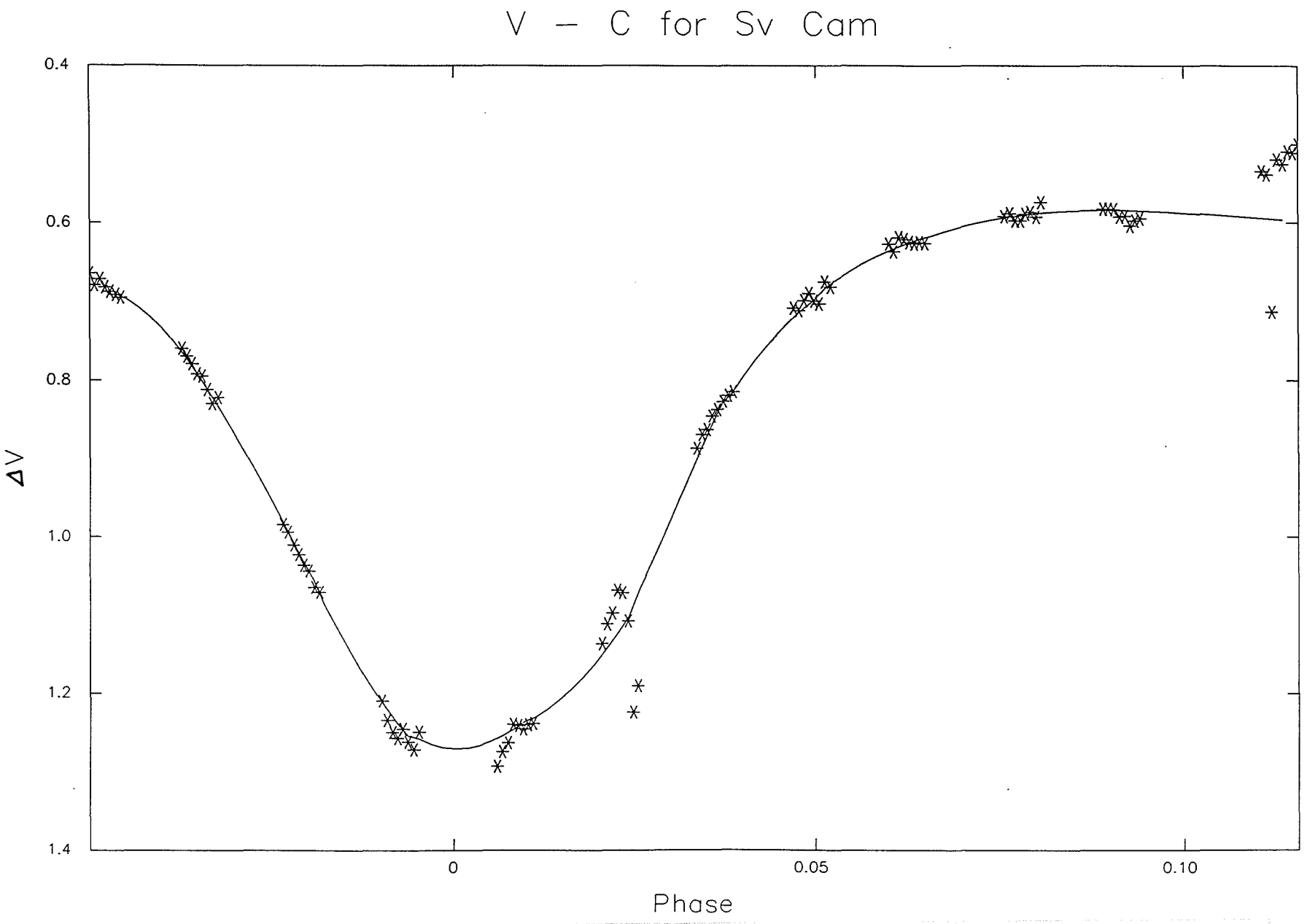

Figure 6.50 Primary minimum for SV CAM.

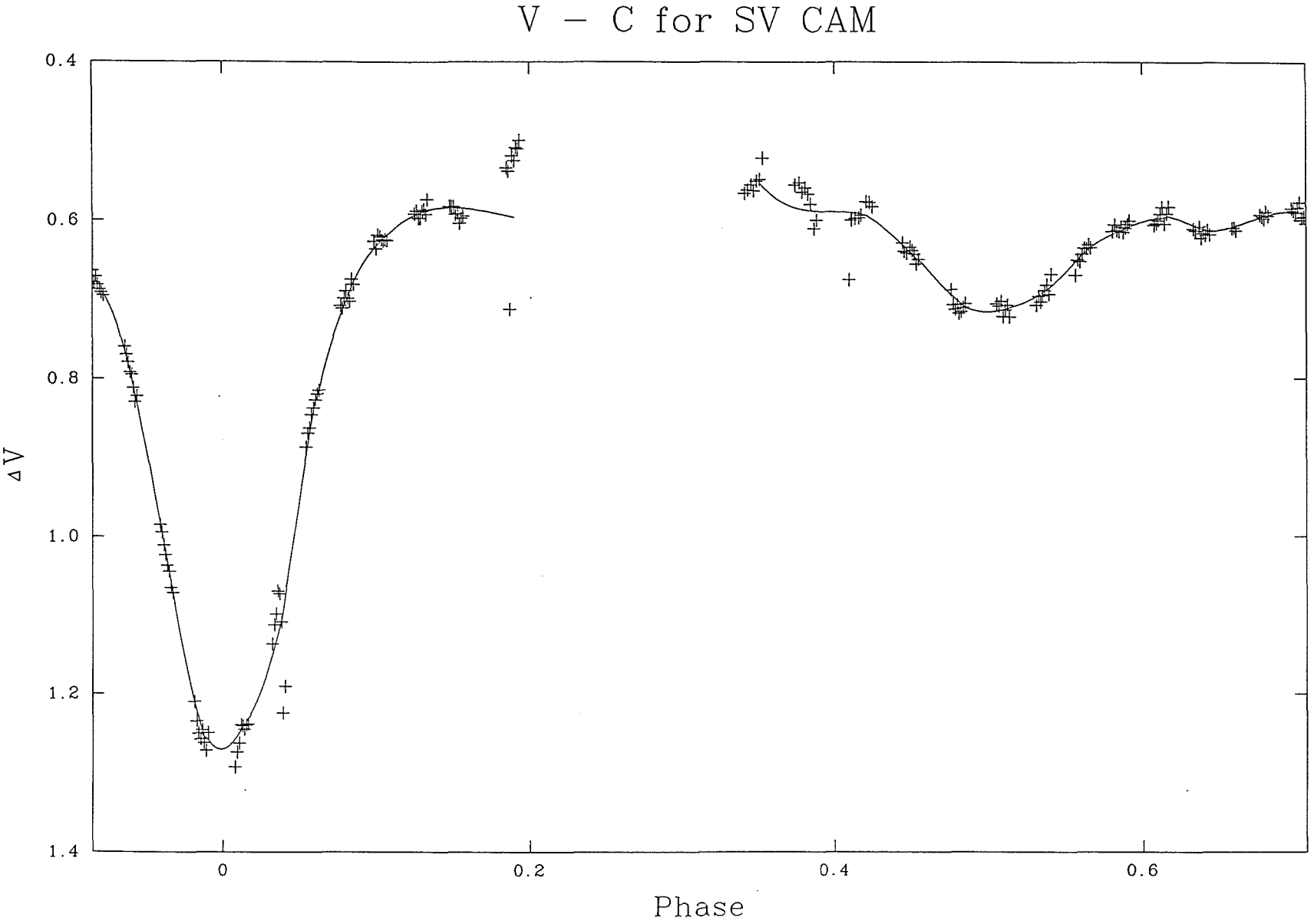

Figure 6.51 Primary and Secondary eclipse for SV Cam.

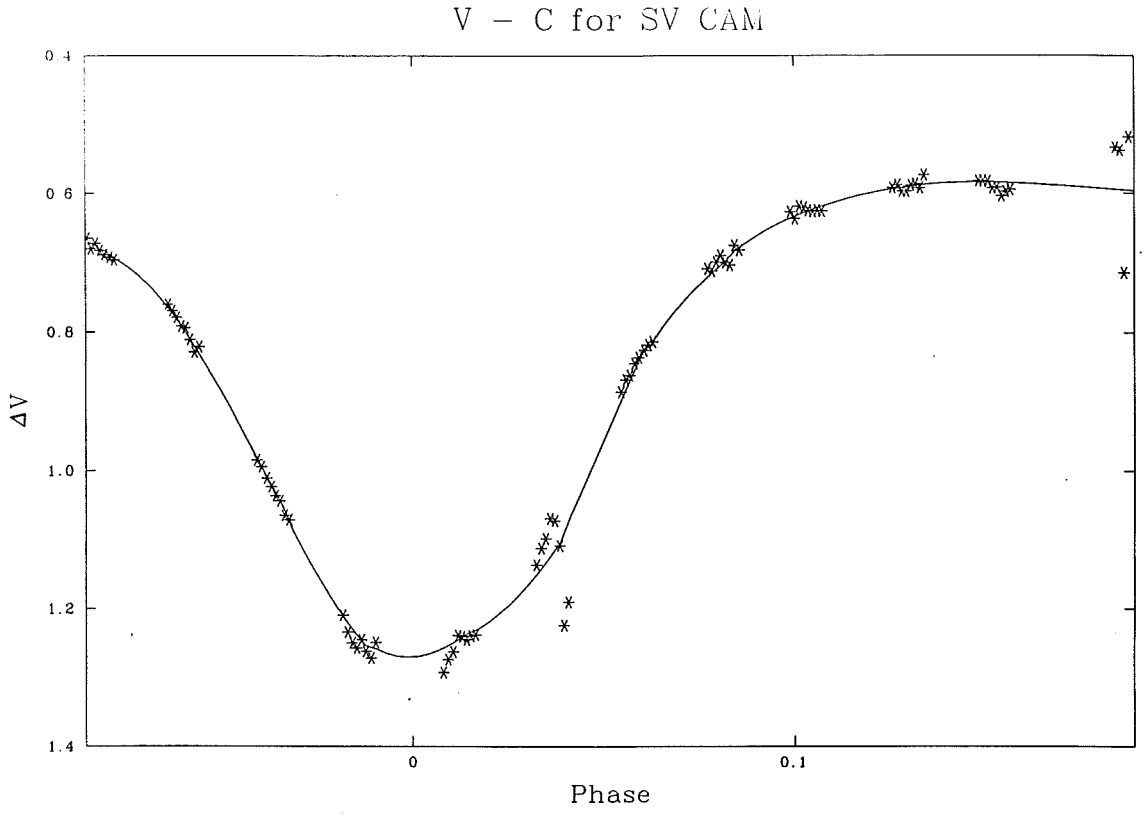

Figure 6.52 Primary eclipse for SV Cam.

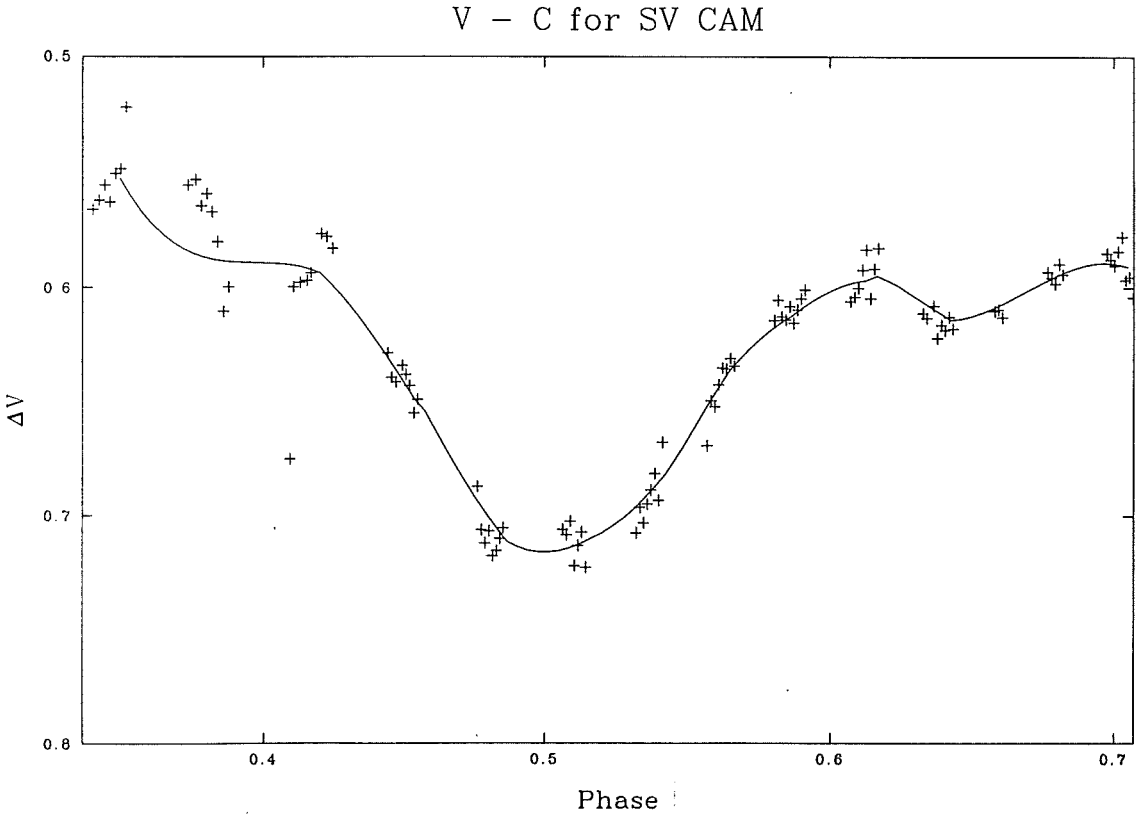

Figure 6.53 Secondary eclipse for SV Cam.

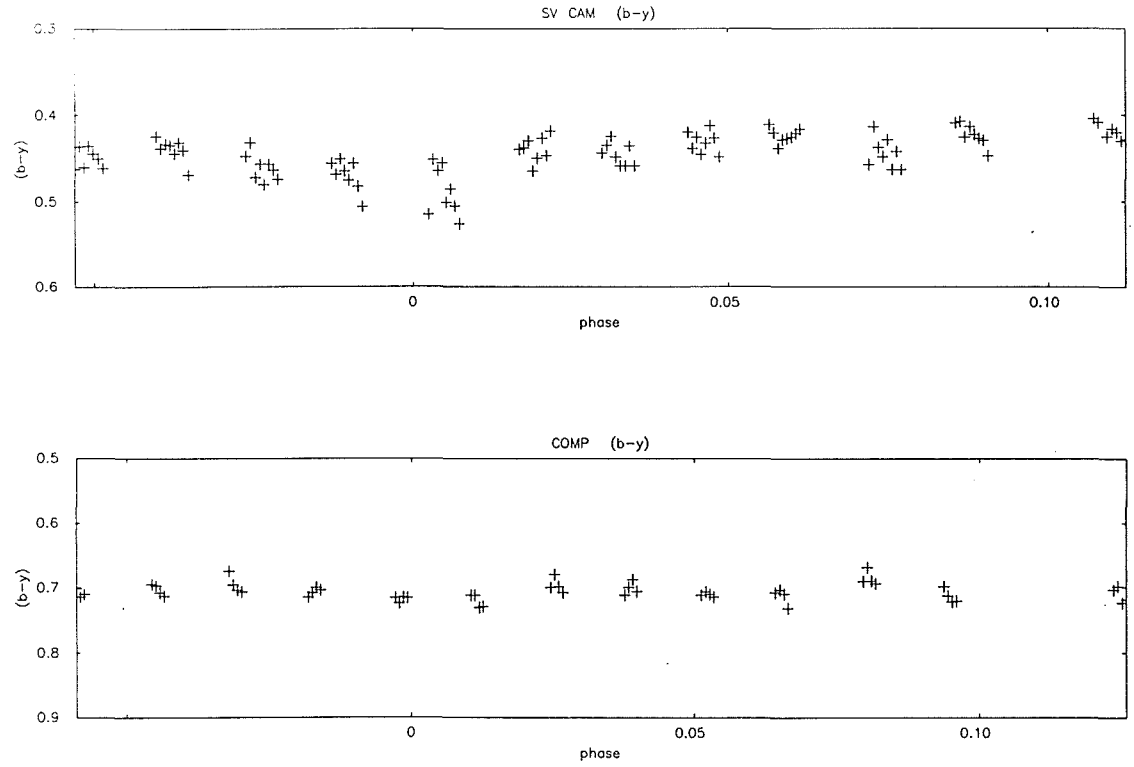

Figure 6.54 (b-y) for SV Cam and Comp at Primary.

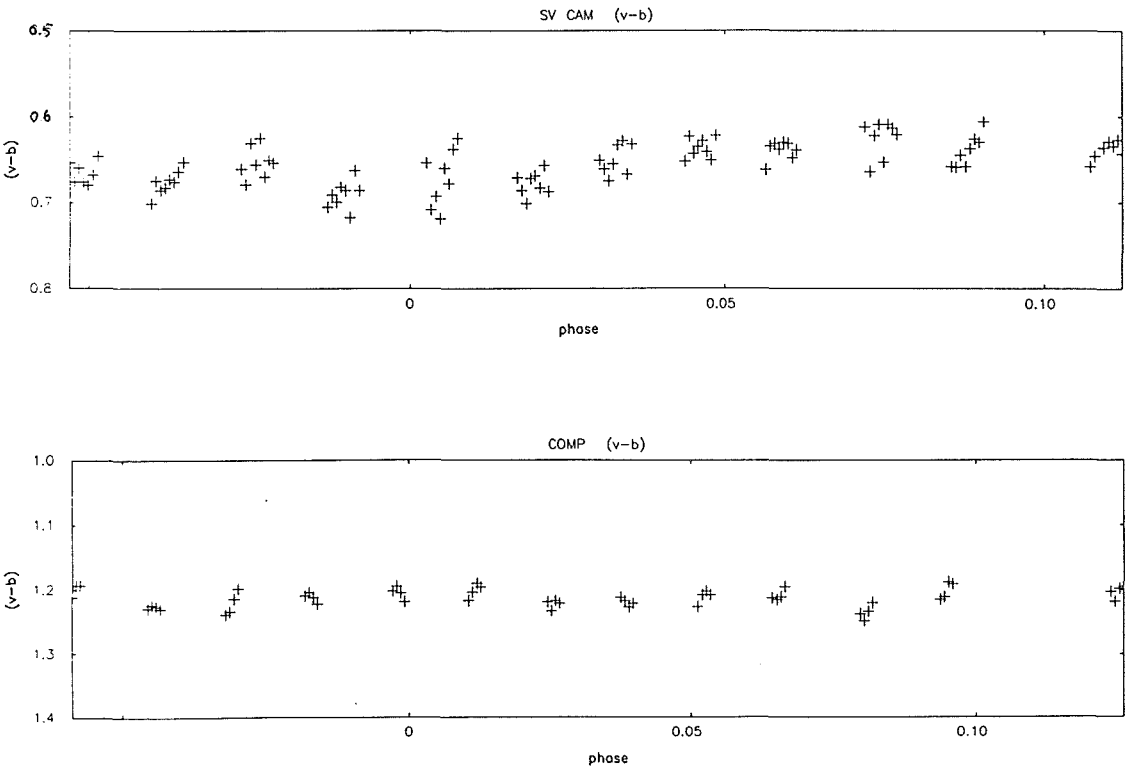

Figure 6.55 (v-b) for SV Cam and Comp at Primary.

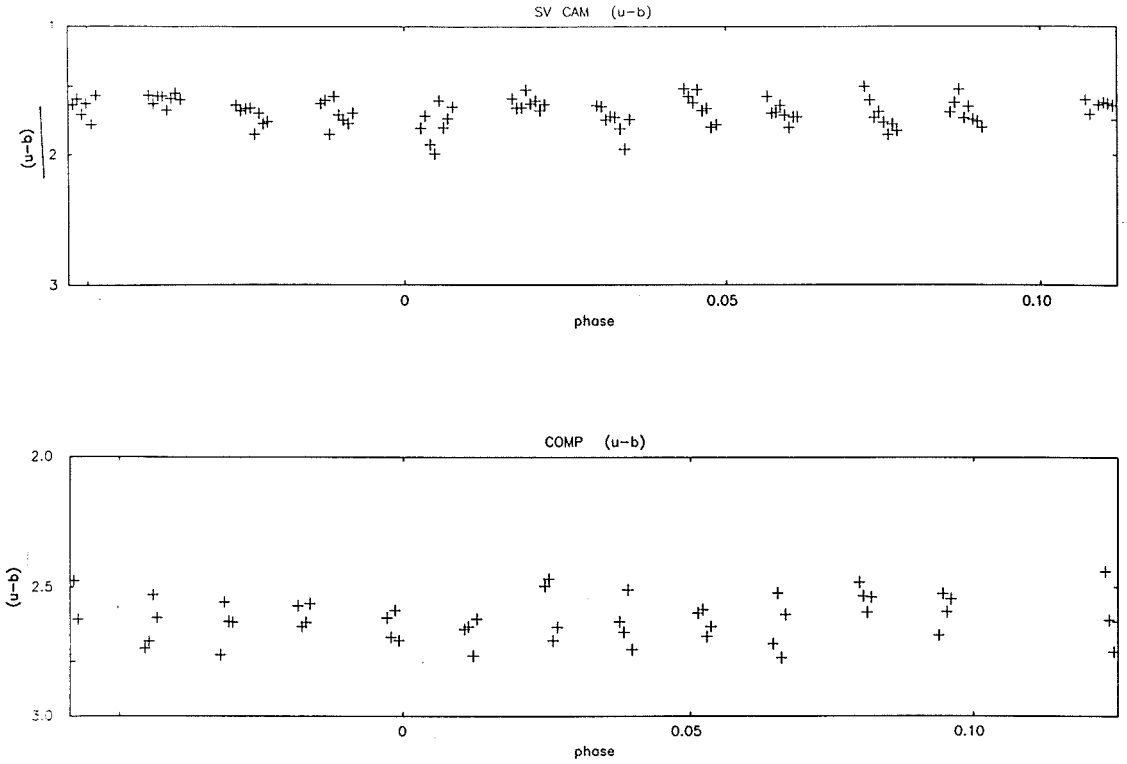

Figure 6.56 (u-b) for SV Cam and Comp at Primary.

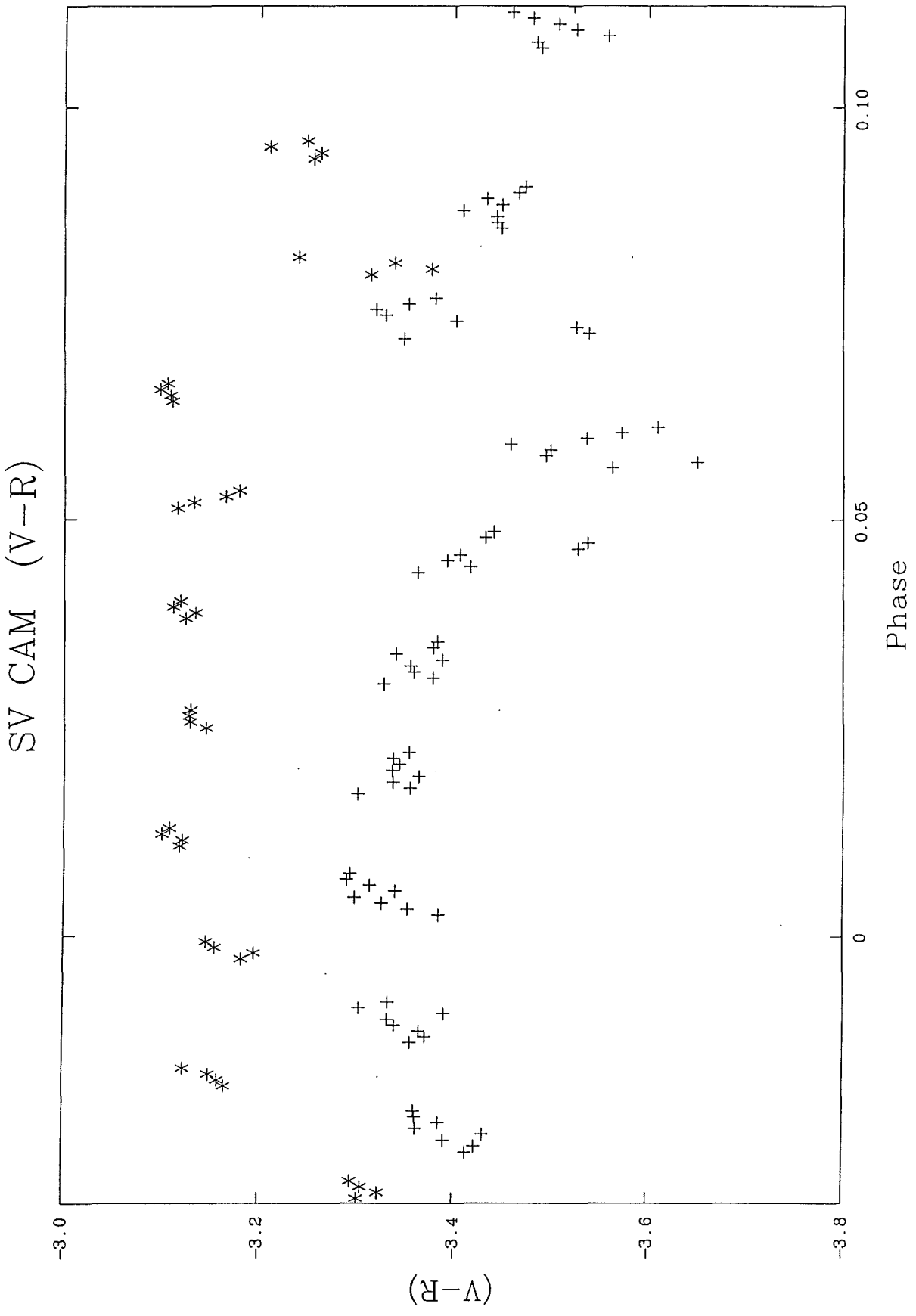

Figure 6.57 (V-R) for SV Cam and Comp at Primary.
+ SV Cam * Comp

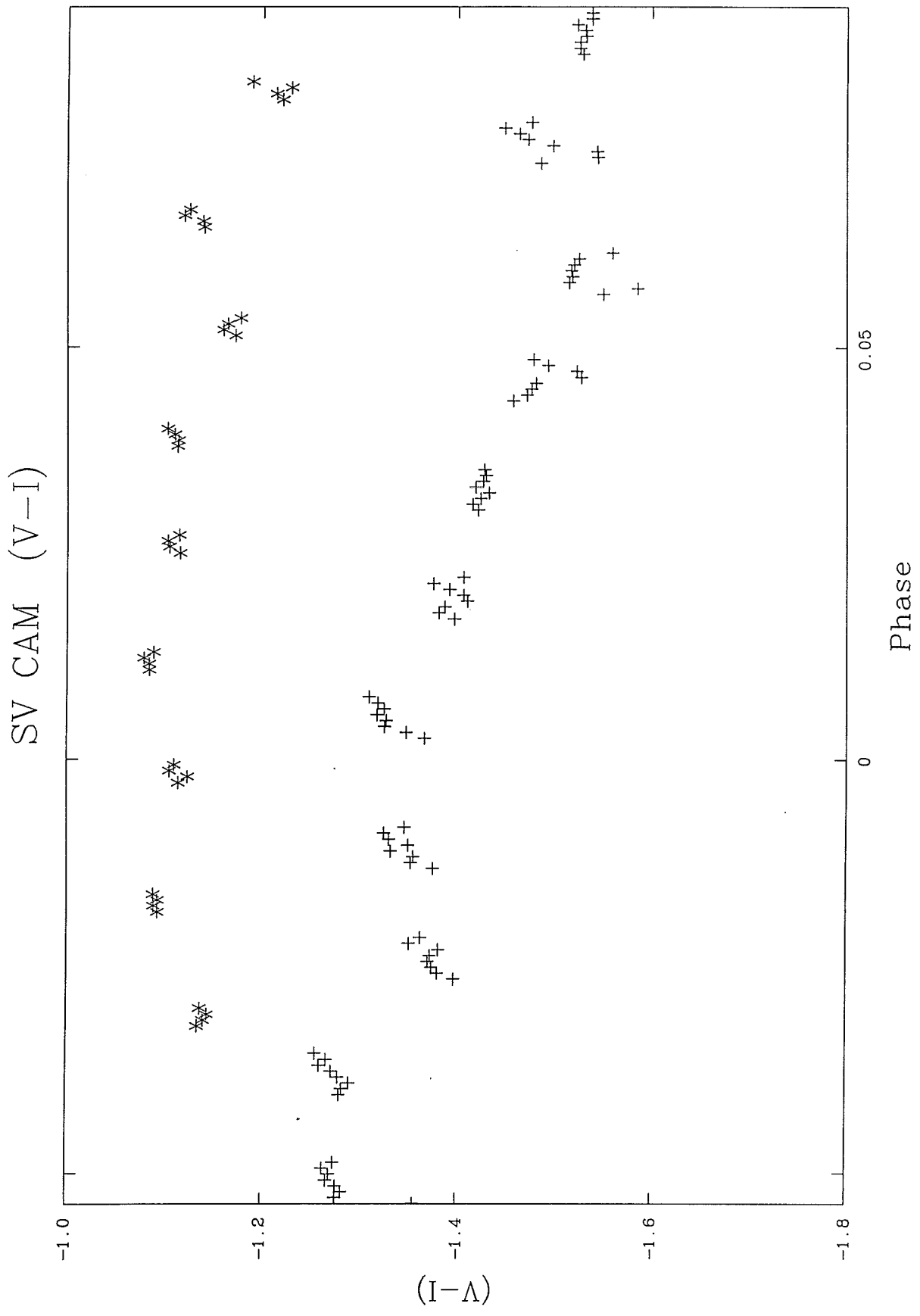

Figure 6.58 (V-I) for SV Cam and Comp at Primary.
+ SV Cam * Comp

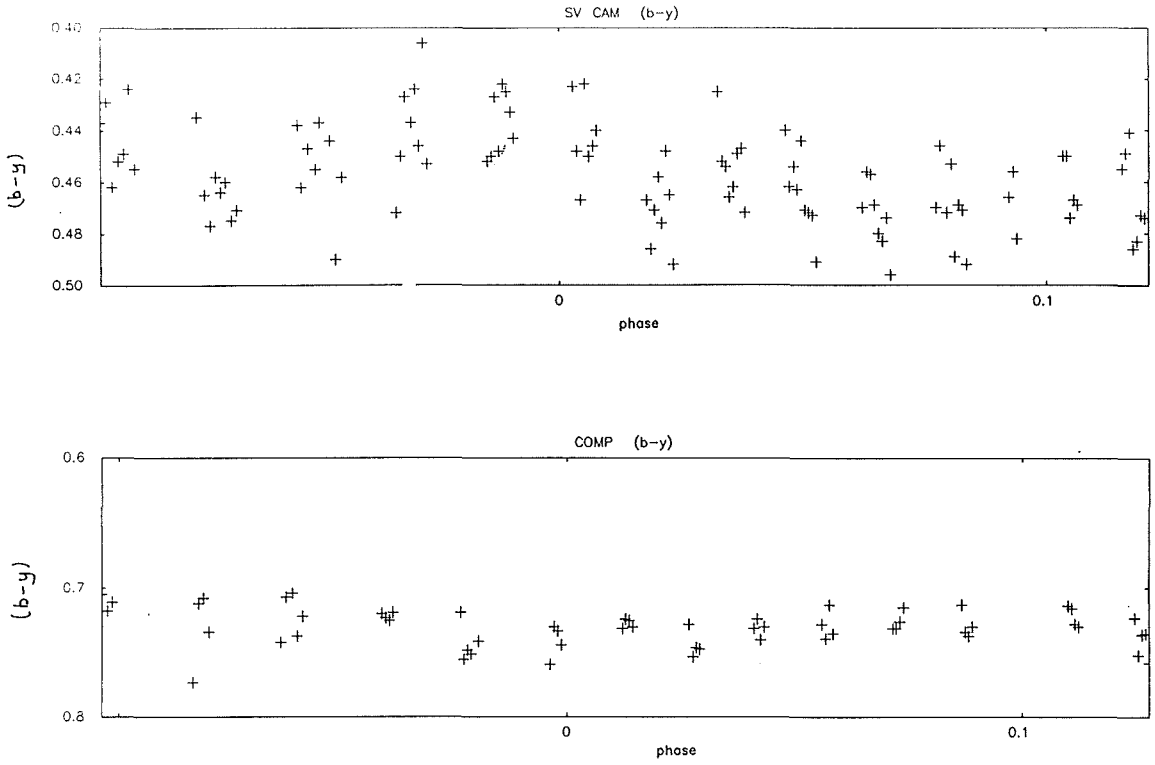

Figure 6.59 (b-y) for SV Cam and Comp at Secondary.

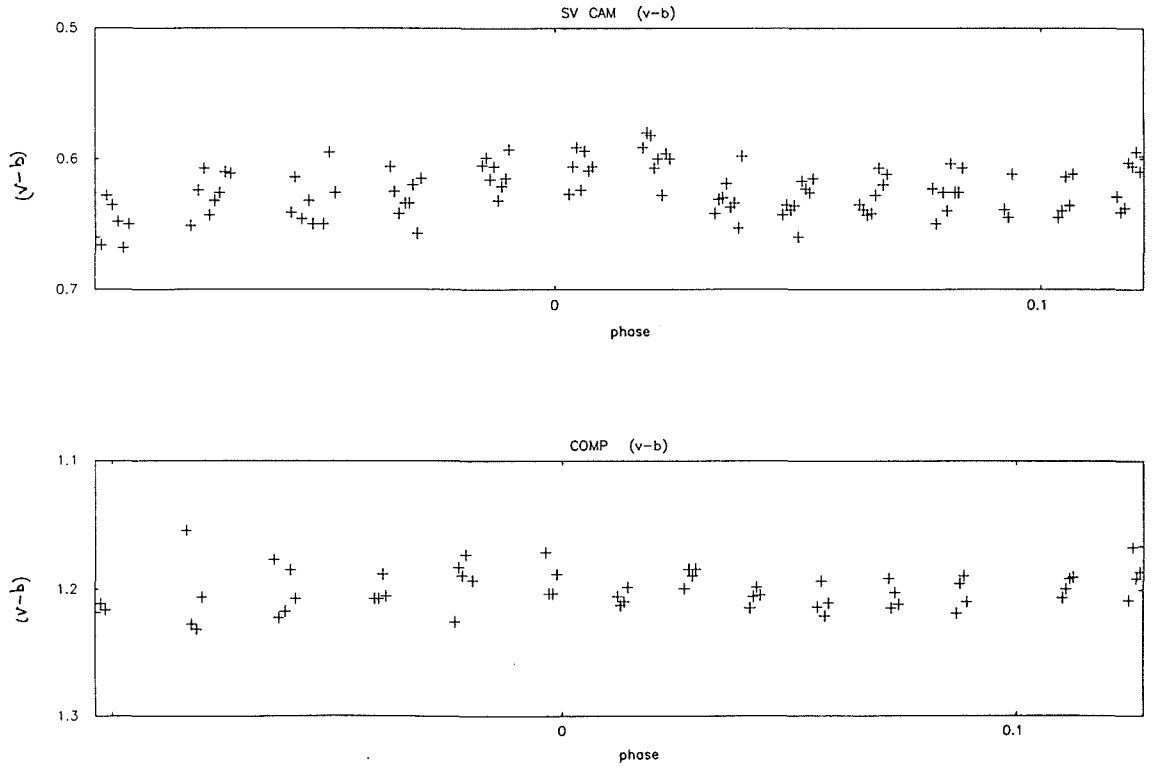

Figure 6.60 (v-b) for SV Cam and Comp at Secondary.

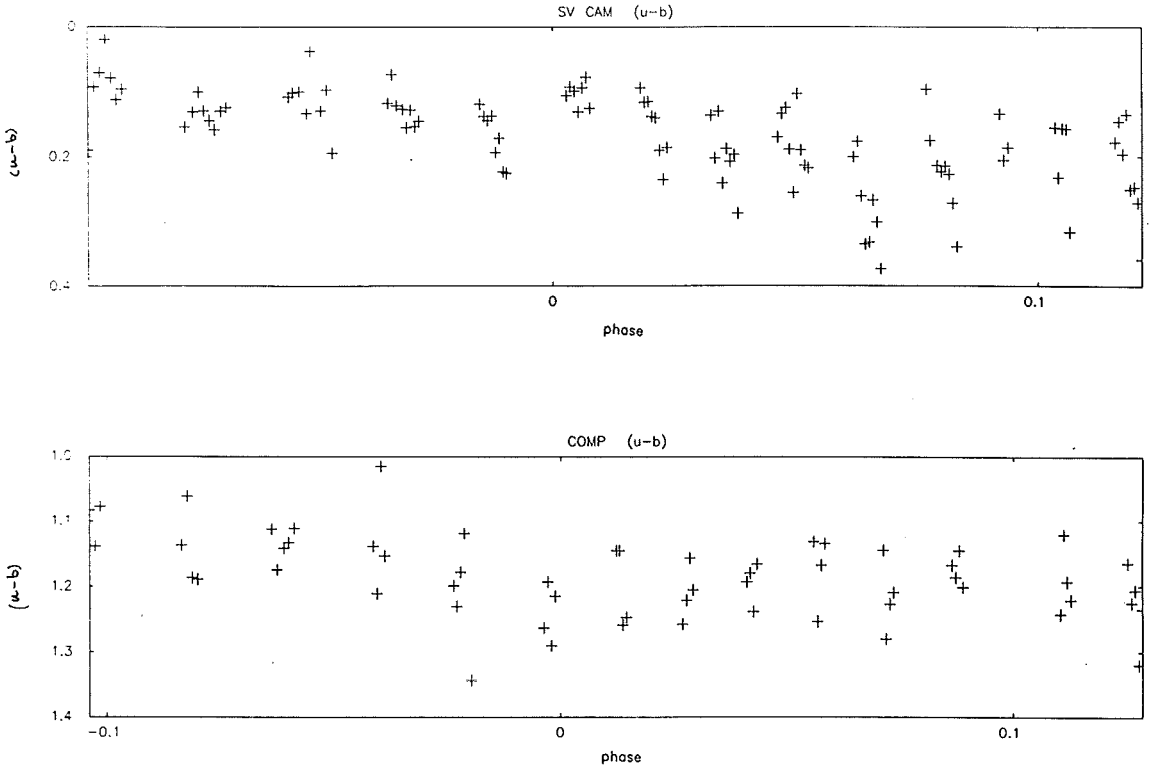

Figure 6.61 (u-b) for SV Cam and Comp at Secondary.

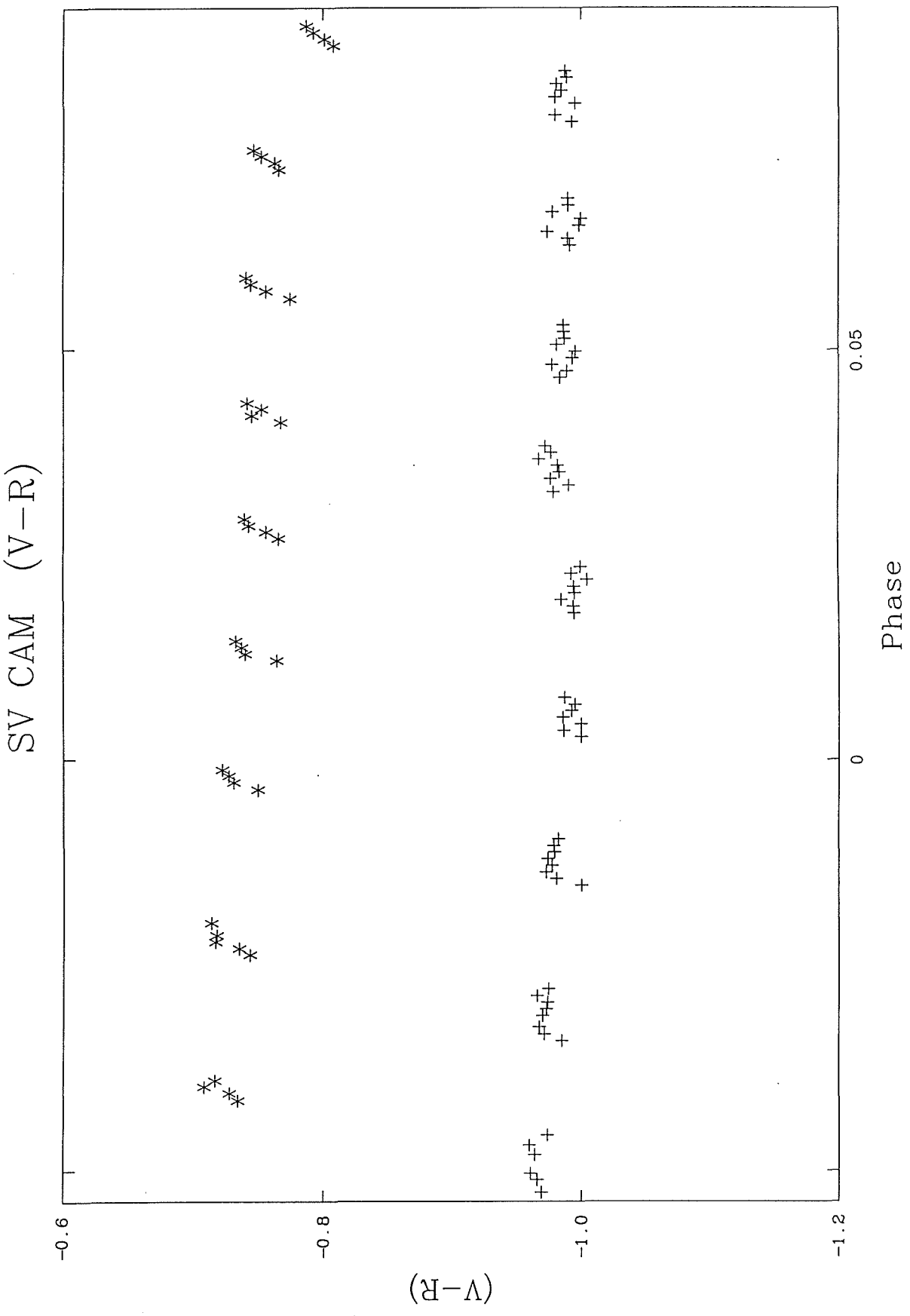

Figure 6.62 (V-R) for SV Cam and Comp at Secondary.
+ SV Cam * Comp

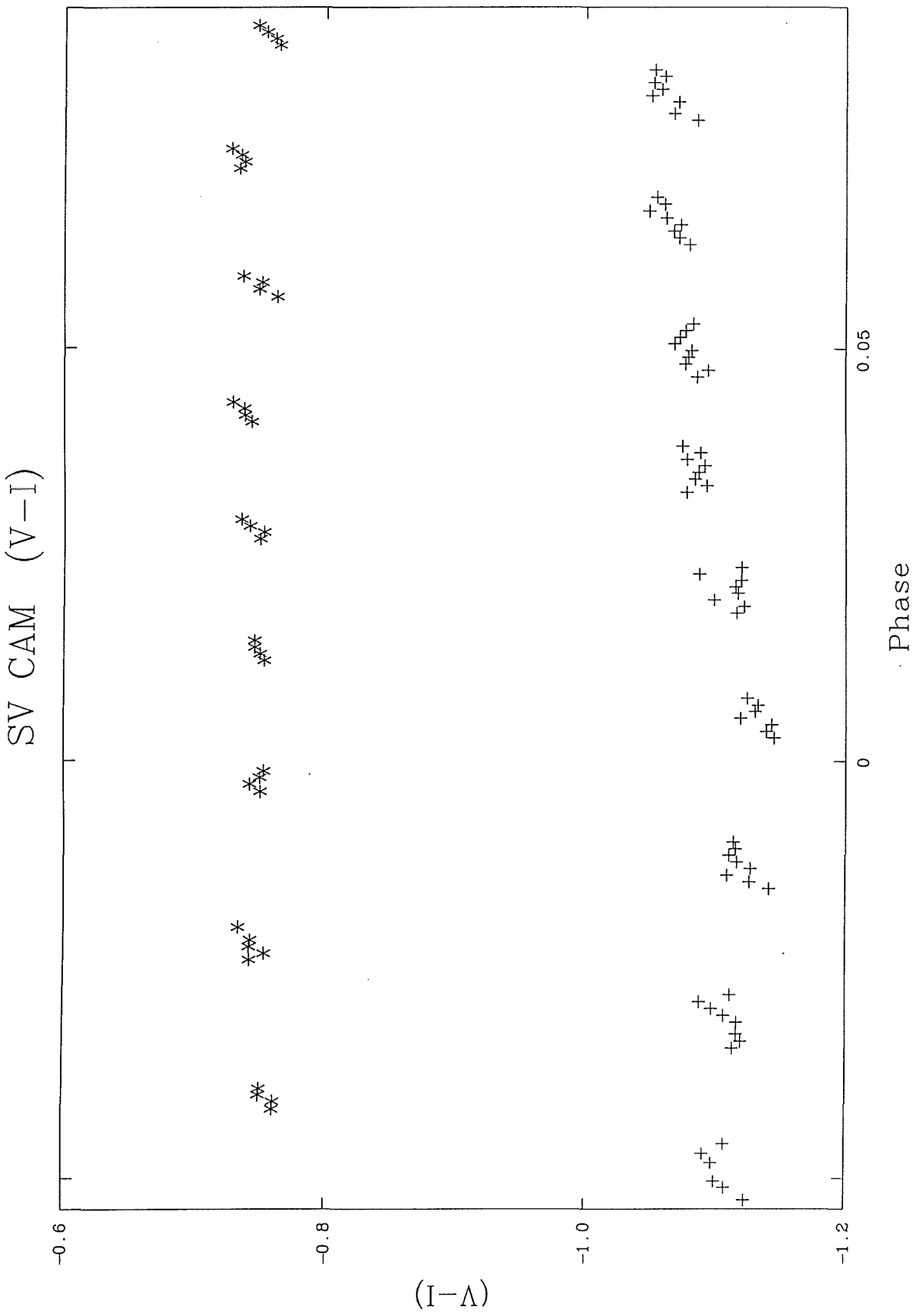

Figure 6.63 (V-I) for SV Cam and Comp at Secondary.
+ SV Cam * Comp

Since the V, R and I observations have not been transformed to a standard system comparisons with other data cannot be made. However we can compare the observed Strömgren indices with those measured by Hilditch and Hill in 1975, (Hilditch and Hill, 1975). They report mean values of 4 uvby observations outside eclipses as,

(b-y)	m1	c1
0.428 mag	0.230 mag	0.324 mag

From the observations presented here we have,

(b-y)	m1	c1
0.431 mag	0.247 mag	0.388 mag

which are consistent with those found before.

CHAPTER 7

SUMMARY

In the previous chapters the development and commissioning of an 8-channel photometer has been described. In certain areas, such as the mechanical and optical design, hindsight and technological advances in, for example, the development of more sensitive detectors, would lead to a radically different end product if the photometer were to be re-designed. In other areas, where constraints have not been imposed by previous design work, recent improvements in the areas of microprocessor and information technology have been exploited, improving the performance of the photometer. No doubt, given the rapid advances being made in these areas the instrument could already benefit from new microprocessing and peripheral hardware which is now available. But it is unwise to place too much emphasis on this aspect of the work, as the primary interest is the ability to perform astronomical photometry.

The goal was to develop a high precision photometer capable of simultaneous measurements in up to 8-passbands. That this has been achieved is demonstrated by the results shown in the last chapter. However there are still certain areas where changes could be made which would improve the performance and quality of the data acquired.

SUMMARY

The principle component of the photometer is a low dispersion grating spectrograph. This is a more efficient way of "splitting" the incoming radiation than using, for example a dichroic beamsplitter. But there are problems with this approach - one of the main objections being the instability of the spectrum produced by the grating. Even if there is no flexure present in the instrument, (which in this case the flexure has been shown to be minimal and insignificant), the movement of the stellar image in the aperture, caused by atmospheric effects, will produce a corresponding movement in the stellar spectrum. If the photometric passbands are to be defined without the use of filters then this movement must be kept to a minimum, particularly if using intermediate or narrow passbands. In using a mirror mosaic to define broad spectral regions and then using filters, whose wavelength coverage lies within these passbands, it should be possible to effectively remove the effects of the shifts in the spectrum.

However, in Ch.5 it was shown that the long wavelength cut-off of the filter used in channel 4 coincided with the mirror mosaic wavelength cut-off, thereby making this channel susceptible to movement of the spectrum. Enhancing this problem was the additional movement of the stellar image in the aperture caused by the inaccuracy of the telescope drive. Whilst a solution to the problem was found, this can only be accepted as a temporary measure. The need for a new mirror mosaic to be manufactured is apparent, with greater care being given to the relation of the mirror and filter passbands. The use of a grating with a higher dispersion would be desirable in reducing the effects of spectrum shift, but must be considered in conjunction with the physical constraints of placing the mosaic within the photometer head.

The other major optical problem is the coupling element used between the telescope and the photometer. The use of a simple camera lens results in the severe reduction of radiation in the ultra-violet region which affects the u passband in particular. Also, the image of the entrance aperture formed by the camera is not at infinity and therefore the performance of the Fabry lenses will suffer. If the photometer is to be used at a site where the ultra-violet transmission is good, then the expense of using a mirror based focal converter would be necessary and justified. Alternatively, the collimator could be matched to the telescope's focal ratio.

With the use of a motor-speed controller the ability to time the up/down integration periods has been seen to be adequate, with the resultant observing dead-time at an acceptable level. However, since the aperchopper is a mechanical device and therefore susceptible to wear it would be expedient to check its accuracy periodically.

In its current state of development the software is adequate for the photometer to be used as a general user instrument. Better use could be made though of the processing power which is available during an integration period to provide a graphical display of the data. Also, telescope time could be used more efficiently if on-line analysis allowed for integrations to be terminated once a pre-set signal-to-noise ratio has been achieved. Since the software has been written in a modular form enhancements can be easily made without affecting any current operations. The use of two separate processing systems has proved to be very successful in this respect and, to this date, no software errors have been encountered.

SUMMARY

The significant advantages of a multi-channel device have been demonstrated in the derivation of the transformation equations. With the observations being acquired in often marginally photometric conditions, we can clearly see that the accuracy attained in measuring a single magnitude is less than that achieved when forming a colour from 2 magnitudes which have been measured simultaneously. There is also the benefit of effectively making more observations in a given time interval.

To a very large extent the performance of the photometer has been hampered by the conditions at the observing site. When installed at a site with good photometric conditions the photometer will undoubtedly be a powerful tool offering significant advantages over classical single-channel photometers. It will be particularly suitable for observing astronomical sources which undergo changes in colour in time-scales of seconds to minutes, prime candidates being cataclysmic variables, flare stars and systems with localised dark and bright regions. The simultaneous nature of the measurements would also greatly reduce the time needed in setting up new photometric sequences. The easy interchangeability of the mirror mosaics gives the potential of using the most suitable photometric system for the observations being made. Furthermore the possibility exists to include a polarization option allowing simultaneous measurements of the four Stokes parameters in each spectral region.

APPENDIX A

CONTROL SOFTWARE

```
 10PROCINITIALISE:PROCMAIN_MENU:STOP
 20DEF PROCMAIN_MENU*FX3,0
 30CLS
 40VDU28,0,24,39,0
 50PROCMSG("M A I N  M E N U",4,12,2):PROCMSG("f0",5,3,5):
   PROCMSG("f1",5,11,5):PROCMSG("f2",5,19,5):PROCMSG("f3",5,27,5):
   PROCMSG("f4",5,35,5):PROCMSG("f5",5,3,11):PROCMSG("f6",5,11,11):
   PROCMSG("f7",5,19,11):PROCMSG("f8",5,27,11)
 60PROCMSG("f9",5,35,11):PROCMSG("Com.So",5,1,7):PROCMSG("AcqMir",5,9,7):
   PROCMSG("Fil.Sh",5,25,7):PROCMSG("Pm.Fil",5,33,7):PROCMSG("Gr.Rot",5,1,13):
   PROCMSG("Status",5,33,13):*FX3,7
 70*FX18
 80*KEY0 PROCCOMP_SOURCE|M
 90*KEY1 PROCACQ_MIR|M
110*KEY3 PROCFIL_SHUT|M
120*KEY4 PROCPM_FILTERS|M
130*KEY5 PROCGRAT_ROT|M
140*KEY9 PROCMAIN_STAT|M
150ENDPROC

160DEF PROCCOMP_SOURCE:*FX3,0
170PROCCLEAR_LEGEND:PROCMSG("Comparison  Source",5,11,2):
   PROCMSG("Main",5,2,7):PROCMSG("SA",5,11,7):PROCMSG("SB",5,19,7):
   PROCMSG("SC",5,27,7):PROCMSG("In Beam",5,32,7):PROCMSG("Out Beam",5,1,13):
   PROCMSG("Recover",5,17,13)
180PROCMSG("Status",5,33,13):*FX3,7
190*FX18
200*KEY0 PROCMAIN_MENU|M
210*KEY1 SOURCE$="A":PROCCOMP_SELECT|M
220*KEY2 SOURCE$="B":PROCCOMP_SELECT|M
230*KEY3 SOURCE$="C":PROCCOMP_SELECT|M
240*KEY4 SOURCE$="I":PROCCOMP_SELECT|M
250*KEY5 SOURCE$="O":PROCCOMP_SELECT|M
260*KEY7 PROCSOURCE_ERROR|M
270*KEY9 PROCCOMP_STAT|M
280ENDPROC

290DEF PROCCLEAR_LEGEND:PROCBLANK(1,2,39):PROCBLANK(1,7,39):
   PROCBLANK(1,13,39):ENDPROC

300DEF PROCCOMP_SELECT:IF SOURCE$="I" OR SOURCE$="O" THEN PROCRACK_MOVE
310PROCRACK_POS
320IF RPOS$="B" THEN PROCRACK_RECOVER
330IF RPOS$="I" THEN PROCNO_MOVE:ENDPROC
```

```
340IF SOURCE$="A" THEN TURNON42:TURNOFF43,44:DUMMY$="A":PROCSO_SEL
350IF SOURCE$="B" THEN TURNON43:TURNOFF42,44:DUMMY$="B":PROCSO_SEL
360IF SOURCE$="C" THEN TURNON44:TURNOFF42,43:DUMMY$="C":PROCSO_SEL
370ENDPROC

380DEF PROCSO_SEL:*FX3,0
390PROCBLANK(9,18,21):PROCMSG("Source being selected",5,9,18):*FX3,7
400REPEAT MOTOR_ON=CH 57:UNTIL MOTOR_ON:*FX3,0
410PROCBLANK(9,18,21):PROCMSG("Source ",5,11,18):PROCMSG(SOURCE$,5,18,18):
   PROCMSG(" selected",5,20,18):*FX3,7
420ENDPROC

430DEF PROCRACK_MOVE:PROCRACK_POS:IF SOURCE$=RPOS$ THEN STOP:ENDPROC
440*FX3,0
450PROCBLANK(11,21,18):PROCMSG("Rack Moving",5,14,21):*FX3,7
460TURNON41:DELAY50:TURNOFF41:REPEAT PROCRACK_POS:
   UNTIL RPOS$="I" OR RPOS$="O":*FX3,0
470PROCBLANK(11,21,18):IF RPOS$="I" THEN PROCMSG("Source in beam",5,13,21)
   ELSE PROCMSG("Source out of beam",5,11,21)
480*FX3,7
490IF RPOS$="O" THEN STATUS$="N"+MID$(STATUS$,2,13) ELSE
   STATUS$=DUMMY$+MID$(STATUS$,2,13)
500STOP:ENDPROC

510DEF PROCRACK_POS:FRONT=CH 55:REAR=CH 56
520IF FRONT AND REAR THEN RPOS$="I"
530IF NOT FRONT AND NOT REAR THEN RPOS$="O"
540IF NOT FRONT AND REAR THEN RPOS$="B"
550ENDPROC

560DEF PROCCOMP_STAT:*FX3,0
570PROCBLANK(9,18,21):PROCBLANK(11,21,18):PROCRACK_POS:
   PROCMSG("Source ",5,11,18):PROCMSG(DUMMY$,5,18,18):
   PROCMSG(" selected",5,20,18)
580IF RPOS$="I" THEN PROCMSG("Source in beam",5,13,21) ELSE
   PROCMSG("Source out of beam",5,11,21)
590*FX3,7
600STOP:ENDPROC

610DEF PROCNO_MOVE:*FX3,0
620PROCMSG("Retract rack first",5,11,23):VDU7:DELAY200:PROCBLANK(11,23,18):
   *FX3,7
630ENDPROC

870DEF PROCGRAT_ROT:PROCCLEAR_LEGEND
880*FX12,20
890*FX18
900*FX3,0
910PROCCLEAR_LEGEND:PROCMSG("Grating Rotator",5,12,2):PROCMSG("Main",5,2,7):
   PROCMSG("+1",5,11,7):PROCMSG("+10",5,18,7):PROCMSG("+100",5,26,7):
   PROCMSG("-1",5,35,7)
920PROCMSG("-10",5,2,13):PROCMSG("-100",5,10,13):PROCMSG("Clear",5,18,13):
   PROCMSG("Ready",5,26,13):PROCMSG("Status",5,33,13):
   PROCMSG("Increment",5,10,18):PROCMSG("Position",5,23,18):*FX3,7
930*FX3,7
940*FX18
950*KEY0 PROCRESET|M
960*KEY1 PROCPLUS1|M
970*KEY2 PROCPLUS10|M
```

```
 980*KEY3 PROCPLUS100¦M
 990*KEY4 PROCMIN1¦M
1000*KEY5 PROCMIN10¦M
1010*KEY6 PROCMIN100¦M
1020*KEY7 PROCCLR_SHIFT¦M
1030*KEY8 PROCGR_RDY¦M
1040*KEY9 PROCGR_STATUS¦M
1050STOP
1060DEF PROCPLUS1:A%=A%+1:PROCDISPINC:ENDPROC
1070DEF PROCPLUS10:A%=A%+10:PROCDISPINC:ENDPROC
1080DEF PROCPLUS100:A%=A%+100:PROCDISPINC:ENDPROC
1090DEF PROCMIN1:A%=A%-1:PROCDISPINC:ENDPROC
1100DEF PROCMIN10:A%=A%-10:PROCDISPINC:ENDPROC
1110DEF PROCMIN100:A%=A%-100:PROCDISPINC:ENDPROC
1120DEF PROCDISPINC:*FX3,0
1130PROCBLANK(12,20,5):AA$=STR$(A%):PROCMSG(AA$,5,12,20):*FX3,7
1140ENDPROC

1150DEF PROCGR_POS
1160MC%=300:WRD=&73:LWRD=&71:X=&72:?WRD=0:?LWRD=0:?X=0:P%=MC%:
    [ OPT 0:.BUILD1:LDA X:LSR A:ROL WRD:RTS:.BUILD2:LDA X:LSR A:
    ROL LWRD:RTS :]
1170?WRD=0
1180FOR COUNT1=16 TO 18:?X=IN (COUNT1):CALL BUILD1:NEXT:FOR COUNT2=19 TO 26:
    ?X=IN (COUNT2):CALL BUILD2:NEXT:GRAT_POS=256*?WRD+?LWRD:ENDPROC
1190DEF PROCGR_RDY:PROCGR_POS:NEW_POS=GRAT_POS+A%:BIGEND=1990:LITTLEND=240
1200IF NEW_POS> BIGEND OR NEW_POS<LITTLEND PROCGRAT_ERR:ENDPROC
1210IF A%> 0 THEN TURNON34 ELSE TURNOFF 34
1220SDELAY=0:PROCGR_MOVE(A%,SDELAY):PROCGR_POS:SGRAT$=STR$(GRAT_POS)
1221REPEAT:L=LEN(SGRAT$):IFL<4 THEN SGRAT$=" "+SGRAT$:UNTIL L=4
1222STATUS$=LEFT$(STATUS$,10)+SGRAT$:ENDPROC

1230DEF PROCGR_MOVE(NO_STEPS,SDELAY)
1240TURNOFF 28:*FX3,0
1250PROCBLANK(24,20,6):PROCMSG("Moving",5,24,20):*FX3,7
1260FOR Y=1 TO ABS(NO_STEPS):TURNOFF 35:DELAY SDELAY:TURNON35:DELAY SDELAY:
    NEXT:ENDPOINT=IN 37
1270IF NOT ENDPOINT THEN PROC_RESET:ENDPROC
1280PROCPOS_ERR:PROCGR_POS:*FX3,0
1290PROCBLANK(24,20,6):GRAT$=STR$(GRAT_POS):PROCMSG(GRAT$,5,25,20):*FX3,7
1300TURNON28:ENDPROC

1310DEF PROCPOS_ERR
1320PROCGR_POS
1330IF GRAT_POS <=(NEW_POS+1) AND GRAT_POS>=(NEW_POS-1) THEN ENDPROC
1340CORRECTION=GRAT_POS-NEW_POS:IF GRAT_POS<NEW_POS THEN TURNON34 ELSE
    TURNOFF 34
1350SDELAY=10:PROCGR_MOVE(CORRECTION,SDELAY)
1360ENDPROC

1370DEF PROCRESET:*FX12,0
1380PROCMAIN_MENU:STOP:ENDPROC

1390DEF PROCGR_STATUS:PROCDISPINC:PROCGR_POS:*FX3,0
1400PROCBLANK(24,20,6):GRAT$=STR$(GRAT_POS):PROCMSG(GRAT$,5,25,20):*FX3,7
1410ENDPROC

1420DEF PROCCLR_SHIFT:A%=0:*FX3,0
1430PROCBLANK(12,20,5):*FX3,7
```

```
1440PROCDISPINC:ENDPROC

1450DEF PROC_RESET
1460PROCGR_POS
1470IF GRAT_POS<240 THEN TURNON34:B%=240-GRAT_POS
1480IF GRAT_POS>1940 THEN TURNOFF34:B%=GRAT_POS-1940
1490DELAY5:TURNON36:TURNOFF 28:FOR X=1 TO B%:TURNOFF35:TURNON35:NEXT
1500TURNON28:TURNOFF36
1510PROCGR_POS:*FX3,0
1520PROCBLANK(24,20,6):GRAT$=STR$(GRAT_POS):PROCMSG(GRAT$,5,25,20):*FX3,7
1530ENDPROC

1540DEF PROCGRAT_ERR:*FX3,0
1550PROCMSG("Attempt to drive past endpoints",5,4,22):VDU7:DELAY200:
    PROCMSG("       Re-enter increment      ",5,4,22):DELAY200:
    PROCBLANK(4,22,31):*FX3,7
1560PROCCLR_SHIFT
1570ENDPROC

1580DEF PROCACQ_MIR:*FX3,0
1590PROCCLEAR_LEGEND
1600PROCMSG("Acquisition Mirror",5,11,2):PROCMSG("Main",5,2,7):
    PROCMSG("M.In",5,10,7):PROCMSG("M.Out",5,18,7):*FX3,7
1610*FX18
1620*KEY0 PROCMAIN_MENU|M
1630*KEY1 C%=1:PROCACQ_MOVE|M
1640*KEY2 C%=0:PROCACQ_MOVE|M
1650PROCACQ_POS:PROCPRINT_ACQPOS
1660ENDPROC

1670DEF PROCACQ_POS
1680X=IN 46:Y=IN 47
1690IF X AND NOT Y THEN STATE$="OUT of":D%=0
1700IF NOT X AND Y THEN STATE$="IN":D%=1
1710IF NOT X AND NOT Y THEN STATE$="INBETWEEN":D%=2
1720ENDPROC

1730DEF PROCPRINT_ACQPOS:*FX3,0
1740PROCBLANK(3,18,33)
1750IF STATE$="OUT of" THEN PROCMSG("Acquisition Mirror is OUT of Beam",5,3,18)
1751IF STATE$="IN" THEN PROCMSG("Acquisition Mirror is IN Beam",5,6,18)
1752IF STATE$="INBETWEEN" THEN PROCMSG("Acquisition Mirror is inbetween ",
    5,5,1,8)
1753*FX3,7
1760ENDPROC

1770DEF PROCACQ_MOVE
1780PROCACQ_POS
1790IF C%=D% THEN PROCPRINT_ACQPOS:ENDPROC
1800TURNON45:DELAY200:TURNOFF45
1810REPEAT:PROCACQ_POS:UNTIL C%=D%
1820PROCPRINT_ACQPOS:ENDPROC

1830DEF PROCFIL_SHUT:*FX3,0
1840PROCCLEAR_LEGEND
1850PROCMSG("Filter Shutter",5,14,2):PROCMSG("Main",5,2,7):
     PROCMSG("FA",5,11,7):PROCMSG("FB",5,19,7):PROCMSG("FC",5,27,7):
     PROCMSG("FD",5,35,7):PROCMSG("FE",5,3,13):PROCMSG("FF",5,11,13):
     PROCMSG("Status",5,33,13):*FX3,7
```

```
1860*FX18
1870*KEY0 PROCMAIN_MENU¦M
1880*KEY1 PROCFS1¦M
1890*KEY2 PROCFS2¦M
1900*KEY3 PROCFS3¦M
1910*KEY4 PROCFS4¦M
1920*KEY5 PROCFS5¦M
1930*KEY6 PROCFS6¦M
1940*KEY9 PROCFIL_SHUT_STATUS¦M
1950STOP

1960DEF PROCFS1:OUT.30=TRUE:OUT,31=FALSE:OUT.32=TRUE:FS$="A":G%=1:
    PROCFS_MOV:ENDPROC
1970DEF PROCFS2:OUT.30=TRUE:OUT.31=TRUE:OUT.32=TRUE:FS$="B":G%=2:
    PROCFS_MOV:ENDPROC
1980DEF PROCFS3:OUT.30=TRUE:OUT.31=TRUE:OUT.32=FALSE:FS$="C":G%=3:
    PROCFS_MOV:ENDPROC
1990DEF PROCFS4:OUT.30=FALSE:OUT.31=TRUE:OUT.32=FALSE:FS$="D":G%=4:
    PROCFS_MOV:ENDPROC
2000DEF PROCFS5:OUT.30=FALSE:OUT.31=TRUE:OUT.32=TRUE:FS$="E":G%=5:
    PROCFS_MOV:ENDPROC
2010DEF PROCFS6:OUT.30=FALSE:OUT.31=FALSE:OUT.32=TRUE:FS$="F":G%=6:
    PROCFS_MOV:ENDPROC

2020DEF PROCFS_MOV
2030IN_POSITION = IN 33
2040IF NOT IN_POSITION THEN GOTO 2070
2050TURNOFF 27
2060REPEAT:FLIP29:DELAY 25:FLIP29:IN_POSITION=IN 33:UNTIL NOT IN_POSITION
2070*FX3,0
2080PROCBLANK(9,18,21):PROCMSG("Filter ",5,11,18):PROCMSG(FS$,5,18,18):
    PROCMSG(" selected",5,20,18):*FX3,7
2090STATUS$=LEFT$(STATUS$,1)+FS$+RIGHT$(STATUS$,12)
2100ENDPROC

2110DEF PROCPM_FILTERS:*FX3,0
2120PROCCLEAR_LEGEND
2130PROCMSG("Photomultiplier  Filters",5,8,2):PROCMSG("Main",5,2,7):
    PROCMSG("F1",5,11,7):PROCMSG("F2",5,19,7):PROCMSG("F3",5,27,7):
    PROCMSG("Clear",5,34,7):PROCMSG("U+",5,3,13):PROCMSG("U-",5,11,13):
    PROCMSG("RDY",5,19,13)
2140PROCMSG("All U",5,25,13):PROCMSG("Status",5,33,13)
2150PROCDISPUNIT:*FX3,7
2160*FX18
2170*FX12,20
2180*KEY0 PROCRESET¦M
2190*KEY1 E%=1:PROCSETPFIL¦M
2200*KEY2 E%=2:PROCSETPFIL¦M
2210*KEY3 E%=3:PROCSETPFIL¦M
2220*KEY4 E%=0:PROCSETPFIL¦M
2230*KEY5 PROCUNIT_UP¦M
2240*KEY6 PROCUNIT_DOWN¦M
2250*KEY7 PROCPM_READY¦M
2260*KEY8 PROCALL_UNITS¦M
2270*KEY9 PROCPMFSTATUS¦M
2280STOP

2290DEF PROCSETPFIL
2300IF E%=1 THEN TURNON48:TURNON49:PMFIL$="F1":PMF$="1":PROCDISPFIL:STOP
```

```
2310IF E%=2 THEN TURNON48:TURNOFF49:PMFIL$="F2":PMF$="2":PROCDISPFIL:STOP
2320IF E%=3 THEN TURNOFF48:TURNOFF49:PMFIL$="F3":PMF$="3":PROCDISPFIL:STOP
2330IF E%=0 THEN TURNOFF48:TURNON49:PMFIL$="F0":PMF$="0":PROCDISPFIL:STOP
2340ENDPROC

2350DEF PROCDISPFIL:*FX3,0
2360PROCMSG(PMFIL$,5,15,18):*FX3,7
2370ENDPROC

2380DEF PROCUNIT_UP
2390IF F%=8 THEN F%=0
2400F%=F%+1
2410PROCDISPUNIT
2420ENDPROC

2430DEF PROCUNIT_DOWN
2440IF F%=1 THEN F%=9
2450F%=F%-1
2460PROCDISPUNIT
2470ENDPROC

2480DEF PROCDISPUNIT:*FX3,0
2490PROCMSG("U",5,23,18):FF$=STR$(F%):PROCMSG(FF$,5,25,18):*FX3,7
2500ENDPROC

2510DEF PROCPM_READY
2520IF F%=1 THEN TURNON50,51,52
2530IF F%=2 THEN TURNOFF50:TURNON51,52
2540IF F%=3 THEN TURNON50,52:TURNOFF51
2550IF F%=4 THEN TURNOFF50,51:TURNON52
2560IF F%=5 THEN TURNON50,51:TURNOFF52
2570IF F%=6 THEN TURNOFF50,52:TURNON51
2580IF F%=7 THEN TURNON50:TURNOFF51,52
2590IF F%=8 THEN TURNOFF50,51,52
2600TURNON 53
2610T=TIME
2620REPEAT
2630T1=TIME-T
2640FIN = IN 54
2650IF T1>400 THEN FIN=FALSE:PMF$="0"
2660UNTIL NOT FIN
2670TURNOFF 53
2680STATUS$=LEFT$(STATUS$,(2+(F%-1)))+PMF$+RIGHT$(STATUS$,(12-F%))
2690ENDPROC

2700DEF PROCMSG(MSG$,C1%,X1%,Y1%)
2710PRINTTAB(X1%-1,Y1%);CHR$(129+C1%);MSG$;
2720ENDPROC

2730DEF PROCBLANK(X1%,Y1%,F1%)
2740PRINT TAB(X1%,Y1%);SPC(F1%);
2750ENDPROC

2760DEF PROCFIL_SHUT_STATUS:IF G%=1 THEN FS$="A":IF G%=2 THEN FS$="B":
    IF G%=3 THEN FS$="C":IF G%=4 THEN FS$="D":IF G%=5 THEN FS$="E":
    IF G%=6 THEN FS$="F":*FX3,0
2761*FX3,0
2762PROCBLANK(9,18,21):PROCMSG("Filter ",5,11,18):PROCMSG(FS$,5,18,18):
    PROCMSG(" selected",5,20,18):*FX3,7
```

```
2780DEF PROCRACK_RECOVER
2790TURNON41:DELAY50:TURNOFF41
2800REPEAT PROCRACK_POS:UNTIL RPOS$="I" OR RPOS$="O":IF RPOS$<>"O" THEN
    GOTO 2790:ENDPROC

2810DEF PROCSOURCE_ERROR:PROCRACK_POS:IF RPOS$="I" THEN SOURCE$="O":
    PROCCOMP_SELECT:IF RPOS$="B" THEN PROCRACK_RECOVER:TURNON59:DELAY100:
    TURNOFF59:ENDPROC

2920DEF PROCALL_UNITS
2930FOR PNEXT = 1 TO 8
2940F%=PNEXT:PROCPM_READY
2950NEXT
2960ENDPROC

2970DEF PROCPMFSTATUS:*FX3,0
2980PROCMSG("U 1  U 2  U 3  U 4  U 5  U 6  U 7  U 8",5,1,21)
2990S1=2
3000FOR XX5%= 0 TO 35 STEP 5
3010S1=S1+1
3020PS$=MID$(STATUS$,S1,1)
3030PROCMSG(PS$,5,(XX5%+2),22)
3040NEXT
3050*FX3,7
3060ENDPROC

3070DEF PROCINITIALISE
3080BASE.=&D000
3090OUTCH 0 TO 63
3100INCH 33,37,54,55,56,57,58,16 TO 26,46,47
3130PROCRACK_POS
3140IF RPOS$<>"O" THEN TURNON41:DELAY25:TURNOFF41:DELAY400:GOTO 3130
3150TURNON42:TURNOFF43,44
3160REPEAT MOTOR_ON = IN 57
3170UNTIL MOTOR_ON
3180SOURCE$="A":DUMMY$="A":A%=0
3190OUT.30=TRUE:OUT.31=TRUE:OUT.32=FALSE
3200FS$="A":G%=1
3210REM PROCFS_MOV
3220E%=0
3230TURNOFF 48:TURNON 49:PMFIL$="F0":PMF$="0"
3240PROCALL_UNITS
3250REM C%=0:PROCACQ_MOVE
3260TURNON27,28
3270PROCGR_POS
3280SGRAT$=STR$(GRAT_POS)
3290REPEAT:L=LEN(SGRAT$):IF L<4 THEN SGRAT$=" "+SGRAT$:UNTIL L=4
3300STATUS$="NA00000000"+SGRAT$
3310*FX3,0
3320FOR Y=0 TO 23
3330NEXT
3340VDU28,0,24,40,0
3350VDU23,1,0;0;0;0;0;
3360*FX3,8
3370ENDPROC
```

APPENDIX B

DATA ACQUISITION SOFTWARE

```
 10CLOSE£ 0
 20INPUT "File Name",FILE_NAME$
 30YY=OPENOUT(FILE_NAME$)
 40LF$=CHR$(10)
 50DIM CNT$(9)
 60DIM CNT(9)
 70DIM STORE 116
 80
 90INPUT "Header",HEADER$
100REM INPUT "WIDE OR NARROW " WORNF$
110REM  IF NOT ((WORNF$="W") OR (WORNF$="N")) THEN GOTO 100
120REM PROCFILTER_CHOICE
130INPUT "Lenght of Integration",LINT
140INPUT "Number of Integrations on Object",NO_INT
150INPUT "Enter ND Filter choice, A,C,D,E or F ",FIL_CHOICE$
160IF NOT ((FIL_CHOICE$="A") OR (FIL_CHOICE$="C") OR (FIL_CHOICE$="D") OR (FIL_CHOICE
170PROC_NDFIL_SELECT
180LINT$= STR$(LINT)
190
200FOR X1=1 TO NO_INT
210
220PROC_READ_STATUS
230PROC_READ_TIME
240PROC_READ_DATE
250PROC_COUNT
260PROC_WRITE_TO_DISC
270
280NEXT X1
290
291TEMP$=FIL_CHOICE$
292FIL_CHOICE$="C"
293PROC_NDFIL_SELECT
294FIL_CHOICE$=TEMP$
300REM INPUT "Same object (S), New Object (N) or Finish (F)",ANS$
310REM IF NOT ((ANS$="S") OR (ANS$="N") OR (ANS$="F")) THEN GOTO 300
320REM IF ANS$="N" GOTO 90
330REM IF ANS$="S" GOTO 100
331VDU7: INPUT "ANY CHANGES " ANS$
332 IF ANS$="Y" GOTO 90
333PROC_NDFIL_SELECT:GOTO200
340CLOSE£ 0
350STOP
360END
370
```

```
380DEF PROC_READ_STATUS
390*FX7,7
400*FX8,7
410*FX15
420*FX2,1
430*FX3,7
440PRINT "PRINT STATUS$"
450*FX3,14
460INPUT " "JUNK$
470INPUT " "STAT$
480*FX3,4
490*FX2,0
500ENDPROC
510
520DEF PROC_READ_TIME
530*FX7,7
540*FX8,7
550*FX15
560*FX2,1
570*FX3,7
580PRINT "PRINT CLOCK$"
590*FX3,14
600INPUT " "JUNK$
610INPUT " "CLK$
620*FX3,4
630*FX2,0
640ENDPROC
645
650DEF PROC_READ_DATE
660*FX7,7
670*FX8,7
680*FX15
690*FX2,1
700*FX3,7
710PRINT "PRINT DATE$"
720*FX3,14
730INPUT " "JUNK$
740INPUT " "DAT$
750*FX3,4
760*FX2,0
770ENDPROC
780
790DEF PROC_COUNT
800?&FCDC=0
810?&FCDD=&03
820?&FCDE=&FC
830?&FCDF=&FF
840N%=LINT*20
850
860A1=-N%-1
870A2=A1 AND &00FF
880A3=A1-A2
890A4=A3/256
900
910?&FCDA=0
920?&FCDB=0
930?&FCDE=A2
940?&FCDF=A4
950Z=?&FCDE
```

```
 960Y=Z AND &80
 970IF Y<>&80 GOTO 950
 980
 990?&FCDA=0
1000Z=?&FCDE
1010Y=Z AND &80
1020IF Y<>&80 GOTO 1000
1030
1040B=-3:CH=0
1050B=B+3:CH=CH+1
1060S=?(&FCC2+B) AND &0F
1070CNT(CH)=?(&FCC0+B)+256*?(&FCC1+B)+65536*S
1080X=?(&FCC2+B) AND &80
1090IF X=&80 THEN CNT(CH)=1048575-CNT(CH)
1100IF CH<8 GOTO 1050
1110
1120?&FCDC=0
1130ENDPROC
1140
1150DEF PROC_WRITE_TO_DISC
1160CH1=0
1170CH1=CH1+1
1180CNT$(CH1)=STR$(CNT(CH1))
1190IF CH1<8 GOTO 1170
1200
1210PROCPAD
1220
1230STORE%=STORE
1240$STORE%=HEADER$
1250STORE%=STORE%+15
1260$STORE%=" "
1270STORE%=STORE%+&1
1280$STORE%=LINT$
1290STORE%=STORE%+&3
1300$STORE%=" "
1310STORE%=STORE%+&1
1320$STORE%=STAT$
1330STORE%=STORE%+&E
1340$STORE%=" "
1350STORE%=STORE%+&1
1360$STORE%=CLK$
1370STORE%=STORE%+8
1380$STORE%=" "
1390STORE%=STORE%+&1
1400$STORE%=DAT$
1410STORE%=STORE%+8
1420$STORE%=" "
1430STORE%=STORE%+&1
1440$STORE%=CNT$(1)
1450STORE%=STORE%+&7
1460$STORE%=" "
1470STORE%=STORE%+&1
1480$STORE%=CNT$(2)
1490STORE%=STORE%+&7
1500$STORE%=" "
1510STORE%=STORE%+&1
1520$STORE%=CNT$(3)
1530STORE%=STORE%+&7
1540$STORE%=" "
```

```
1550STORE%=STORE%+&1
1560$STORE%=CNT$(4)
1570STORE%=STORE%+&7
1580$STORE%=" "
1590STORE%=STORE%+&1
1600$STORE%=CNT$(5)
1610STORE%=STORE%+&7
1620$STORE%=" "
1630STORE%=STORE%+&1
1640$STORE%=CNT$(6)
1650STORE%=STORE%+&7
1660$STORE%=" "
1670STORE%=STORE%+&1
1680$STORE%=CNT$(7)
1690STORE%=STORE%+&7
1700$STORE%=" "
1710STORE%=STORE%+&1
1720$STORE%=CNT$(8)
1730STORE%=STORE%+&7
1740$STORE%=LF$
1750PROCBPUT
1760ENDPROC
1770
1780DEF PROCPAD
1790CH2=0
1800CH2=CH2+1
1810L1=LEN(CNT$(CH2))
1820IF L1<7 THEN CNT$(CH2)=CNT$(CH2)+" ":GOTO 1810
1830PRINTCH2," ",CNT$(CH2)
1840IF CH2<8 GOTO 1800
1850PRINT
1860
1870L2=LEN(HEADER$)
1880IF L2<15 THEN HEADER$=HEADER$+" ":GOTO1870
1890
1900L3=LEN(LINT$)
1910IF L3<3 THEN LINT$=LINT$+" ":GOTO 1900
1920
1930ENDPROC
1940
1950DEF PROCBPUT
1960FOR K=0 TO 117
1970BPUT&YY,STORE?K
1980NEXT
1990ENDPROC
2000
2010DEF PROCFILTER_CHOICE
2020IF WORNF$="W" THEN EE1=0 ELSE EE1=1
2030*FX7,7
2040*FX8,7
2050*FX2,1
2060*FX3,7
2070PRINT "INPUT E%"
2080PRINT EE1
2090PRINT "PROCSETPFIL"
2100PRINT "INPUT F%"
2110PRINT 5
2120PRINT "PROCPM_READY"
2130PROCDELAY
```

```
2140*FX3,14
2150*FX21,1
2160*FX21,2
2170*FX3,4
2180*FX2,0
2190*FX21,1
2200*FX21,2
2210ENDPROC
2220
2230DEF PROCDELAY
2240T=TIME
2250T1=TIME
2260IF T1<T+300 GOTO 2250
2270ENDPROC
2280
2290DEF PROC_NDFIL_SELECT
2300IF FIL_CHOICE$="A" THEN SELECT$="PROCFS1"
2310IF FIL_CHOICE$="C" THEN SELECT$="PROCFS3"
2320IF FIL_CHOICE$="D" THEN SELECT$="PROCFS4"
2330IF FIL_CHOICE$="E" THEN SELECT$="PROCFS5"
2340IF FIL_CHOICE$="F" THEN SELECT$="PROCFS6"
2350*FX 7,7
2360*FX8,7
2370*FX2,1
2380*FX3,7
2390PRINT SELECT$
2400PROCDELAY
2410*FX3,14
2420*FX21,1
2430*FX21,2
2440*FX3,4
2450*FX2,0
2460*FX21,1
2470*FX21,2
2480ENDPROC
```

APPENDIX C

It is impossible to get a measure of the signal-to-noise ratio for each individual integration since the counters used automatically subtract the contribution from the sky+dark-count. But, if we have a typical Sky+dark-count count then we can find a typical measured count for which will give a signal-to-noise of 100.

Let n_s = sky + dark-count

and n_* = star + sky + dark-count

Using Poisson statistics the error in n_s and n_* are,

$$\sigma n_s = \sqrt{n_s}$$

$$\sigma n_* = \sqrt{n_*}$$

Since

$$n_{star} = n_* - n_s$$

$$\sigma^2 n_{star} = \sigma^2 n_s + \sigma^2 n_*$$

$$= n_s + n_*$$

$$r = \frac{n_* - n_s}{\sqrt{n_s + n_*}}$$

where r = signal-to-noise ratio

For a typical sky+dark-count count of 6000 counts we find that $n_{*}-n_{s}$ = 17000 counts. Therefore we need to measure at least 17000 counts to achieve a signal-to-noise ratio of 100.

REFERENCES

d'Arsonval, A. 1886, Soc. Fran. Phys., 30.

Barwig,H. and Schoembs,R. 1984, I.A.U. Coll.No.79 p.665

Barwig,H. and Schoembs,R. 1986, in Instrumentation and Research
Programmes for Small Telescopes. eds. J.B.Hearnshaw and
P.C.Cottrell. p.61

Barwig,H.,Schoembs,R.,Buckenmayer,C. 1987,
Atron. Astrophys. 175, 327.

Baum,W.A.,Hiltner,W.A.,Johnson,H.L. and Sandage,A.R. 1959,
Ap. J. 130, 749.

Bell,S.A. and Hilditch,R.W., 1984, Mon. Not. R. astr. Soc.,
211, 229, (Paper 1).

Belvedere,G., and Paterio,L. 1976, Astron. Astrophys.
51, 199.

Bernacca,P.L.,Canton,G.,Stagni,R.,Leschiutta,S.,Sedmak,G. 1978,
Astron. Astrophys. 38, 359.

Blitzstein,W. 1951, in Astonomical Photoelectric Photometry,
ed. F.B.Wood, p.64.

Bopp,B.W. and Fekel,F. 1977, Astr. J., 82, 490.

Boys,F.S., 1800, Phil. Trans., 90, 284.

REFERENCES

van Breda,I.G., 1970, Physics Bulletin, 21, p.207.

Burnet,M. and Rufner,F., 1979, Astron. Astrophys., 74, 54.

Caplan,J. and Grec,G., 1975, Astron. Astrophys., 47, 59.

Caton,D.B. and Pollock,J.T., 1986, in Instrumentation and Research

Programmes for Small Telescopes, eds. J.B.Hearnshaw and

P.C.Cottrel, p.81.

Cellino,A.,Scaltriti,F. amd Busso,M., 1985, Astron. Astrophys.,

144, 315.

Clampin,M., 1985, Ph.D. Thesis, St.Andrews.

Coblentz,W.W., Lick Obs. Bull., 1915, 8, 104.

Crawford,D.L. and Barnes,J.V., 1970, Atron. J., 75, 978.

Davidson,J.K.,Neff,J.S. and Enermark,D.C., 1976, Pub.A.S.P.,

88,209.

De Baise,G.A.,Paterno,L.,Pucillo,M. and Sedmak,G. 1978,

Appl. Optics. Vol. 17, No. 3, p.345.

Eccles,M.J.,Sim,.M.E. and Tritton,K.P., 1983, in Low Light level

Detectors in Astronomy, Cambridge University Press.

Elster,J. and Geitel,H. 1916, Physik. Z., 17, 268.

Engstrom,R.W., 1947, J. Opt. Soc. America, 37, 420.

Genet,R.M., 1974, in Microprocessors in Astronomy,

Fairborn Observatory.

Geyer,E.H. and Hoffmann,M., 1974, Astron. Atrophys. 70, 821.

Gianni,G.,Mazzitelli,I. and Natali,G., 1975, Astron. Astrophys.

44, 277.

REFERENCES

Giovannelli,F.,Auriemma,G.,Costa,E.,Massimo,F.,
Mastropietro,M., and Pica,F., 1980,
Acta. Astron. 30, 565.

Golay,M., 1974, Introduction to Astronomical Photometry.
D. Reidel Publ. Co., Dordrecht, Holland.

Goudis,C. and Meaburn,J., 1973, Astrophys. and Space Science,
20, 149.

Grauer,A.D. and Bond,H.E., 1981, Publ. A. S. P., 93, 388.

Griffin,R.F. and Redman,R.O., 1960, Mon. Not. R. astr. Soc.,
120, 287.

Gronbech,B.,Olsen,E.H.,Stromgren,B., 1975, Astron. Astrophys.
Suppl., 26, 155.

Guthnick,P., 1929, Astron. Nachr., 235, 83.

Guthnick,P., 1913, Astron. Nachr., 196, 357.

Guthnick,P., 1918, Varoff. sterw. Babelsberg, Vol II/3, 140.

Guthnick,P., 1947, Abhandl. Berhiner Akad. Wiss. Jahrg, 1947/2.

Hall,D.S., 1976, Multiple Periodic Variable Stars, IAU coll. No.29,
p.287, ed Fitch,W.S., D Reidel, Dordrecht, Holland.

Hardie,R.H., 1962, in Astronomical Techniques, ed. W.A.Hiltner,
University of Chicago Press, p.181.

Hardie,R.H., 1959, Ap. J. 130, 663.

Herschel,W., 1800, Phil. Trans., 30.

Hertzsprung,E., 1928, Bul. Astr. Inst. Neth., 4, 179.

Hilditch,R.W., 1988, Private Communication.

REFERENCES

Hilditch,R.W., Harland,D.M. and McLean,B.J., 1979, Mon. Not. R. astr. Soc., 187, 39.

Hilditch,R.W. and Hill,G., 1975, Mem. R. astr. Soc., 79, 101.

Hiltner,W.A., 1956, Ap. J. Suppl., 2, 389.

Huggins,A., 1868, Proc. Roy. Soc. London, 17, 309.

Johnson,H.L. and Morgan,W.W., 1953, Astrophys. J., 117, 313.

Johnson,H.L., 1955, Ann. Rev. Astron., 18, 4.

Johnson,H.L., 1958, Sky and Telescope, 14, 558.

Johnson,H.L. and Morgan,W.W., 1951, Ap. J. Suppl., 2, 389.

Kinamn,T.D. and Mahaffey,C.T., 1974, Publ. A. S. P., 86, 336.

Kron,G.E., 1946, Ap. J., 103, 326.

Kunkel,W.E., 1975, I.A.U. Symp. 67, p.15.

Latham,D.W., 1968, Astron. J., 73, 515.

Linnel,A.P., 1975, Publ. A. S. P., 87, 273.

Llyod Evans,T., 1967, The Observatory, 87, 956, p.32.

McClure,R.D. and Van Den Bergh,S., 1968, Astron. J., 73, 313.

Minchin,G.M., 1895, Proc. Roy. Soc. London, 17, 309.

Moor,C.H. and Rather,E.D., 1974, Ast. Astro. (Suppl.), 15, 497.

Nather,E.R. and Warner,B., 1971, Mon. Not. R. astr. Soc., 152, 209.

Nelson,B., 1963a, Publ. A. S. P., 75, 18.

Nelson,B., 1963b, Publ. A. S. P., 756, 417.

Nelson,B. and Duckworth.E., 1968, Publ.A. S. P., 80, 562.

Nelson,B., 1951, B. A. J., 56, 136.

Nielsen,R.F., 1983, Inst.Theor, Astrophys., Oslo, Report 59, p.141.

REFERENCES

Oke,J.B., 1969, Publ. A. S. P., 81, 11.

Paterno,L., 1976, Astron. Asrophys., 47, 437.

Patkos,L., 1982a, Astrophys. Letters, 22, 131.

Patkos,L., 1982b, Comm. Konkoly Obs., No.80.

Pfund,H., 1913, Pub. of the Allegheny Obs., 3, 43.

Piccioni,A.,Bartolini,C.,Guarnien,A., 1979, Acta Astronomica,
Vol.29, No.3, p.463.

Rajewsky,B., 1931, Physik Z., 32, 121.

Robinson,L., 1975, Ann. Rev. Astron. Astrophys., 13, 165.

Rosenberg,H., 1913, Viert.der Ast. Gesell, 48, 210.

Schilt,J., 1922, B. A. N., 1, 51.

Sedmak,G., 1973, Astron. Astrophys., 18, 232.

Serkowski,K., 1970, Publ. A. S. P., 82, 908.

Sorvari,J.M., 1975, Publ. A. S. P., 87, 443.

Stebbins,J. and Brown,F.C., 1907, Ap. J., 26, 326.

Stebbins,J., 1910, Ap.J., 32, 185.

Stebbins,J. and Kron,G.E., 1956, Astrophys. J., 123, 440.

Stebbins,J. and Whittford,A.E., 1945, Astrophys. J., 102, 318.

Steinke,Z., 1926, Physik Z., 38, 378.

Stetson,H.T., 1914, Pop. Astr., 23, 23.

Stetson,H.T., 1916, Ap. J., 43, 253.

Strömgren,B., 1966, Ann. Rev. Astron. Astrophys., 4, 433.

Taylor,D.J., 1980, Publ. A. S. P., 92, 108.

Visvanathen,N., 1972, Publ. A. S. P., 84, 248.

Walker,G.A.H.,Andrews,D.H.,Hill,G,Morris,S.C.,Smyth,W.G. and White,J.R., 1971, Pub. of the Dom. Astr. Obs., Vol.,13, 415.

Walker,E.N., 1984, Vistas in Astronomy, 27, 421.

Walraven,Th. and Walraven,J.H., 1960, B. A. N., 15, 67.

REFERENCES

Warner,B., 1971, I.A.U. Coll., 15, p.44.

Warner,B., 1972, Sky and Telescope, 23, 82.

Weaver,H.F., 1946, Pop. Astron., 54, 5, p.230.

Whitford,A.E., 1932, Ap. J., 76, 213.

Whitford,A.E. and Kron,G.E., 1937, Rev. Sci. Inst., 8, 78.

Willingale,G.P.H., 1988, Private Communication.

Wireless World, 1972, July, p.333.

van Woerden,H., 1957, Leiden Ann., 21, p.40.

Wood,F.B., 1946, Contr. Princeton Obs., 21, p.40.

Yates,G.G., 1948, Mon. Not. R. astr. Soc., 108, 476.

Young,A.T., 1974, in Experimental Methods in Physics, Vol. 12,

p.37, ed. N.Carleton, Academic Press.